Design, Synthesis and Evaluation of Novel HIV-1 Integrase Inhibitors

THESIS

Submitted in partial fulfillment

of the requirements for the degree of

DOCTOR OF PHILOSOPHY

by

Pankaj Wadhwa

Under the Supervision of

Prof. Hemant R Jadhav

BITS Pilani

Pilani | Dubai | Goa | Hyderabad

BIRLA INSTITUTE OF TECHNOLOGY AND SCIENCE, PILANI

2017

BIRLA INSTITUTE OF TECHNOLOGY AND SCIENCE, PILANI

CERTIFICATE

This is to certify that the thesis entitled "Design, Synthesis and Evaluation of Novel HIV-1 Integrase Inhibitors" and submitted by Mr. Pankaj Wadhwa, ID No 2012PHXF0406P for award of Ph.D. degree of the Institute embodies original work done by him under my supervision.

Signature of the Supervisor

Name in capital letters: Prof. HEMANT R JADHAV

Designation: Associate Professor, Dept. of Pharmacy

Associate Dean, Academic Research Division

Birla Institute of Technology and Science Pilani, Pilani Campus

Date:

ACKNOWLEDGEMENT

"In the name of the most beneficent, the most merciful"

Completion of this doctoral dissertation was possible with the support of several people. I would like to express my sincere gratitude to all of them. Firstly, I would like to express my sincere gratitude to my advisor **Prof. Hemant R Jadhav** for the continuous support of my Ph.D study and related research, for his patience, motivation, and immense knowledge. His guidance helped me in all the time of research and writing of this thesis. I could not have imagined having a better advisor and mentor for my Ph.D study. Thank you Sir, for all your help and support.

I am immensely thankful to **Prof. Souvik Bhattacharyya**, Vice-Chancellor, BITS, Pilani, **Prof. A. K. Sarkar**, Director, BITS Pilani, Pilani Campus and **Prof. B.N Jain** (ex Vice-Chancellor, BITS-Pilani, Pilani Campus), for permitting me to carry out this research work in BITS, Pilani. I would like to express my gratitude to **Prof. R. N. Saha**, Director, BITS Pilani, Dubai Campus and **Prof. R. Mahesh**, Dean, Faculty Affairs, BITS, Pilani for their suggestions and impetus during my research work. I am grateful to **Prof. S. C. Sivasubramanian**, Dean, Administration, BITS Pilani, Pilani Campus, **Prof. S. K. Verma**, Dean, Academic Research Division, BITS, Pilani, and **Dr. Anshuman**, Unit Chief, Estate Management, BITS Pilani, Pilani Campus for their support during the period of stay at BITS.

Besides my advisor, I would like to thank my Doctoral Advisory Committee members **Dr. S. Murugesan**, and **Dr. Atish T. Paul**, for their insightful comments and encouragement, but also for the hard questions that incented me to widen my research from various perspectives.

I owe my gratitude to **Dr. Anil Gaikwad**, Head, Department of Pharmacy for his constant support and guidance to pursue my doctoral thesis. I sincerely thank **Dr. Rajeev Taliyan, Dr. Priti Jain, Ms. Archana K Kakkar**, **Mr. Subhash Chander Saini, Mr. Almesh Kadakol and Mr. Ram Partap Suthar** for their continuous help and support. They have been helpful for their constructive suggestions and moral support.

Further, my sincere thanks to **Dr. Gautam Singhvi**, **Dr. Shvetank Bhatt**, **Dr. Sunil Dubey**, **Dr. Anil Jindal**, **Dr. Mahaveer Singh**, **Dr. Deepak Chitkara**, **Dr. Anupama Mittal**, **Dr. Aniruddha Roy** and **Dr. Murali Monohar Pandey** for making the journey a memorable one. They all supported me personally as well as professionally.

I sincerely express my gratitude to our collaborator **Prof. Christophe Pannecouque**, Rega Institute for Medical Research, Laboratory of Virology and Chemotherapy, Belgium for carrying out cell based assays.

My heartfelt thanks to my seniors **Dr. Vadiraj**, **Dr. Ankur**, **Dr. Emil**, **Dr. Prashant**, **Dr. Muthu**, **Dr. Arghya**, **Dr. Sourabh Mundra**, **Dr. Sushil**, **Dr. Garima Balwani**, **Dr. Vibhu Nagpal**, **Dr. Yeshwant**, **Dr. Mukund**, **Dr. Deepali**, **Dr. Pallavi** and **Mr. Satish Reddy**. I will always cherish the warmth shown by them.

A special mention of thanks to my friends **Sridhar**, **Sorabh Sharma**, **Santosh Goru**, **Anuradha**, **Shruti**, **Nisha**, **Vajir**, **Kishan**, **Saurabh Sharma, Ginson**, **Krishna**, **Parcheta**, **S.K. Das**, **Dinesh Kumar**, **Shiv Dhiman**, **Hitesh Saini**, **Sachin**, **Anoop Singh**, **Nitesh**, **Saleem Pasha**, **Faiyaz Baig**, **Manish Mehra**, **Venkata Reddy**, **Santosh Khandagale**, **Vimal Kumar**, **Vishal Kachwal** and **Vandana Tomar**.

I overwhelmingly acknowledge the nonteaching staff of ARD and Department of Pharmacy for their help in one form or other.

I owe my deepest gratitude towards my **parents** and my better half **Priyanka Wadhwa** for their eternal support and understanding of my goals and aspirations. Their infallible love and support has always been my strength. Their patience and sacrifice will remain my inspiration throughout my life. I am thankful to my niece **Peehu Upveja** and my son **Parth**. Their presence has filled my life with full of joy.

My warmest thanks belong to my family members for their never ending love, encouragement and support. I owe a lot to my siblings, who encouraged and helped me at every stage of my personal and academic life.

I acknowledge University Grants Commission (UGC), Govt. of India for the financial support in the form BSR Scholarship. I also would like to thank **Department of Science & Technology**, **Science and Engineering Research Board**, New Delhi for providing the travel grant for attending conferences abroad.

I gratefully acknowledge **Department of Pharmacy** and **BITS, Pilani** for providing me an opportunity to carry out my research as well as for providing institute fellowship.

My sincere thanks and regrets to all friends and people I missed to acknowledge, who had directly or indirectly helped me to accomplish this task.

Last but not the least; I pay my obeisance to GOD, the almighty to have bestowed upon me good health, courage, inspiration, zeal and grace due to which I became able to finish this task.

Pankaj Wadhwa

DEDICATED

TO

MY FAMILY

LIST OF ABBREVIATIONS

^{1}H NMR	Proton Nuclear Magnetic Resonance
α	Alpha
β	Beta
δ	Delta
°C	Degrees Centigrade
µl	Micro Liters
3P	3'-End Processing
AIDS	Acquired Immune Deficiency Syndrome
ART	Anti-Retroviral Treatment
CD4	Cluster of Differentiation 4
cDNA	Complementary DNA
5-ClTEP	1-(5-Chloroindol-3-Yl)-3-Hydroxy-3-(2*H*-Tetrazol-5-Yl)-Propenone
ClogP	Calculated Log Partition Coefficient
d	Doublet
dd	Doublet Of Doublet
DCM	Dichloromethane
DNA	Deoxyribonucleic Acid
DMF	*N,N*-Dimethylformamide
DMSO	Dimethyl Sulfoxide
ds	Double Stranded
EDC.HCl	1-(3-Dimethylaminopropyl)-3-Ethylcarbodiimide hydrochloride
Eqv.	Equivalent
ELISA	Enzyme-Linked Immunosorbent Assay
ESI-MS	Electrospray Ionization Mass Spectrometry
gp120	Glycoprotein 120
Gscore	Glide Score
h	Hour(s)
HAART	Highly Active Anti-Retroviral Therapy
HBA	Hydrogen Bond Acceptors
HBD	Hydrogen Bond Donors

HIV	Human Immunodeficiency Virus
HOBt	1-Hydroxy benzotriazole
IC_{50}	Half Maximal Inhibitory Concentration
IR	Infra-Red
LTR	Long Terminal Repeats
mg	Milligram
ml	Milli Liters
mM	Milli Moles
m.p.	Melting Point
mol	Mole
MW	Molecular Weight
nM	Nanomoles
OB	Oral Bioavailibilty
pdb	Protein Data Bank
ppm	Parts Per Million
RNA	Ribonucleic Acid
RPM	Round Per Minute
RT	Reverse Transcriptase
rt	Room Temperature
SAR	Structure-Activity Relationship
ST	Strand Transfer
TEA	Triethylamine
TLC	Thin Layer Chromatography
TMS	Trimethylsilane
XP	Extra Precision

TABLE OF CONTENTS

LIST OF TABLES

LIST OF FIGURES

CHAPTER 1: INTRODUCTION

1.1 HIV/AIDS

Acquired Immuno deficiency Syndrome (AIDS) is one of the most widespread worldwide infectious diseases caused by Human Immunodeficiency Virus (HIV). In 2016, UNAIDS estimated that around 36.7 million people were living with HIV with over 5000 new infections occuring each day, and in the same year, AIDS claimed one million lives. In India, about 2.1 million people were suffering from HIV infection (UNAIDS data, 2017).

In 1992, India's first National AIDS Control Programme (1992-1999) was launched and National AIDS Control Organization (NACO) was constituted to implement it. In 2009, India framed a "National HIV and AIDS Policy and the World of Work", which sought to end discrimination against workers based on their real or perceived HIV status. Under this policy, all enterprises in the public, private, formal and informal sectors are encouraged to establish workplace policies and programmes based on the principles of non-discrimination, gender equity, health work environment, non-screening for the purpose of employment, confidentiality, prevention and care and support.

Human immunodeficiency viruses (HIV) are lentiviruses, a family of mammalian retroviruses that are evolved to create chronic persistent infection with slow onset of clinical symptoms. Once infection is established, replication is constant indicating that there generally is no true period of viral latency. However, some of the infected cells may host nonreplicating but infectious virus for years. These viruses are hosted only by humans and chimpanzees. There are two major families of HIV viz. HIV-1 and HIV-2. Globally, HIV-1 infection occurs while HIV-2 is distributed mainly in western Africa. HIV-1 has at least five distinct subfamilies or clades, all are equally susceptible to drugs. Most of the drugs inhibit HIV-1 and HIV-2 *in vitro* but the nonnucleoside reverse transcriptase inhibitors (NNRTIs) do not inhibit HIV-2 (Brunton, 2011).

1.1.1 HIV-1

An HIV virus particle is spherical with a diameter of about 120 nm and constitutes two copies of positive sense single-stranded genomic RNA of approximately 9.3 kilo bases in nucleocapsid core surrounded by envelop. Envelop is a lipid bilayer derived from host cell plasma membrane during budding of the virus. There are three major open reading frames viz *gap*, *pol* and *env* encoded in viral genome. *Gag* encodes a polyprotein that is processed to release the major structural proteins of the virus. *Pol* encodes three important enzymes—an RNA-dependent DNA polymerase or reverse transcriptase with RNAase activity, protease, and integrase. *Pol* overlaps *gag* and *Env* encodes the large transmembrane envelope protein

responsible for host cell recognition and fusion entry. *Env* consists of a cap made of a trimeric glycoprotein, GP120 (or gp120), which masks a transmembrane glycoprotein 41 (or gp41) stalk that anchor the structure into the viral envelope. Several other small genes are also there which encode regulatory proteins known enhance virion production or combat host defenses. These include tat, rev, nef, and vpr. A proteinous matrix made up of viral protein p17 lie between the envelope and core provides structural support and integrity of the virion particle (Crandall, 1999; Brunton, 2011).

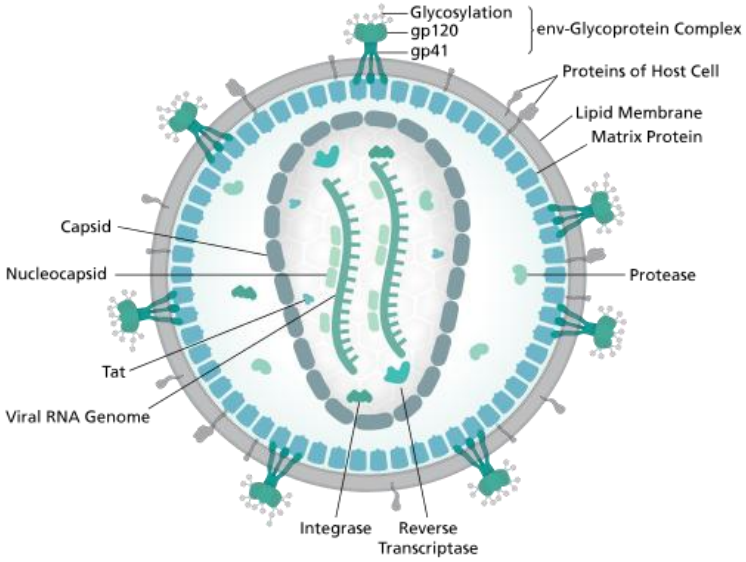

Figure 1: Schematic diagram of HIV structure

(https://en.wikipedia.org/wiki/Structure_and_genome_of_HIV#/media/File:HI-virion-structure_en.svg)

1.1.2 HIV-1 infection and life cycle

HIV spreads in three ways: through sexual intercourse, from mother to child (during birth and breastfeeding), and by blood (through transfusion, blood products, or contaminated needles). The surface glycoprotein gp120 attaches to the receptors on surface of CD4 cell that triggers conformational changes in gp120 followed by discharge of viral nucleocapsid into the cytoplasm. After uncoating, reverse transcriptase (RT) transcribes the viral RNA. The resulting double stranded DNA migrates into the cell's nucleus and integrated by HIV integrase (IN) enzyme. Resultant proviral DNA is further transcribed by cellular RNA polymerase II. For making larger proteins, mRNAs are translated by cellular polysomes. The viral proteins and genomic RNA are transported to cell membrane where they assemble, form a viral bud and are released into the lymphocyte membrane. These immature virions are released, and polypeptide precursors are processed by the viral protease (PR) to produce mature viral particles.

The final stage is known as assembling, maturation and budding of immature virions to bind to a new CD4 cell and receptors and begin the process again, as given in Figure 2 (Brunton, 2011; Clercq, 2009).

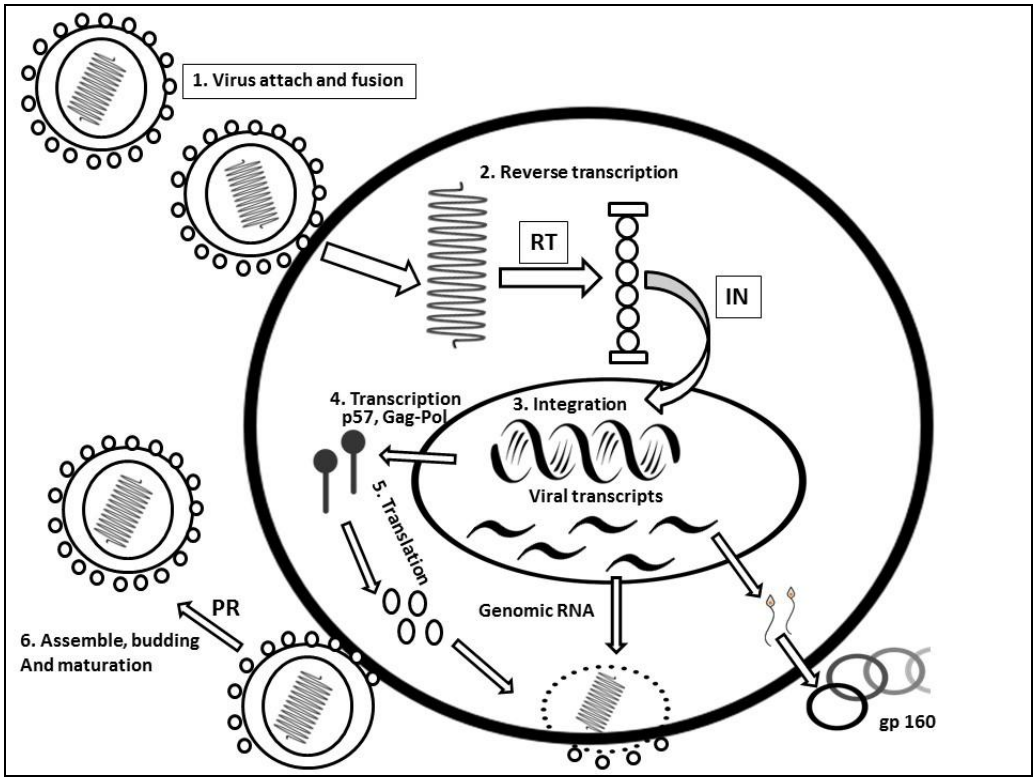

Figure 2: Stages of HIV life cycle.

1.2 Drug therapy for HIV/AIDS

Drugs have been developed to delay disease by keeping blood viral load at minimum. The first antiretroviral drug Azidothymidine (AZT, zidovudine) was approved in 1987. So far, there are 32 FDA approved antiretroviral (ARV) drugs which target various stages of HIV life cycle. These ARVs are classified into five different classes: (i) fusion or entry inhibitors (EIs); (ii) nucleoside (and nucleotide) reverse transcriptase inhibitors (NRTIs and NtRTIs); (iii) non-nucleoside reverse transcriptase inhibitors (NNRTIs); (iv) protease inhibitors (PIs) and (v) integrase inhibitors (Foye, 2008).

(i) Entry and fusion inhibitors

The first FDA approved fusion inhibitor is enfuvirtide (36 amino acid polypeptide) that prevents HIV entry by binding to glycoprotein 41 on the viral envelope, preventing the creation of an entry pore for capsid of virus. Maraviroc is the only approved C-C chemokine receptor type 5 (CCR5) antagonist. It prevents infection by binding of HIV gp 120 to CCR5 and blocks subsequent membrane fusion events

required for viral entry. It is best used in combination with a C-X-C chemokine receptor type 4 (CXCR-4) antagonists such as Plerixafor and BL-8040 (Fumakia, 2016).

(ii) Nucleoside/Nucleotide reverse transcriptase inhibitors (NRTIs and NtRTIs)

These are structurally similar to the naturally occurring building blocks of DNA. They inhibit reverse transcriptase and prevent HIV from replicating. NRTIs require three phosphorylation steps for activation while NtRTIs are already chemically activated and have one phosphate group attached. This phosphate group is non-cleavable by hydrolases, so NtRTI cannot be removed after incorporation. The examples of approved NRTIs are zidovudine (AZT), didanosine (ddI), zalcitabine (ddC), lamivudine (3TC), stavudine (d4T), emtricitabine (FTC), abacavir (ABC), entecavir (ETV) and tenofovir D (TDF). During reverse transcription, these nucleoside/nucleotide analogues are incorporated into viral DNA, but because of absence of 3'-OH, which is essential to make phospho-ester linkage with incoming deoxynucleoside triphosphate, DNA synthesis is prematurely suppressed (Arts, 2012).

(iii) Non-nucleoside reverse transcriptase inhibitors (NNRTIs)

NNRTIs are non-competitive inhibitors of RT and exert their effect by binding with allosteric site proximal to the catalytic site of RT. Their binding causes conformational change in three-dimensional structure of enzyme and inhibit normal interaction with viral RNA, blocking DNA-dependent and RNA dependent polymerase activities. NNRTIs in clinic are nevirapine, delavirdine, efavirenz, rilpivirine and etravirine (Arts, 2012).

(iv) Protease inhibitors (PIs)

PIs prevent viral replication by inhibiting proteolytic cleavage of HIV polypeptide precursors into mature enzymes and structural proteins via binding to viral proteases (e.g. HIV-1 protease). There are presently ten approved PIs for clinical use such as saquinavir, nelfinavir, ritonavir, tipranavir, atazanavir, indinavir, lopinavir, fosamprenavir and Darunavir. These mimic the peptide linkage that interacts with viral protease catalytic site and deactivate protease irreversibly (Lv, 2015).

(v) Integrase (IN) inhibitors

Many IN inhibitors have been reported in last 30 years. However, not many have advanced to clinical trials. First IN inhibitor approved was raltegravir, approved in 2007. Later on, elvitegravir and dolutegravir were also approved (Wang, 2011; Johns, 2013). These will be discussed later in chapter 2.

Highly Active Anti-Retroviral Therapy (HAART)

Highly Active Antiretroviral Therapy (HAART) is a triple cocktail of two N- or NtRTIs and one NNRTI or PI or IN inhibitor. It suppresses viral replication via reducing the patient's total burden of HIV, maintaining function of immune system and preventing opportunistic infections. Antiretroviral combination therapy

defends against resistance by suppressing HIV replication as much as possible, thus reducing the potential pool of spontaneous resistance mutations (Arts, 2012).

HAART, although efficiently diminishes viral load, is unable to eliminate the virus completely. Furthermore, HAART is a multi-drug therapy, which leads increased pill load, toxic side effects and affects pharmacokinetic properties of respective other drugs (Brunton, 2011; Peterson, 2013).

1.3 HIV Integrase

1.3.1 Integrase as a target in anti-HIV drug development

HIV-1 Integrase has been recognized as an attractive target for treatment of HIV because of following reasons:

1. *In vitro* inhibition of IN demonstrated significant reduction of integrated provirus in host cell DNA.
2. No human analog of this enzyme is present making it highly selective and low toxic.
3. Reduction in viral load was observed in human clinical trials by use of specific integrase inhibitors.
4. Presently there are only three IN inhibitors approved, so there is lot of scope for further research.
5. Generally, inhibition of integration of viral DNA is exciting as a valid biological target because this can be seen as a point of no return.

However, multiple DNA-protein interactions in pre-integration complex (PIC) occur and it may obstruct inhibitors from reaching the catalytically active sites (Ingale, 2011).

1.3.2 Integrase Structure

HIV-1 integrase is a 288 amino acid containing protein, encoded by the pol gene. It is folded into three distinct functional or canonical domains viz. zinc binding N-terminal domain (NTD) (residues 1-50), central/ catalytic core domain (CCD) (residues 50-212) and non-specific DNA binding C-terminal domain (CTD) (residues 212-288), associated by flexible linkers, as shown in Figure 3. The NTD contains a His-His-Cys-Cys (HHCC) zinc-finger motif, which is vastly conserved in retroviruses and retrotransposases. Coordination of this zinc-finger motif with a Zn^{2+} ion stabilizes protein folding and multimerization, which is necessary for normal enzymatic activity. The catalytic core domain consists of residues of three-amino acid Asp-64, Asp-116 and Glu-152 (DDE motif), which is highly conserved in all integrases (INs) and is supposed to form a coordination complex with two Mg^{2+} ions (Mg1001 and Mg 1002) and viral DNA. Mutation of any of these three acidic residues abolishes enzymatic activities of IN and viral replication. The CTD is the least conserved, and exhibits some structural homology with SH_3 DNA binding domains. This lysine-rich positively charged domain has nonspecific but strong DNA binding function (Wadhwa, 2017).

Earlier *in vitro* studies reported that monomeric form of IN is inactive. Later, NTD, CCD, and CTD were isolated as dimers which catalyze 3'-end processing and integration of one viral DNA end (Chen, 2000). In further studies, tetrameric IN was extracted from human cells expressing HIV-1 IN. Structural modeling studies have confirmed that tetrameric form catalyzes the insertion of two viral DNA ends into target DNA (Faure, 2005).

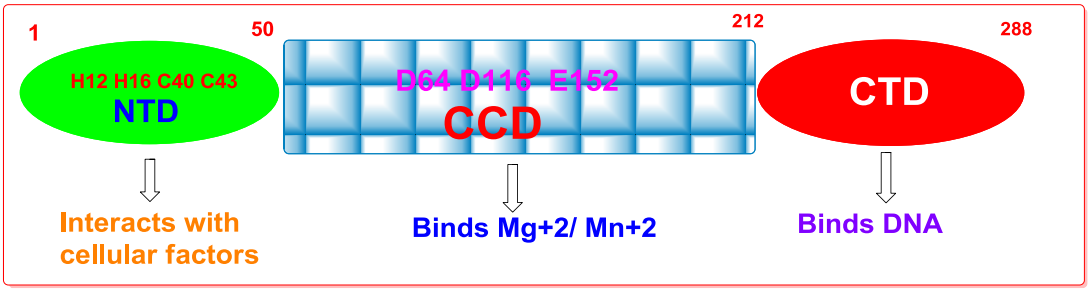

Figure 3: Structure of HIV-1 Integrase

1.3.3 Integrase Mechanism

After action of RT enzyme on viral RNA in the host cytoplasm, integrase binds with two conserved sequences 5'-GCAGT-3' of the viral ds-DNA long terminal repeats (LTR). Preintegration complex (PIC) is an intracellular nucleoprotein particle partly made of integrase-HIV DNA complex. PIC complex consists of linear HIV DNA, host proteins and viral proteins such as integrase, nucleocapsid, matrix, viral protein R (Vpr), and reverse transcriptase. Although several host proteins are parts of this complex, their role as well as their joining (some or all) before nuclear transport is not clear.

IN catalyzes two metal dependent reactions viz. 3'-end processing (3P) and strand transfer (ST). In 3P, IN binds with long terminal repeat (LTR) at the end of viral DNA resulting in endonucleolytic cleavage of two conserved nucleotides from 3' end (Johns, 2013). Chemically, this reaction takes place in cytoplasm as part of pre-integration complex (PIC), which leads to nucleophilic activation of a water molecule by Mg^{2+} ion (coordinated with Glu152 and Asp64). Further, the activated water molecule subsequently attacks phosphodiester bond of viral DNA to generate free 3'-OH ends. Later, HIV IN catalyzes second reaction called strand transfer (also known as 3'-end joining reaction). It occurs simultaneously at both ends of the viral DNA, involves dynamic transportation of activated PIC into nucleus where it works as a substrate for integration of viral DNA into host/nuclear DNA. Chemically, strand transfer reaction involves a second nucleophilic attack by 3'-end product to cellular DNA. Finally, host enzymes remove the two mismatched nucleotides at each 5'- end of viral DNA followed by filling in single stranded gaps and ligating the remaining ends (Maertens, 2010; Ribeiro, 2012).

Two divalent ions, Mg^{2+} or Mn^{2+}, are required for both 3P and ST, as shown in Figure 4. It is also assumed that the 3P processes conformational change in HIV-1 IN that permits host chromosome to bind and allows successive ST to take place (Johns, 2013). It is also reported that there are two separate cavities named cavity 3P and cavity ST, which are perpendicular to each other. The first cavity ST covers the area of the flexible loop (Phe 139–Ile 151, part of α-4 helix) and pocket is made up of hydrophilic amino acids Gln146, Ser147, Gln148 and hydrophobic amino acids Ile141, Pro142, Tyr143, Pro145, Val150. The cavity 3P is made of amino acids Asp64, Cys65, Thr66, His67, Glu92, Asp116 and Asn120. Here, Asp64 and Asp116 could chelate with Mg^{2+}, which is important for 3'-processing activity (Dayam, 2004).

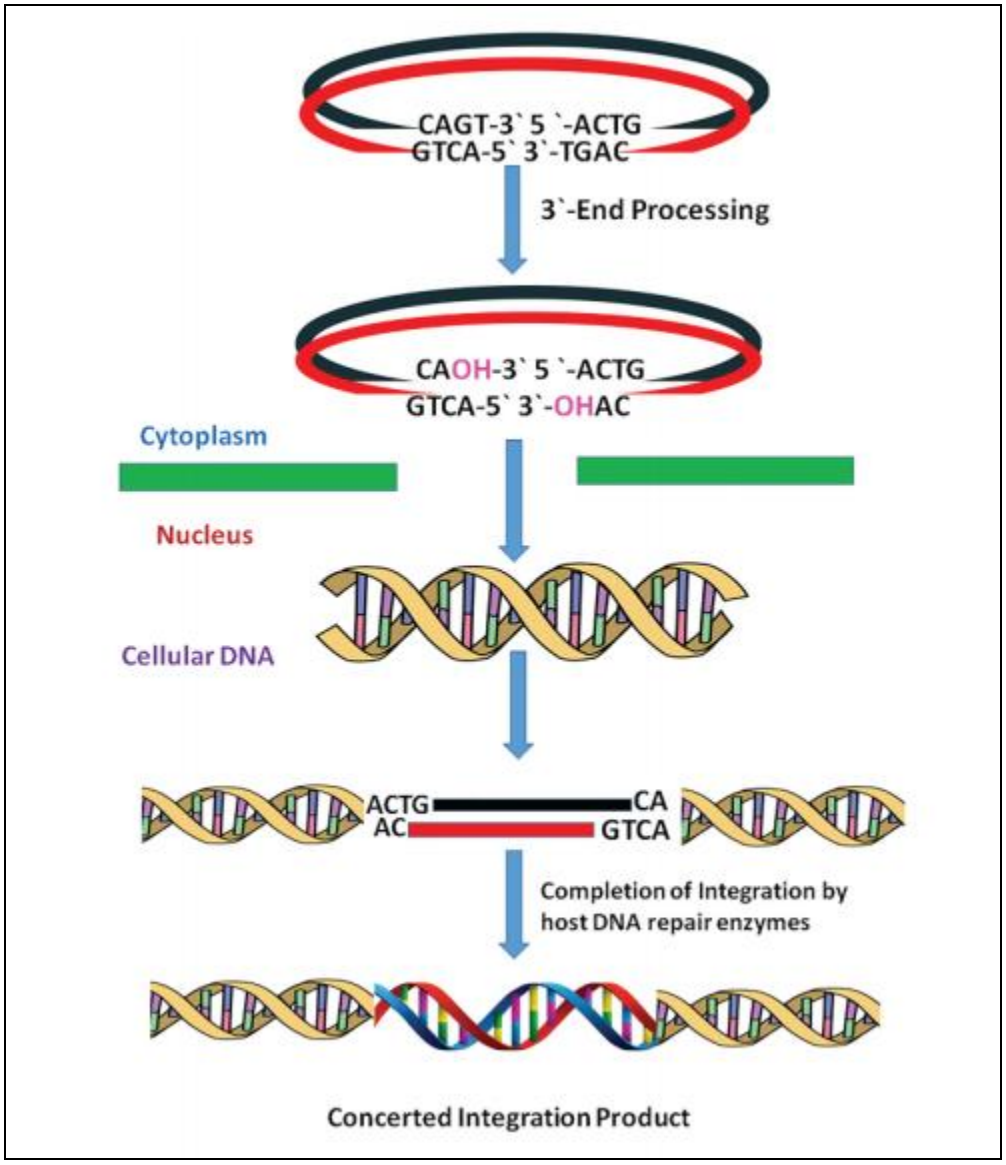

Figure 4: Catalytic activities of HIV-1 integrase (Wadhwa, 2017).

CHAPTER 2: REVIEW OF LITERATURE

Compared to other classes of anti-HIV drugs such as NRTIs, NNRTIs and PIs, the development of integrase inhibitors has taken a long time and has been particularly rigorous. The reasons behind slow development were: nonexistence of specificity in initial identification assays, lack of a standard and absence of a full-length protein crystal structure (Nowotny, 2009).

During last 20 years of research, large numbers of IN inhibitors have been discovered. However, only few have advanced to clinical trials and only three, raltegravir, elvitegravir and dolutegravir have been approved for clinical use. HIV integration occurs in two well-characterized catalytic steps and inhibitors are categorized on the basis of selectively inhibiting the 3P end processing stage, second class that inhibits both 3P and Strand transfer (ST), and third class that selectively inhibits the ST catalytic step. As a result, many scientists' use substrate-based drug design methodology and high-throughput screening methods to explore chemical or natural product libraries (Li, 2015). In general, for ST inhibition, two hydrogen bond acceptor groups and one aromatic ring are considered essential. In literature, different scaffolds such as arylamides, aurintricarboxylic acids, catechols, curcumin derivatives, diarylsulfones, depsides, flavones, integrinic acid derivatives, lignanolides, nucleotides analogs, styrylquinoline derivatives, salicylhydrazides, tyrphostins, thiazolothiazepines, triazine derivatives, tetracyclines and naturally extracted derivatives have been reported as HIV IN inhibitors (Wadhwa, 2017). Some of these are discussed below:

2.1 Diketo compounds or Diketo acids

The β-diketo acids and their related compounds represent most important and explored class HIV IN inhibitors wherein β-diketo acid is present on different hetercyclic scaffolds (Li, 2015; Hajimahdi, 2016). Hazuda *et al.* screened almost 250,000 samples and found that two compounds L-731988 (compound **1**) and L-708906 (compound **2**) show selective strand transfer inhibition with an IC_{50} of 0.17 and 0.10 μM, respectively. Their results concluded that diketo acid functionality is an intrinsic feature of integrase inhibitors (Hazuda, 2000). Further reports screened compounds having either heterocyclic ring on L-731988 diketo acid (compound **3**) or monobenzyl analogue of L-708906 (compound **4)** without loss of activity (Wai, 2002; Costi 2003; Yoshinaga 2003; Pais, 2002).

Costi *et al.* evaluated series of 6-aryl-2,4-dioxo-5-hexenoic acids, quinolinonyl diketo acids, 1-benzyl-pyrrolyl diketohexenoic derivatives. Their results showed that few of these compounds (**5-6**) exhibit significant inhibition of HIV IN catalyzed 3P and ST steps at nano molar range (Costi, 2004; Santo, 2008; Costi, 2013; Costi, 2014).

Zhang *et al.*reported that compounds bearing the azido and nitrilomethano groups were found to elicit potent inhibition of IN at non-cytotoxic concentrations. The compound **7** gave IC_{50} of 2.0 μM in extracellular IN assays. But its isomeric 3,4-di-(azidomethyl) analogue **8** was approximately 10-fold more potent (Zhang, 2003).

Sechi *et al.* performed molecular modelling studies on a series of substituted indole-β-diketo acids and concluded that compounds with free acid adopted different bound conformations than the esters. Their studies showed that two compounds **9-10** showed moderate inhibitory effects on HIV-1 IN (Sechi, 2004). Same group further designed a series of 5-aryl (heteroaryl)-isoxazole-3-carboxylic acids as bioisosteric analogues of β-diketo acid by identifying several pharmacophoric fragments and incorporated them on various aromatic or heteroaromatic rings. Their result showed that cyano keto acid (compound **11**) was most potent with an IC_{50} of 10.0 μM (Sechi, 2005). Walker *et al.* reported triketoacid-based derivatives (compound **12**) having moderate activities that were weaker as compared to molecules containing diketo acids (Walker, 2006).

Long *et al.* evaluated dimeric β-diketoacids interconnected *via* diverse type of linkers such as piperazine, diamines and reported that most showed significant inhibition of ST with IC_{50} in range of 0.2-2.7 μM. They reported that decrease in intrinsic selectivity was observed by increasing the length of linear chain from two carbons to six carbons. Further, it was also found that benzyl-linked bis-phenyl diketoacids (compound **13-14**) exhibits potent inhibition of IN (Long, 2004).

Li *et al.* reported that carbazol-1-one containing diketo acid analogues (compound **15**) showed better activity as compared to carbazol-4-one diketo acid analogues at IC_{50} value of 10 μM (Li, 2006). Same group further reported that both- diketo acid analogues of delavirdine as well as 1-[(2-hydroxyethoxy) methyl]-6-(phenylthio) thymine - had significatory inhibitory effects on HIV-1 IN and RT (Wang, 2008; Wang, 2010).

Nair *et al.*evaluated β-diketo acids with purine nucleobase scaffolds and reported that Compound **16** showed significant inhibition of ST (Nair, 2006). Same group also prepared phosphonic acid analogues of β-diketo acids as ST inhibitors (Chi, 2007). Patil *et al.* reported that lipophilic phenanthrene diketo acids exhibited potent inhibition of ST with an IC_{50} ranging from 2.7–0.38 μM (Patil, 2007). Kawasuji *et al.* explored 2-hydroxy-3-heteroarylic acrylic acid derivatives (HHAAs) having hydrophilic domain at one side followed by the hydrophobic substituent as the hydrophobic domain on other side for inhibition of integrase. Two compounds **17-18** showed significant inhibitory activity against ST step at nano molar range (Kawasuji, 2006; Kawasuji, 2012). Zeng *et al.* synthesized a set of aryl diketo acids and dimers and

two compounds (**19-20**) were found to possess significant inhibition of ST process (IC_{50} 0.4 & 0.6 µM, respectively) (Zeng, 2008).

Vandurm and co-authors evaluated quinolonyl diketo acids and its derivatives, bearing various substituents at position 6 of the quinolone scaffold and three compounds (**21-23**) were found to exhibited significant inhibition of both 3P and ST reactions (Vandurm, 2009; Vandurm, 2011).

Sharma *et al.* evaluated series of 3-keto salicylic acid chalcones of which two compounds (**24-25**) showed inhibition of ST step. Further, same group reported that halogen-substituted phenanthrene β-diketo acid derivatives (compound **26**) showed activity at IC_{50} value 1.3 µM (Sharma, 2011; Sharma, 2013). Serafin *et al.* prepared series of ethyl malonate amides (EMA) with terminal free acid group. They found that compound **27** exhibits significant inhibition of ST (Serafin, 2011).

Hu *et al.*evaluated β-diketo derivatives which combined the characteristics of 1,3-diketo, 1,2,3-triazole and polyhydroxylated aromatic moieties of which compound **28** was most active (IC_{50} 2.6 µM). Further, they evaluated a series of aromatic diketo derivatives and calix[4]arene based β-diketo analogues. Their results showed that compound **29** showed significant inhibition of ST (Hu, 2012; Hu, 2015; Luo, 2015).

Although it has been reported that the cytotoxicity and probably hepatotoxicity of HIV IN inhibitors is the result of α-diketo or diketo acid functionality (Hajimahdi *et al.* 2013), it still remains a favoured structure due to its success rate. Structures of some of representative compounds is given in figure 5.

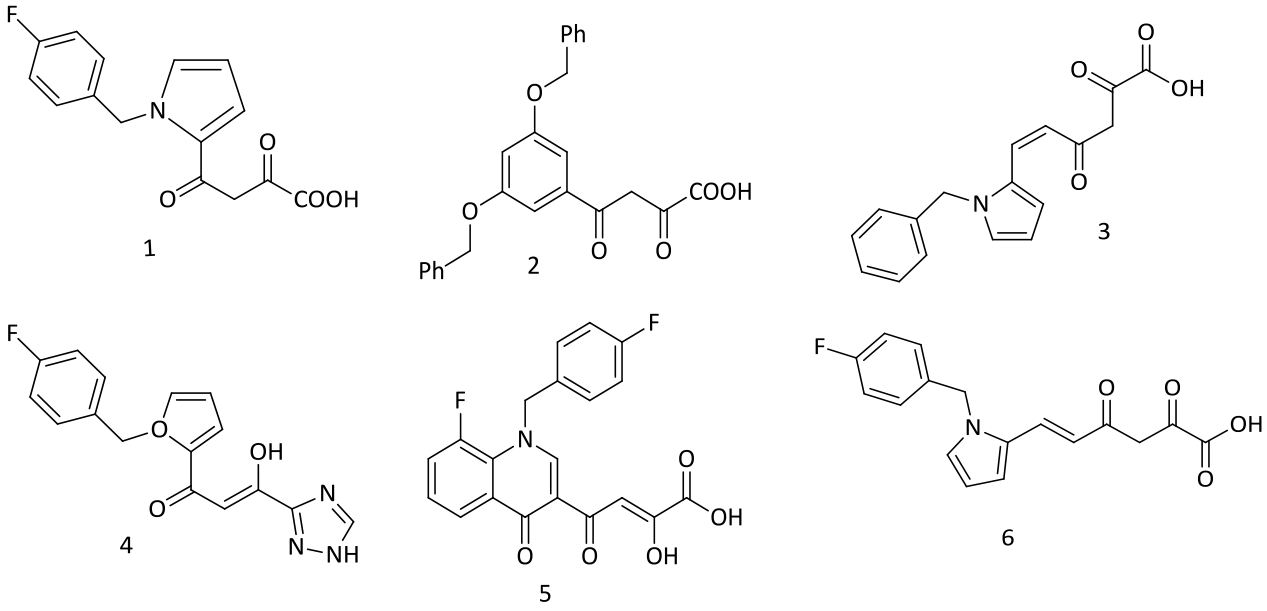

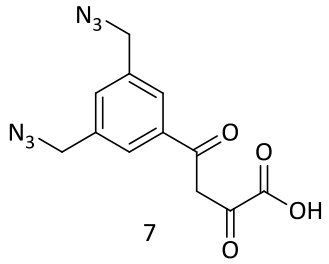

7

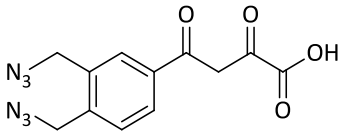

8

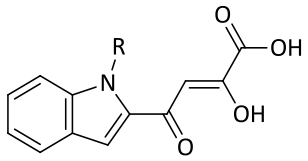

9= R= $-C_2H_5$

10= R=- CH_2-Ph

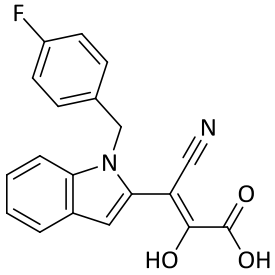

11

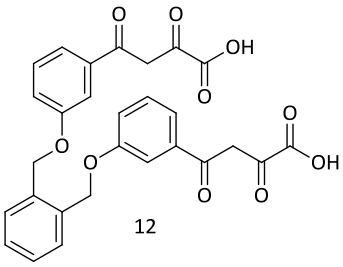

12

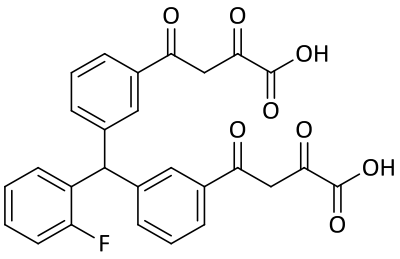

13

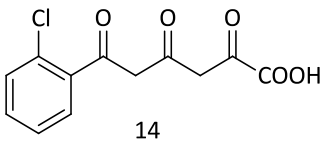

14

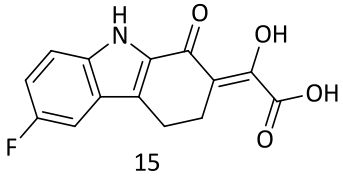

15

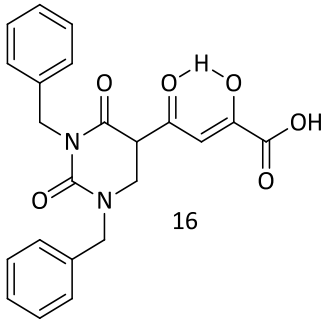

16

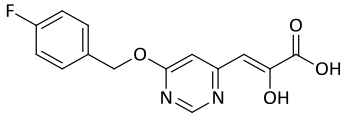

17

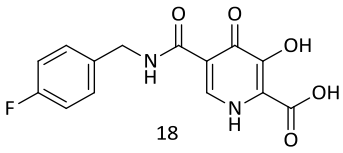

18

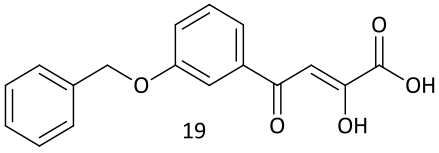

19

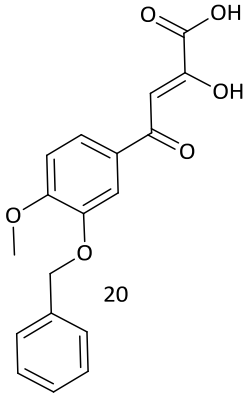

20

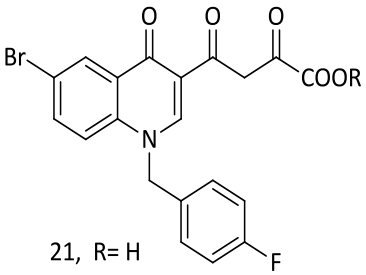

21, R= H

22,. R= Et

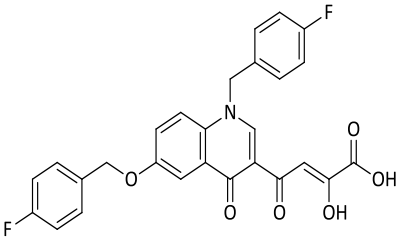

23

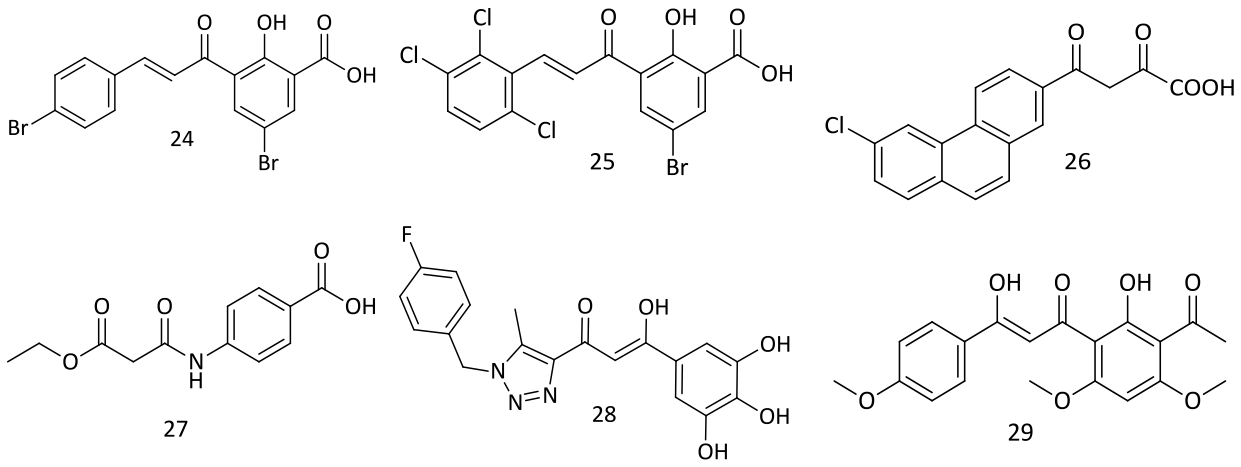

Figure 5: Reported diketo derivatives as HIV-1 IN inhibitors

2.2 Indole derivatives

Goldgur *et al.* reported crystal structure of a complex of HIV-1 integrase core domain with its inhibitor, 5-ClTEP, 1-(5-chloroindol-3-yl)-3-hydroxy-3-(2H-tetrazol-5-yl)-propenone (compound **30**) having 2.1 Å resolution. 5-ClTEP binds with catalytic residues Asp-64, Asp-116, and Glu-152 and inhibits enzyme activity with IC_{50} of 2.3µM (Goldgur, 1999). Ferro *et al.* evaluated a series of 4-[(1-Benzyl-1H-indol-3-yl)carbonyl]-3-hydroxyfuran-2(5*H*)-ones derivatives and found that compound **31** exhibits activity with an IC_{50} of 4.0 µM. They further developed pharmacophore model and concluded that compound **32** exhibits anti-integrase activity with an IC_{50} value of 0.03 µM. Same group evaluated the 1*H*-benzylindole derivatives having fluorine substitution and observed that two compounds (**33, 34**) showed significant inhibition of ST reaction with IC_{50} of 0.012 & 0.02 µM (Ferro, 2007; Luca, 2008; Ferro, 2008). Later, same group evaluated series of chloro and fluorobenzylindole derivatives and found that compounds (**35, 36**) exhibit most promising activity with IC_{50} values of 0.03 & 0.06 µM, respectively. They also prepared small molecules containing indole moiety (example, compound **37**) for inhibition of the interaction between enzyme HIV-1 IN and nuclear protein lens epithelium growth factor LEDGF/p75 (Ferro, 2010; Luca, 2010). It was also observed that another analogue (compound **38**) of 1*H*-benzylindole derivatives inhibited *in vitro* ST step with IC_{50} value of 1.36 µM (Ferro, 2011). Same group further indicated that compound **39** exhibits best inhibition of integrase catalyzed ST reaction with IC_{50} value of 6.0 nM. Recently, they reported compound **40** to exhibit ST inhibition at IC_{50} value of 0.026µM (Luca, 2011 and Ferro, 2014).

Parallely, Xu *et al.* reported that N-aryl indole derivatives (compound **41**), showed anti-HIV-1 integrase activity (Xu, 2008) and Plewe *et al.* synthesised a set of azaindole carboxylic acids and azaindole

hydroxamic acids (compounds **42, 43)** with potent inhibition of ST reaction with IC_{50} values of 84 and 145 nM (Plewe, 2009; Tanis, 2010).

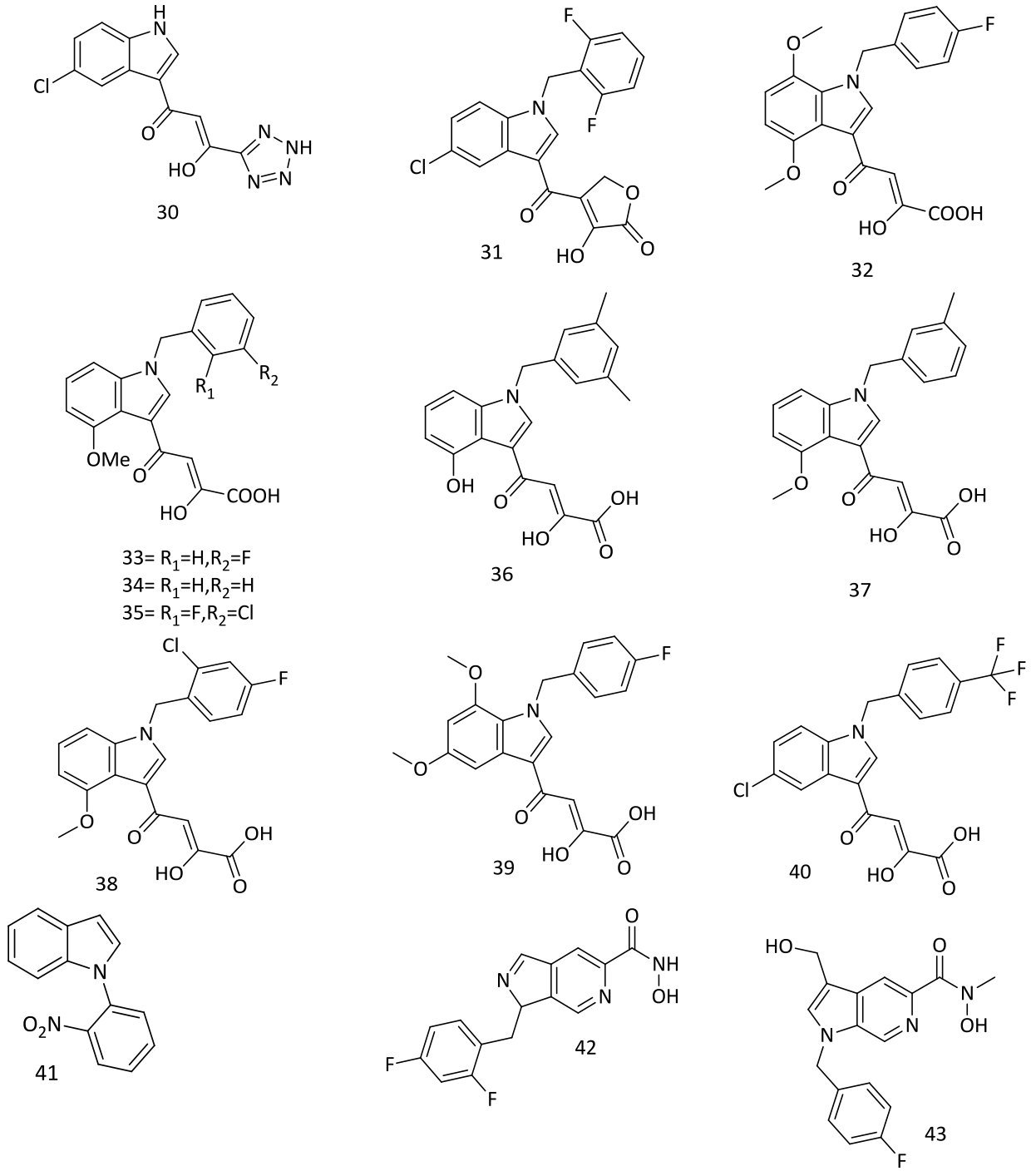

Figure 6: Representative indole derivatives as HIV-1 IN inhibitors

2.3 Sulphonamides and sulphur containing analogues

Xu *et al.* evaluated caffeoyl naphthalene sulfonamide derivatives and reported that substitution of *p*-fluoro group (compound **44)** in *N*-phenylsulfonamide derivative increased the HIV IN inhibitory activity while substitution of *p*-chloro and *p*-bromo groups decreased the inhibitory activity (Xu, 2003).

Brzozowski *et al.* designed benzodithiazines and later evaluated 4-chloro-*N*-(4-oxopyrimidin-2-yl)-2-mercapto benzene sulfonamide derivatives and found that compound **45** inhibits 3P and ST with an IC_{50} value of 6 & 4 µM. Further, another series of 3-aryl-2,3-dihydro-1,1-dioxo-1,4,2-benzodithiazines was evaluated and compound **46** was found to possess most promising inhibition of both 3P and ST steps with an IC_{50} value of 4.0 and 3.0 µM (Brzozowski, 2004; Brzozowski, 2008; Brzozowski, 2009).

Meadows *et al.* evaluated a series of neutral non-hydrolysable geminal disulfone derivatives of the chicoric acids. Their study reported that compound **47** inhibits HIV-1 IN at 0.3 µM. Same group further reported analogue of vinyl geminal disulfones (compound **48)** showing anti-IN activity (Meadows, 2005; Meadows, 2007).

Jin *et al.* reported that two compounds (**49, 50**) showed significant anti-integrase activity with an IC_{50} value of 28.0 & 13.0 nM, respectively. Same group further evaluated novel series of tricyclic HIV integrase inhibitors and compound **51** showed significant inhibition of ST with an IC_{50} of 5.0 nM (Jin, 2008; Jin, 2009).Muraglia *et al.* found that sulfamide compound **52** showed significant inhibition of ST with an IC_{50} of 7.0 µM (Muraglia, 2008).

Wang *et al.* reported series of compounds in which most active compound *N*-(4-(*N*-(4-butylphenyl)sulfamoyl)phenyl)-3,4,5-trihydroxybenzamide (**53**) showed significant activity against HIV-1 integrase catalysed 3P and ST steps with an IC_{50} value of 3.0 & 2.5 µM, respectively (Wang, 2009).

Jiao *et al.* evaluated a novel series of *N*-(5-Chloro-8-Hydroxy-2-Styrylquinolin-7-yl) benzene sulphonamide analogues (eg. Compound **54**) (Jiao, 2010). Zhao *et al.* investigated a series of 6,7-Dihydroxy-1-oxoisoindoline-4-sulfonamides and reported that compound **55** exhibited inhibition of IN catalysed 3P and ST steps with IC_{50} values of 6.8 and 0.047 µM, respectively (Zhao, 2012).

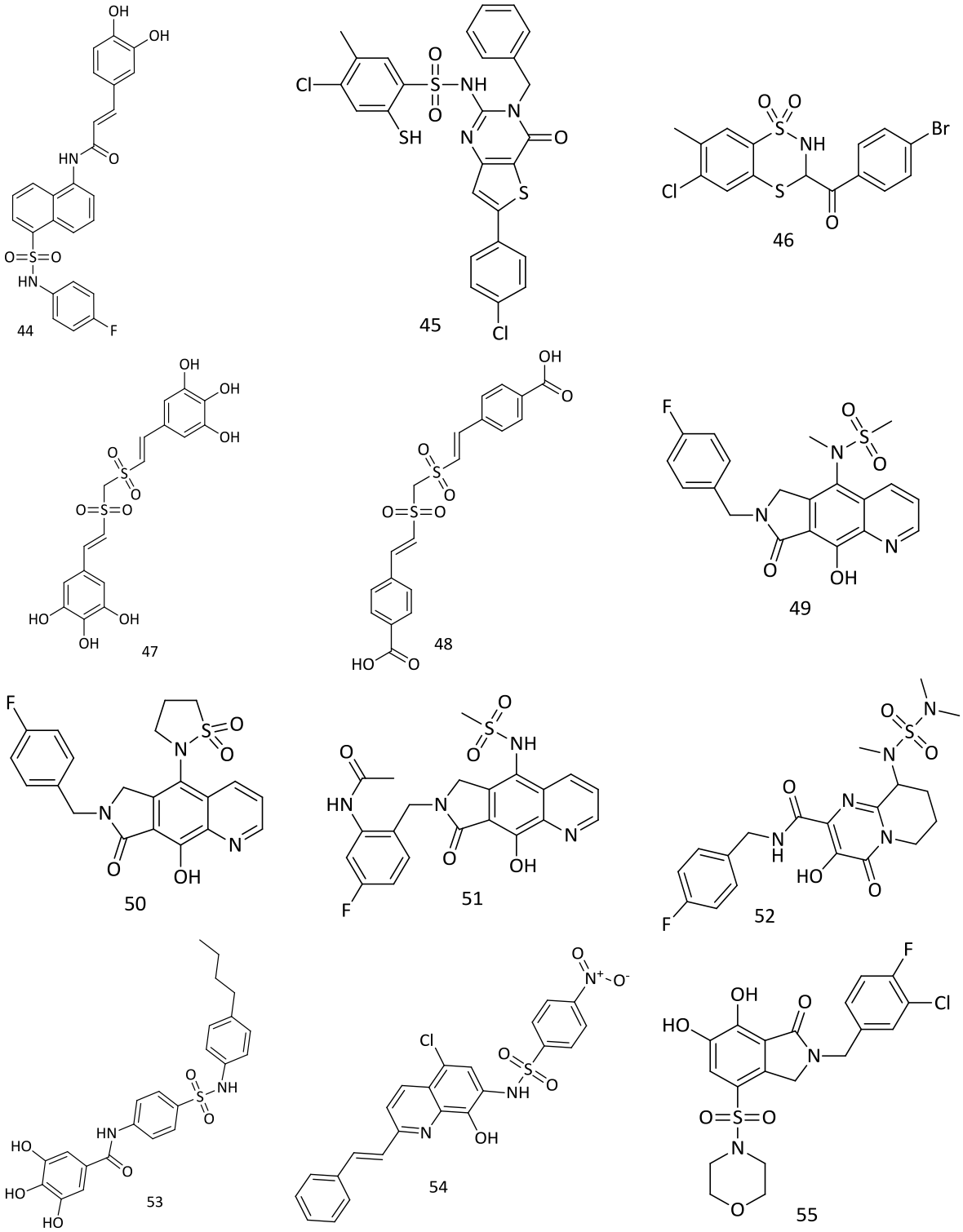

Figure 7: Some of the reported Sulphonamides and sulphur containing derivatives as HIV-1 IN inhibitors

2.4 Polyhydroxylated derivatives and salicylhydrazines

Neamati *et al.* evaluated forty-five analogues of salicylhydrazines derivatives and found that hydroxy group is essential for anti-integrase activity. Most of derivatives of this class having 2-hydroxyphenyl, the α-keto, and the hydrazine moieties in a planar conformation showed high potent activity with IC_{50} value of less than 3.0 μM *via* chelating metal in the integrase active site. Same group further reported that three novel mercapto salicylhydrazides (MSH, compounds **56-58**) derivatives inhibited 3P and ST reactions in the presence of $Mn^{2+}$with a range of IC_{50} 5.0-35.0 μM. They observed that MSHs inhibit IN in Mg^{2+} based assays by chelating and interacting with Mg^{2+} and cysteine 65 *via* disulphide bond formation on the active site of IN (Neamati, 1998; Neamati, 2002).

Artico *et al.* synthesized and evaluated cinnamoyl derivatives of caffeic acid phenethyl ester (CAPE) against HIV-1 IN. They observed that compound **59** showed submicromolar activity but its methylated product is devoid of activity. Further, it was also found that analogues of the cyclovalone compounds (compound **60**) inhibits 3P at IC_{50} 0.6 μM, when the bis-catechol moiety is preserved otherwise reduction in anti-integrase activity was observed. They hypothesized that for binding with IN, the residue C=C-C=O of cinnamoyl compounds should be in a *syn* disposition. This was also concluded that the distance between the catechol units and the nature of the central linker does not affect much but the presence of *o*-hydroxyls is necessary for anti-integrase activity. Same group further found that 3,5-Bis(3,4,5-trihydroxybenzylidene)-4-oxocyclohexaneacetic acid **61** inhibits both 3P and disintegration with IC_{50} values of 0.2 and 0.5 μM, respectively (Artico, 1998; Costi, 2004).

Dupont *et al.* reported that bis-catechols-1 **62** and bis-catechols-2 **63** exhibited promising inhibitory activity against ST reaction with an IC_{50} value of 1.3 μM and 2.1 μM respectively (Dupont, 2001).

Lee *et al.* evaluated different catechols substituted L-chicoric acid derivatives and observed that analogues having methyl substitution at *o*-position are devoid of activity. It was also observed that compound **64** having malic anhydride substitution showed significant potent activity with IC_{50} value of 3.8 μM. They also reported that catechol-substituted pyrrole-dicarboxylic acid **65** exhibited about 2-fold more potent inhibitory activity than L-chicoric acid (Lee, 2003).

Maurin *et al.* reported that catechol–DKA hybrids inhibits the 3P and ST reactions at inhibitory concentration ranging from 1.9-11.3 μM and 0.9-3.7 μM, respectively.They also evaluated a series of 4,5-diaryl-3-hydroxy-2(5*H*)-furanones and reported that compound **66** was found to be most potent with an IC_{50} of 1.0 μM. They further reported the synthesis of polyphenols analogues, which were structurally similar to isolated product of Salvia genus (isolated from *Salvia miltiorrhiza*). Their reports showed that during the synthesis of salvianolic acid E **67**, a side product rac-12 **68** (IC_{50} 0.30 μM) obtains,

which exhibit better anti-integrase activity compare to **67** (IC_{50} 0.73 µM). Further, Same group also reported that 2-aryl naphthalene diols and triol showed significance activity against both 3P and ST reactions with an IC_{50} value of 0.45 & 0.17 µM, respectively (Maurin, 2006; Bailly, 2008, Queffelec, 2008; Maurin, 2010).

Marchand *et al.* evaluated a new class of madurahydroxylactone derivatives and found that compound **69** showed most promising inhibition of HIV-1 IN with an IC_{50} of 0.41µM. Further, their group reported that compound **70** exhibit significant inhibition when Mn^{2+} is used as cofactor and compound **71** showed anti-integrase activity in the presence of cofactor Mg^{2+} (Marchand, 2008; Zhao, 2007).

Fan and co-authors evaluated a novel series by merging the pharmacophores of salicylate and catechol against the catalytic domain as well as its interaction with LEDGF/p75 of HIV-1 IN. Their results showed that compound **72** showed inhibition of ST with an IC_{50} value of 35.0 µM (Fan, 2011).

Pawar *et al.* reported that labdane analogs with *o*-quinol, catechol and hydroquinone moiety (compounds **73-75**) showed significant anti integrase activity with an IC_{50} value of 13.4, 11.1 and 11.5 µM, respectively (Pawar, 2014). Tupchiangmai *et al.* evaluated a series of substituted polyhydroxylated mono, bis and tris-cinnamoyl analogues and compound **76** showed significant inhibition of ST with an IC_{50} value of 3.5 µM (Tupchiangmai, 2014).

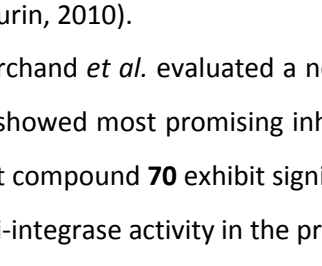

56

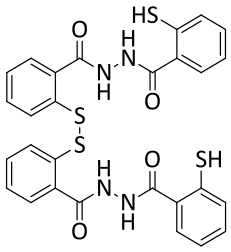

57

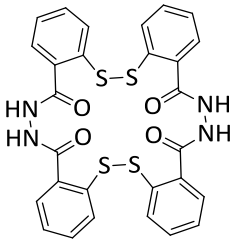

58

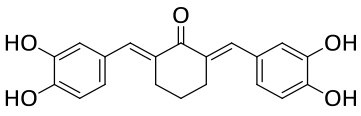

59

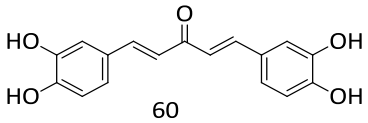

60

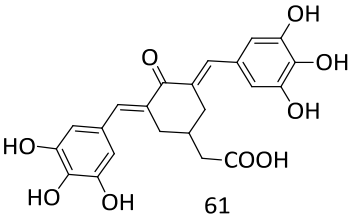

61

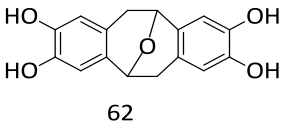

62

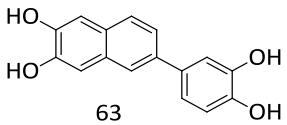

63

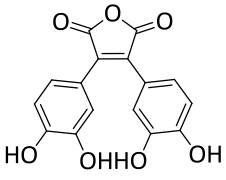

64

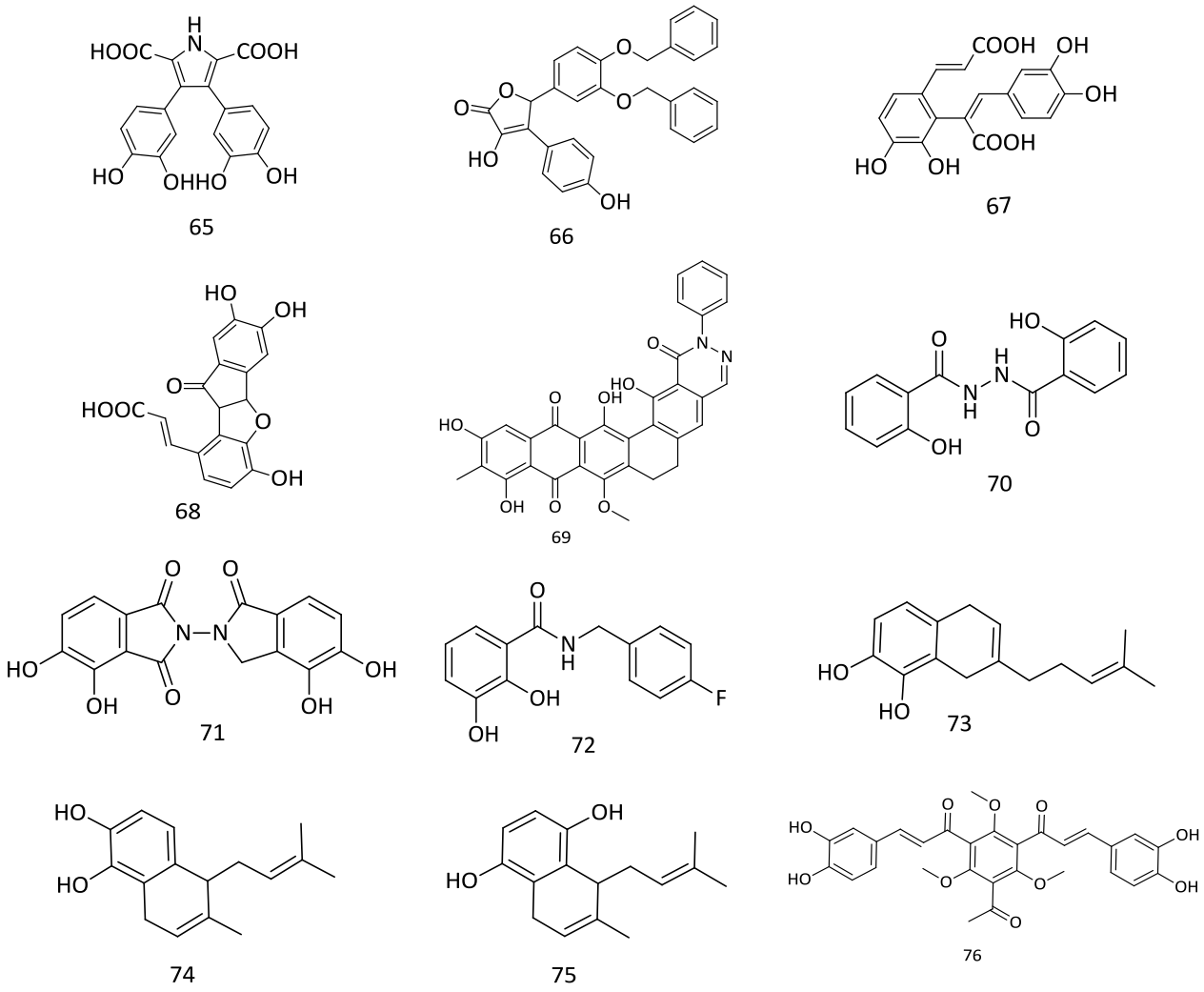

Figure 8: Reported Polyhydroxylated derivatives and salicylhydrazines as HIV-1 IN inhibitors

2.5 Amides and carboxamides

Ryabinin *et al.* reported that oligo-1,3-thiazolecarboxamide derivatives block IN activity with a IC_{50} range of 0.3-2.2 µM (Ryabinin, 2000). Benard *et al.* synthesised a series containing quinoline subunit and an ancillary aromatic ring linked by functionalized spacers such as amide, hydrazide, urea and 1-hydroxyprop-1-en-3-one moiety. Their results showed that molecules (**77-79**) had significant anti-integrase activity with IC_{50} values from 1.5 µM to 6.5 µM in *in-vitro* 3P activity and 2-4 µM in Ex vivo methods (Bénard, 2004).

Embrey *et al.* evaluated a series of 5-(dihydrouracil or uracil) substituted 8-hydroxy-[1,6]naphthyridine-7-carboxylic acid 4-fluorobenzylamides analogues. They reported that compound **80** inhibits the ST with

an IC_{50} of 33.4 nM. Further, they found that a novel orally active HIV-1 integrase inhibitor L-900564 (compound **81**) showed most promising anti-integrase activity at IC_{50} of 10.0 nM with good pharmacokinetic profile. Same group members also reported that compound **82** showed significant activity with an IC_{50} of 0.10 µM against ST process (Embrey, 2005; Egbertson, 2007; Wai, 2007). Further, Guare *et al.* extended the work and reported that compound **83** showes remarkable increase in potency against strand transfer process with an IC_{50} of 25.0 nM (Guare, 2006).

Kehlenbeck *et al.* evaluated dihydroxythiophenes carboxamides (compounds **84, 85**) showing selective inhibition of IN with IC_{50} in nanomoles (Kehlenbeck, 2006). Boros *et al.* reported 7-hydroxythiazolo-pyridin-6-carboxamide analogues. Later, they reported novel naphthyridinone GSK364735 (**86**) having ST inhibition at IC_{50} value of 7.8 nM. Recently, a N1 acetamide substituted naphthyridinone derivative (compound **87**) with IC_{50} of 3.0 nM against ST was reported (Boros, 2006; Garvey, 2008 and Johns, 2014).

Walker *et al.* evaluated anilide-ketoacids and benzyl amide-ketoacids potent activity as also a series of pyrrolidinedione analogs (eg. compound **88**) (Walker, 2006; Walker, 2007; Pendri, 233). Later, Naidu *et al.* reported that several C2-linked heterocyclic pyrimidinone-4-carboxamides (compounds **89, 90**) have significant activity with IC_{50} value upto 3.0 nM (Naidu, 2015). Petrocchi *et al.* reported that three dihydroxypyrimidine carboxamides were found to possess significant inhibition of IN. Their reports concluded that two compounds **91** and **92** showed significant anti-integrase activity with an IC_{50} 0.05 µM and 3.0 nM in the cell-based assay (Summa 2006; Petrocchi, 2007; Pace, 2007; Petrocchi, 2009).

Tang *et al.* prepared a series of dihydroxypyrimidine (DHP) derivatives and found that compound **93** showed better inhibition with an IC_{50} of 2.6 µM. Jones *et al.* reported bicyclic pyrimidinone core analogues also showed potent anti-integrase activity (Tang, 2010; Jones, 2010).

In literature, 3-Hydroxy-1,5-dihydro-pyrrol-2-one (HDPO), substituted 4-oxo-4,5,6,7-tetra hydropyrazolo[1,5-a]pyrazine-2-carboxamide and *N*-Methyl pyrimidine-4-carboxamide (compounds **94, 95**) derivatives have been given to chelate with Mg^{2+} ions of IN active site and exhibit significant ST inhibitory activity at nano molar range (Kawasuji, 2007; Langford, 2008; Gardelli, 2007; Francesco, 2008; Nizi, 2009; Donghi, 2009; Ferrara, 2010; Yu, 2013).

Billamboz *et al.* investigated a series of 2-Hydroxyisoquinoline-1,3 (2*H*,4*H*)-diones as a dual inhibitors of HIV-1 IN and RT RNase H domain. Their results showed that two analogues (compounds **96, 97**), had significant anti-integrase activity with IC_{50} values of 0.09 & 0.13 µM, respectively (Billamboz, 2008). Zhao *et al.* evaluated dihydroquinoline-3-carboxamides, naphthyridine-3-carboxamides and found that compound **98** exhibit significant inhibition of ST step at IC_{50} 0.14 µM (Zhao, 2014). Further, Zhang *et al.*

reported that one analogue (compound **99**) of series of 5-hydroxy-6-oxo-1,6-dihydropyrimidine-4-carboxamides inhibits both 3P & ST with an IC_{50} value of 11.0 & 0.5 µM, respectively (Zhang, 2014).

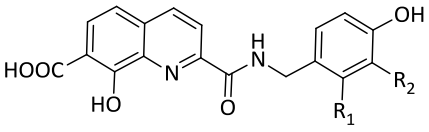

77= R_1, R_2= OH
78= R_1=H, R_2= OH

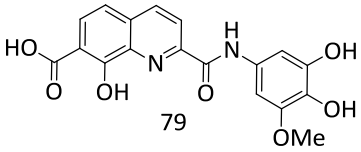

79

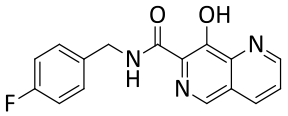

80

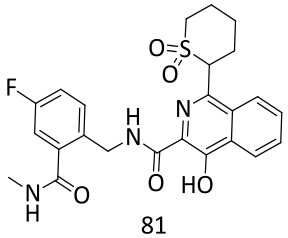

81

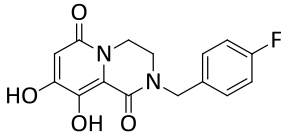

82

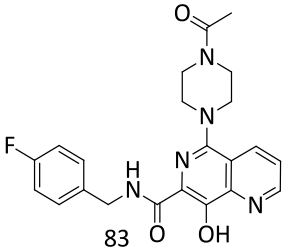

83

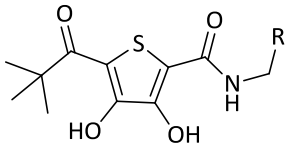

84= R=Benzyl
85= R=Phenyl

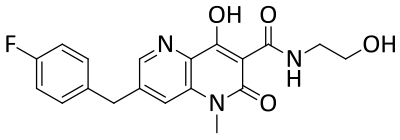

86

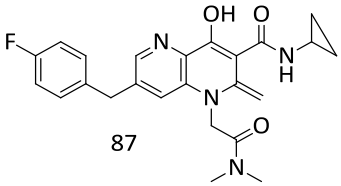

87

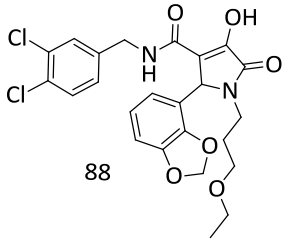

88

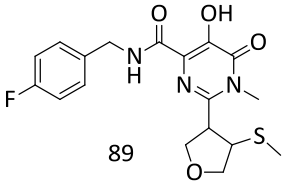

89

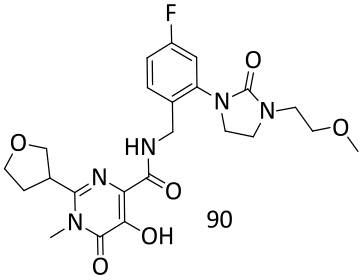

90

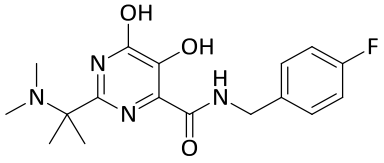

91

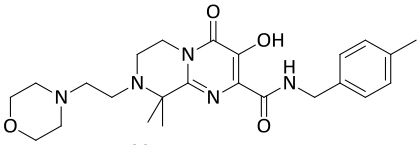

92

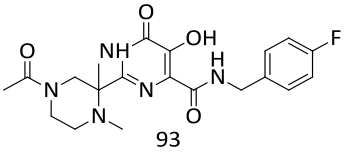

93

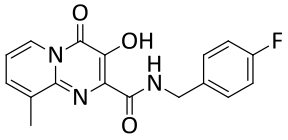

94

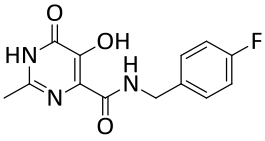

95

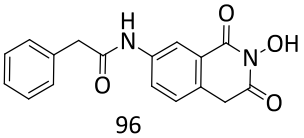

96

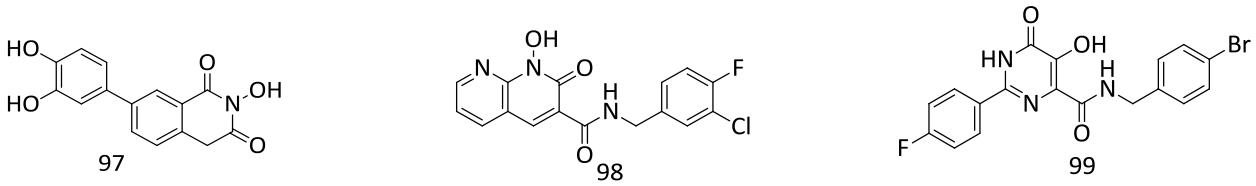

Figure 9: Literature reported amides and carboxamides as HIV-1 IN inhibitors

2.6 Quinoline and its structural analogues

Quinoline is considered a privileged structure as several quinoline derivatives have been used in treatment of various diseases. Therefore, lot of work has been done on quinolines and its structural analogues as anti-HIV. Lee and co-authors prepared different analogues of styrylquinazoline by Perkin condensation of 2-methylquinazoline and various aromatic aldehydes. Most of them showed potent inhibitory activity against 3P of IN (Lee, 2002).

Sato *et al.* synthesised a novel HIV-1 IN inhibitor JTK-303 (GS-9137) by modifying quinolone antibiotic Ciprofloxacin. Compound **100** (JTK-303 or GS9137) having the coplanarity of diketo acid functional groups showed significant inhibition of ST process with an IC_{50} of 7.2 nM. This compound later became known as Elvitegravir. They also modified the N-1 substitution and compounds **101** showed significant inhibition of HIV-1 IN catalyzed ST with an IC_{50} value of 5.6 and 5.8 nM, respectively (Sato, 2006; Sato, 2009).

Santo *et al.* designed and synthesized a series of novel bifunctional quinolonyl diketo acid derivatives. Compound **102** having *p*-fluorobenzyl substitution was the most potent derivative, which binds with both DNA acceptor and donor site of HIV-1 IN, and thus inhibits ST with IC_{50} value of 15 nM. The group further reported that even monofunctional diketo acids such as compound **103** also exhibit anti-integrase activity (Di Santo, 2006; Di Santo, 2008).

Fardis *et al.* reported that spirocyclopropyl analogue having *p*-fluoro benzyl substitution on pyrrol nitrogen (compound **104**) showed HIV-1 IN inhibition at IC_{50} of 7.0 nm. Same group members further modified the substitution pattern and reported that C-3 halobenzyl substituted tricyclic pyrroloquinolines derivative (for example compound **105)** was found to possess good inhibitory activity with an IC_{50} of 14.0 nM. They further also reported another series of similar compounds of which, compound **106** showed significant inhibition of HIV-1 IN with an IC_{50} of 50 nM *via* chelating with Mg^{2+} ions in catalytic core of enzyme (Fardis, 2006; Metobo, 2006; Metobo, 2009).

Pasquini *et al.* designed a set of 4-quinolone-3-carboxylic acids, structurally related to elvitegravir as potent inhibitors of HIV-1 IN. In the study, compound **107** possesses significant inhibition with an IC_{50} of 0.2 µM by chelating the metal ion between E326 and D97. Further, dihydroquinoline-3-carboxylic acids

have also been screened against HIV-1 IN. Compound **108** bearing *p*-fluorobenzyl substitution at C-6 and methyl group on N1 was found to possess significant IN inhibitory activity with an IC_{50} of 0.9 µM. It was also reported that fluorine group exhibits positive influence on inhibitory activity (Pasquini, 2008; Sechi, 2009).

He and co-authors took the clue from work of Sato, *et al*. and synthesized and evaluated a novel series of 5-hydroxylquinolone-3-carboxylic acids (HQCAs) with various aryl or benzyl substituents on N-1 position against HIV-1 integrase. It was found that compound **109** having *N*-benzyl substitution possessed significant activity against wild-type HIV-1 and HIV-1 mutant virus A17 with an EC_{50} value of 3.17 and 17.88 µM, respectively (He, 2011).

Nagasawa *et al*. evaluated new analogues of 6-benzylamino 4-oxo-1, 4-dihydro-1, 8-naphthyridines and 4-oxo-1, 4-dihydroquinolines against HIV-1 integrase. Two compounds (**110, 111**) were found to possess better inhibition of ST with an EC_{50} value of 9.9 and 7.6 nM, respectively (Nagasawa, 2011).

Billamboz *et al.* prepared a set of 2-hydroxyisoquinoline-1,3(2*H*,4*H*)-diones of which, compound **112** is reported to be most active. Using computational studies, it was shown that the phenylpropyl side chain of compound **113** perfectly occupies active site of IN. This compound inhibits *in vitro* integrase activity with an IC_{50} of 2.6 µM. Further, the authors report that magnesium complex of 2-hydroxyisoquinoline-1,3(2*H*,4*H*)-dione, Compound **114**, was found to inhibit overall IN as well as ST reaction of IN with an IC_{50} value of 4.11 & 2.89 µM, respectively (Billamboz, 2011 and Billamboz, 2011).

Wang *et al.* reported a novel class of 5-hydroxyquinazolinones as potent HIV-1 IN inhibitors. Compound **115** showed 77.5 % inhibition rate at 10 µM against HIV-1 IN (Wang, 2012).

Suchaud *et al.* reported series of 2-hydroxyisoquinoline-1,3(2*H*,4*H*)-diones (HIDs) as potent HIV-1 IN inhibitors. All analogues showed anti-integrase activity at submicromolar range. Four Compounds (**116-118**) were found to possess overall anti-integrase activity at IC_{50} value of 0.010 µM (Suchaud, 2014).

Recently, Tandon and his group reported the new class of 1,2-dihydroisoquinolines having different functionality at the C-1, C-3, C-7 and N-2 positions. The synthesized derivatives also revealed strong interaction with both the active site magnesium ions *via* chelation. Compounds (**119, 120**) were found to be potent integrase inhibitors in *in vitro* strand transfer (ST) assay, with IC_{50} value of 0.7 and 0.8 µM, respectively (Tandon,2015).

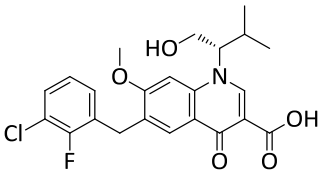

100

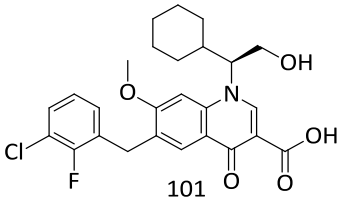

101

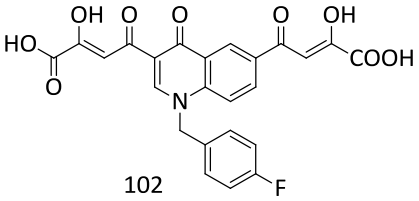

102

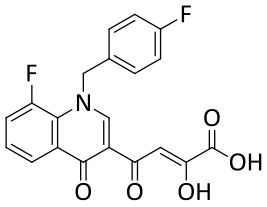

103

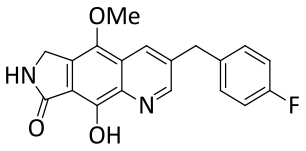

104

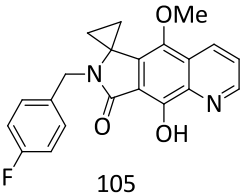

105

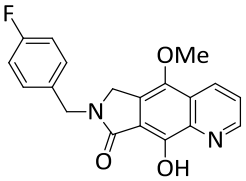

106

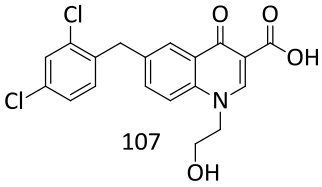

107

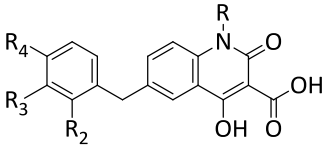

108= R=Methyl, R_2, R_3=H, R_4= F
109= R=Benzyl, R_2=F, R_3=Cl, R_4= H

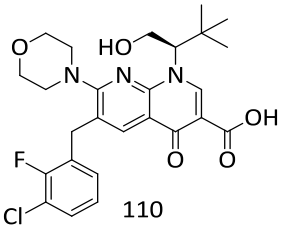

110

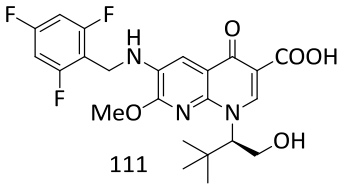

111

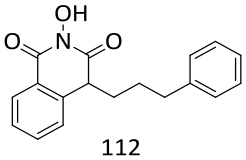

112

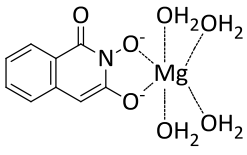

113

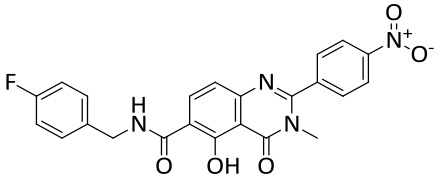

114

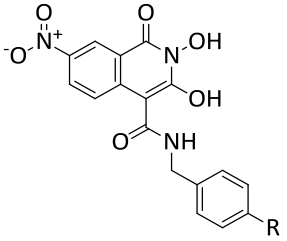

115, R = H
116, R = F
117, R = OMe

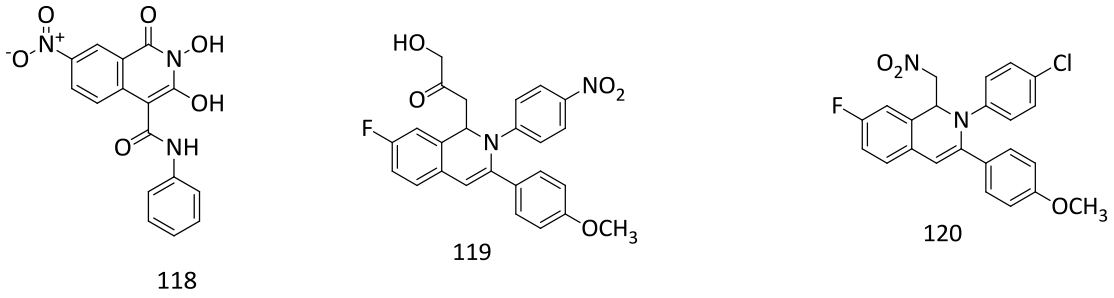

118 119 120

Figure 10: Reported quinoline and its structural analogues as HIV-1 IN inhibitors

2.7 Coumarin and their analogues

In an effort to derive new inhibitors, replacing nitrogen in quinolones by oxygen, certain coumarin based analogues having HIV integrase inhibitory potency have been reported by various groups.

Mao *et al.* explored the pharmacophore (compound **121**) as HIV IN inhibitor and synthesized modified coumarin dimers. They divided these synthesized analogues into two categories based on aryl-substitution attached to either benzoyloxy or sulfonyloxy linker. Authors found that these compounds exhibited potent inhibitory activity against HIV IN with IC_{50} value in the range of 0.5-3.9 µM (Mao, 2002).

Su and co-workers further modified these biscoumarins to have free and modified hydroxyl substituents at benzoyloxyphenyl linker. They found that 3,3-[4-(3,4-Dihydroxybenzoyloxy) benzylidene] bis-4-hydroxycoumarin **122** and its acetate analogue **123** inhibit integration of viral cDNA with an IC_{50} of 1.5 and 1.9 µM, respectively. Chiang *et al.* further modified these compounds and synthesized compounds **124-126**, which exhibit significant anti-integrase activity at IC_{50} values of 0.96, 0.58, and 0.49 µM, respectively (Su, 2006; Chiang, 2007).

Bailly *et al.* reported two caffeoyl-coumarin conjugates against HIV-1 integrase in Mg^{2+}-dependent 3'-end processing reaction. Both compounds (**127-128**) were found to exhibit HIV-1 IN inhibitory potencies at 2.0 and 1.0 µM, respectively (Bailly, 2005).

Li *et al.* synthesized and evaluated a series of mono substituted flavonoids, of which most active compound **129** showed inhibition of 3P and ST with an IC_{50} value of 20 and 4.0 µM, respectively (Li, 2014).

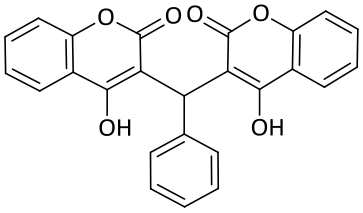

121

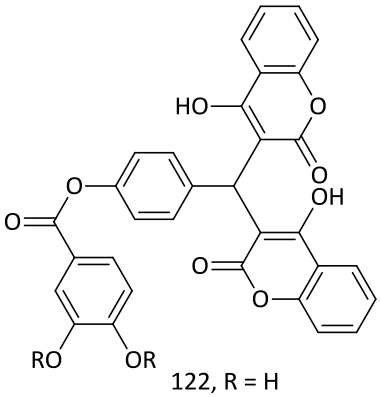

122, R = H
123, R =-$COCH_3$

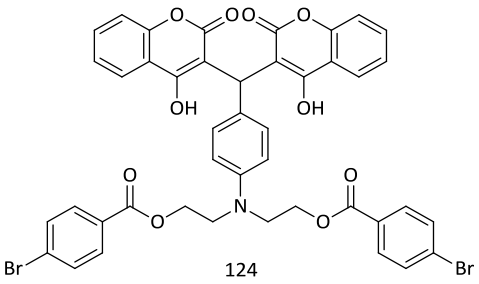

124

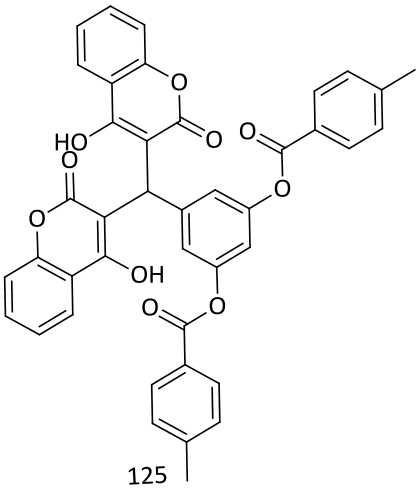

125

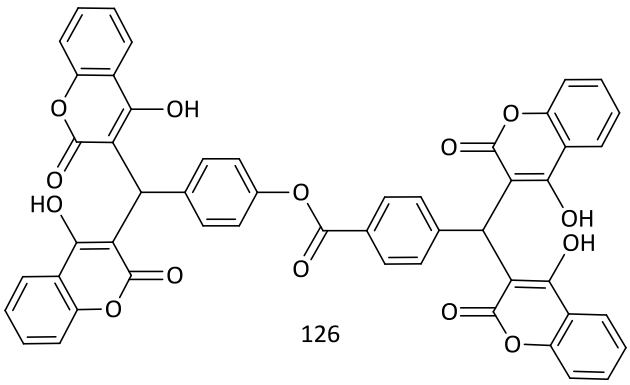

126

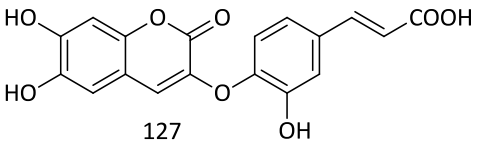

127

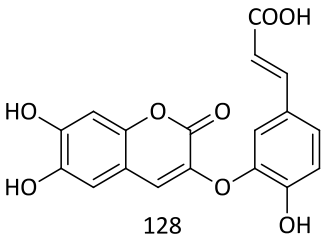

128

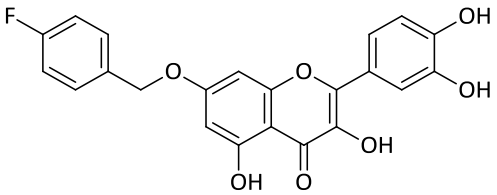

129

Figure 11: Literature reported coumarin and their analogues as HIV-1 IN inhibitors

2.8 Miscellaneous analogues

Zhuang *et al.* prepared a set of designed 8-hydroxy-[1,6]naphthyridine derivatives and investigated them for the inhibition of the integration of double-stranded viral DNA into the host cell's genomic DNA. Compound **130** is reported to inhibit the ST with an IC_{50} of 10.0 nM and it also inhibits 95 % spread of HIV-1 infection in cell culture at 0.39 µM (Zhang, 2003).

Middleton and co-workers reported the anti-integrase activity of naphthamidines and 2-aminobenzimidazoles in cell culture. Among the tested compounds, compound **131**, a 2-aminobenzimidazole, inhibited HIV-1 IN at IC_{50} 1.8 µM (Middleton, 2004).

Verschueren and co-authors reported the design and synthesis of novel series of phthalimide analogues. It was proposed using molecular docking studies, that presence of a single carbonyl-hydroxy-aromatic nitrogen motif was necessary for the enzymatic activity. They found that compound **132** inhibited HIV-1 IN enzyme with an IC_{50} value of 112 nM (Verschueren, 2005).

Jin *et al.* reported new tricyclic succinimide analogues using molecular modelling studies of already reported quinoline derivatives. Of these, two compounds (**133, 134**) showed good anti IN activity with an IC_{50} of 0.08 and 0.05 µM, respectively (Jin, 2006).

Mugnaini and co-authors developed a three-dimensional ligand-based pharmacophoric model and evaluated a new series of (*E*)-3-(5-(2-(1H-benzo[d]imidazol-2-yl)-2-cyanovinyl) furan-2-yl) benzoic acid analogues. Their results showed that only one compound **135** having nitro group in the *meta* position of the phenyl ring exhibited significant activity with an IC_{50} value of 12 µM (Mugnaini, 2007).

Fisher *et al.* evaluated a series of 8-Hydroxy-3,4-dihydropyrrolo[1,2-a]pyrazine-1(2*H*)-one analogues and reported that compound **136** was found to be most potent inhibitor with an IC_{50} of 0.01 µM and CIC_{95} of 0.31 µM against ST step and replication of HIV-1 in cell culture, respectively. Same group later modified these pyrazino-pyrrolopyrazine integrase inhibitors by changing one of the pyrazinone rings to a pyridazinone, which resulted the improved chemical properties such that stable alkali metal salts. Compound **137** showed significant inhibition with an IC_{50} value of 10 nM. Further, structure–activity studies indicated that high antiviral potency against wild-type virus as well as viruses containing integrase mutations was achieved by incorporating small aliphatic groups at certain positions on the core template (Fisher, 2007; Wiscount, 2008).

Zeng *et al.* evaluated novel phenyl-substituted isoxazole- or 1*H*-pyrazole-3-carboxylic acids by conversion of the biologically labile 1,3-diketo unit. They reported that compound **138**, which is a hydroxamate derivative of 5-phenylisoxazole-3-carboxylic acid, displayed significant inhibition of ST process with an IC_{50} value of 27.0 µM (Zeng, 2008).

Johns *et al.* evaluated a series of HIV-1 integrase inhibitors consisting of the 8-hydroxy-1,6-naphthyridine core and either an oxadiazole or triazole ring system. The revealed that 4-fluoro derivative with oxadiazole ring system (compound **139**) showed most promising anti ST activity with an IC_{50} of 0.042 µM as compared to unsubstituted benzyl group *via* two-metal coordination(John, 2009).

Zhao and their group investigated the effect of halogen substitution on benzyl ring of 4,5-dihydroxy-1*H*-isoindole-1,3(2*H*)-dione and reported that four compounds (**140-143**) having different halogen substituents showed significant inhibition of IN catalyzed ST reaction in range of 0.1 - 0.7 µM. It was also observed that dihalo-substituted analogues have higher potency than monohalo-substituted compounds. Further, same group also evaluated effect of changing phenyl ring of isoindolinedione by synthesizing a series of tricyclic hydroxy-1*H*-pyrrolopyridine-trione analogues. In this series, they combined structural features of bicyclic pyrimidinones with 4,5-dihydroxy-1H-isoindole-1,3(2*H*)-diones. They also observed the effect of *N*-arylmethyl substituents on IN inhibitory potencies of hydroxy-pyrrolopyridine triones and found that compound **144** showed significant inhibition at IC_{50} of 6.0 µM. Same group later reported bicyclic hydroxy-1*H*-pyrrolopyridine-triones as a new family of HIV-1 IN inhibitors. Of these, compound **145** was found to be most potent against the three major raltegravir-resistant IN mutant enzymes, G140S/Q148H, Y143R, and N155H and showed low micromolar inhibitory potency (IC_{50} 6.4 µM) with selectivity for strand transfer reactions as compared with 3P inhibition (IC_{50}> 111 µM)(Zhao, 2009; Zhao, 2011; Zhao, 2012).

Johnson *et al.* synthesized orally bioavailable HIV-1 IN inhibitors belonging to novel tricyclic *N*-hydroxy-dihydronaphthyridinones class, which expresses excellent ligand and lipophilic efficiencies. They reported that compound **146** showed reasonable combination of cellular potency, clearance properties and most promising activity with an IC_{50} value of 8.8 nM (Johnson, 2011).

Tang *et al.* reported the structure-activity relationship (SAR), molecular modelling, and resistance profile of 3-hydroxypyrimidine-2,4-diones analogues. Molecular modelling studies showed that compound **147** fits perfectly into the IN binding site through two major binding domains such as the chelation of two Mg^{2+} ions and the placement of the 4-fluorobenzyl group into the protein-DNA interfacial hydrophobic pocket. Compound **147** was found to possess high potency against ST process with an IC_{50} value of 0.44 and 0.56 µM, respectively. Same group then modified the substitution pattern and further synthesized a series of analogues featuring benzoyl group at C-6 position of the pyrimidine ring and reported that compound **148** inhibits IN in low micromolar range (IC_{50} 4.1 µM). They further modified the substituents and reported that N-3 OH is essential for IN inhibition and that the benzyl group on N-1 side chain is

more important for IN binding than the one on C-6.It wasfound that compound **149** showed significant inhibition of IN catalyzed ST process with an IC_{50} value of 3.5 µM (Tang, 2011; Tang, 2011; Tang, 2010).

Ma and his group designed and synthesized eight analogues of 2-pyrrolinones from developed pharmacophore model. The overall study demonstrated that presence of a bulky hydrophobic group at the nitrogen atom seems to be important and the character of acyl-diketo can function as a selective ST inhibitor. Further, they reported that compound **150** having pyridinyl substitution showed good inhibition of HIV-1 IN catalysed 3P and ST reactions with an IC_{50} value of 77 and 40 µM, respectively. Further mapping analysis and docking studies affirmed these results (Ma, 2011).

Sanchez *et al.* evaluated a new series of acylhydrazones, hydrazines, and diazenes as potent inhibitor of human lens epithelium-derived growth factor (LEDGF)/p75-IN interaction and IN catalytic activity. Mechanistic studies revealed that most of the IN inhibitors chelate with magnesium ions in the catalytic active site. This region is topologically distant from the LEDGF/p75 binding site. Compound **151** having pyridine nitrogen at *ortho* position showed most significant activity against LEDGF/p75-IN (IC_{50} 1.3 µM), integrase catalyzed 3P (17 µM) and ST (13 µM) (Sanchez, 2013).

Billamboz *et al.* reported the synthesis and biological activity of a series of 2-hydroxy-1,3-dioxoisoquinoline-4-carboxamides featuring an *N*-hydroxyimide chelating functionality. The result of the study demonstratedthat substitution of the 2-hydroxyisoquinoline-1,3-dione scaffold at position 4 by carboxamido chains was found to be favourable for antiviral activity. Furthermore, two derivatives (**152, 153**) possessed remarkable inhibition of IN catalyzed 3P (IC_{50} value of 0.010 and 0.08 µM) and ST step (IC_{50} value of 0.110 and 0.03 µM) (Billamboz, 2013).

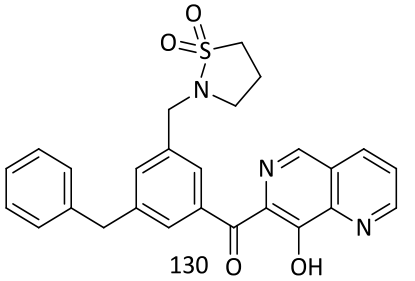

130

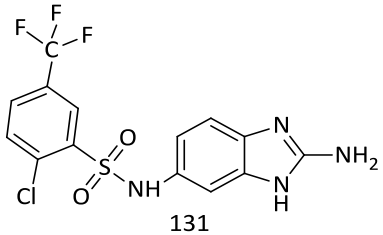

131

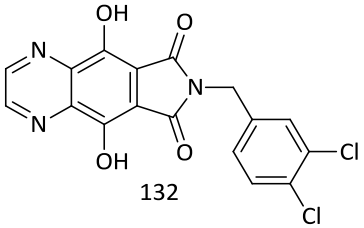

132

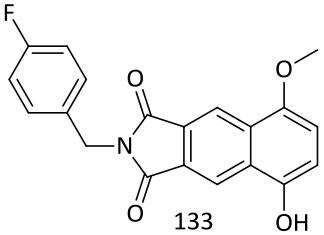

133 OH

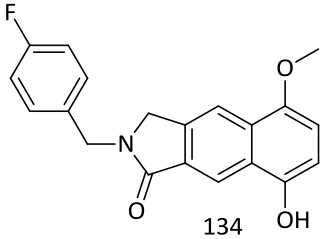

134 OH

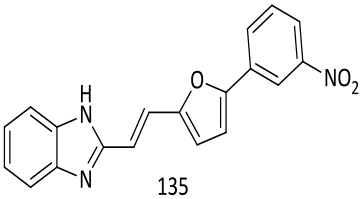

135

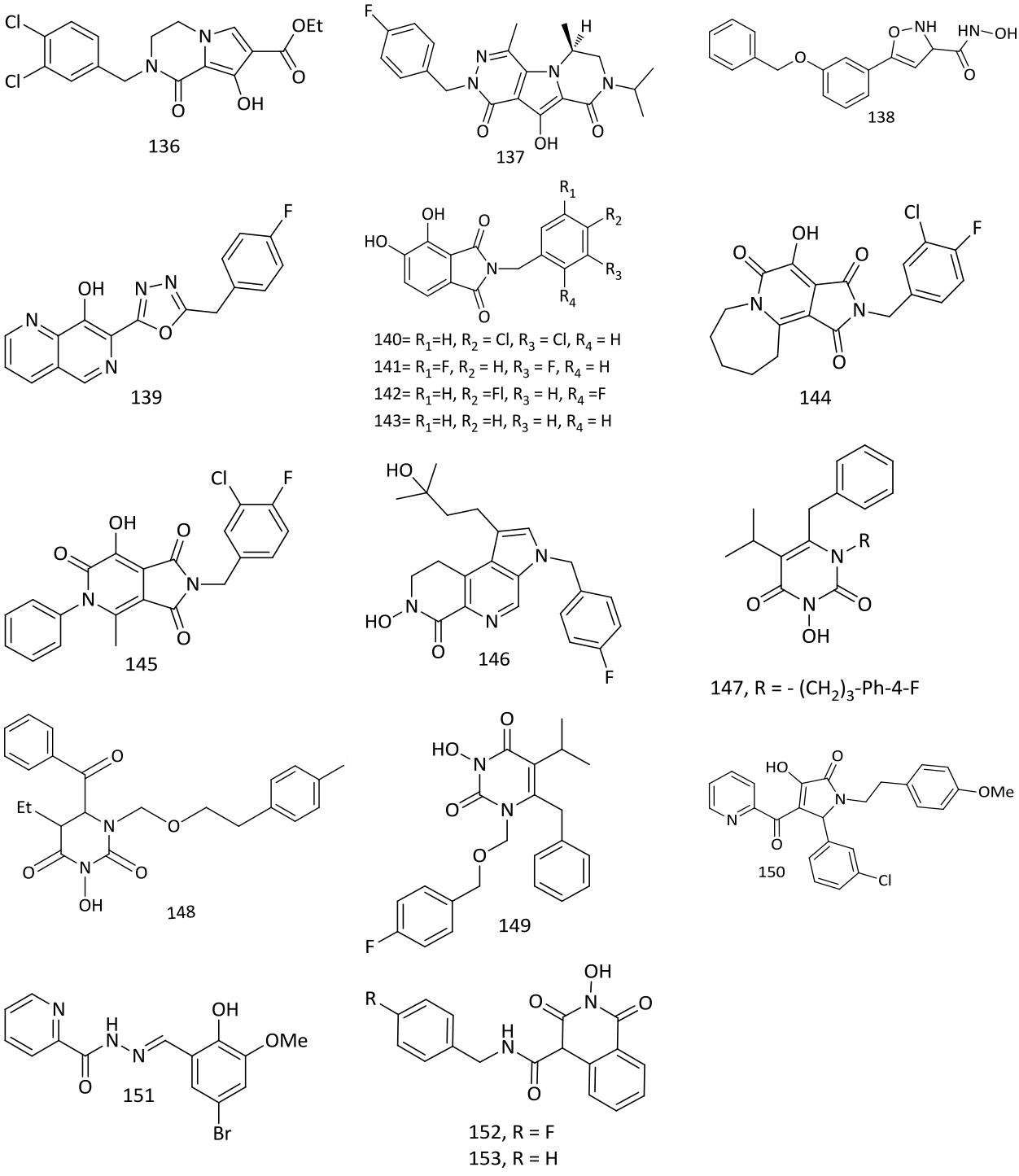

Figure 12: Some of the reported miscellaneous analogues as HIV-1 IN inhibitors

CHAPTER 3: AIM AND OBJECTIVES

3.1. Need for newer HIV-1 IN inhibitors

Although many compounds have been reported to inhibit integrase, only three drugs have been approved for clinical use so far. Raltegravir is used in combination with optimized background therapy while elvitegravir is used as first line treatment. Recently, dolutegravir has been approved by the U.S. FDA in 2013 and has gained European approval in January 2014. Second generation IN strand transfer inhibitors (INSTI) are being developed to find a treatment against viruses resistant to first generation inhibitors. Among this class, MK-2048, cabotegravir and bictegravir are new investigational drugs exhibiting strong antiviral activity as compared to Dolutegravir (Li, 2015; Hajimahdi, 2016).

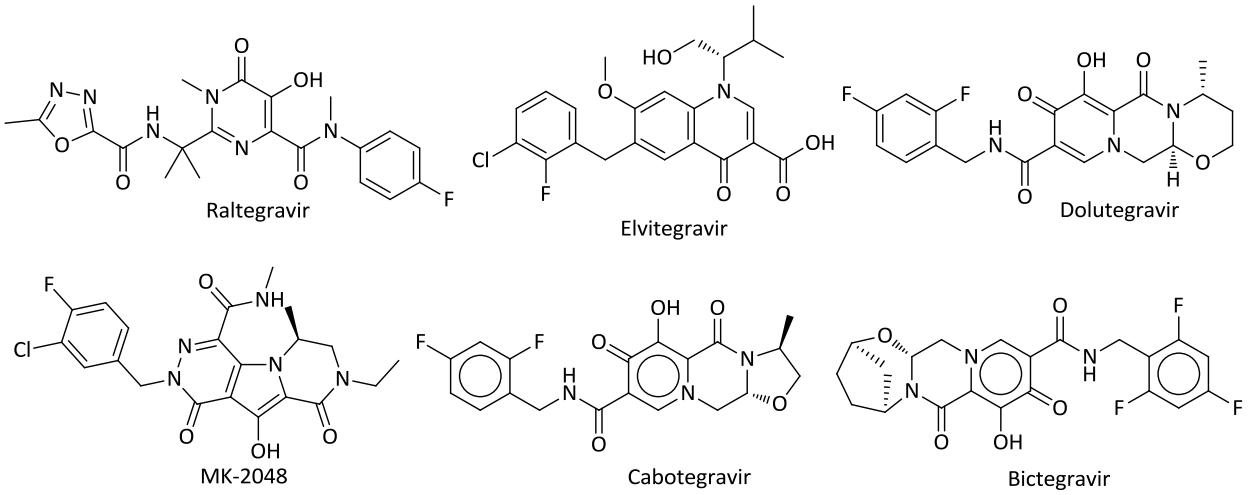

Figure 13: HIV integrase inhibitors in clinic and in clinical trials

Although triple therapy or highly active antiretroviral therapy (HAART) has improved the longevity of affected population, due to high mutation rate, rapid emergence of resistance is a serious concern. There is a need for development of new anti-HIV drugs to tackle the problems of resistance, toxicity and drug availability (Hajimahdi, 2016). Earlier reports are on focused libraries around the lead compounds, in which majority did not succeed due to several reasons that include structural complexity, poor biological activity, decreased drug susceptibility and resistance due to mutated catalytic core domain of IN. Considering these facts, the present thesis work was aimed to design, synthesize and evaluate HIV-1 IN inhibitors. It was envisioned to generate structurally different library of compounds so as to obtain few leads.

3.2 Objective of the study

The objective of the present work was to synthesize and evaluate structurally diverse library of anti-integrase compounds representing dissimilar scaffolds.

To achieve the aim, following steps were envisaged:

Step 1: Based on literature report and gap therein, synthesize few series of structurally diverse compounds by different synthetic methods followed by purification and characterization.

Step 2: To evaluate the HIV IN inhibition activity of synthesized compounds using the *in-vitro* assay, first at a single concentration and evaluate IC_{50} of few having good percent inhibition.

Step 3: Provide rationale for the *in vitro* activity by studying the *in silico* docking and derive *in silico-in vitro* correlation.

Step 4: Study the anti HIV effect of compounds in cell based assay.

CHAPTER 4: MATERIALS AND METHODS

Materials

Chemicals used in synthetic work were purchased from Spectrochem Pvt Ltd, Mumbai, SD Fine Chem Limited, Mumbai and Sigma Aldrich, Mumbai. All the solvents used were of analytical grade without further purification. Analytical TLC was carried out with plates precoated with silicagel 60 F_{254} (0.25 mm thick) by using mobile phase ethyl acetate and hexane in suitable portion. Melting points were determined in open capillary tubes on a Precision Buchi B530 (Flawil, Switzerland) apparatus containing silicon oil. The IR spectra of the synthesized compounds were recorded using FTIR spectrophotometer (Shimadzu IR Prestige 21, Shimadzu, Mumbai, India). ^{1}H NMR and ^{13}C NMR spectra were recorded on Bruker DPX-400 spectrometer (Bruker India Scientific Pvt. Ltd., Mumbai, India) using tetramethylsilane (TMS) as an internal standard (chemical shifts indicated in δ). ESI-MS were recorded on MICROMASS Quattro-II LCMS system (Waters Corporation, Milford, USA).

Methods

4.1 Docking Protocol

X-ray crystal structure of the HIV-1 IN-5CITEP complex (PDB ID: 1QS4) protein was downloaded from RCSB protein data bank and further adapted for Glide docking calculations (Goldgur, 1999). For Glide (Schrödinger 2013) calculations, HIV-1 IN complex was imported to Maestro (Schrödinger 2013), the co-crystallized ligands were identified and removed from the structure and non-bridge water molecules were also removed from the complex, and hydrogen atoms were added to the structure followed by assignment of Partial atomic charges according to the force field. Protein was minimized until the average root mean square deviation (RMSD) of the non-hydrogen atoms reached 0.3Å by applying OPLS-2005 force field to remove the steric hindrance using the protein preparation wizard of maestro. Grid file was generated by using prepared protein as an input file for docking simulation. The grid of active site was procreated at centroid of -17.27, 29.10, 66.61 on x, y, z-axis respectively using Maestro. Grid box dimension was set to 10, 10 and 10 Å along x, y and z directions respectively. Preparation of ligands was executed using “LigPrep” module of Schrodinger Suite 2013. Compounds were imported into the software’s workspace and energy minimized using two algorithms: steepest descent and conjugate gradient, of the Impact module having default options (Friesner, 2004). Poses with an RMSD of less than 0.5Å and a maximum atomic displacement of less than 1.3Å were removed as redundant in order to increase diversity in the retained ligand/compound poses. The application of LigPrep is to construct a particular, low-energy, 3D structure with accurate chirality for each successfully processed input

structure. LigPrep can also produce a number of structures from each input structure with numerous ionization states, tautomers, stereochemistries, and ring conformations. Chemaxon Marvin Sketch was used for drawing structures of all compounds and energy minimization was done by using OPLS_2005 Force Field of LigPrep of Maestro (http://www.chemaxon.com).

The ionization states in a given pH range of 7 ± 2 were produced by addition or deletion of protons from the ligand using EPIK 2.1 module. During docking simulation, using different modules of Schrödinger suite, potential of non-polar parts of ligands was softened by scaling Vander Waals radii of ligand atoms by 0.8 Å with partial charge cut-off of 0.15. During docking simulation, glide first places the Centre of ligand at various grid positions of a 1 Å grid and then by rotating ligand in all the Euler angles it generates various possible conformations which pass through a filter series composed of initial rough positioning followed by scoring phase. The docking simulation was performed by allowing flexible torsions in ligands with the use of XP mode.

All docking simulations were achieved by means of the Induced Fit Docking module of the Schrödinger suite. It executes flexible protein-ligand docking and examines for favorable interactions between one characteristically small ligand molecule and a typically bigger receptor molecule, usually protein. Docking procedure is classified into three different stages such as Initial Glide Docking, in which protein preparation constrained refinement is carried out with a maximum of 20 poses. Prime Induced Fit, which includes optimization of side chains and refinement of residues, takes place, if the ligand poses are within 5.0Å. Step 3 consists of the Glide redocking phase by applying Standard Precision (SP) or extra precision (XP) mode. After completion of each docking steps almost 20 poses per compound were generated. The best-docked structure/pose were selected on basis of Glide score (Gscore) function, Glide Energy and the number of residual matches (hydrogen bonds, hydrophobic interactions) with the original drug complex.

4.2 Selection and validation of docking protocol

The validation of docking protocol is crucial to manage the reliability and reproducibility of docking parameters used for study. The protocol was established using Schrodinger suite 2013. The chemical structure of ligand was drawn using Chemdraw ultra 11.0 and 3D energy minimized structures were obtained using LigPrep module of Schrodinger 2013. The docking study revealed that the docked ligand superimposed well on the reference ligand (co-crystallized ligand) with RMSD value of 0.28 Å (figure 14) and glide score of -7.8 with similar binding interactions with amin acids Thr 66, Lys 156, Lys 159 and DDE motif (Asp 64, Asp 116 and Glu 152).

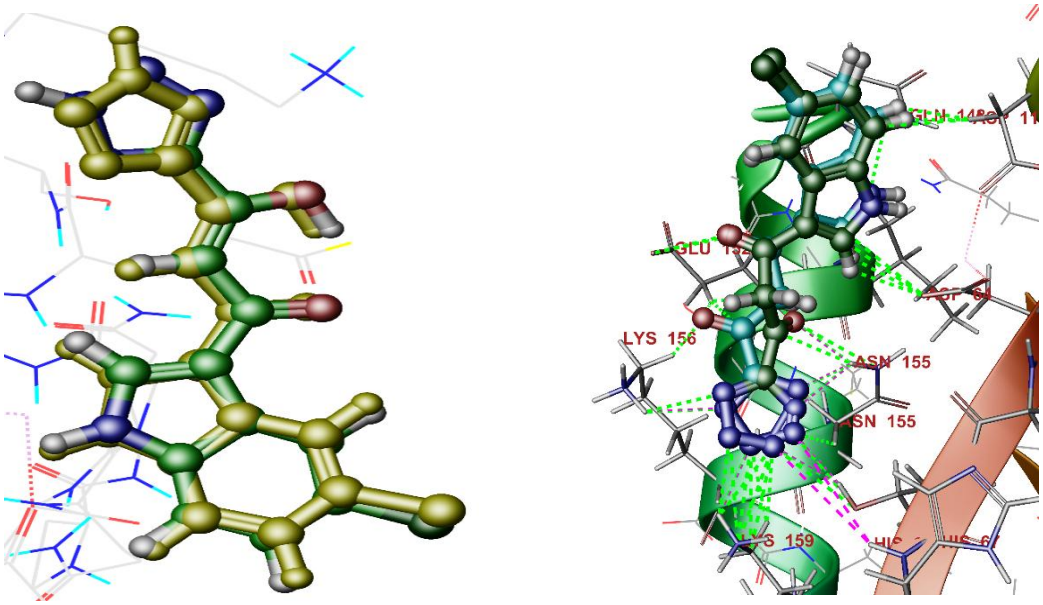

(A) (B)

Figure 14: Docking validation of 1QS4 (A) Redocked pose of 5ClTEP (blue) superimposed with the co-crystallized ligand (green); (B) Secondary view of docked ligand and co-crystallized ligand.

4.3 *In vitro* screening

For studying the HIV-1 integrase inhibitory potency of all the synthesized compounds, *in vitro* enzyme inhibition assay was done. The concentration used was 10 µM in duplicate using colorimetric assay method (Elisa kit supplied by XpressBio Life Science Products, USA). Dolutegravir was used as standard to compare the inhibitory potency of tested derivatives. From amongst designed compounds, those showing maximum inhibitory potential were also subjected to IC_{50} value determination (Debyser, 2001). HIV- 1 IN inhibition was analyzed according to manufacturer's procedure. The principle for IN inhibition is explained in figure 15. Streptavidin coated 96-well plates were coated with a double-stranded HIV-1 LTR U5 donor substrate (DS) oligonucleotide containing an end-labeled biotin. Full-length recombinant HIV-1 integrase protein was then loaded onto this oligo substrate. Compounds were added to the reaction at 10 µM concentration in duplicates and then a different double-stranded target substrate (TS) oligo containing 3'-end modifications was added to the plate. The HIV-1 integrase catalyzes 3P reaction by slicing the terminal two bases from the exposed 3'-end of the HIV-1 LTR DS and followed by a strand-transfer reaction (ST) to integrate the DS into the TS. The products of the reaction were detected colorimetrically using an HRP-labeled antibody directed against the TS 3'-end modification. The percentage inhibition of integrase activity was calculated by dividing the mean value in the presence of

the tested antiviral compound with that in the presence of the dolutegravir as a positive control in this experiment.

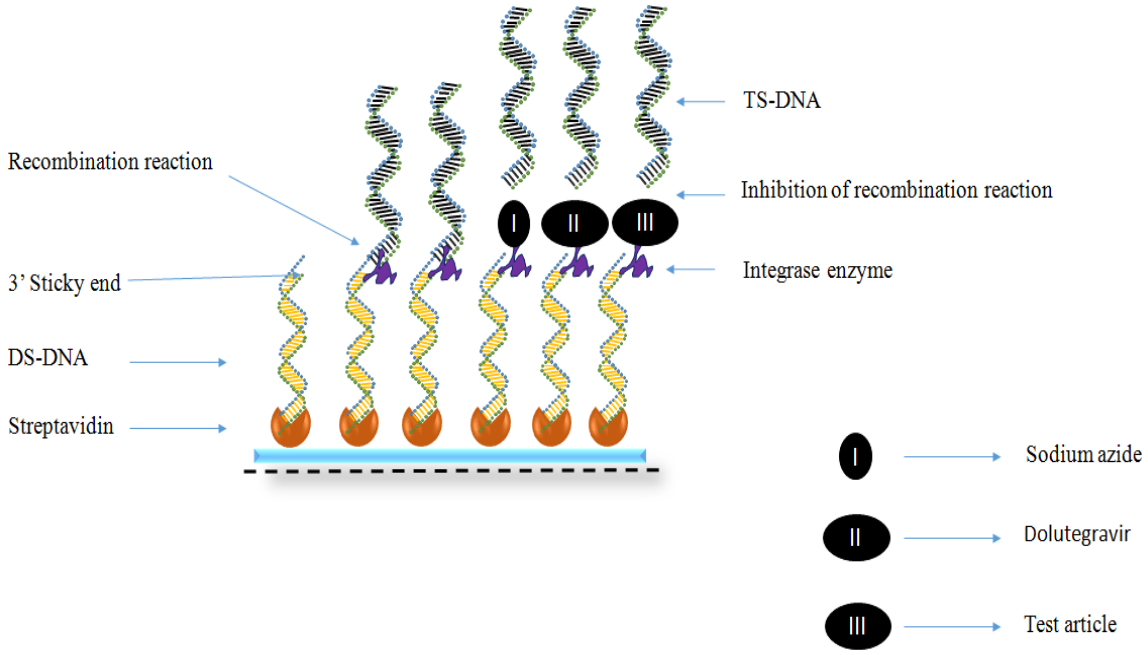

Figure 15: Diagrammatic representation of *in vitro* HIV-1 integrase assay

4.4 Anti-HIV assay

3-(4,5-dimethylthiazol-2-yl)-2,5-diphenyltetrazolium bromide (MTT) assay was performed for evaluating the antiviral activity of the compounds. The principle of MTT assay is based on spectrophotometric measurement of blue-purple formazan produced by reduction of MTT (Acros Organics, Geel, Belgium) by metabolically active cells. The absorbance was read in an eight-channel computer-controlled photometer (Infinite M1000, Tecan, Mechelen, Belgium), at two wavelengths (540 and 690 nm). All data were calculated using the median OD (optical density) value of three wells.

The procedure involved addition of stock solutions (10 x final concentration) of test compounds in 25 µl volumes to two series of triplicate wells for evaluation of their effects on mock- and HIV-infected cells at the start of each experiment. In flat-bottomed 96-well microtiter trays, serial five-fold dilutions of the test compounds were supplemented using Biomek 3000 robot (Beckman instruments, Fullerton, CA). Further, untreated control HIV and mock-infected cell samples followed by HIV-1 (IIIB) stock (50 µl) at 100–300 $CCID_{50}$ (50 % cell culture infectious dose) or culture medium were added for each sample. Cytotoxicity effect of test compounds was measured by evaluating mock-infected cells. It involves centrifugation of exponentially growing MT-4 cells for 5 min at 220 g. Then the obtained supernatant was discarded and MT-4 cells were re-suspended at 6 x 10^5 cells/ml and followed by transfer of 50 µl

volumes to the microtiter tray wells. After five days of infection, the viability of mock and HIV infected cells were examined spectrophotometrically (Vercruysse, 2012).

Here, EC_{50} (50 % effective antiviral concentration) is defined as the concentration of the tested compound achieving 50 % protection from virus-induced cytopathic effect and CC_{50} (50 % cytotoxic concentration) was defined as the compound concentration that reduced the viability of mock-infected cells by 50 %.

4.5 *In Silico* Prediction of Physicochemical Properties

USFDA explained oral bioavailability (OB) as the rate and extent to which the active constituent is absorbed and becomes available at the site of action. For development of bioactive molecules, high OB is a major consideration in drug discovery research. Different physiochemical properties which influence OB such as molecular weight, log partition coefficient (logP), topological polar surface area (TPSA), hydrogen bond acceptor count (HBA) and hydrogen bond donor (HBD) count were calculated using pkCSM software. This software is freely available on http://structure.bioc.cam.ac.uk/pkcsm.

LogP is defined as the logarithm of partition coefficient between octanol and water. HBA are molecules that have a lone pair of electrons located on an electronegative atom (for example, oxygen, nitrogen, or fluorine) whereas HBD is described as number of oxygen or nitrogen atoms with at least one hydrogen attached. TPSA is defined as the sum of polar atom surfaces in the molecule (Fernandes, 2009).

Rule of five or Lipinski rule was also investigated which states that for good oral bioavailability given molecule should not violate more than one of the following rules:

a. Molecular weight should be less than 500 kDa.

b. LogP should be less than 5

c. Should have less than 10 hydrogen-bond acceptors (sum of oxygen and nitrogen atoms)

d. Should have less than 5 hydrogen bond donors (sum of hydroxyl and amine groups)

Some of the major properties such as water solubility and Caco2 permeability were also predicted *in silico* using pkCSM software (Pires, 2015).

CHAPTER 5: *N*-(4-FLUOROPHENYL)-6-METHYL-2-OXO-1,2,3,4-TETRAHYDROPYRIMIDINE-5-CARBOXAMIDES

Tetrahydropyrimidines have been extensively evaluated for muscarinic; anti-inflammatory; antiviral; anticancer and acetyl cholinesterase inhibitory activity (Fátima, 2015). Recently, antiretroviral potential of tetrahydropyrimidine analogues having 2-chlorophenyl group has been reported (Elumalai, 2015); wherein one of the compound *N*-(4-fluorophenyl)-6-methyl-2-oxo-4-phenyl-1,2,3,4-tetrahydro pyrimidine-5-carboxamide (**PK-A1**) was found inactive but its bromo analogue ie. *N*-(4-bromophenyl)-6-methyl-2-oxo-4-phenyl-1,2,3,4-tetrahydropyrimidine-5-carboxamide was found to be active (Zabihollahi, 2012). Clinically approved (**I**-**III**) as well as other reported HIV IN inhibitors (**IV**-**VI**) also have p-fluoro phenyl (aromatic ring) feature on a heterocyclic ring along with carboxamide linkage. Therefore, structural similarity with integrase inhibitors was the reason to explore compound (**PK-A1**) further. For this, *p*-fluoro phenyl, which helps to penetrate the active site pocket, vacated by 3' adenine and forms a more favourable π-stacking interaction with the base of nucleotide and carboxamide being other common feature in reported structures were not modified (Sepehri, 2015; Billamboz, 2013). In addition, the 2-tetrahydropyridinone nucleus was kept the same and modification was done by changing substitution pattern on 4-phenyl ring and its effect on integrase inhibition was evaluated.

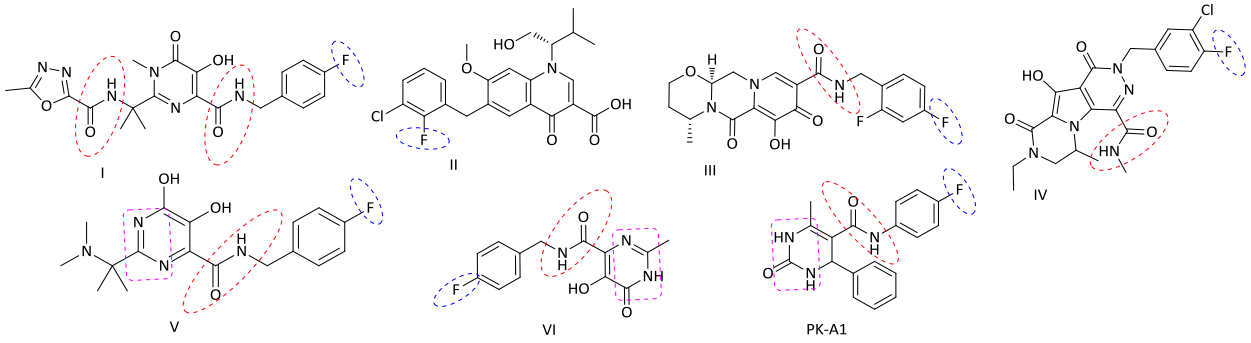

Figure 16: Literature reported HIV-1 IN inhibitors and general structure of designed molecule (PK-A1)

5.1 Chemistry

The synthetic route is illustrated in **Scheme 1.** Ethyl acetoacetate was condensed with 4-fluoro aniline in presence of pyridine under reflux to give key intermediate *N*-(4-fluorophenyl)-3-oxobutanamide (compound **PK-A0**). Second step involves formation of *N*-acyl iminium by treatment of compound **PK-A0** with different substituted aromatic aldehydes and urea in ethanol at 80°C. The final step comprises attack of **PK-A0** on *N*-acyl iminium to give final products **PK-A1 to PK-A18**, in 67-75% yields.

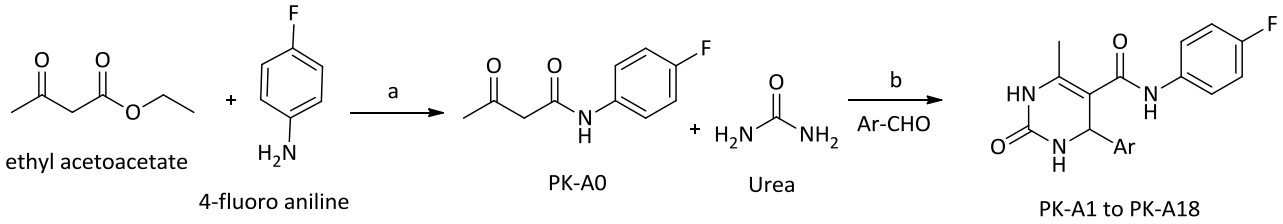

Scheme 1: Reagents and conditions: (a) pyridine, xylene, 8.5 h, reflux (b) hydrochloric acid, 7-9 h, reflux.

Reaction Mechanism

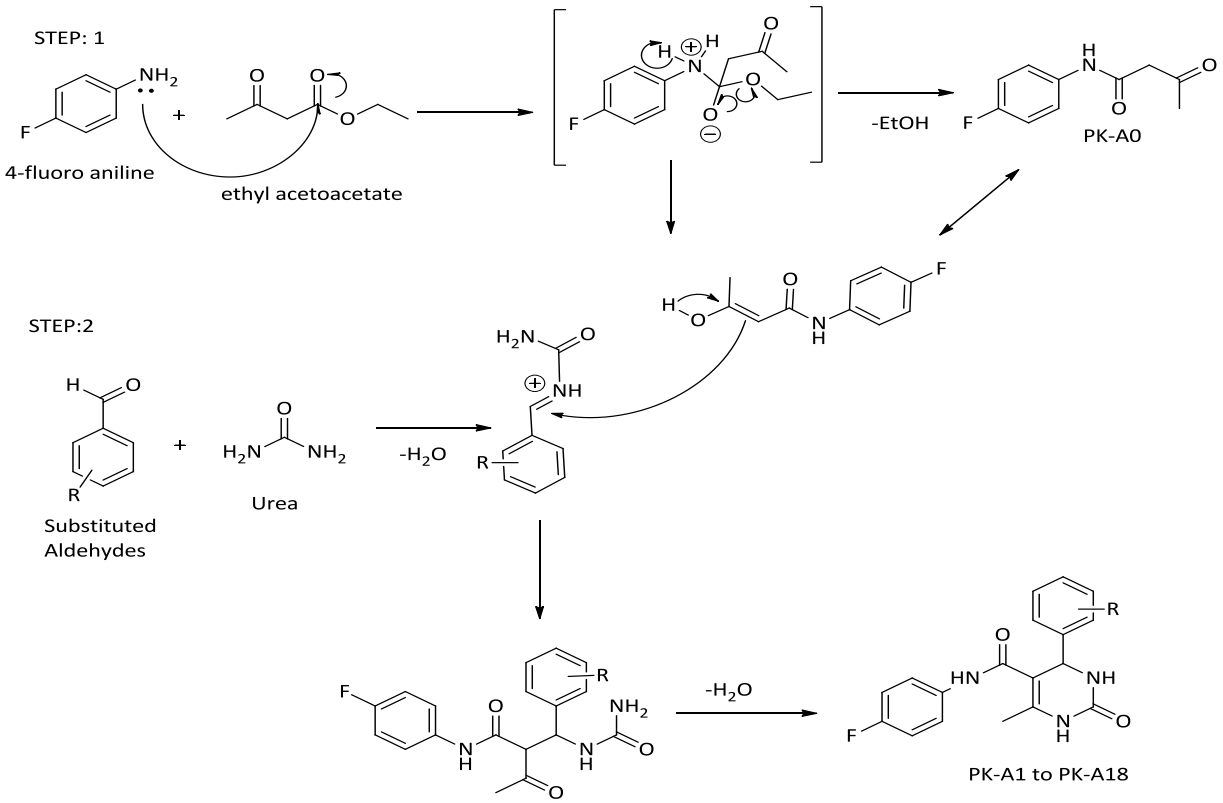

Figure 17: Reaction mechanism for substituted phenyl tetrahydro pyrimidine-5-carboxamides

Synthesis of *N*-(4-fluorophenyl)-3-oxobutanamide (PK-A0)

To a two-necked 100 ml RBF fitted with condenser, was added ethylacetoacetate (12.75 ml, 0.10 mol) in xylene (30 ml) and pyridine (1 ml) under nitrogen atmosphere. The reaction mass was gently refluxed for 0.5 h, 4-fluoroaniline (10 ml, 0.10 mol) was then added drop wise and further refluxed for 8 h, with removal of distillate through a Dean-Stark tube. The progress of reaction was monitored by TLC. After completion, the mixture was cooled to room temperature (RT) and extracted with 2M solution of NaOH

solution (50 ml). The aqueous layer was separated and made weakly acidic with concentrated HCl. The resulting precipitate was collected by filtration, washed with water, and dried to give the desired product as white crystals. Yield 63%; Mp: 105–107°C; IR (KBr) cm^{-1}: 3310 ($NH_{str.}$), 2985 (Ar-$CH_{str.}$), 1715, 1675 (C=$O_{str.}$), 1520 (C=C); ^{1}H-NMR (400 MHz, DMSO-d_6): δ (ppm): 2.20 (s, 2H), 3.39 (s, 3H), 7.17 (t, 2H, J = 8.4 Hz), 7.71 (t, 2H), 10.16 (s, 1H); ^{13}C-NMR (100 MHz, DMSO-d_6): δ (ppm): 30.6, 52.7, 115.6, 115.8, 135.7, 157.3, 159.6 and 203.4; EI-MS (m/z): 196.04 $[M+H]^+$.

Synthesis of *N* -(4-fluorophenyl)-6-methyl-2-oxo-4-substituted-phenyl-1,2,3,4-tetrahydro pyrimidine-5-carboxamides (PK-A1 to PK-A18):

Three necked RBF was charged with *N*-(4-fluoro-phenyl)-3-oxo-butyramide (**PK-A0**) dissolved in 30 ml of ethanol. Then substituted aryl aldehydes (0.01 mol), and urea (0.015 mol) were added and the resultant solution was heated under reflux for 7–9 h in presence of a catalytic amount of concentrated HCl. The progress of reaction was monitored by TLC. After the reaction was complete, mixture was kept overnight and the precipitate obtained was filtered. Products were recrystallized from ethanol and purity was assessed using HPLC. For this purpose, column used was Agilent Extend – C18 (250 x 4.6mm, 5µ), mobile phase: Water: Methanol (50:50), flow rate of 1 mL/min. Detection was done at 254 nm.

***N*-(4-fluorophenyl)-6-methyl-2-oxo-4-phenyl-1,2,3,4-tetrahydropyrimidine-5-carboxamide (PK-A1):** White solid; yield 71%; Mp: 179-182 °C; IR (KBr) cm^{-1}: 3385 ($NH_{str.}$), 3085 (Ar-$CH_{str.}$), 2957 (Ali-$CH_{str.}$), 1712, 1678 (C=$O_{str.}$), 1513 (C=C); ^{1}H-NMR (400 MHz, DMSO-d_6): δ 2.65 (s, 3H), 5.75 (s, 1H), 7.14– 7.75 (m, 9H), 7.17 (t, 2H, J = 8.4 Hz), 7.71 (t, 2H), 9.56 (s, 1H); ^{13}C-NMR (100 MHz, DMSO-d_6): δ (ppm): 18.4, 53.2, 107.1, 126.0, 126.1, 132.6, 143.9, 146.7, 150.3, 162.1 and 163.6; ESI-MS m/z: 326.06 $[M+H]^+$.

***N*-(4-fluorophenyl)-6-methyl-4-(2-nitrophenyl)-2-oxo-1,2,3,4-tetrahydropyrimidine-5-carboxamide (PK-A2):** Yellow solid; yield 68%; Mp: 204-206°C; IR (KBr) cm^{-1}: 3415 ($NH_{str.}$), 3082 (Ar-$CH_{str.}$), 2984 (Ali-$CH_{str.}$), 1708, 1672 (C=$O_{str.}$), 1510 (C=C); ^{1}H-NMR (400 MHz, DMSO-d_6): δ(ppm): 2.58 (s, 3H), 5.30 (s, 1H), 7.10– 7.52 (m, 8H), 9.58 (s, 1H); ^{13}C-NMR (100 MHz, DMSO-d_6): δ (ppm): 20.3, 51.1, 108.4, 127.2, 127.3, 131.4, 144.1, 152.2, 167.2, 163.2; ESI-MS m/z: 371.14 $[M+H]^+$.

***N*-(4-fluorophenyl)-6-methyl-4-(3-nitrophenyl)-2-oxo-1,2,3,4-tetrahydropyrimidine-5-carboxamide (PK-A3):** Yellow solid; yield 75%; Mp: 201-203°C; IR (KBr) cm^{-1}: 3385 ($NH_{str.}$), 3085 (Ar-$CH_{str.}$), 2957 (Ali-$CH_{str.}$), 1712, 1678 (C=$O_{str.}$), 1513 (C=C); ^{1}H-NMR (400 MHz, DMSO-d_6): δ(ppm): 1.98 (s, 3H), 5.71 (s, 1H), 6.30– 7.10 (m, 8H), 8.21 (s, 1H); ^{13}C-NMR (100 MHz, DMSO-d_6): δ (ppm): 20.4, 58.3, 104.7, 109.5, 119.5, 119.4,126.7, 126.9, 134.3, 144.6, 151.6, 153.8, 170.7; EI-MS (m/z): 371.21 $[M+H]^+$.

***N*-(4-fluorophenyl)-6-methyl-4-(4-nitrophenyl)-2-oxo-1,2,3,4-tetrahydropyrimidine-5-carboxamide (PK-A4):** Yellow solid; yield 68%; Mp: 203-205°C; IR (KBr) cm^{-1}: 3449 ($NH_{str.}$), 3068 (Ar-$CH_{str.}$), 2943 (Ali-

$CH_{str.}$), 1719, 1669 (C=$O_{str.}$), 1524 (C=C); ^{1}H-NMR (400 MHz, DMSO-d_6): δ(ppm): 2.32 (s, 3H), 5.41 (s, 1H), 7.19– 7.56 (m, 8H), 9.41 (s, 1H); ^{13}C-NMR (100 MHz, DMSO-d_6): δ (ppm): 19.4, 52.7, 107.2, 126.2, 127.1, 132.5, 143.4, 151.1, 166.4, 170.6; ESI-MS m/z: 371.10 $[M+H]^+$.

4-(2-chlorophenyl)-*N*-(4-fluorophenyl)-6-methyl-2-oxo-1,2,3,4-tetrahydropyrimidine-5-carboxamide (PK-A5): Yellow creamish solid; yield 67%; Mp: 211-213°C; IR (KBr) cm^{-1}: 3438 ($NH_{str.}$), 3041 (Ar-$CH_{str.}$), 2935 (Ali-$CH_{str.}$), 1705, 1670 (C=$O_{str.}$), 1504 (C=C); ^{1}H-NMR (400 MHz, DMSO-d_6): δ (ppm): 3.36 (s, 3H), 5.32 (s, 1H), 7.06– 8.20 (m, 8H), 10.23 (s, 1H); ^{13}C-NMR (100 MHz, DMSO-d_6): δ (ppm): 19.4, 50.7, 108.1, 127.4, 127.3, 131.2, 135.3, 150.4, 165.3, 167.3; ESI-MS m/z: 360.11 $[M+H]^+$.

4-(4-chlorophenyl)-*N*-(4-fluorophenyl)-6-methyl-2-oxo-1,2,3,4-tetrahydropyrimidine-5-carboxamide (PK-A6): Light yellow solid; yield 69%; Mp: 211-213°C; IR (KBr) cm^{-1}: 3368 ($NH_{str.}$), 3071 (Ar-$CH_{str.}$), 2987 (Ali-$CH_{str.}$), 1721, 1676 (C=$O_{str.}$), 1509 (C=C); ^{1}H-NMR (400 MHz, DMSO-d_6): δ(ppm): 2.51 (s, 3H), 5.45 (s, 1H), 7.30– 7.72 (m, 8H),10.0 (s, 1H); ^{13}C-NMR (100 MHz, DMSO-d_6): δ (ppm): 19.5, 53.4, 108.5, 115.6, 115.7, 126.1, 126.2, 126.4, 126.5, 133.6, 133.8, 141.5, 146.2, 150.7, 162.3,163.4; ESI-MS m/z: 360.10 $[M+H]^+$.

4-(2,4-dichlorophenyl)-N-(4-fluorophenyl)-6-methyl-2-oxo-1,2,3,4-tetrahydropyrimidine-5-carboxamide (PK-A7): Light brown solid; yield 67%; Mp: 237-240°C; IR (KBr) cm^{-1}: 3461 ($NH_{str.}$), 3069 (Ar-$CH_{str.}$), 2965 (Ali-$CH_{str.}$), 1701, 1678 (C=$O_{str.}$), 1512 (C=C); ^{1}H-NMR (400 MHz, DMSO-d_6): δ (ppm): 2.38 (s, 3H), 5.49 (s, 1H), 7.24 – 7.51 (m, 7H), 9.60 (s, 1H); ^{13}C-NMR (100 MHz, DMSO-d_6): δ (ppm): 21.3, 52.1, 108.4, 116.1, 116.4, 126.4, 126.2, 127.1, 133.7, 133.6, 140.8, 146.2, 150.8, 162.8, 163.4; ESI-MS m/z: 409.06 $[M+H]^+$.

***N*-(4-fluorophenyl)-4-(2-hydroxyphenyl)-6-methyl-2-oxo-1,2,3,4-tetrahydropyrimidine-5-carboxamide (PK-A8):** Dark reddish brown solid; yield 70%; Mp: 207-210°C; IR (KBr) cm^{-1}: 3387 (NHstr.), 3054 (Ar-CHstr.), 2974 (Ali-CHstr.), 1689, 1673 (C=Ostr.), 1508 (C=C); ^{1}H-NMR (400 MHz, DMSO-d_6): δ (ppm): 3.30 (s, 3H), 5.39 (s, 1H), 7.16– 8.04 (m, 8H), 10.04 (s, 1H); ^{13}C-NMR (100 MHz, DMSO-d_6): δ (ppm): 20.1, 52.4, 108.9, 126.8, 127.0, 130.4, 135.6, 150.7, 163.6, 165.7; ESI-MS m/z: 342.21 $[M+H]^+$.

***N*-(4-fluorophenyl)-4-(4-hydroxyphenyl)-6-methyl-2-oxo-1,2,3,4-tetrahydropyrimidine-5-carboxamide (PK-A9):** Yellow solid; yield 67%; Mp: 211-214°C; IR (KBr) cm^{-1}: 3385 ($NH_{str.}$), 3024 (Ar-$CH_{str.}$), 2968 (Ali-$CH_{str.}$), 1711, 1679 (C=$O_{str.}$), 1516 (C=C); ^{1}H-NMR (400 MHz, DMSO-d_6): δ (ppm): 3.32 (s, 3H), 5.47 (s, 1H), 7.21– 8.22 (m, 8H), 9.54 (s, 1H); ^{13}C-NMR (100 MHz, DMSO-d_6): δ (ppm): 19.4, 53.5, 108.3, 124.7, 128.6, 130.1, 136.0, 150.1, 162.1, 165.0; ESI-MS m/z: 342.19 $[M+H]^+$.

***N*-(4-fluorophenyl)-4-(4-methoxyphenyl)-6-methyl-2-oxo-1,2,3,4-tetrahydropyrimidine-5-carboxamide (PK-A10):** White solid; yield 69%; Mp: 211-214°C; IR (KBr) cm^{-1}: 3398 ($NH_{str.}$), 3051 (Ar-$CH_{str.}$), 2977 (Ali-

$CH_{str.}$), 1712, 1672 ($C=O_{str.}$), 1523 (C=C); ^{1}H-NMR (400 MHz, DMSO-d_6): δ (ppm): 3.36 (s, 3H), 3.71 (s, 3H), 5.36 (s, 1H), 6.90– 7.57 (m, 8H), 8.72 (s, 1H), 9.59 (s, 1H); ^{13}C-NMR (100 MHz, DMSO-d_6): δ (ppm): 17.5, 54.6, 55.5, 60.2, 114.5, 115.3, 115.6, 121.6, 127.3, 152.9, 158.9, 165.6; ESI-MS m/z: 356.21 $[M+H]^+$.

4-(3,4-dimethoxyphenyl)-*N*-(4-fluorophenyl)-6-methyl-2-oxo-1,2,3,4-tetrahydropyrimidine-5-carboxamide (PK-A11): White solid; yield 72%; Mp: 285-287°C; IR (KBr) cm^{-1}: 3374 ($NH_{str.}$), 3029 (Ar-$CH_{str.}$), 2997 (Ali-$CH_{str.}$), 1711, 1678 ($C=O_{str.}$), 1525 (C=C); ^{1}H-NMR (400 MHz, DMSO-d_6): δ (ppm): 2.82 (s, 3H), 3.85-3.87 (s, 6H), 5.46 (s, 1H), 7.17-7.79 (m, 7H), 9.51 (s, 1H); ^{13}C-NMR (100 MHz, DMSO-d_6): δ (ppm): 18.9, 53.4, 55.9, 103.8, 104.7, 108.8, 115.4, 115.8, 126.1, 126.5, 131.4, 132.7, 134.8, 141.5, 144.7, 146.8, 160.4, 162.4; ESI-MS m/z: 386.16 $[M+H]^+$.

4-(2,5-dimethoxyphenyl)-*N*-(4-fluorophenyl)-6-methyl-2-oxo-1,2,3,4-tetrahydropyrimidine-5-carboxamide (PK-A12): Light yellow solid; yield 67%; Mp: 281-283°C; IR (KBr) cm-1: 3452 ($NH_{str.}$), 3065 (Ar-$CH_{str.}$), 2987 (Ali-$CH_{str.}$), 1701, 1688 ($C=O_{str.}$), 1522 (C=C); ^{1}H-NMR (400 MHz, DMSO-d_6): δ (ppm): 2.89 (s, 3H), 3.83-3.85 (s, 6H), 5.67 (s, 1H), 7.20-7.71 (m, 7H), 9.51 (s, 1H); ^{13}C-NMR (100 MHz, DMSO-d_6): δ (ppm): 17.6, 54.8, 56.4, 104.5, 105.4, 107.7, 114.4, 115.9, 125.8, 126.2, 130.7, 133.5, 135.7, 140.8, 143.8, 145.8, 161.3, 163.4; ESI-MS m/z: 386.22 $[M+H]^+$.

***N*-(4-fluorophenyl)-6-methyl-2-oxo-4-(3,4,5-trimethoxyphenyl)-1,2,3,4-tetrahydropyrimidine-5-carboxamide (PK-A13):** Yellowish white solid; yield 69%; Mp:184-187°C; IR (KBr) cm^{-1}: 3417 ($NH_{str.}$), 3057 (Ar-$CH_{str.}$), 2963 (Ali-$CH_{str.}$), 1712, 1682 ($C=O_{str.}$), 1517 (C=C); ^{1}H-NMR (400 MHz, DMSO-d_6): δ (ppm): 2.42 (s, 3H), 3.82-3.84 (s, 9H), 5.61 (s, 1H), 7.14-7.61 (m, 6H), 9.62 (s, 1H); ^{13}C-NMR (100 MHz, DMSO-d_6): δ (ppm): 18.4, 56.8, 56.7, 60.7, 104.1, 106.7, 106.5, 113.5, 115.9, 126.1, 131.7, 132.8, 134.7, 138.1, 141.8, 144.8, 160.5, 162.9; ESI-MS m/z: 416.08 $[M+H]^+$.

***N*-(4-fluorophenyl)-4-(4-hydroxy-3,5-dimethoxyphenyl)-6-methyl-2-oxo-1,2,3,4-tetrahydropyrimidine-5-carboxamide (PK-A14):** Creamish yellow solid; yield 72%; Mp:199-201°C; IR (KBr) cm^{-1}: 3446 ($NH_{str.}$), 3069 (Ar-$CH_{str.}$), 2967 (Ali-$CH_{str.}$), 1707, 1683 ($C=O_{str.}$), 1521 (C=C); ^{1}H-NMR (400 MHz, DMSO-d_6): δ (ppm): 3.32 (s, 3H), 3.84-3.86 (s, 6H), 4.48 (s, 1H), 5.46 (s, 1H), 7.15-7.70 (m, 6H), 9.62 (s, 1H); ^{13}C-NMR (100 MHz, DMSO-d_6): δ (ppm): 17.9, 54.4, 56.3, 104.1, 104.4, 109.2, 115.3, 115.4, 125.7, 125.9, 132.4, 133.4, 136.3, 144.2, 146.5, 148.9, 162.4, 163.2; ESI-MS m/z: 400.22 $[M+H]^+$.

***N*-(4-fluorophenyl)-4-(4-hydroxy-3-methoxyphenyl)-6-methyl-2-oxo-1,2,3,4-tetrahydropyrimidine-5-carboxamide (PK-A15):** White solid; yield 67%; Mp: 204-206°C; IR (KBr) cm^{-1}: 3396 ($NH_{str.}$), 3077 (Ar-$CH_{str.}$), 2969 (Ali-$CH_{str.}$), 1715, 1680 ($C=O_{str.}$), 1519 (C=C); ^{1}H-NMR (400 MHz, DMSO-d_6): δ (ppm): 3.32 (s, 3H), 3.84 (s, 3H), 4.56 (s, 1H), 5.40 (s, 1H), 7.04-7.66 (m, 7H), 9.48 (s, 1H); ^{13}C-NMR (100 MHz, DMSO-d_6):

δ (ppm): 19.3, 55.4, 56.3, 107.2, 112.8, 115.5, 116.6, 126.7, 133.4, 137.3, 145.5, 148.0, 164.2; ESI-MS m/z: 370.12 $[M+H]^+$.

4-(3-ethoxy-4-hydroxyphenyl)-*N*-(4-fluorophenyl)-6-methyl-2-oxo-1,2,3,4-tetrahydropyrimidine-5-carboxamide (PK-A16): Yellowish brown solid; yield 70%; Mp: 209-211°C; IR (KBr) cm^{-1}: 3414 ($NH_{str.}$), 3041 (Ar-$CH_{str.}$), 2925 (Ali-$CH_{str.}$), 1703, 1676 (C=$O_{str.}$), 1524 (C=C); ^{1}H-NMR (400 MHz, DMSO-d_6): δ (ppm): 0.95 (s, 3H), 2.25 (s, 3H), 2.84 (s, 2H), 4.33 (s, 1H), 5.40 (s, 1H), 6.50-7.50 (m, 7H), 9.50 (s, 1H); ^{13}C-NMR (100 MHz, DMSO-d_6): δ (ppm): 15.4, 19.6, 54.4, 63.3, 108.1, 111.2, 115.6, 115.7, 115.9, 125.6, 126.3, 133.9, 136.9, 144.2, 146.5, 146.2, 148.4, 150.6, 162.8, 163.9; ESI-MS m/z: 384.17 $[M+H]^+$.

***N*-(4-fluorophenyl)-4-(1H-indol-3-yl)-6-methyl-2-oxo-1,2,3,4-tetrahydropyrimidine-5-carboxamide (PK-A17):** White solid; yield 65%; Mp: 208-210°C; IR (KBr) cm^{-1}: 3468 ($NH_{str.}$), 3048 (Ar-$CH_{str.}$), 2965 (Ali-$CH_{str.}$), 1709, 1684 (C=$O_{str.}$), 1516 (C=C); ^{1}H-NMR (400 MHz, DMSO-d_6): δ (ppm): 2.34 (s, 3H), 5.32 (s, 1H), 7.01-7.83 (m, 8H), 9.27 (s, 1H),10.03 (s, 1H); ^{13}C-NMR (100 MHz, DMSO-d_6): δ (ppm): 18.7, 55.1, 107.1, 111.3, 111.8, 114.7, 115.3, 118.2, 122.4, 124.5, 126.2, 132.3, 134.1, 143.2, 149.8, 162.7, 163.8; ESI-MS m/z: 365.09 $[M+H]^+$.

***N*-(4-fluorophenyl)-4-(furan-2-yl)-6-methyl-2-oxo-1,2,3,4-tetrahydropyrimidine-5-carboxamide (PK-A18):** Black solid; yield 68%; Mp:178-180°C; IR (KBr) cm^{-1}: 3425 ($NH_{str.}$), 3018 (Ar-$CH_{str.}$), 2924 (Ali-$CH_{str.}$), 1720, 1688 (C=$O_{str.}$), 1511 (C=C); ^{1}H-NMR (400 MHz, DMSO-d_6): δ (ppm): 3.36 (s, 3H), 5.47 (s, 1H), 6.37 (t, 1H), 7.11-7.72 (m, 5H), 8.83 (s, 1H), 9.66 (s, 1H); ^{13}C-NMR (100 MHz, DMSO-d_6): δ (ppm): 8.9, 17.6, 45.8, 49.2, 106.3, 110.7, 115.6, 115.9, 121.7, 121.8, 142.9, 150.2, 166.8; ESI-MS m/z: 316.09 $[M+H]^+$.

5.2 Results and Discussion

The results of *in vitro* evaluation as well as Gscore of designed compounds with dolutegravir as standard are given in **table 1**. The results of cytoxicity and anti-HIV assay are shown in **table 2**.

Unsubstituted phenyl ring at 4 position of pyrimidine was used as starting point and effect of various electron donating and electron withdrawing substituents on this ring was checked. Compound **PK-A1** having unsubstituted phenyl ring showed hydrogen bonding interactions with Thr 66, Lys 159 (by amidic carbonyl group) and hydrophobic interactions with Asn 155, Lys 156 and Lys 159 were also observed. It did not show interaction with DDE motif (Asp 64, Asp 116 and Glu 152) and was also least active against IN *in vitro*.

Substitution of electron withdrawing nitro group, either at ortho position (**PK-A2**) or at para position (**PK-A2**), showed hydrophobic interactions with Asp 116, Gln 148 and Glu 152 as well as hydrogen bonding interactions with Thr 66 (*via* carbonyl group of pyridine ring) and Glu 152 (by –NH group of

pyridine ring). In addition, **PK-A2** showed hydrogen bonding interactions with Cys 65 (by amidic carbonyl group and *o*-NO_2 group) and His 67 by carbonyl of pyrimidine ring; whereas **PK-A4** displayed hydrogen-bonding interactions Lys 156 and Lys 159 (via *p*-NO_2 group). The % inhibition profile of both compounds was better than **PK-A1**, however **PK-A4** was less active than **PK-A2**, which may be attributed to lack of interactions with Cys 65 and His 67. Substitution of nitro group at *meta* position (**PK-A3**) further reduced activity because it did not show interaction with Asp 116, Gln 148 and Glu 152 as well as with Cys 65 and His 67 as compared to *o* & *p* substituted compounds (**PK-A2** and **PK-A4**).

Compounds **PK-A5** and **PK-A6** were substituted with *o*-chloro and *p*-chloro group, respectively and displayed high inhibition; **PK-A5** showed 88.36% and **PK-A6** showed 90.11% inhibition. Analysis of docked poses revealed that amidic carbonyl has hydrogen bonding interaction with Cys 65, carbonyl of pyrimidine ring also showed hydrogen bonding with Thr 66 and His 67; and -NH of pyrimidine formed hydrogen bond with Glu 152. Also, hydrophobic interactions of chlorophenyl ring with Asp 64, Asp 116 and Gln 148 were seen. Moreover, the amidic carbonyl also showed interaction with Mg 1001 and hence these compounds showed very good activity. The *o*-chloro group of **PK-A5** showed hydrophobic interaction with Cys 65 which was not observed in **PK-A6**. But **PK-A6** showed π-π stacking interaction with His 67 which was absent in **PK-A5**. The *p*-chloro group of **PK-A6** appeared to come out of the cavity and hence it showed less docking score. However, **PK-A6** was found to be more active than **PK-A5** *in vitro*. Substitution of chlorine at both ortho and para positions (compound **PK-A7**) showed absence of docking interactions with Asp 64 and Asp 116 (G score -5.21) leading to reduction in Gscore as well as activity as compared to **PK-A5** and **PK-A6**.

Substitution of electron donating hydroxy group at *o*- or *p*- position (**PK-A8** and **PK-A9**, respectively) showed more than 70 % HIV-1 IN inhibition. Compound **PK-A8** showed highest docking score (G Score -7.40) and visual analysis indicated that *o*-hydroxyl group formed hydrogen bonding interactions with Cys 65 and Thr 66 and also formed salt bridge with Mg1001. The carbonyl of pyrimidine also formed hydrogen bond with His 67 and Lys 159; and amidic carbonyl formed hydrogen bond with Asn 155. Apart from these, hydrophobic interactions were observed with Asp 64, Asp 116, Cys 65, Thr 66, Gln 148, Ile 151, Glu 152, Lys 156 and Lys 159.

Substitution of *p*-OH (Compound **PK-A9**) displayed hydrogen-bonding interactions with Cys 65 via –NH of amide and pyrimidine ring and His 67 (via carbonyl group of pyrimidine ring). Hydrophobic interactions were observed with Asp 64, Gln 148 (by *p*-fluoro group), Ile 151, Glu 152, Lys 156 and Lys 159. The *p*-hydroxy group was found to interact with Mg1001. However, other interactions like **PK-A8** were not seen, which might be reason for less docking score as compare to **PK-A8**. Replacing *p*-OH with

p-methoxy (**PK-A10**) further reduced the activity as well as docking score because it was observed that the methoxy substituted aryl ring did not enter the active site cavity.

After analyzing the results of **PK-A8**, **PK-A9** and **PK-A10**, next logical step was to check the effect of di- or tri- substitution on activity. Keeping this in mind, compounds **PK-A11** (having 3,4-dimethoxy substitution) and **PK-A12** (having 2,5-dimethoxy substitution) were designed. It was observed that in compound **PK-A11**, there was no improvement in activity although docking score was improved as compared to **PK-A10**. It showed hydrogen bonding interactions with Thr 66 (via 3-methoxy group) and His 67 (by 4-methoxy group) and hydrophobic interactions with Gln 148, Ile 151, Glu 152, Asn 155, Lys 156 and Lys 159. However, compound **PK-A12**, substituted with dimethoxy groups at 2 and 5 positions of aryl ring, displayed similar interactions but the docking score was less and % inhibitory potential was marginally more as compared to **PK-A11**. It displayed hydrogen bonding interactions with Cys 65 (via amidic carbonyl group), Thr 66, His 67 and Glu 152 (via carbonyl and –NH group of pyrimidine ring). Hydrophobic interactions with Asp 64, Glu 92, Gln 148 and Glu 152 were also observed. The π-π stacking between dimethoxy-substituted aryl ring and His 67 were also seen, that might be responsible for better activity as compare to **PK-A11**.

When the ring is substituted with 3,4,5-trimethoxy (compound **PK-A13**), it was noted that there was no interaction with DDE motif although hydrogen bonding interactions with Cys 65 (via carbonyl of amide) and Thr 66 (by methoxy) and also hydrophobic interactions with His 67, Asn 155 and Lys 156 were seen. It reduced the inhibitory activity drastically.

Since compound **PK-A9**, having 4-hydroxy substitution showed good activity, effect of replacing 4-methoxy with 4-hydroxyl (**PK-A14**) was studied. Indeed, it enhanced the docking score as well as activity but very slightly. It established some interactions with DDE motif, particularly Asp 116 and Glu 152, as also 4-hydroxy was found to have interaction with Lys 156. The observation that 4-hydroxy substitution and 3-methoxy substitution has positive effect on activity, compound **PK-A15** was considered and since methoxy group takes part in hydrophobic interactions, replacing methoxy with ethoxy in compound **PK-A16** was envisaged.

Interestingly, it was noted that methoxy substitution decreases the activity and score but ethoxy substitution enhances the interactions and thus potentiates activity. These compounds had similar interactions such as hydrogen bonding with Cys 65 (via *p*-OH); Gln 148 (via amidic carbonyl group); Glu 152 and Lys 156 (via carbonyl and –NH group of pyrimidine ring) as well as hydrophobic interactions with Asp 64, Asp 116, and formed salt bridge with Mg 1001. However, **PK-A16** additionally showed hydrophobic interactions with Cys 65, Gln 148 and DDE motif (via ethoxy group) and hydrogen bonding

interaction of 4-hydroxy and oxygen of ethoxy with Thr 66, which might be the reason for better activity of **PK-A16**.

Effect of replacing the substituted phenyl ring with fused ring like indole (compound **PK-A17**) or small ring like furan (**PK-A18**) was also thought of. Compound **PK-A17** showed hydrogen bonding interactions with Asp 116 (via -NH of indole ring) and Glu 92 (via –NH- of pyrimidine ring). Hydrophobic interactions with Cys 65, His 67 and Asn 155 were also seen. However, it did not interact with DDE motif and the indole ring was more or less solvent exposed, which might be the reason for less docking score as well as IN inhibitory activity. However, substitution of small heterocyclic furan ring displayed hydrogen bonding interactions with His 67, Thr 66 and Lys 159 (via carbonyl of pyrimidine ring), Asn 155 (via oxygen of furan ring) and Cys 65 (with amidic oxygen); hydrophobic interactions with Asp 64, Asp 116, Thr 66, His 67, Asn 155, Glu 152 and salt bridge with Mg 1001 (with amidic oxygen). Due to these interactions, its docking score was good and showed 84% inhibition of IN.

Overall, it was observed that the HIV-1 IN inhibitory potency of designed compounds altered significantly with variation in nature as well as position of substituent. In general, compounds having *o*-chloro (**PK-A5**) and *p*-chloro substitution (**PK-A6**); electron donating group like 4-hydroxy-3-ethoxy substitution (**PK-A16**) and small furan ring in place of phenyl ring (**PK-A18**) exhibited significant IN inhibitory activity. Since these compounds showed % inhibition more than 80%, these were further tested for calculation of IC_{50} values (given in table 1). It was observed that compounds **PK-A5** and **PK-A6** with electron withdrawing substituent showed IC_{50} value of 4.01 µM and 0.65 µM respectively. Compound **PK-A16** had IC_{50}value of 1.91 µM and furan substituted compound **PK-A18** displayed IC_{50}value of 4.91 µM. Encouraged by the *in silico* and *in vitro* results, all the compounds were tested for anti-HIV activity against HIV-1 (III_B) and HIV-2 (ROD) in cell based assay. It was however observed that, all the compounds did not show any anti-HIV activity below their cytotoxic concentration (as shown in **table 2**). The compounds showed very good potential *in vitro* however in cell culture assay the activity was not seen.

5.3 Oral bioavailability and toxicity prediction

All the designed compounds fulfilled the criteria of Lipinski rule. The log P values were in range of 2.68 to 4.32 and hydrogen bond donor count between 3 to 4, hydrogen bond acceptor count from 2 to 4. The results are shown in **table 3**.

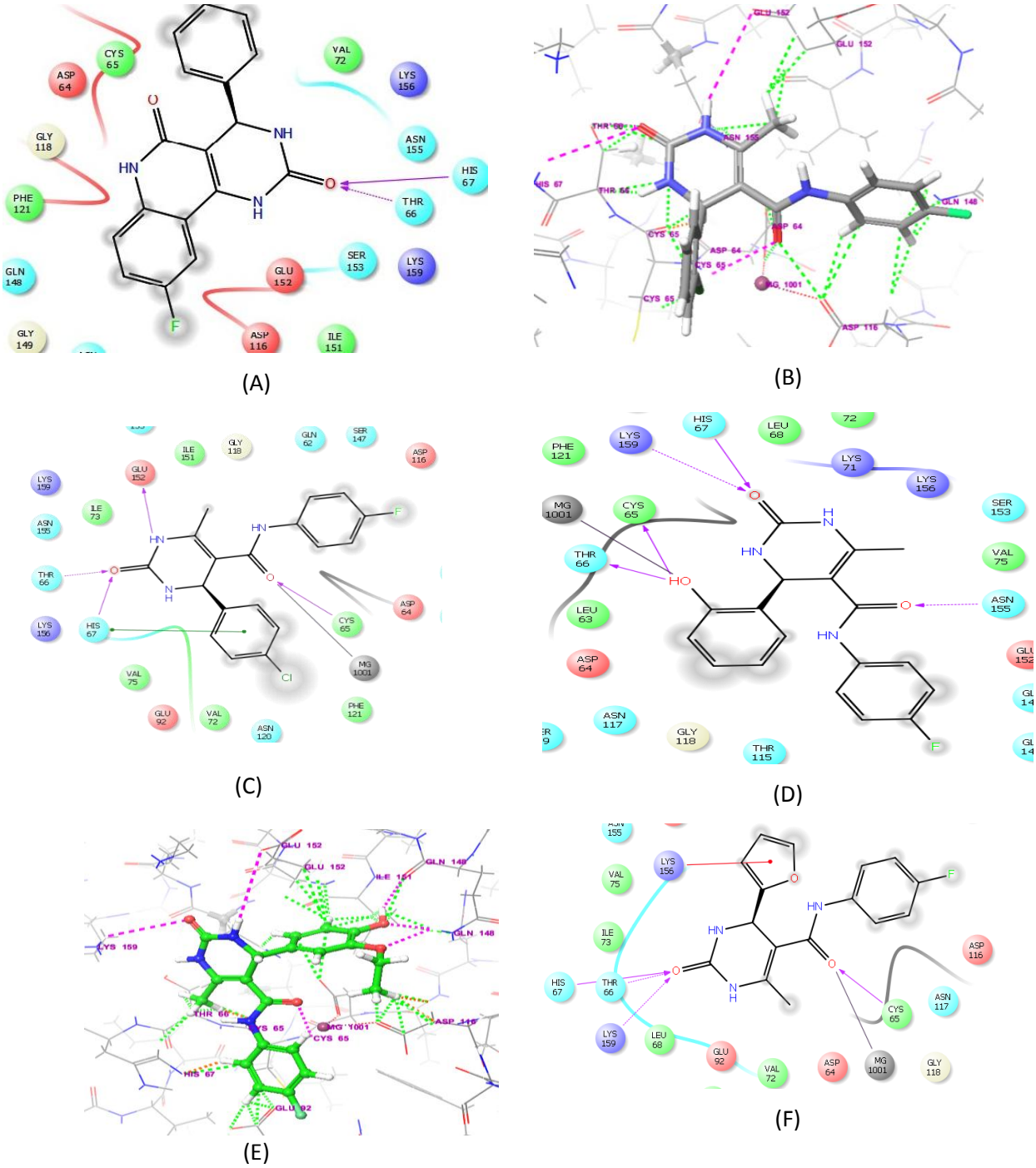

Figure 18: Docking poses of few representative compounds A: Docking pose of PK-A1; B: 2D interaction plot of PK-A5; C: 2D interaction plot of PK-A6; D: Docking pose of PK-A8; E: 2D interaction plot of PK-A16; F: 2D interaction plot of PK-A18

Table 1: Results of in-vitro HIV-1 IN inhibition and docking studies of compounds PK-A1 to PK-A18

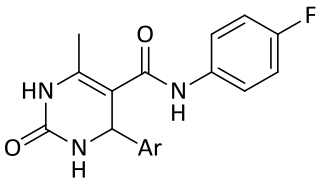

Compound code	Ar	Glide Score (G score)	% IN INHIBITION*	IC_{50} value**
Dolutegravir	-----	-7.65	95	nd
PK-A1	Ph	-4.85	27.35	nd
PK-A2	2-NO_2-Ph	-6.07	45.50	nd
PK-A3	3-NO_2-Ph	-5.82	30.20	nd
PK-A4	4-NO_2-Ph	-5.93	40.82	nd
PK-A5	2-Cl-Ph	-5.95	88.36	4.01±0.84
PK-A6	4-Cl-Ph	-5.66	90.11	0.65±0.04
PK-A7	2,4-diCl-Ph	-5.21	69.31	nd
PK-A8	2-OH-Ph	-7.40	72.80	nd
PK-A9	4-OH-Ph	-6.66	73.40	nd
PK-A10	4-OMe-Ph	-5.85	65.60	nd
PK-A11	3,4-diOMe-Ph	-6.37	67.20	nd
PK-A12	2,5-diOMe-Ph	-6.01	72.50	nd
PK-A13	3,4,5-triOMe-Ph	-6.16	49.20	nd
PK-A14	4-OH-3,5-diOMe-Ph	-6.69	56.62	nd
PK-A15	4-OH-3-OMe-Ph	-6.70	60.18	nd
PK-A16	4-OH-3-OEt-Ph	-7.03	87.83	1.91±0.65
PK-A17	1H-indol-3-yl	-5.81	47.30	nd
PK-A18	furan-2-yl	-6.50	84.13	4.91±0.99

*% inhibition at 10µM concentration, values are mean of duplicate experiment performed independently, nd = not done; ** in µM

Table 2: Anti-HIV activity of synthesized compounds PK-A1 to PK-A18

Compounds	HIV-1 (III_B)			HIV-2 (ROD)		
	EC_{50}[1] (µM)	CC_{50}[2] (µM)	HIV-1[3] SI	EC_{50}[1] (µM)	CC_{50}[2] (µM)	HIV-2[3] SI
Dolutegravir	0.0006±0.000001	1.275±0.3	2110.00	0.00232±0.00061	1.495±0.165	597.00
PK-A1	>86.00±13.00	85.75±12.00	<1	>87.00±10.40	87.00±10.40	<1
PK-A2	>17.00±0.60	17.25±0.50	<1	>18.10±2.40	18.10±2.40	<1
PK-A3	>61.00±0.50	60.80±0.50	<1	>60.70±5.10	60.70±5.10	<1
PK-A4	>11.00±0.30	11.00±0.30	<1	>13.09±2.30	13.09±2.30	<1
PK-A5	>61.00±1.60	60.90±1.60	<1	>64.40±5.60	64.40±5.60	<1
PK-A6	nd	nd	nd	nd	nd	nd
PK-A7	>4.60±1.50	4.59±1.50	<1	>5.10±0.50	5.10±0.50	<1
PK-A8	>66.00±2.10	66.25±2.00	<1	>69.00±8.30	69.00±8.30	<1
PK-A9	>122.00±3.00	122.00±3.00	<1	>123.05±7.40	123.05±7.40	<1
PK-A10	>59.00±1.30	59.20±1.30	<1	>58.50±4.30	58.50±4.30	<1
PK-A11	>80.00±4.20	80.00±4.20	<1	>83.00±7.20	83.00±7.20	<1
PK-A12	>64.00±12.00	63.70±12.40	<1	>68.50±8.50	68.50±8.50	<1
PK-A13	>124.00±0.80	124.20±0.80	X1	>124.50±8.20	124.50±8.20	<1
PK-A14	>64.00±0.13	63.65±1.15	<1	>68.50±4.53	68.50±4.53	<1
PK-A15	>61.00±2.50	60.78±2.50	<1	>63.05±6.40	63.05±6.40	<1
PK-A16	>58.00±0.85	58.45±0.85	<1	>54.05±3.50	54.05±3.50	<1
PK-A17	nd	nd	nd	nd	nd	nd
PK-A18	>58.00±9.20	58.30±9.20	<1	>57.04±6.80	57.04±6.80	<1

[1] EC_{50}: concentration of compound required to achieve 50% protection of MT-4 cell cultures against HIV induced cytotoxicity, as determined by MTT method. [2] CC_{50}: concentration required to reduce the viability of mock-infected cells by 50%, as determined by MTT method. [3] SI: selectivity index (CC_{50}/EC_{50}); nd= not done.

Table 3: *In-silico* predicted physiochemical parameters of compounds PK-A1 to PK-A18

CODE	Mol. Formula	M.Wt.	log P[a]	RB[b]	HBA[c]	HBD[d]	PSA[e]	log S[f]	PCaco[g]
PK-A1	$C_{18}H_{16}FN_3O_2$	325.35	3.09	4	2	3	138.16	-4.41	1.05
PK-A2	$C_{18}H_{15}FN_4O_4$	370.33	3.00	5	4	3	142.60	-5.16	-5.16
PK-A3	$C_{18}H_{15}FN_4O_4$	370.33	3.00	5	4	3	142.60	-5.16	0.32
PK-A4	$C_{18}H_{15}FN_4O_4$	370.33	3.00	5	4	3	142.60	-5.16	0.32
PK-A5	$C_{18}H_{15}ClFN_3O_2$	359.78	3.71	4	2	3	136.78	-5.15	1.03
PK-A6	$C_{18}H_{15}ClFN_3O_2$	359.78	3.71	4	2	3	136.78	-5.15	1.03
PK-A7	$C_{18}H_{14}Cl_2FN_3O_2$	394.54	4.32	4	2	3	140.43	-5.84	0.91
PK-A8	$C_{18}H_{16}FN_3O_3$	341.35	2.79	4	3	3	139.43	-4.21	1.07
PK-A9	$C_{18}H_{16}FN_3O_3$	341.35	2.79	4	3	3	139.43	-4.21	1.07
PK-A10	$C_{19}H_{18}FN_3O_3$	355.36	3.10	5	3	3	144.92	-4.63	1.07
PK-A11	$C_{20}H_{20}FN_3O_4$	385.39	3.11	6	3	3	133.08	-4.85	1.08
PK-A12	$C_{20}H_{20}FN_3O_4$	385.39	3.11	6	3	3	133.08	-4.85	1.08
PK-A13	$C_{21}H_{22}FN_3O_5$	415.14	3.15	7	3	3	140.56	-5.03	0.43
PK-A14	$C_{20}H_{20}FN_3O_5$	401.39	2.81	6	4	4	138.76	-4.66	0.33
PK-A15	$C_{19}H_{18}FN_3O_4$	371.36	2.80	5	4	4	142.52	-4.44	0.42
PK-A16	$C_{20}H_{20}FN_3O_4$	385.39	2.81	6	4	4	136.40	-4.65	-4.65
PK-A17	$C_{20}H_{17}FN_4O_2$	364.37	3.51	4	4	4	137.88	-4.66	1.08
PK-A18	$C_{16}H_{14}FN_3O_3$	315.30	2.68	4	3	3	130.99	-3.92	0.99

[a]Partition coefficient, [b]No. of rotatable bonds, [c] No. of hydrogen bond acceptors, [d] No. of hydrogen bond donors, [e]polar surface area, [f]water solubility, [g]caco-2 permeability.

CHAPTER 6: 4-OXO-6-SUBSTITUTED PHENYL-2-THIOXO 1,2,3,4-TETRAHYDROPYRIMIDINE-5-CARBONITRILE DERIVATIVES

Pyrimidines are an important constituent of nucleic acids and many times they were used for the synthesis of antiviral, antineoplastic, antibacterial and antifungal agents as building blocks in pharmaceuticals. Likewise, the associated thiouracil derivatives are prospective therapeutics as antiviral, anticancer and antimicrobial agents. Generally, most of the anti-HIV agents like NNRTIs were synthesized by consuming pyrimidine as a common heterocyclic core but very few are reported as IN inhibitors (Jain, 2016).

Summa *et al.* explored dihydroxypyrimidine-4-carboxylic acid derivatives as HIV-1 IN inhibitors but no activity against HIV IN mediated ST was observed. Same group further reported dihydroxypyrimidine-4-carboxamides (for example, compound **I**) as potent reversible inhibitors of HIV IN (Summa, 2006; Petrocchi, 2007).

Ramajayam *et al.* synthesized and evaluated a new series of 2-phenethyl/benzylthio-6-oxo-4-phenyl-1,6-dihydropyrimidine-5-carbonitrile. They found that compound **II** inhibited both 3P and ST reactions with IC_{50} of 58 & 16 µM, respectively (Ramajayam, 2009). Novel thiobarbituric acid analogue (compound **III**) was reported to inhibit HIV-1 IN catalyzed ST reaction with an IC_{50} of 2.74 µM (Rajamaki, 2009).

Earlier, Mazumder *et al.* reported that tyrosine kinase inhibitors such as tyrphostins (compound **IV**), also inhibit both HIV-1 IN mediated 3P and ST steps at micromolar concentrations (Mazumder, 1995).

Previous series of tetrahydro pyrimidine-5-carboxamide derivatives was found to inhibit HIV-1 IN. Taking clue, it was hypothesized that 4-oxo-6-substituted phenyl-2-thioxo1,2,3,4-tetrahydropyrimidine-5-carbonitrile analogues (**PK-B1** to **PK-B14**) would also be inhibitors of HIV-1 INST. As shown in figure 2, prototype compound **PK-B** can be viewed as hybrid structure having characteristics of dihydropyrimidine derivatives **I-III** and tyrphostin **IV**.

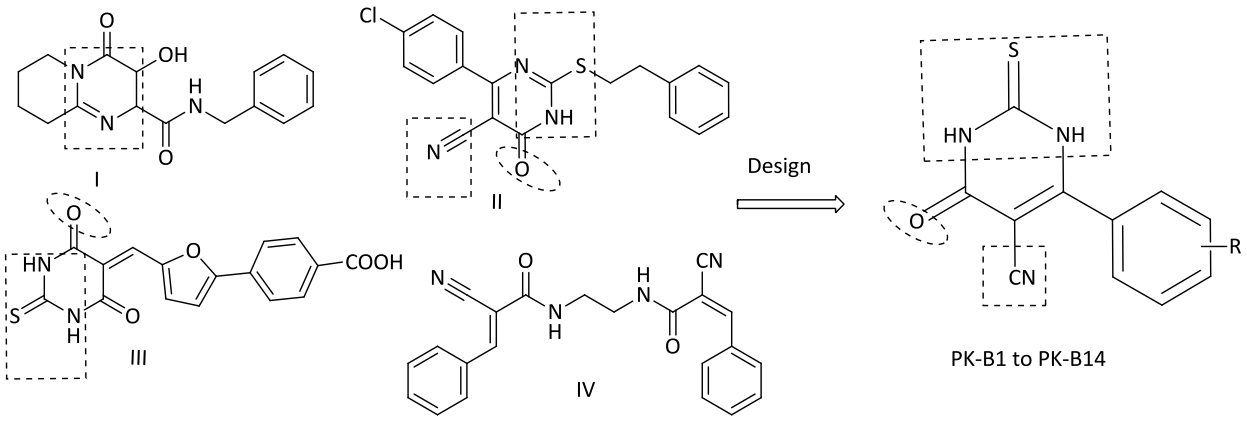

Figure 19: Derivation of 4-oxo-6-substituted phenyl-2-thioxo1,2,3,4-tetrahydropyrimidine-5-carbonitrile analogues

6.1 Chemistry

The synthetic approach (shown in **scheme 2**) adopted to obtain compounds **PK-B1** to **PK-B14** involved tertiary condensation of ethyl cyanoacetate with appropriate aldehydes and thiourea in presence of anhydrous potassium carbonate to yield corresponding tetrahydropyrimidine-5-carbonitrile analogues. In the presence of base potassium carbonate, reaction proceeds smoothly giving desired products in short time and in a quantitative yield.

The designed analogue has been developed *via* initial Knoevenagal, subsequent addition and final cyclization. In the presence of base potassium carbonate, reaction proceeds smoothly giving desired products in short time and in a quantitative yield.

The IR spectra of these compounds were characterized by the presence of NH stretching bands at 3415–3125 cm^{-1}, C≡N bands at 2210–2155 cm^{-1} along with C=O bands at 1660–1620 cm^{-1} and C=S bands at 1258–1224 cm^{-1} .

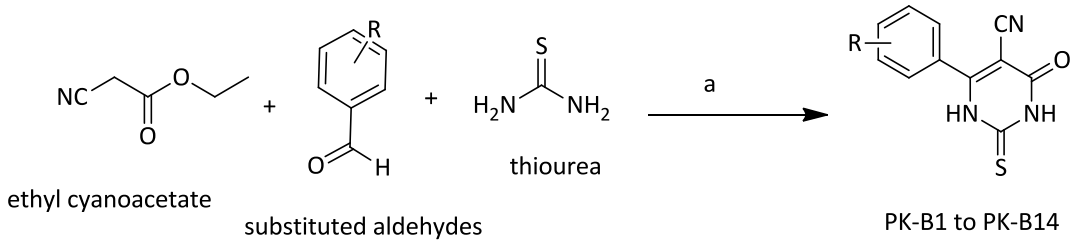

Scheme 2: Reagents and conditions: (a) potassium carbonate, ethanol and reflux.

Reaction Mechanism

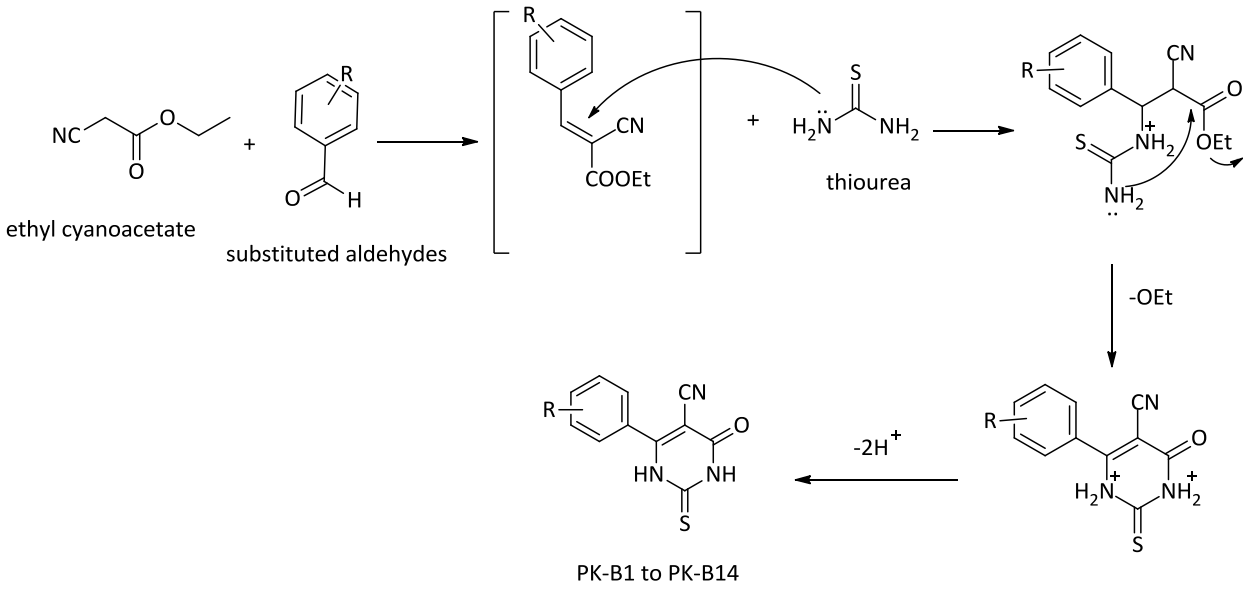

Figure 20: Plausible mechanism for synthesis of tetrahydropyrimidine-5-carbonitrile analogues

Synthesis of 4-oxo-6-substituted phenyl-2-thioxo1,2,3,4-tetrahydropyrimidine-5-carbonitrile analogues (PK-B1 to PK-B14)

In a 50 ml RBF, mixture of ethyl cyanoacetate (0.1 mol), thiourea (0.1 mol), anhydrous potassium carbonate (0.15 mol) and the appropriate aromatic aldehydes (0.1 mol) in absolute ethanol (25 mL) was refluxed for 8-12 h. The progress of reaction was monitored by thin layer chromatography (ethyl acetate: hexane; 7:3). After completion of reaction, reaction mixture was cooled to RT and then the reaction mixtures were poured in ice water and neutralized with acetic acid. The solid compound thus formed was filtered and crystallized using absolute ethanol to afford tetrahydropyrimidine-5-carbonitrile derivatives (**PK-B1** to **PK-B14**).

4-oxo-6-phenyl-2-thioxo-1,2,3,4-tetrahydropyrimidine-5-carbonitrile (PK-B1): White Solid; Yield 62%; Mp: 238-240°C; IR (KBr) cm^{-1}: 3220 ($NH_{str.}$), 3093 (Ar-$CH_{str.}$), 2245 ($CN_{str.}$), 1648 ($C=O_{str.}$), 1610(C=C), 1143 (C=S); ^{1}H-NMR (400 MHz, DMSO-d_6): δ (ppm): 7.58-7.60 (d, 2H, ArH), 7.66-7.67 (d, 2H, ArH), 7.69 (t, 1H, ArH), 13.15 (s, 1H, NH), 13.29 (s, 1H, NH); ^{13}C-NMR (100 MHz, DMSO-d_6): δ (ppm): 75.2, 114.3, 126.2, 126.5, 126.9, 127.3, 127.8, 132.4, 166.4, 169.3, 175.4; ESI-MS m/z: 230.04 $[M+H]^+$.

6-(2-nitrophenyl)-4-oxo-2-thioxo-1,2,3,4-tetrahydropyrimidine-5-carbonitrile (PK-B2): Yellow Solid; Yield 48%; Mp: 254-256°C; IR (KBr) cm^{-1}: 3229, ($NH_{str.}$), 3058 (Ar-$CH_{str.}$), 2269 ($CN_{str.}$), 1662 ($C=O_{str.}$), 1598 (C=C), 1149 (C=S); ^{1}H-NMR (400 MHz, DMSO-d_6): δ (ppm): 7.21 (d, 2H, ArH), 7.26 (t, 2H, ArH), 11.61 (s,

1H, NH), 12.15 (s, 1H, NH); ^{13}C-NMR (100 MHz, DMSO- d_6): δ (ppm): 73.1, 114.2, 126.4,126.7,126.9, 127.2, 127.6, 131.6, 166.2,167.5,172.1; ESI-MS m/z: 275.02 $[M+H]^+$.

6-(4-nitrophenyl)-4-oxo-2-thioxo-1,2,3,4-tetrahydropyrimidine-5-carbonitrile (PK-B3): Yellow Solid; Yield 51%; Mp: 253-255°C; IR (KBr) cm^{-1}: 3241, ($NH_{str.}$), 3058 (Ar-$CH_{str.}$), 2267 ($CN_{str.}$), 1668 ($C=O_{str.}$), 1624 (C=C), 1151 (C=S); ^{1}H-NMR (400 MHz, DMSO-d_6): δ (ppm): 7.73-7.74 (d, 2H, ArH), 7.75-7.76 (d, 2H, ArH), 10.34 (s, 1H, NH), 11.91 (s, 1H, NH); ^{13}C-NMR (100 MHz, DMSO- d_6): δ (ppm): 73.6, 113.9, 124.8,125.5,126.1, 126.7, 127.2, 131.7, 164.5,167.2,174.7; ESI-MS m/z: 275.06 $[M+H]^+$.

6-(2-chlorophenyl)-4-oxo-2-thioxo-1,2,3,4-tetrahydropyrimidine-5-carbonitrile (PK-B4): Pale Yellow Solid; Yield 62%; Mp: 263-265°C; IR (KBr) cm^{-1}: 3265, ($NH_{str.}$), 3071 (Ar-$CH_{str.}$), 22451 ($CN_{str.}$), 1674 ($C=O_{str.}$), 1580 (C=C), 1159 (C=S); ^{1}H NMR (DMSO -d_6) δ (ppm): 7.40-7.41 (d, 2H, ArH), 7.47-7.49 (t, 2H, ArH), 7.86 (s, 1H, NH), 10.19 (s, 1H, NH); ^{13}C-NMR (100 MHz, DMSO-d_6): δ (ppm): 75.4, 114.6, 126.5,126.7,126.8, 127.6, 127.7, 132.9, 166.6,168.8,174.6; ESI-MS m/z: 263.42 $[M+H]^+$.

6-(4-chlorophenyl)-4-oxo-2-thioxo-1,2,3,4-tetrahydropyrimidine-5-carbonitrile (PK-B5): Light Yellow Solid; Yield 56%; Mp: 260-262°C; IR (KBr) cm^{-1}: 3275, ($NH_{str.}$), 3077 (Ar-$CH_{str.}$), 2253 ($CN_{str.}$), 1657 ($C=O_{str.}$), 1560 (C=C), 1142 (C=S); ^{1}H-NMR (400 MHz, DMSO-d_6): δ (ppm): 7.20-7.22 (d, 2H, ArH), 7.26-7.28 (d, 2H, ArH), 8.96 (s, 1H, NH), 9.23 (s, 1H, NH); ^{13}C-NMR (100 MHz, DMSO-d_6): δ (ppm): 74.6, 114.7, 125.4,125.8,126.4, 126.7, 127.1, 131.7, 162.8, 170.3,173.8; ESI-MS m/z: 263.34 $[M+H]^+$.

6-(2,4-dichlorophenyl)-4-oxo-2-thioxo-1,2,3,4-tetrahydropyrimidine-5-carbonitrile (PK-B6): Light Brown Solid; Yield 60%; Mp: 264-266°C; IR (KBr) cm^{-1}: 3218, ($NH_{str.}$), 3045 (Ar-$CH_{str.}$), 2242 ($CN_{str.}$), 1662 ($C=O_{str.}$), 1619 (C=C), 1146 (C=S); ^{1}H-NMR (400 MHz, DMSO-d_6): δ (ppm): 6.33-6.35 (d, 2H, ArH), 6.48 (s, 1H, ArH), 7.23 (s, 1H, NH), 8.89 (s, 1H, NH); ^{13}C-NMR (100 MHz, DMSO-d_6): δ (ppm): 76.8, 115.8, 127.6,127.9,128.5, 128.9, 129.2, 133.5, 162.8, 169.8,176.4; ESI-MS m/z: 298.04 $[M+H]^+$.

6-(2-hydroxyphenyl)-4-oxo-2-thioxo-1,2,3,4-tetrahydropyrimidine-5-carbonitrile (PK-B7): Yellow Creamish Solid; Yield 56%; Mp: 234-236°C; IR (KBr) cm^{-1}: 3456, ($OH_{str.}$), 3257, ($NH_{str.}$), 3027 (Ar-$CH_{str.}$), 2246 ($CN_{str.}$), 1665 ($C=O_{str.}$), 1596 (C=C), 1142 (C=S); ^{1}H-NMR (400 MHz, DMSO-d_6): δ (ppm): 5.46 (s, 1H, OH), 7.06 (d, 2H, ArH), 7.26 (t, 1H, ArH), 7.45 (d, 1H, ArH), 7.81 (s, 1H, NH), 8.21 (s, 1H, NH); ^{13}C-NMR (100 MHz, DMSO-d_6): δ (ppm): 77.2, 116.3, 128.2,128.5,128.9, 129.3, 130.2, 134.6, 163.2, 171.4, 176.4; ESI-MS m/z: 246.05 $[M+H]^+$.

6-(4-hydroxyphenyl)-4-oxo-2-thioxo-1,2,3,4-tetrahydropyrimidine-5-carbonitrile (PK-B8): White Solid; Yield 53%; Mp: 239-241°C; IR (KBr) cm^{-1}: 3442, ($OH_{str.}$), 3301, ($NH_{str.}$), 3064 (Ar-$CH_{str.}$), 2256 ($CN_{str.}$), 1651 ($C=O_{str.}$), 1574 (C=C), 1160 (C=S); ^{1}H-NMR (400 MHz, DMSO-d_6): δ (ppm): 5.74 (s, 1H, OH), 6.91-6.93 (d, 2H, ArH), 7.55-7.57 (d, 2H, ArH), 10.42 (s, 1H, NH), 13.08 (s, 1H, NH); ^{13}C-NMR (100 MHz, DMSO-d_6): δ

(ppm): 73.9, 116.5, 128.1,128.4, 128.7, 129.5, 130.4, 134.8, 164.4, 174.4, 176.8; ESI-MS m/z: 246.06 $[M+H]^+$.

6-(2,5-dimethoxyphenyl)-4-oxo-2-thioxo-1,2,3,4-tetrahydropyrimidine-5-carbonitrile (PK-B9): Yellow Solid, Yield 47%, mp 271-273°C; IR (KBr) cm^{-1}: 3288, ($NH_{str.}$), 3038 (Ar-$CH_{str.}$), 2257 ($CN_{str.}$), 1681 ($C=O_{str.}$), 1621 (C=C), 1140 (C=S); ^{1}H-NMR (400 MHz, DMSO-d_6): δ (ppm): 3.94-3.98 (s, 6H, OCH_3), 7.03 (s, 1H, ArH), 7.40-7.42 (d, 2H, ArH), 7.88 (s, 1H, NH), 8.18 (s, 1H, NH); ^{13}C-NMR (100 MHz, DMSO-d_6): δ (ppm): 55.4, 56.8, 74.6, 110.5, 111.8, 115.8, 117.8, 145.8, 148.7, 164.8, 168.2, 177.5; ESI-MS m/z: 290.14 $[M+H]^+$.

4-oxo-2-thioxo-6-(3,4,5-trimethoxyphenyl)-1,2,3,4-tetrahydropyrimidine-5-carbonitrile (PK-B10): White Solid; Yield 62%; Mp: 290-292°C; IR (KBr) cm^{-1}: 3289, ($NH_{str.}$), 3058 (Ar-$CH_{str.}$), 2258 ($CN_{str.}$), 1674 ($C=O_{str.}$), 1641 (C=C), 1152 (C=S); ^{1}H-NMR (400 MHz, DMSO-d_6): δ (ppm): 3.83-3.86 (s, 9H, OCH_3), 7.14 (s, 1H, ArH), 7.23 (s, 1H, ArH), 7.61 (s, 1H, NH), 8.10 (s, 1H, NH); ^{13}C-NMR (100 MHz, DMSO- d_6): δ (ppm): 55.4, 56.8, 58.2, 77.8, 112.5, 114.8, 115.6, 147.2, 148.8, 149.3, 164.2, 167.9, 178.2; ESI-MS m/z: 320.03 $[M+H]^+$.

6-(4-hydroxy-3,5-dimethoxyphenyl)-4-oxo-2-thioxo-1,2,3,4-tetrahydropyrimidine-5-carbonitrile (PK-B11): Yellow Solid; Yield 64%; Mp: 282-284°C; IR (KBr) cm^{-1}: 3416, ($OH_{str.}$), 3269, ($NH_{str.}$), 3074 (Ar-$CH_{str.}$), 2274 ($CN_{str.}$), 1678 ($C=O_{str.}$), 1543 (C=C), 1141 (C=S); ^{1}H-NMR (400 MHz, DMSO-d_6): δ (ppm): 3.82-3.84 (s, 6H, OCH_3), 5.32 (s, 1H, OH), 7.56 (s, 1H, ArH), 7.57 (s, 1H, ArH), 8.26 (s, 1H, NH), 8.27 (s, 1H, NH); ^{13}C-NMR (100 MHz, DMSO-d_6): δ (ppm): 55.8, 56.2, 74.3, 111.3, 113.2, 114.6, 116.5, 146.6, 151.7, 169.2, 172.7, 179.5; ESI-MS m/z: 306.09 $[M+H]^+$.

6-(3-ethoxy-4-hydroxyphenyl)-4-oxo-2-thioxo-1,2,3,4-tetrahydropyrimidine-5-carbonitrile (PK-B12): Brown Solid; Yield 57%; Mp: 276-278°C; IR (KBr) cm^{-1}: 3465, ($OH_{str.}$), 3218, ($NH_{str.}$), 3037 (Ar-$CH_{str.}$), 2987 (Ali $CH_{str.}$), 2248 ($CN_{str.}$), 1662 ($C=O_{str.}$), 1542 (C=C), 1135 (C=S); ^{1}H-NMR (400 MHz, DMSO-d_6): δ (ppm): 1.35-1.37 (t, 3H, CH_3), 4.01-4.03 (d, 2H, OCH_2), 5.15 (s, 1H, OH), 7.04 (d, 1H, ArH), 7.14 (d, 1H, ArH), 7.52 (s, 1H, NH), 8.01 (s, 1H, NH); ^{13}C-NMR (100 MHz, DMSO-d_6): δ (ppm): 15.9, 65.8, 78.2, 110.9, 114.2, 119.6, 125.4, 147.4, 147.9, 162.7, 167.8, 172.4; ESI-MS m/z: 290.18 $[M+H]^+$.

6-(4-(dimethylamino)phenyl)-4-oxo-2-thioxo-1,2,3,4-tetrahydropyrimidine-5-carbonitrile (PK-B13): Yellow Solid; Yield 65%; Mp: 263-265°C; IR (KBr) cm^{-1}: 3274, ($NH_{str.}$), 3064 (Ar-$CH_{str.}$), 2940 (Ali $CH_{str.}$), 2243 ($CN_{str.}$), 1669 ($C=O_{str.}$), 1534 (C=C), 1128 (C=S); ^{1}H-NMR (400 MHz, DMSO-d_6): δ (ppm): 3.15-3.17 (s, 36, CH_3), 6.71-6.73 (d, 2H, ArH), 7.97-7.99 (d, 2H, ArH), 7.52 (s, 1H, NH), 8.01 (s, 1H, NH), 8.11 (s, 1H, NH); ^{13}C-NMR (100 MHz, DMSO-d_6): δ (ppm): 47.4, 47.4, 76.4, 112.2, 112.5, 115.7, 123.4, 128.2, 151.3, 162.4, 166.3, 171.9; ESI-MS m/z: 271.09 $[M+H]^+$.

6-(1*H*-indol-3-yl)-4-oxo-2-thioxo-1,2,3,4-tetrahydropyrimidine-5-carbonitrile (PK-B14): Creamish Yellow Solid; Yield 61%; Mp: 269-271°C; IR (KBr) cm^{-1}: 3365, ($NH_{str.}$), 3288, ($NH_{str.}$), 3047 (Ar-$CH_{str.}$), 2925 (Ali $CH_{str.}$), 2245 ($CN_{str.}$), 1673 ($C=O_{str.}$), 1550 (C=C), 1139 (C=S); ^{1}H-NMR (400 MHz, DMSO-d_6): δ (ppm): 6.35 (s, 1H, ArH), 7.01-7.63 (m, 4H, ArH), 7.59 (s, 1H, NH), 8.34 (s, 1H, NH), 8.66 (s, 1H, NH); ^{13}C-NMR (100 MHz, DMSO-d_6): δ (ppm): 76.1, 107.8, 112.5, 115.7, 122.4, 122.5, 126.8, 128.2, 138.4, 166.8, 169.2, 178.1; ESI-MS m/z: 269.08 $[M+H]^{+}$.

6.2 Results and Discussion

The outcomes of *in vitro* study as well as Gscore of designed compounds with dolutegravir as standard drug are shown in **table 4**. Further, the results of cytoxicity and anti-HIV assay are shown in **table 5**. Dolutegravir showed hydrogen bonding interactions with Cys 65, Thr 66, His 67, Asn 155, Lys 156 and Lys 159. Hydrophobic interactions with Asp 64, Asp 116, Gln 148, Glu 152, Asn 155, Lys 156, Lys 159 and metal coordination with Mg 1001 were also observed.

All 4-oxo-6-substituted phenyl-2-thioxo1,2,3,4-tetrahydropyrimidine-5-carbonitrilederivatives (**PK-B1** to **PK-B14**) displayed consistent HIV-1 IN inhibition profile. Compound **PK-B1** having unsubstituted phenyl ring inhibited IN moderately and displayed hydrogen bonding interactions with Cys 65 (via –NH at C-3), Thr 66 (by thio group) and Glu 152 (via –NH at C-1). Hydrophobic interactions with Asp 64, Asp 116, Gln 148, Glu 152, Asn 155 and metal coordination with Mg 1001 (via –C=O of pyrimidine ring) were also observed. It showed 65.82% inhibition of HIV IN at 10 µM concentration.

Substitution of electron withdrawing nitro group either at ortho (**PK-B2**) or para position (**PK-B3**) reduced the docking score as well as % inhibition. In silico, it showed absence of hydrogen bonding with Glu 152 as also hydrophobic interactions with Asp 64, Asp 116, and Gln 148 as compared to **PK-B1**. Similarly, substitution of chloro group at *o* position (**PK-B4**) showed comparable interactions (except for absence of hydrophobic interactions with Gln 148 and Glu 152) as well as % inhibition to that of **PK-B1**.

However, *p*-chloro substitution (**PK-B5**) showed significant improvement in activity and it was most active compound in the series. It showed 84.18 % inhibition of HIV IN at 10 µM concentration. This is may be because of hydrogen bonding interactions with Cys 65 (*via* –NH at C-3 position and –C=O at C-4 position of pyrimidine ring, respectively), Thr 66 and Lys 156 (*via* –C=S at C-2 position of pyrimidine ring), Glu 152 (via –NH at C-1 position of pyrimidine ring) and Asp 64, Gln 148 and Glu 152. The metal coordination bond with Mg 1001 (via –C=O at C-4 position of pyrimidine ring) was also seen. It was hypothesized that by having both- *o*- and *p*- Chloro substitution (**PK-B6**) may enhance the activity but it pushes the pyrimidine ring away from catalytic site. It displayed absence of any interactions with DDE

motif and hence it showed less docking score as well as activity than either **PK-B4** or **PK-B5**. Thus, it was clear indication that only substitution at 4th position is favored. Substitution of electron donating groups also showed similar trend.

Substitution of hydroxy group at *o*- position (**PK-B7)** showed reduction in activity as compared to **PK-B1**. However, *p*-hydroxy substitution (**PK-B8)** showed highest docking score (GScore -6.39) and more than 70% HIV-1 IN inhibition. In silico, hydrogen bonding interactions with Gln 148 (via *p*-OH), Glu 152 (via –NH at C-1 position of pyrimidine ring), Lys 156 and Lys 159 (via –C=S at C-2 position of pyrimidine ring) were seen along with other hydrophobic interactions with Asp 64, His 67 and Asn 155.

After analyzing the results of **PK-B8**, next logical step was to check the effect of di- or tri- substitution on activity and for this purpose, compounds **PK-B9** (having 2,5-dimethoxy substitution) and **PK-B10** (having 3,4,5-trimethoxy substitution) were thought of. It was observed that there is slight decrease in activity as well as docking score, which prompted us not to change hydroxyl at 4th position and make changes at 3 or 5 positions. Compounds **PK-B11** (having 3,5-dimethoxy substitution) and **PK-B12** (having 3-ethoxy substitution) with hydroxyl at 4 position were found to have further reduction in activity as well as docking score, even less than that of compound **PK-B1**.

Substitution of *N,N*-dimethyl group at para position (**PK-B13**) drastically reduces the docking interactions as well as activity. Moreover, replacing the substituted phenyl ring with fused ring like indole (compound **PK-B14**), although having hydrogen bonding interactions with Cys 65 (via –NH at C-1 position of pyrimidine ring), Thr 66 via –C=S at C-2 position of pyrimidine ring) and hydrophobic interactions with Asp 64, Gln 148 and Asn 155; did not interact with DDE motif. It was seen that the indole ring was more or less solvent exposed, which might be the reason for less docking score as well as IN inhibitory activity. Thus, only substitution at 4th position is favored and substitution at other positions reduced the activity as well as in silico interactions. Overall, compounds having unsubstituted phenyl (**PK-B1**) and para substitution (**PK-B5** and **PK-B8**) exhibited significant IN inhibitory activity. These were further tested for calculation of IC_{50} values (given in table 3). It was observed that compound **PK-B5** was most active with IC_{50} value 2.31 µM.

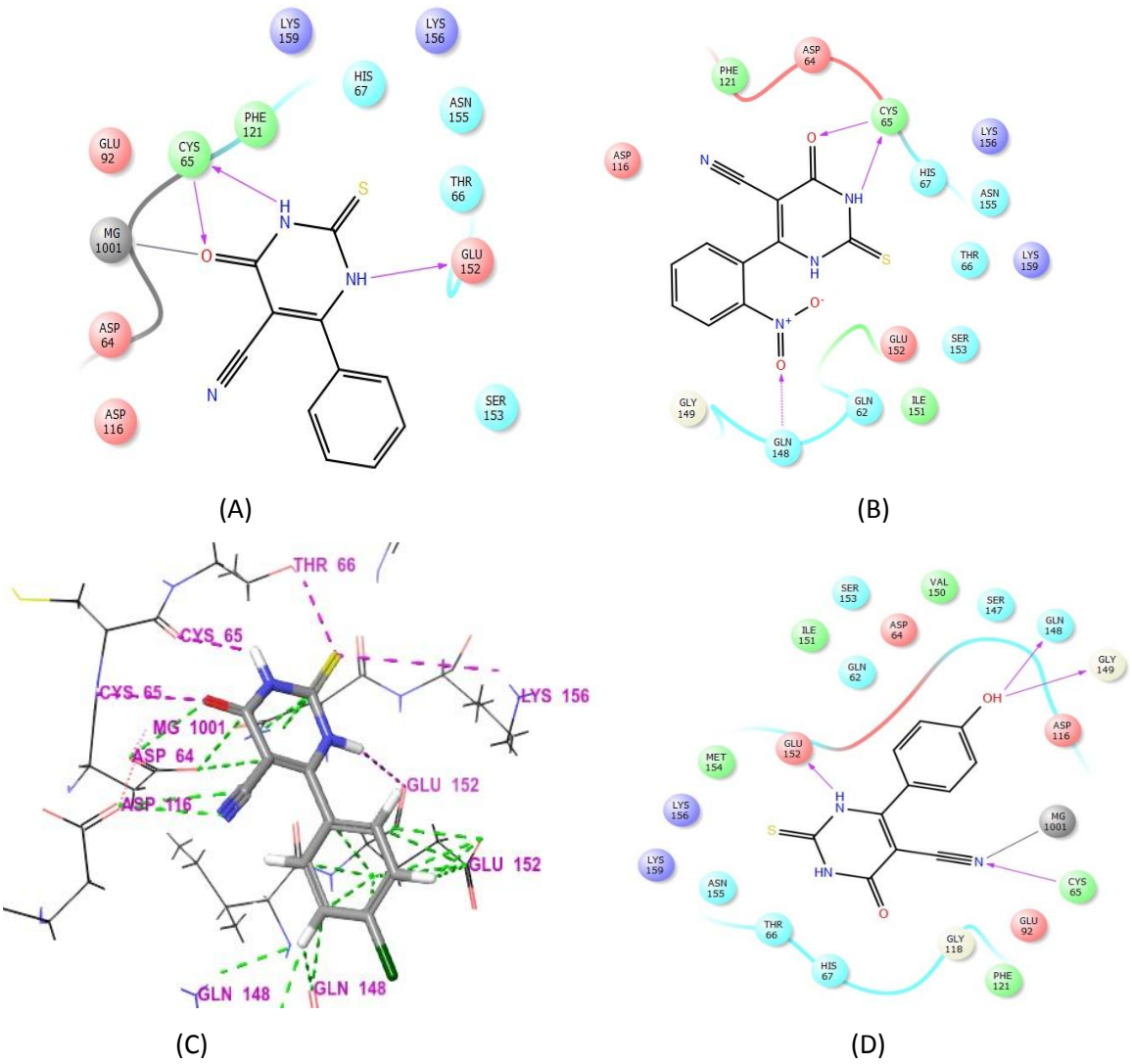

Figure 21: Docking poses of few representative compounds A: 2D interaction plot of PK-B1; B: 2D interaction plot of PK-B2; C: 3D interaction plot of PK-B5; 2D docking pose of PK-B8

Table 4: Docking Score and Inhibition of HIV-1 IN by tetrahydropyrimidine-5-carbonitrile analogues (PK-B1 to PK-B14)

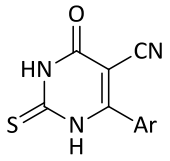

Code	Ar	DOCKING SCORE	% IN INHIBITION*	IC_{50} value**
Dolutegravir	----------	-7.3	95.00	nd
PK-B1	Ph	-5.60	65.82	7.45±0.9
PK-B2	2-NO_2-Ph	-5.37	41.50	nd
PK-B3	4-NO_2-Ph	-5.41	41.84	nd
PK-B4	2-Cl-Ph	-5.53	60.18	nd
PK-B5	4-Cl-Ph	-5.84	84.18	2.31±0.61
PK-B6	2,4-diCl-Ph	-5.44	49.19	nd
PK-B7	2-OH-Ph	-5.39	42.71	nd
PK-B8	4-OH-Ph	-6.39	71.92	6.24±0.29
PK-B9	2,5-diOMe-Ph	-5.62	69.31	nd
PK-B10	3,4,5-triOMe-Ph	-5.56	66.75	nd
PK-B11	4-OH-3,5-diOMe-Ph	-5.51	55.72	nd
PK-B12	4-OH-3-OEt-Ph	-5.49	53.21	nd
PK-B13	4-(*N,N*-diCH_3)-Ph	-5.38	42.72	nd
PK-B14	1H-indol-3-yl	-5.47	50.25	nd

*Percentage inhibition at 10µM concentration, values are mean of duplicate experiment performed independently; nd: not done; ** in µM.

After evaluating in silico and in vitro results, all the compounds were investigated for anti-HIV activity against HIV-1 (III_B) and HIV-2 (ROD) in cell based assay. It was, however, observed that no compound showed anti-HIV activity below their cytotoxic concentration (as shown in **table 5**). The compounds showed very good potential in vitro however, in cell culture assay, the activity was absent. However, the results of cytotoxicity assay indicate that these compounds can be tapped for their cytotoxic potential.

Table 5: Anti-HIV activity of synthesized compounds PK-B1 to PK-B14

Compounds	HIV-1 (III_B)			HIV-2 (ROD)		
	EC_{50}[1] (µM)	CC_{50}[2] (µM)	HIV-1[3] SI	EC_{50}[1] (µM)	CC_{50}[2] (µM)	HIV-2[3] SI
Dolutegravir	0.0006±0.000001	1.275±0.3	2110.00	0.00232±0.00061	1.495±0.165	597.00
PK-B1	>10.80±0.60	10.80±0.60	<1	>10.50±0.69	10.50±0.69	<1
PK-B2	>12.05±2.05	12.05±2.05	<1	>13.51±1.98	13.51±1.98	<1
PK-B3	>92.55±13.40	92.55±13.40	<1	>99.81±10.60	99.81±10.60	<1
PK-B4	>100.50±4.50	100.50±4.50	<1	>95.72±6.44	95.72±6.44	<1
PK-B5	>92.05±8.95	92.05±8.95	<1	>91.85±7.85	91.85±7.85	<1
PK-B6	>35.15±15.20	35.15±15.20	<1	>39.95±10.14	39.95±10.14	<1
PK-B7	>64.25±9.45	64.25±9.45	<1	>74.25±8.60	74.25±8.60	<1
PK-B8	>69.95±1.75	69.95±1.75	<1	>66.91±2.62	66.91±2.62	<1
PK-B9	>125.00±0.65	125.00±0.65	<1	>102.12±4.23	102.12±4.23	<1
PK-B10	>71.20±1.40	71.20±1.40	<1	>69.87±1.86	69.87±1.86	<1
PK-B11	>113.00±12.00	113.00±12.00	<1	>125.00±2.60	125.00±2.60	<1
PK-B12	>66.55±4.55	66.55±4.55	<1	>62.15±0.3	62.15±0.3	<1
PK-B13	>47.75±1.65	47.75±1.65	<1	>42.15±4.50	42.15±4.50	<1
PK-B14	>58.10±2.00	58.10±2.00	<1	>41.95±4.65	41.95±4.65	<1

[1] EC_{50}: concentration of compound required to achieve 50% protection of MT-4 cell cultures against HIV induced cytotoxicity, as determined by MTT method. [2] CC_{50}: concentration required to reduce the viability of mock-infected cells by 50%, as determined by MTT method. [3] SI: selectivity index (CC_{50}/EC_{50}).

6.3 Oral bioavailability and toxicity prediction

Designed molecules of tetrahydropyrimidine-5-carbonitrile series were subjected to *in silico* oral bioavailability. All the compounds fulfilled the criteria for Lipinski rule of five. LogP of these derivatives varied from 1.68 to 3.28. The polar surface area was found to be in range of 96.20 to 130.64 and water solubility (log S) was in range of -2.99 to -4.66 log mol/L. The results are shown in **table 6**.

Table 6: *In silico* predicted physiochemical parameters of compounds PK-B1 to PK-B14

CODE	Mol.Formula	M.Wt.	log P[a]	RB[b]	HBA[c]	HBD[d]	PSA[e]	log S[f]	PCaco[g]
PK-B1	$C_{11}H_7N_3OS$	229.03	1.97	1	3	2	96.20	-2.99	0.99
PK-B2	$C_{11}H_6N_4O_3S$	274.02	1.88	2	5	2	110.86	-4.06	0.03
PK-B3	$C_{11}H_6N_4O_3S$	274.02	1.88	2	5	2	110.86	-3.82	-0.02
PK-B4	$C_{11}H_6ClN_3OS$	262.99	2.62	1	3	2	106.51	-3.77	0.96
PK-B5	$C_{11}H_6ClN_3OS$	262.99	2.62	1	3	2	106.51	-3.77	0.96
PK-B6	$C_{11}H_5Cl_2N_3OS$	296.95	3.28	1	3	2	116.81	-4.60	0.94
PK-B7	$C_{11}H_7N_3O_2S$	245.03	1.68	1	4	3	101.00	-3.09	-0.29
PK-B8	$C_{11}H_7N_3O_2S$	245.03	1.68	1	4	3	101.00	-3.09	-0.29
PK-B9	$C_{13}H_{11}N_3O_3S$	289.05	1.99	3	5	2	119.16	-3.75	1.02
PK-B10	$C_{14}H_{13}N_3O_4S$	319.06	2.00	3	6	2	130.64	-4.14	0.16
PK-B11	$C_{13}H_{11}N_3O_4S$	305.05	1.69	3	6	3	123.96	-3.93	-0.27
PK-B12	$C_{13}H_{11}N_3O_3S$	289.05	2.08	3	5	3	118.84	-3.77	0.18
PK-B13	$C_{13}H_{12}N_4OS$	272.07	2.04	2	4	2	114.70	-3.55	1.01
PK-B14	$C_{13}H_8N_4OS$	268.04	2.45	1	3	3	112.10	-3.81	0.97

[a]Partition coefficient, [b]No. of rotatable bonds, [c] No. of hydrogen bond acceptors, [d] No. of hydrogen bond donors, [e]polar surface area, [f]water solubility, [g]caco-2 permeability.

CHAPTER 7: TETRAHYDROQUINAZOLINE-2,5(1*H*,6*H*)- DIONE DERIVATIVES

Among several attempts to develop IN inhibitors (**I-III**), the keto-enol acid class (generally represented to as the diketo acid class) of compounds has been most aggressively considered because of the noticeable anti HIV activities revealed. Since the keto-enol acid compounds often showed adverse hepatic effects (Hajimahdi, 2013), there is an attempt to find new replacement for keto-enol acid motif. Earlier, various derivatives were synthesized having different basic aromatic heterocycle bearing a lone pair donor atom, such as a thiazolothiazepines **IV**, Styrylquinazoline derivatives **V**, furoyl pyrazolones **VI**, C-methyl chalcones **VII** and 1,3,4-oxadiazole- and 1,3,4-thiadiazole **VIII** as a part of the metal chelation (Lee, 2002,Hajimahdi, 2013; Babu, 2014).

Quinazoline derivates have been reported to have diverse pharmacological properties such as analgesic, anticancer, anticonvulsant, antidepressant, antifungal, hypolipidemic, antiHIV, antiinflammatory, antimicrobial, antitubercular and antiulcer (Hajimahdi, 2013; He, 2017). Based on structural requirements for IN inhibition and considering that quinzaolines have not been explored, we synthesized quinazolinones derivatives (**PK-C1** to **PK-C14**) as HIV-1 integrase inhibitors. It was hypothesized that carbonyl group on position 2 would bind with mangensium and aromatic ring on 4th position would be placed in hydrophobic pocket of enzyme. Investigating the effect of changing substituents on 4-phenyl ring of the quinazoline subunit on IN inhibition was also planned (as general structure shown in Figure 22).

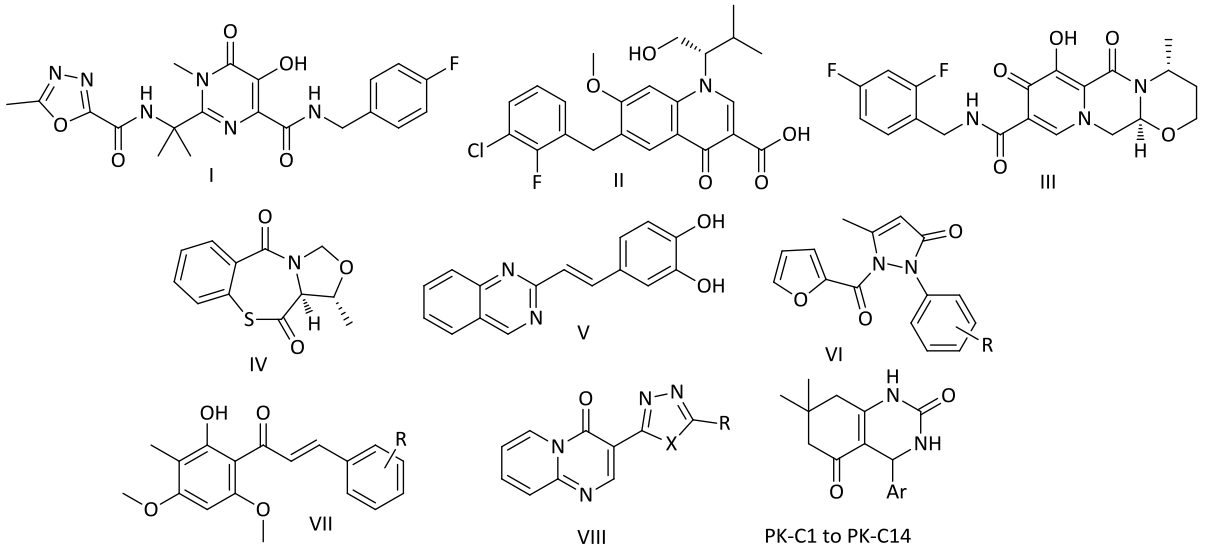

Figure 22: Literature reported HIV-1 IN inhibitors and general structure of designed molecule (PK-C1 to PK-C14)

7.1 Chemistry

Target compounds (**PK-C1** to **PK-C14**) were prepared by three step reaction illustrated in Scheme 3. First step involves Michael addition of dimethyl malonate with mesityl oxide under basic condition, followed by hydrolysis of intermediate to yield 5,5-dimethyl-1,3-cyclohexanedione, or "dimedone", in step 2. Final step was carried out under solvent free condition by condensing dimedone, urea and substituted aromatic aldehydes under reflux condition. All the synthesized compounds were purified using column chromatography. Purified compounds were characterized by spectral analysis.

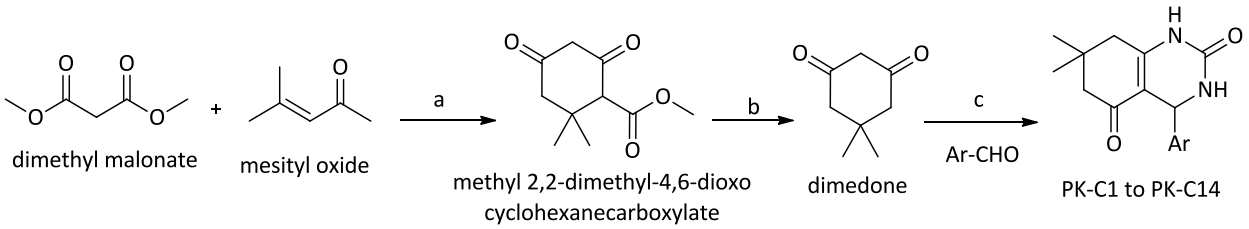

Scheme 3: Reagents and conditions: (a) Sodium methoxide, methanol, 5 h, reflux (b) 4M sodium hydroxide, 6N hydrochloric acid, 1.5 h, reflux (c) urea, hydrochloric acid, 2.5-4.5 h, reflux

Reaction Mechanism

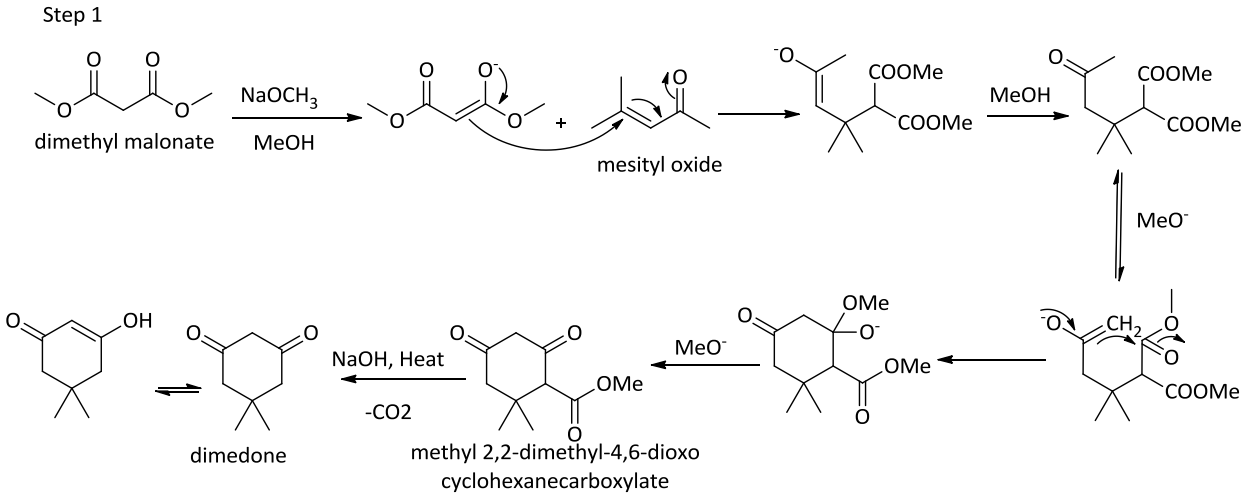

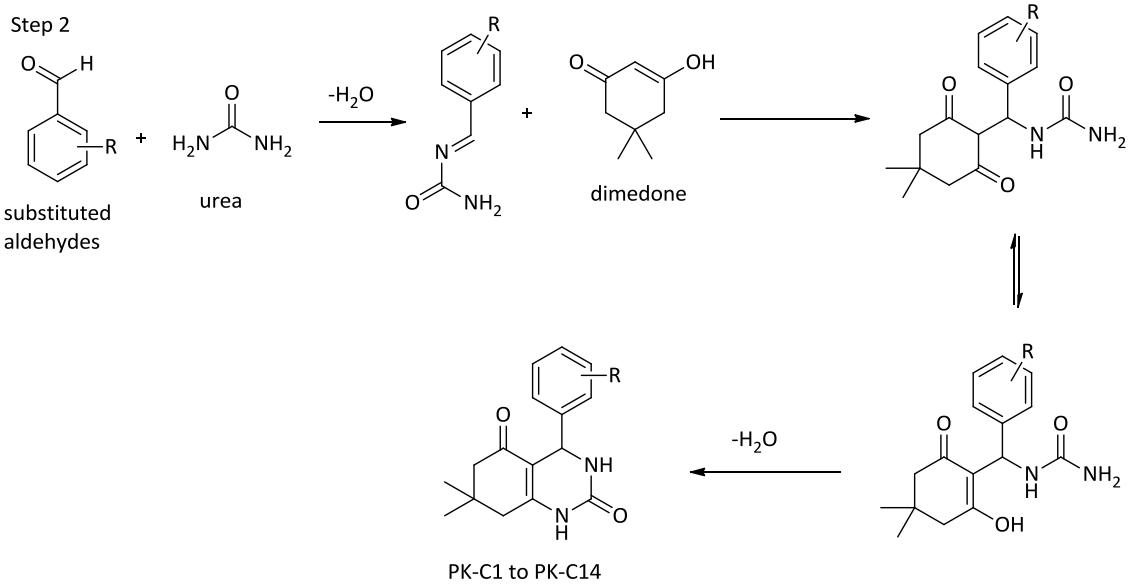

Figure 23: Reaction mechanism of tetrahydroquinazoline-2,5(1*H*,6*H*)-dione analogues (PK-C1 to PK-C14)

Synthesis of methyl 2,2-dimethyl-4,6-dioxocyclohexanecarboxylate

In a two necked 100 ml RBF fitted with a magnetic stirbar and reflux condenser with $CaCl_2$ drying tube, sodium methoxide (1.5 g) was dissolved in methanol (15 ml). Then dimethyl malonate (10.6 ml) with a boiling stone was added. The reaction mixture was refluxed for 4 hrs. After this, heating source was carefully removed and reaction mass was allowed to cool to room temperature (RT). Mesityl oxide (11,3 ml) dissolved in methanol (5 ml) was added slowly *via* syringe. The reaction mixture was again refluxed for 45 minutes. The progress of the reaction was monitored by TLC (ethyl acetate: hexane; 2:8). After completion of reaction, solvent was removed under vacuum at 50^{o}C. The crude methyl ester precipitate was used as such for next step. Brown yellow solid; Yield 70%; Mp: 105–107°C; IR (KBr) cm^{-1}: 2962 ($CH_{str.}$), 1710, 1735 ($C{=}O_{str.}$); ^{1}H-NMR (400 MHz, DMSO-d_6): δ (ppm): 1.05 (s, 6H), 2.30 (dd, 2H), 3.25 (s, 1H), 3.45 (dd, 2H), 3.75 (s, 3H); ^{13}C-NMR (100 MHz, DMSO-d_6): δ (ppm): 16.5, 25.8, 52.9, 58.4, 60.5, 72.4, 165.7, 203.8 and 208.4; EI-MS (m/z): 199.04 $[M+H]^{+}$.

b. Synthesis of 5,5-dimethylcyclohexane-1,3-dione

To a 100 ml RBF, methyl 2,2-dimethyl-4,6-dioxocyclohexanecarboxylate (1.0 g) was dissolved in 10 ml ethanol and water mixture (1: 1). Then 15 ml of 4M sodium hydroxide was added and solution was refluxed for 1.5 hr. Reaction mixture was cooled to RT and slowly poured into beaker containing 15 ml of 6N HCl. The beaker was kept into ice bath for half an hour. Completion of reaction was monitored by TLC (ethyl acetate: hexane; 3:7). The solution was filtered and dried. The crude material was crystallized using acetone and collected as yellow crystals (0.75 g). Yield 78%; Mp: 150–152°C; IR (KBr) cm^{-1}:

2984($CH_{str.}$), 1715, 1728 ($C=O_{str.}$); ^{1}H-NMR (400 MHz, DMSO-d_6): δ (ppm): 1.02-1.03 (s, 6H), 2.29-2.30 (dd, 2H), 3.27 (s, 1H), 3.43 (dd, 2H); ^{13}C-NMR (100 MHz, DMSO-d_6): δ (ppm): 29.7, 29.8, 32.4, 54.9, 55.1, 58.8, 204.2 and 204.4; EI-MS (m/z): 141.10 [M+H]+.

Synthesis of 7,7-dimethyl-4-substituted phenyl-3,4,7,8-tetrahydroquinazoline-2,5(1*H*,6*H*)-dione analogues (PK-C1 to PK-C14)

In a 50 ml RBF, a mixture of aromatic aldehydes (0.5 g), dimedone (,0.75 g), urea (0.5 g) and 3-4 drops of concentrated hydrochloric acid was mixed and refluxed for appropriate time as mentioned in table 7. The progress of completion of reaction was monitored by thin layer chromatography (ethyl acetate: hexane; 7:3). After completion of reaction, reaction mixture was cooled to RT and ice cold water (15 ml) was added. The solid compound thus formed was filtered and crystallized from absolute ethanol to afford the pure corresponding octahydroquinazolinone derivatives (**PK-C1 to PK-C14**) in 55-75 % yields, as shown in **table 7**. All the products were characterized using their spectral data. The synthetic procedure was modified of the literature protocol (Ladani, 2009).

7,7-dimethyl-4-phenyl-3,4,7,8-tetrahydroquinazoline-2,5(1*H*,6*H*)-dione (PK-C1): Dark Brown Solid; IR (KBr) cm^{-1}: 3274, 3175 ($NH_{str.}$), 3097 (Ar-$CH_{str.}$), 2962 (Ali $CH_{str.}$), 1692 ($C=O_{str.}$), 1634 (C=C); ^{1}H-NMR (400 MHz, $CDCl_3$ + DMSO-d_6, 1:1): δ (ppm): 0.96 (s, 3H, 7-Me), 1.03 (s, 3H, 7-Me), 2.02 (s, 2H, CH_2), 2.28 (s, 2H, CH_2), 5.12 (d, 1H, CH), 7.25 -7.37 (m, 5H, ArH), 7.88 (s, I H, NH), 9.36 (s, I H, NH); ^{13}C-NMR (100 MHz, $CDCl_3$ + DMSO-d_6, 1:1): δ (ppm): 27.4, 29.7, 32.8, 40.2, 50.3, 53.8, 107.9, 126.7, 127.2, 128.1, 145.3, 152.2, 152.8 and 193.2; ESI-MS m/z: 271.14 $[M+H]^+$.

7,7-dimethyl-4-(2-nitrophenyl)-3,4,7,8-tetrahydroquinazoline-2,5(1*H*,6*H*)-dione (PK-C2): Pale Yellow Solid; IR (KBr) cm^{-1}: 3324, 3198 ($NH_{str.}$), 3074 (Ar-$CH_{str.}$), 2981 (Ali $CH_{str.}$), 1690 ($C=O_{str.}$), 1629 (C=C); ^{1}H-NMR (400 MHz, $CDCl_3$ + DMSO-d_6, 1:1): δ (ppm): 0.94 (s, 3H, 7-Me), 1.01 (s, 3H, 7-Me), 2.06 (s, 2H, CH_2), 2.24 (s, 2H, CH_2), 5.14 (d, IH, CH), 7.21 -7.30 (m, 4H, ArH), 7.83 (s, I H, NH), 9.31 (s, I H, NH); ^{13}C-NMR (100 MHz, $CDCl_3$ + DMSO-d_6, 1:1): δ (ppm): 27.4, 29.5, 32.8, 40.1, 50.3, 53.8, 108.2, 126.6, 127.1, 128.9, 145.8, 152.2, 152.9 and 193.4; ESI-MS m/z: 316.24 $[M+H]^+$.

7,7-dimethyl-4-(3-nitrophenyl)-3,4,7,8-tetrahydroquinazoline-2,5(1*H*,6*H*)-dione (PK-C3): Yellow Solid; IR (KBr) cm^{-1}: 3347, 3208 ($NH_{str.}$), 3041 (Ar-$CH_{str.}$), 2989 (Ali $CH_{str.}$), 1698 ($C=O_{str.}$), 1610 (C=C); ^{1}H-NMR (400 MHz, $CDCl_3$ + DMSO-d_6, 1:1): δ (ppm): 0.97 (s, 3H, 7-Me), 1.04 (s, 3H, 7-Me), 2.04 (s, 2H, CH_2), 2.21 (s, 2H, CH_2), 5.13 (d, IH, CH), 7.18 -7.27 (m, 4H, ArH), 7.84 (s, I H, NH), 9.34 (s, I H, NH); ^{13}C-NMR (100 MHz, $CDCl_3$ + DMSO-d_6, 1:1): δ (ppm): 27.6, 29.4, 32.7, 40.2, 50.4, 53.6, 108.3, 126.9, 127.4, 128.5, 144.4, 151.9, 153.3 and 192.8; ESI-MS m/z: 316.26 $[M+H]^+$.

7,7-dimethyl-4-(4-nitrophenyl)-3,4,7,8-tetrahydroquinazoline-2,5(1*H*,6*H*)-dione (PK-C4): Pale Yellow Solid; IR (KBr) cm^{-1}: 3304, 3241 ($NH_{str.}$), 3018 (Ar-$CH_{str.}$), 2971 (Ali $CH_{str.}$), 1694 (C=$O_{str.}$), 1627 (C=C); ^{1}H-NMR (400 MHz, $CDCl_3$ + DMSO-d_6, 1:1): δ (ppm): 0.95 (s, 3H, 7-Me), 1.06 (s, 3H, 7-Me), 2.01 (s, 2H, CH_2), 2.27 (s, 2H, CH_2), 5.19 (d, IH, CH), 7.22 -7.33 (m, 4H, ArH), 7.89 (s, I H, NH), 9.37 (s, I H, NH); ^{13}C-NMR (100 MHz, $CDCl_3$ + DMSO-d_6, 1:1): δ (ppm): 26.9, 28.8, 31.4, 41.2, 51.6, 52.9, 109.4, 127.4, 128.2, 129.1, 144.6, 152.6, 153.1 and 194.2; ESI-MS m/z: 316.26 $[M+H]^+$.

4-(2-chlorophenyl)-7,7-dimethyl-3,4,7,8-tetrahydroquinazoline-2,5(1*H*,6*H*)-dione (PK-C5): Creamish White Solid; IR (KBr) cm^{-1}: 3287, 3209 ($NH_{str.}$), 3058 (Ar-$CH_{str.}$), 2965 (Ali $CH_{str.}$), 1686 (C=$O_{str.}$), 1549 (C=C); ^{1}H-NMR (400 MHz, $CDCl_3$ + DMSO-d_6, 1:1): δ (ppm): 1.02 (s, 3H, 7-Me), 1.04 (s, 3H, 7-Me), 2.08 (s, 2H, CH_2), 2.36 (s, 2H, CH_2), 5.63 (d, IH, CH), 7.24 -7.31 (m, 4H, ArH), 7.35 (s, I H, NH), 9.21 (s, I H, NH); ^{13}C-NMR (100 MHz, $CDCl_3$ + DMSO-d_6, 1:1): δ (ppm): 26.4, 27.7, 31.5, 40.2, 49.3, 50.4, 52.1, 105.4, 126.2, 127.5, 127.6, 131.1, 150.1, 154.1 and 192.4; ESI-MS m/z: 305.79 $[M+H]^+$.

4-(4-chlorophenyl)-7,7-dimethyl-3,4,7,8-tetrahydroquinazoline-2,5(1*H*,6*H*)-dione (PK-C6): White Solid; IR (KBr) cm^{-1}: 3369, 3248 ($NH_{str.}$), 3098 (Ar-$CH_{str.}$), 2947 (Ali $CH_{str.}$), 1686 (C=$O_{str.}$), 1604 (C=C); ^{1}H-NMR (400 MHz, $CDCl_3$ + DMSO-d_6, 1:1): δ (ppm): 0.99 (s, 3H, 7-Me), 1.01 (s, 3H, 7-Me), 2.02 (s, 2H, CH_2), 2.31 (s, 2H, CH_2), 5.67 (d, IH, CH), 7.20 -7.27 (m, 4H, ArH), 7.37 (s, I H, NH), 9.18 (s, I H, NH); ^{13}C-NMR (100 MHz, $CDCl_3$ + DMSO-d_6, 1:1): δ (ppm): 25.7, 27.4, 31.7, 40.8, 49.1, 50.1, 53.0, 104.9, 126.5, 127.9, 128.6, 132.1, 150.6, 155.1 and 191.1; ESI-MS m/z: 305.76 $[M+H]^+$.

4-(2,4-dichlorophenyl)-7,7-dimethyl-3,4,7,8-tetrahydroquinazoline-2,5(1*H*,6*H*)-dione (PK-C7): Off-white Yellow Solid; IR (KBr) cm^{-1}: 3354, 3147 ($NH_{str.}$), 3052 (Ar-$CH_{str.}$), 2942 (Ali $CH_{str.}$), 1684 (C=$O_{str.}$), 1585 (C=C); ^{1}H-NMR (400 MHz, $CDCl_3$ + DMSO-d_6, 1:1): δ (ppm): 1.02 (s, 3H, 7-Me), 1.04 (s, 3H, 7-Me), 2.09 (s, 2H, CH_2), 2.37 (s, 2H, CH_2), 5.62 (d, 1H, CH), 7.17 -7.24 (m, 3H, ArH), 7.42 (s, 1H, NH), 8.74 (s, I H, NH); ^{13}C-NMR (100 MHz, $CDCl_3$ + DMSO-d_6, 1:1): 28.4, 29.3, 33.4, 40.8, 52.6, 54.4, 107.5, 124.3, 126.3, 127.5, 143.3, 156.8, 157.4 and 192.6; δ (ppm): ESI-MS m/z: 340.18 $[M+H]^+$.

4-(2-hydroxyphenyl)-7,7-dimethyl-3,4,7,8-tetrahydroquinazoline-2,5(1*H*,6*H*)-dione (PK-C8): Dark Brown Solid; IR (KBr) cm^{-1}: 3425 ($OH_{str.}$), 3328, 3167 ($NH_{str.}$), 3065 (Ar-$CH_{str.}$), 2977 (Ali $CH_{str.}$), 1688 (C=$O_{str.}$), 1580 (C=C); ^{1}H-NMR (400 MHz, $CDCl_3$ + DMSO-d_6, 1:1): δ (ppm): 0.99 (s, 3H, 7-Me), 1.05 (s, 3H, 7-Me), 2.07 (s, 2H, CH_2), 2.24 (s, 2H, CH_2), 5.18 (d, IH, CH), 7.34 -7.47 (m, 4H, ArH), 7.92 (s, I H, NH), 9.21 (s, I H, NH), 9.40 (s, I H, OH); ^{13}C-NMR (100 MHz, $CDCl_3$ + DMSO-d_6, 1:1): δ (ppm): 25.6, 27.8, 30.7, 40.2, 50.9, 52.6, 107.7, 113.2, 113.5, 126.2, 131.7, 145.3, 154.8 and 194.2; ESI-MS m/z: 287.16 $[M+H]^+$.

4-(4-hydroxyphenyl)-7,7-dimethyl-3,4,7,8-tetrahydroquinazoline-2,5(1*H*,6*H*)-dione (PK-C9): Yellow Solid; IR (KBr) cm^{-1}: 3469 ($OH_{str.}$), 3374, 3120 ($NH_{str.}$), 3060 (Ar-$CH_{str.}$), 2974 (Ali $CH_{str.}$), 1696 (C=$O_{str.}$), 1594

(C=C); ^{1}H-NMR (400 MHz, $CDCl_3$ + DMSO-d_6, 1:1): δ (ppm): 0.97 (s, 3H, 7-Me), 1.06 (s, 3H, 7-Me), 2.05 (s, 2H, CH_2), 2.34 (s, 2H, CH_2), 5.13 (d, IH, CH), 6.94 -7.14 (m, 4H, ArH), 7.61 (s, I H, NH), 9.34 (s, I H, NH), 9.36 (s, I H, OH); ^{13}C-NMR (100 MHz, $CDCl_3$ + DMSO-d_6, 1:1): δ (ppm): 25.5, 27.8, 30.8, 40.2, 50.1, 52.7, 107.4, 113.7, 113.5, 126.6, 131.7, 145.8, 154.7 and 194.4; ESI-MS m/z: 287.19 $[M+H]^+$.

4-(3,4-dimethoxyphenyl)-7,7-dimethyl-3,4,7,8-tetrahydroquinazoline-2,5(1*H*,6*H*)-dione (PK-C10): Yellow Solid; IR (KBr) cm^{-1}: 3352, 3162 ($NH_{str.}$), 3064 (Ar-$CH_{str.}$), 2972 (Ali $CH_{str.}$), 1695 (C=$O_{str.}$), 1599 (C=C); ^{1}H-NMR (400 MHz, $CDCl_3$ + DMSO-d_6, 1:1): δ (ppm): 1.03 (s, 3H, 7-Me), 1.05 (s, 3H, 7-Me), 2.11 (s, 2H, CH_2), 2.30 (s, 2H, CH_2), 3.85 (s, 6H, OCH_3), 5.59 (d, 1H, CH), 7.11 -7.18 (m, 3H, ArH), 7.38 (s, 1H, NH), 8.91 (s, 1H, NH); ^{13}C-NMR (100 MHz, $CDCl_3$ + DMSO-d_6, 1:1): δ (ppm): 27.4, 27.6, 31.9, 38.9, 50.7, 52.9, 56.4, 56.5, 107.9, 113.4, 113.4, 118.2, 146.6, 148.7, 149.8, and 198.4; ESI-MS m/z: 331.39 $[M+H]^+$.

4-(2,5-dimethoxyphenyl)-7,7-dimethyl-3,4,7,8-tetrahydroquinazoline-2,5(1*H*,6*H*)-dione (PK-C11): Yellow Solid; IR (KBr) cm^{-1}: 3344, 3151 ($NH_{str.}$), 3068 (Ar-$CH_{str.}$), 2976 (Ali $CH_{str.}$), 1696 (C=$O_{str.}$), 1624 (C=C); ^{1}H-NMR (400 MHz, $CDCl_3$ + DMSO-d_6, 1:1): δ (ppm): 0.98 (s, 3H, 7-Me), 1.02 (s, 3H, 7-Me), 2.13 (s, 2H, CH_2), 2.25 (s, 2H, CH_2), 3.81 (s, 6H, OCH_3), 5.51 (d, 1H, CH), 7.17 -7.21 (m, 3H, ArH), 7.35 (s, 1H, NH), 8.81 (s, 1H, NH); ^{13}C-NMR (100 MHz, $CDCl_3$ + DMSO-d_6, 1:1): δ (ppm): 27.8, 27.9, 32.6, 39.5, 51.1, 52.6, 55.1, 56.3, 107.5, 113.8, 113.8, 118.9, 146.7, 149.8, 155.2, and 199.3; ESI-MS m/z: 331.31 $[M+H]^+$.

4-(4-hydroxy-3-methoxyphenyl)-7,7-dimethyl-3,4,7,8-tetrahydroquinazoline-2,5(1*H*,6*H*)-dione (PK-C12): Light Yellow Solid; IR (KBr) cm^{-1}: 3452 ($OH_{str.}$), 3362, 3135 ($NH_{str.}$), 3067 (Ar-$CH_{str.}$), 2971 (Ali $CH_{str.}$), 1682 (C=$O_{str.}$), 1553 (C=C); ^{1}H-NMR (400 MHz, $CDCl_3$ + DMSO-d_6, 1:1): δ (ppm): 1.01 (s, 3H, 7-Me), 1.04 (s, 3H, 7-Me), 1.89 (s, 2H, CH_2), 2.27 (s, 2H, CH_2), 3.45 (s, 3H, OCH_3), 5.11 (d, 1H, CH), 6.32 (s, 1H, OH), 6.96 -7.04 (m, 3H, ArH), 7.34 (s, 1H, NH), 8.89 (s, 1H, NH); ^{13}C-NMR (100 MHz, $CDCl_3$ + DMSO-d_6, 1:1): δ (ppm): 27.8, 27.8, 32.4, 38.3, 50.6, 52.8, 56.7, 56.9, 106.4, 112.9, 113.6, 119.6, 148.4, 149.8, 152.6, and 195.3; ESI-MS m/z: 317.22 $[M+H]^+$.

4-(1*H*-indol-3-yl)-7,7-dimethyl-3,4,7,8-tetrahydroquinazoline-2,5(1*H*,6*H*)-dione (PK-C13): Yellow Solid; IR (KBr) cm^{-1}: 3412, 3354, 3170 ($NH_{str.}$), 3024 (Ar-$CH_{str.}$), 2958 (Ali $CH_{str.}$), 1684 (C=$O_{str.}$), 1581 (C=C); ^{1}H-NMR (400 MHz, $CDCl_3$ + DMSO-d_6, 1:1): δ (ppm): 0.99 (s, 3H, 7-Me), 1.01 (s, 3H, 7-Me), 2.16 (s, 2H, CH_2), 2.27 (s, 2H, CH_2), 5.61 (d, 1H, CH), 7.14 -7.32 (m, 5H, ArH), 7.38 (s, 1H, NH), 8.91-8.95 (s, 2H, NH); ^{13}C-NMR (100 MHz, $CDCl_3$ + DMSO-d_6, 1:1): δ (ppm): 27.7, 27.9, 32.6, 38.7, 51.6, 52.4, 105.4, 110.1, 112.6, 118.6, 119.2, 121.8, 123.5, 127.4, 136.5, 146.4, 150.8, and 202.5; ESI-MS m/z: 310.41 $[M+H]^+$.

4-(furan-2-yl)-7,7-dimethyl-3,4,7,8-tetrahydroquinazoline-2,5(1*H*,6*H*)-dione (PK-C14): Brown Solid; IR (KBr) cm^{-1}: 3314, 3150 ($NH_{str.}$), 3046 (Ar-$CH_{str.}$), 2978 (Ali $CH_{str.}$), 1691 (C=$O_{str.}$), 1590 (C=C); ^{1}H-NMR (400 MHz, $CDCl_3$ + DMSO-d_6, 1:1): δ (ppm): 1.02-1.04 (s, 6H, 7-Me), 2.19 (s, 2H, CH_2), 2.23 (s, 2H, CH_2), 5.67 (d,

1H, CH), 7.07 -7.11 (m, 3H, ArH), 7.18 (s, 1H, NH), 7.75 (s, 1H, NH); ^{13}C-NMR (100 MHz, $CDCl_3$ + DMSO-d_6, 1:1): δ (ppm): 27.6, 27.7, 32.8, 38.8, 51.4, 52.8, 105.8, 107.8, 110.9, 140.5, 147.4, 151.5, 153.5, and 198.4; ESI-MS m/z: 261.23 $[M+H]^+$.

Table 7: Synthesis of tetrahydroquinazoline derivatives (PK-C1 to PK-C14)

Compounds	Time (h)	% Yield	Melting Point (°C)
PK-C1	3.0	77	285-287
PK-C2	3.5	68	291-292
PK-C3	4.5	74	297-298
PK-C4	4.0	67	> 300
PK-C5	5.0	55	295-297
PK-C6	4.5	58	203-205
PK-C7	3.0	55	228-230
PK-C8	3.5	58	212-214
PK-C9	4.0	55	205-207
PK-C10	4.0	57	284-286
PK-C11	4.0	56	268-270
PK-C12	4.5	56	271-273
PK-C13	2.5	62	219-221
PK-C14	2.5	64	249-250

7.2 Results and Discussion

The results of *in vitro* evaluation as well as Gscore of designed compounds with dolutegravir as standard are given in **table 8**. The results of cytoxicity and anti-HIV assays are given in **table 9**.

It was observed that all compounds showed metal coordination with Mg 1001 by C2-carbonyl of quinazoline and one of the –NH formed hydrogen bond with Asp 116. In addition, most of the compounds showed hydrogen bond interaction between C-5 carboxyl and Asn 155 or Lys 156. This meant that in all compounds, the quinazoline ring occupied same cavity. Also, it was observed that more or less the phenyl ring did not affect the activity much. Therefore, the % IN inhibition in almost all compounds was consistent between 44 to 55% at 10 µM concentration except for four compounds viz. **PK-C2**, **PK-C3, PK-C4** and **PK-C13** for which % IN inhibition was between 60 to 70%.

Compounds **PK-C2, PK-C3** and **PK-C4** had substitution of electron withdrawing nitro group at 2nd, 3rd and 4th position, respectively. Compound **PK-C2** (percentage inhibition 69.25, G Score -7.35) showed hydrogen bonding interaction between Cys 65 and C-2 carbonyl, which also coordinated Mg1001; Asp 116 and C1–NH; Lys 156 and C-5 Carbonyl and between Thr 66, His 67, Lys 159 and 2-nitro group of 4-phenyl ring. Compounds **PK-C3** and **PK-C4** showed similar interactions but lacked hydrogen bonding interactions with Cys 65, His 67 and it might be the reason for their less docking score and HIV-1 IN inhibitory activity as compared to **PK-C2**. Compound **PK-C4** formed hydrogen bonding interaction with Asn 155 with 4-nitro group and hence was more active than **PK-C3**. In compound **PK-C13**, 4-phenyl ring was replaced with indole. It also showed hydrogen bonding interactions with amino acids Cys 65 (C-2 carbonyl, which also coordinated Mg1001), Asp 64, Asp 116 (by C-3 -NH), Glu 152 (by –NH of indole ring) and Lys 156 (by C-5 carbonyl). Hydrophobic interactions with Glu 152, Asn 155, Lys 156 and Lys 159 were also seen. It also showed comparable IN inhibition to that of **PK-C2**.

Since compounds **PK-C2**, **PK-C4** and **PK-C13** showed inhibition more than 65%, these were further tested for calculation of IC_{50} values (given in table 1). Both nitro substituted compounds (**PK-C2**, **PK-C4**) showed IC_{50} value of 1.20 µM and 5.36 µM respectively. Compound **PK-C13** having indole in place of phenyl ring had IC_{50} value of 4.56 µM.

Encouraged by the consistent *in vitro* results, all the compounds were tested for anti-HIV activity against HIV-1 (III_B) and HIV-2 (ROD) in cell based assay. It was however observed that these compounds did not show any anti-HIV activity below their cytotoxic concentration (as shown in **table 9**).

Table 8: Results of in-vitro HIV-1 IN inhibition and docking studies of compounds PK-C1 to PK-C14

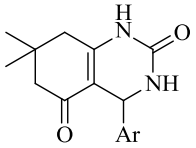

Compounds	Ar	Docking score	% IN Inhibition*	IC_{50} value**
Dolutegravir	-----	-7.65	95.00	nd
PK-C1	Ph	-6.61	44.32	nd
PK-C2	2-NO_2-Ph	-5.72	69.25	1.20±0.12
PK-C3	3-NO_2-Ph	-7.95	62.84	nd
PK-C4	4-NO_2-Ph	-6.73	65.80	5.36±0.83
PK-C5	2-Cl-Ph	-5.81	45.28	nd

PK-C6	4-Cl-Ph	-5.76	48.74	nd
PK-C7	2,4-diCl-Ph	-5.59	46.42	nd
PK-C8	2-OH-Ph	-6.15	52.25	nd
PK-C9	4-OH-Ph	-6.26	54.37	nd
PK-C10	3,4-diOMe-Ph	-6.19	46.33	nd
PK-C11	2,5-diOMe-Ph	-6.27	49.72	nd
PK-C12	4-OH-3-OMe-Ph	-5.35	46.69	nd
PK-C13	1*H*-indol-3-yl	-5.71	67.83	4.56±0.56
PK-C14	furan-2-yl	-5.62	46.62	nd

*% inhibition at 10µM concentration, values are mean of duplicate experiment performed independently, nd = not done; ** in µM

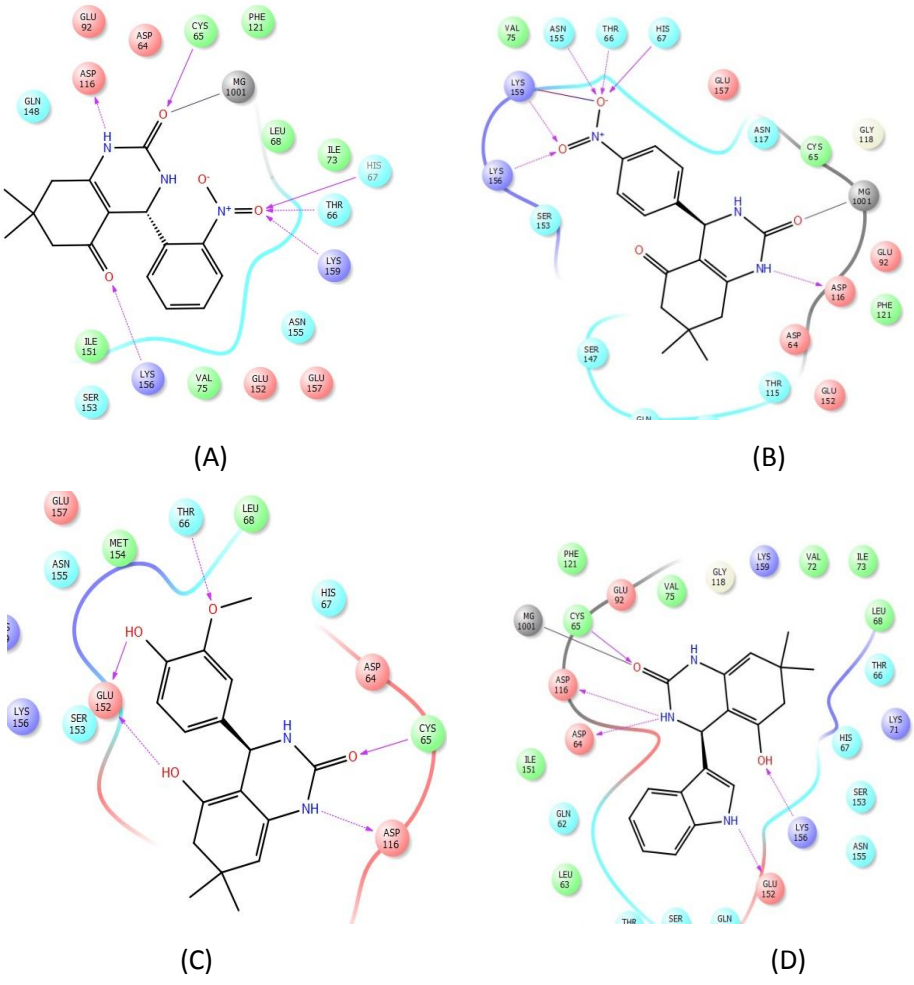

Figure 24: 2D docking poses of few representative compounds A: PK-C2; B: PK-C4; C: PK-C12; C: PK-C13

Table 9: Anti-HIV activity of the synthesized compounds PK-C1 to PK-C14

Compounds	HIV-1 (III_B)			HIV-2 (ROD)		
	EC_{50}[1] (µM)	CC_{50}[2] (µM)	HIV-1[3] SI	EC_{50}[1] (µM)	CC_{50}[2] (µM)	HIV-2[3] SI
Dolutegravir	0.0006±0.000001	1.275±0.3	2110.00	0.00232±0.00061	1.495±0.165	597.00
PK-C1	>82.30±1.50	82.30±1.50	<1	>80.59±4.62	80.59±4.62	<1
PK-C2	>116.65±2.25	116.65±2.25	<1	>113.51±1.98	113.51±1.98	<1
PK-C3	>29.30±0.90	29.30±0.90	<1	>29.81±0.60	29.81±0.60	<1
PK-C4	>71.45±1.30	71.45±1.30	<1	>75.78±2.44	75.78±2.44	<1
PK-C5	>60.18±1.25	60.18±1.25	<1	>61.85±2.85	61.85±2.85	<1
PK-C6	nd	nd	nd	nd	nd	nd
PK-C7	>4.49±0.45	4.49±0.45	<1	>4.25±0.60	4.25±0.60	<1
PK-C8	>55.15±1.75	55.15±1.75	<1	>56.51±2.62	56.51±2.62	<1
PK-C9	>108.00±1.65	108.00±1.65	<1	>109.12±4.23	109.12±4.23	<1
PK-C10	>92.10±1.40	92.10±1.40	<1	>93.87±1.86	93.87±1.86	<1
PK-C11	>25.00±1.10	25.00±1.10	<1	>25.75±2.60	25.75±2.60	<1
PK-C12	>11.40±0.85	11.40±0.85	<1	>12.15±0.3	12.15±0.3	<1
PK-C13	nd	nd	nd	nd	nd	nd
PK-C14	nd	nd	nd	nd	nd	nd

[1] EC_{50}: concentration of compound required to achieve 50% protection of MT-4 cell cultures against HIV induced cytotoxicity, as determined by MTT method. [2] CC_{50}: concentration required to reduce the viability of mock-infected cells by 50%, as determined by MTT method; [3] SI: selectivity index (CC_{50}/EC_{50}); nd: not done.

7.3 Oral bioavailability and toxicity prediction

It was observed that estimated parameters such as molecular weight, number of hydrogen bond donor, number of hydrogen bond acceptor, octanol/water partition coefficient (logP) were within the acceptable range. All compounds satisfied the lipinsky rule of five.

Table 10: Predicted physiochemical properties of tetrahydroquinazolinedione analogs (PK-C1 to PK-C14)

CODE	Mol.Formula	M.Wt.	log P[a]	RB[b]	HBA[c]	HBD[d]	PSA[e]	log S[f]	PCaco[g]
PK-C1	$C_{16}H_{18}N_2O_2$	270.32	2.68	1	2	2	117.83	-3.61	1.37
PK-C2	$C_{16}H_{17}N_3O_4$	315.29	2.59	2	4	2	132.68	-4.52	0.57
PK-C3	$C_{16}H_{17}N_3O_4$	315.29	2.59	2	4	2	132.68	-4.42	0.41
PK-C4	$C_{16}H_{17}N_3O_4$	315.29	2.59	2	4	2	132.68	-4.42	0.41
PK-C5	$C_{16}H_{17}ClN_2O_2$	304.77	3.33	1	2	2	128.12	-4.52	1.30
PK-C6	$C_{16}H_{17}ClN_2O_2$	304.77	3.33	1	2	2	128.12	-4.52	1.30
PK-C7	$C_{16}H_{16}Cl_2N_2O_2$	339.22	3.99	1	2	2	138.45	-5.31	1.35
PK-C8	$C_{16}H_{18}N_2O_3$	286.33	2.38	1	3	3	122.59	-3.83	1.01
PK-C9	$C_{16}H_{18}N_2O_3$	286.33	2.38	1	3	3	122.59	-3.83	1.01
PK-C10	$C_{18}H_{22}N_2O_4$	330.38	2.71	3	4	2	140.75	-4.38	1.02
PK-C11	$C_{18}H_{22}N_2O_4$	330.38	2.71	3	4	2	140.75	-3.97	0.98
PK-C12	$C_{17}H_{20}N_2O_4$	316.35	2.39	2	4	3	134.03	-4.15	1.03
PK-C13	$C_{18}H_{19}N_3O_2$	309.36	3.16	1	2	3	133.69	-4.39	0.98
PK-C14	$C_{14}H_{16}N_2O_3$	260.29	2.27	1	3	2	110.59	-3.49	0.98

[a]Partition coefficient, [b]No. of rotatable bonds, [c] No. of hydrogen bond acceptors, [d] No. of hydrogen bond donors, [e]polar surface area, [f]water solubility, [g]caco-2 permeability.

CHAPTER 8: 4-SUBSTITUTED BENZYLIDENE ISOQUINOLINE-1,3(2*H*,4*H*)-DIONE DERIVATIVES

Isoquinoline scaffold is considered druggable and hence has been explored widely for biological activities such as kinase inhibition, hepatitis B virus inhibition, HIV-1 non-nucleoside reverse transcriptase inhibition, tyrosyl DNA phosphodiesterase II inhibition, anticancer, antimicrobial, anti-hypertensive and antifungal (Tsou, 2008). Most of the work on isoquinolinediones as HIV IN inhibitors is done by Billiamboz *et al.*(Billiamboz, 2008, Billiamboz, 2011, Billiamboz, 2011, Billiamboz, 2013 and Billiamboz, 2016). Since diketo acids were reported to inhibit HIV-1 IN as well as anti RNase H activities, they planned to synthesize dual inhibitors. Initially, their group reported 7-substituted 2-hydroxyisoquinoline-1,3(2*H*,4*H*)-dione derivatives (compounds **I**) (Billiamboz, 2008), followed by 4-substituted 2-hydroxyisoquinoline-1,3(2*H*,4*H*)-diones (compounds **II**) (Billiamboz, 2011) and later 4-alkylated 2-hydroxyisoquinoline-1,3(2*H*,4*H*)-diones (compounds **III**) (Billiamboz, 2011) . Based on these, they studied the effect of phenyl or benzyl carboxamido side chain at position 4 of the 2-hydroxyisoquinoline-1,3-dione scaffold (compounds **IV**) (Billiamboz, 2013). Almost all the compounds in these three papers had limited application because of cytotoxicity.

Suchaud *et al.* took clue from these and studied the effect of substitution at 7th position on HIV IN inhibition of hydrophobic carboxamido substituted 2-hydroxyisoquinoline-1,3(2*H*,4*H*)-diones (compounds **V**), expecting it to reduce the cytotoxic nature. However, the compounds, although less cytotoxic, showed reduced potency due to low cell permeability and high protein binding (Suchaud, 2014). Same group also reported that phenyl or benzyl substituents on 4-carboxamido function (compounds **VI**) can be efficiently replaced by an n-alkyl group. But it was found that the compounds lacked significant antiviral activities due to unfavorable tautomeric equilibrium (keto form), that is, failure to achieve enol form. They postulated that displacement of the keto-enol equilibrium towards enol will lead to higher lipophilicity and hence improved anti-HIV activity (Billiamboz, 2016). Recently, dihydroisoquinolines substituted with nucleophiles having differential ability to chelate with Mg^{2+} ions have been reported.

But recently, Tandon *et al.* designed and synthesized three types of 1,2-dihydroisoquinolines derivatives bearing different functional groups at the C-1, C-3, C-7, and N-2 positions. After optimizing this scaffold, their results showed that dihydroisoquinolines lacking hydroxy group at C-2 positions are also exhibits significant activity against HIV-1 IN (compounds **VII**) (Tandon, 2015). Considering these reports and the fact that there are many scaffolds lacking hydroxy functionality but having HIV-1 IN inhibition, modification of compound 1 was attempted by removing the hydroxyls of C-2 position and substituting

at C-4 position to obtaining the prototype 4-substituted-benzylideneisoquinoline-1,3(2*H*,4*H*)-dione derivatives (**PK-D1 to PK-D16**) as one of pharmacophore with different electron withdrawing, electron releasing substitutent on different positions of attached aromatic ring (see **Figure 16**).

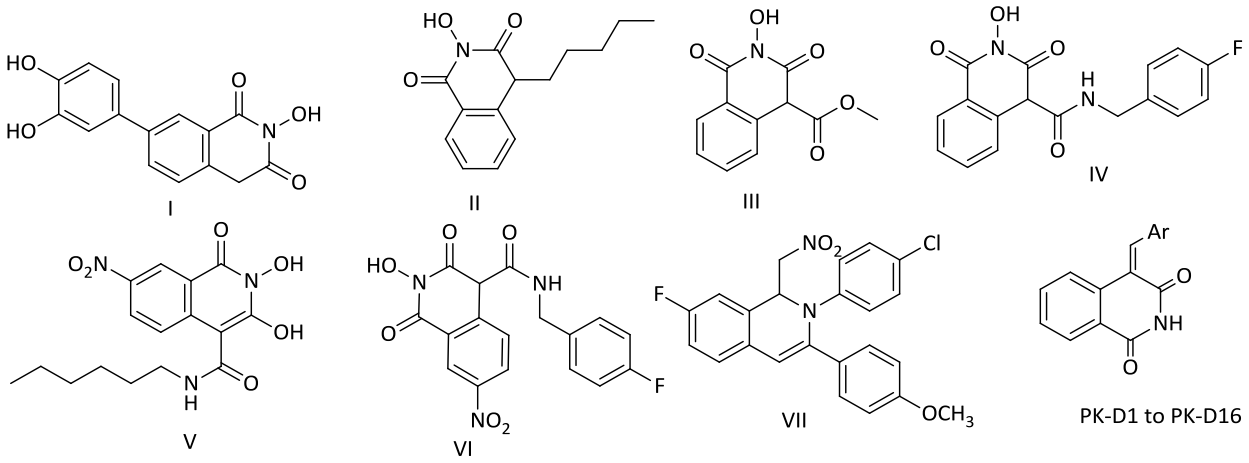

Figure 25: Literature reported HIV-1 IN inhibitors and general structure of designed molecule (PK-D1 to PK-D16)

8.1 Chemistry

The synthetic routes for 4-substituted-benzylideneisoquinoline-1,3(2*H*,4*H*)-dione derivatives are summarized in Scheme 4. The synthetic procedure involves reaction of 2-(carboxymethyl) benzoic acid with urea to form intermediate by loss of a water molecule. The intermediate further rearranges and cyclise to produce isoquinoline-1,3(2*H*,4*H*)-dione, which is also known as homophthalimide. In second step compound homophthalimide was stirred with base piperidine, which abstracts a proton of homophthalimide, and further, different substituted aromatic aldehydes attacks on carbanion followed by another loss of water molecule to give moderate yields of desired targeted molecules (53-74%, **PK-D1** to **PK-D16**).

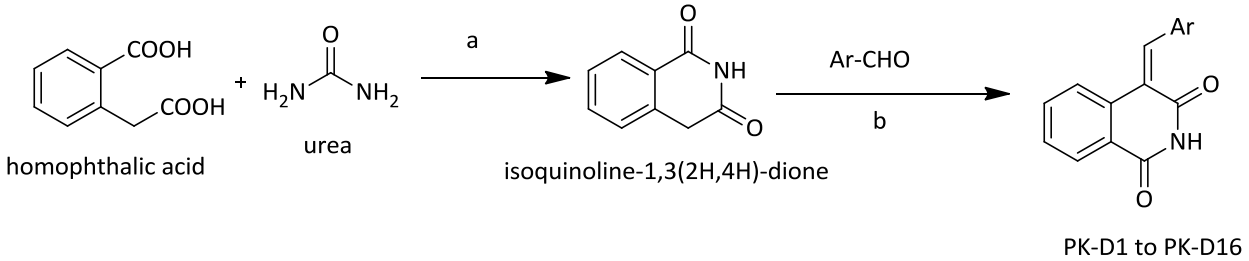

Scheme 4: Reagents and conditions: (a) MW, 8 minutes, 185˚C, cool to RT, MeOH, reflux 1.5h (b) EtOH: Toluene (1:1), Piperidine, reflux 4-8 h.

Reaction mechanism

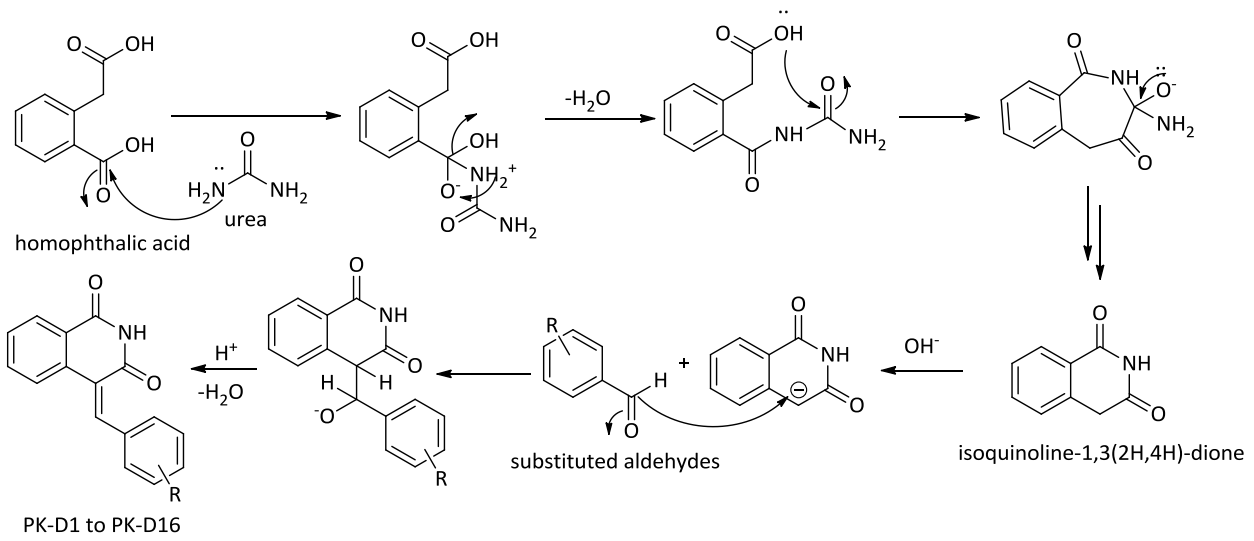

Figure 26: Plausible mechanism for synthesis of benzylideneisoquinoline-1,3(2*H*,4*H*)-dione derivatives (PK-D1 to PK-D16)

Synthesis of isoquinoline-1,3(2*H*,4*H*)-dione

In mortar pestle 2-(carboxymethyl) benzoic acid (also known as homophthalic acid, 0.0832 mol) and urea (0.0989 mol) was ground to a fine powder. The powder was transferred to 250 ml RBF and heated at 185 °C in microwave for about 8 minute at 720 watt. The mixture was further cooled to ambient temperature and methanol (150 mL) was added. The reaction mixture was then refluxed for 90 minutes, filtered, and allowed to cool to ambient temperature. The solvent was removed under vacuum and resulted solid was treated with hexane (40 ml), collected by filtration, and dried under vacuum to give isoquinoline-1,3(2*H*,4*H*)-dione (also known as homophthalimide). Light Green Yellow Solid; Yield: 84%; Mp: 237-239°C; IR (KBr) cm^{-1}: 3324, ($NH_{str.}$), 2947 ($CH_{str.}$), 1714, 1722 ($C=O_{str.}$), 1630 (C=C); ^{1}H-NMR (400 MHz, $CDCl_3$): δ (ppm): 3.65 (s, 2H, CH_2), 7.24-7.28 (d, 2H, ArH), 7.35-7.43 (t, 2H, ArH), 8.68 (s, 1H, NH); ^{13}C-NMR (100 MHz, $CDCl_3$): δ (ppm): 40.2, 124.5, 126.7, 128.2, 129.6, 133.9, 136.3, 158.8, 172.4; ESI-MS m/z: 162.08 $[M+H]^+$.

Synthesis of 4-substituted-benzylideneisoquinoline-1,3(2*H*,4*H*)-dione (PK-D1 to PK-D16)

In 100 ml RBF isoquinoline-1,3(2*H*,4*H*)-dione (0.0043 mol) was dissolved in a mixture of ethanol and toluene (1:1, 10 ml) at room temperature. Then base piperidine (0.00645 mol) was added to reaction mixture. The resulting mixture was stirred for 10-15 minutes. The appropriate aldehydes were slowly added to the mixture and the mixture was refluxed for 4-8 hours. The progress of reaction was

monitored by TLC and after completion of reaction, reaction mass was cooled to room temperature. The solvents were removed by rota evaporator and the residue was diluted with ethyl acetate (50 ml) and washed successively with aqueous water (60 ml). Concentration of solvent under vacuum gave crude solids (**PK-D1** to **PK-D16**). The compounds were further purified by column chromatography.

4-benzylideneisoquinoline-1,3(2H,4H)-dione (PK-D1): Light Yellow Solid; Yield 66%; Mp: 212-214°C; IR (KBr) cm^{-1}: 3395, ($NH_{str.}$), 3097 (Ar-$CH_{str.}$), 3021 (Ali-$CH_{str.}$), 1687, 1696 (C=$O_{str.}$), 1612 (C=C); ^{1}H-NMR (400 MHz, $CDCl_3$): δ (ppm): 7.28 (s, 1H, C=CH), 7.42-8.24 (m, 9H, Ar-H), 8.30 (s, I H, NH); ^{13}C-NMR (100 MHz, $CDCl_3$): δ (ppm): 122.6, 123.3, 124.7, 126.2, 128.5, 129.1, 133.2, 135.2, 136.4, 136.7, 137.3, 138.4, 139.6, 140.1, 159.2 and 168.6; ESI-MS m/z: 250.18 $[M+H]^+$.

4-(2-nitrobenzylidene)isoquinoline-1,3(2*H*,4*H*)-dione (PK-D2): Yellow Solid; Yield 66%; Mp: 228-230°C; IR (KBr) cm^{-1}: 3461, ($NH_{str.}$), 3129 (Ar-$CH_{str.}$), 3054 (Ali-$CH_{str.}$), 1684, 1690 (C=$O_{str.}$), 1618 (C=C); ^{1}H-NMR (400 MHz, $CDCl_3$): δ (ppm): 6.39 (s, 1H, C=CH), 6.45-7.72 (m, 8H, Ar-H), 7.92 (s, I H, NH); ^{13}C-NMR (100 MHz, $CDCl_3$): δ (ppm): 124.2, 124.9, 125.6, 126.8, 127.9, 130.3, 132.2, 134.8, 135.3, 137.1, 137.5, 139.2, 139.9, 141.6, 161.3, 169.1; ESI-MS m/z: 295.20 $[M+H]^+$.

4-(4-nitrobenzylidene)isoquinoline-1,3(2*H*,4*H*)-dione (PK-D3): Yellow Solid; Yield 56%; Mp: 223-225°C; IR (KBr) cm^{-1}: 3454, ($NH_{str.}$), 3119 (Ar-$CH_{str.}$), 3059 (Ali-$CH_{str.}$), 1689, 1697 (C=$O_{str.}$), 1615 (C=C); ^{1}H-NMR (400 MHz, $CDCl_3$): δ (ppm): 7.33 (s, 1H, C=CH), 7.43-8.14 (m, 8H, Ar-H), 8.31 (s, I H, NH); ^{13}C-NMR (100 MHz, $CDCl_3$): δ (ppm): 124.5, 125.3, 125.8, 126.2, 127.5, 130.6, 132.9, 133.7, 134.6, 136.8, 138.5, 139.6, 140.2, 141.3, 158.5 and 172.9; ESI-MS m/z: 295.17 $[M+H]^+$.

4-(2-chlorobenzylidene)isoquinoline-1,3(2*H*,4*H*)-dione (PK-D4): White Solid; Yield 58%; Mp: 217-219°C; IR (KBr) cm^{-1}: 3461, ($NH_{str.}$), 3112 (Ar-$CH_{str.}$), 3062 (Ali-$CH_{str.}$), 1683, 1694 (C=$O_{str.}$), 1611 (C=C); ^{1}H-NMR (400 MHz, $CDCl_3$): δ (ppm): 7.28 (s, 1H, C=CH), 7.37-8.29 (m, 8H, Ar-H), 8.32 (s, I H, NH); ^{13}C-NMR (100 MHz, $CDCl_3$): δ (ppm): 123.8, 124.9, 125.2, 126.4, 127.1, 128.6, 129.3, 131.8, 132.6, 134.5, 136.1, 138.4, 140.6, 140.9, 160.9 and 170.2; ESI-MS m/z: 284.04 $[M+H]^+$.

4-(3-chlorobenzylidene)isoquinoline-1,3(2*H*,4*H*)-dione (PK-D5): Light green Solid; Yield 61%; Mp: 216-218°C; IR (KBr) cm^{-1}: 3467, ($NH_{str.}$), 3123 (Ar-$CH_{str.}$), 3064 (Ali-$CH_{str.}$), 1685, 1692 (C=$O_{str.}$), 1617 (C=C); ^{1}H-NMR (400 MHz, $CDCl_3$): δ (ppm): 7.28 (s, 1H, C=CH), 7.30-8.24 (m, 8H, Ar-H), 8.27 (s, I H, NH); ^{13}C-NMR (100 MHz, $CDCl_3$): δ (ppm): 123.1, 123.5, 125.2, 126.8, 127.9, 129.6, 131.3, 133.4, 134.2, 136.9, 138.1, 139.5, 141.2, 142.5, 161.3 and 171.1; ESI-MS m/z: 284.15 $[M+H]^+$.

4-(4-chlorobenzylidene)isoquinoline-1,3(2*H*,4*H*)-dione (PK-D6): Yellow Solid; Yield 67%; Mp: 220-222°C; IR (KBr) cm^{-1}: 3451, ($NH_{str.}$), 3127 (Ar-$CH_{str.}$), 3069 (Ali-$CH_{str.}$), 1682, 1699 (C=$O_{str.}$), 1604 (C=C); ^{1}H-NMR (400 MHz, $CDCl_3$): δ (ppm): 7.28 (s, 1H, C=CH), 7.32-8.20 (m, 8H, Ar-H), 8.27 (s, I H, NH); ^{13}C-NMR (100

MHz, $CDCl_3$): δ (ppm): 125.4, 125.9, 126.3, 127.0, 128.2, 129.1, 130.9, 132.5, 135.3, 136.7, 138.9, 140.2, 141.7, 142.3, 162.4 and 173.7; ESI-MS m/z: 284.09 $[M+H]^+$.

4-(2,4-dichlorobenzylidene)isoquinoline-1,3(2*H*,4*H*)-dione (PK-D7): Light Brown Solid; Yield 53%; Mp: 239-241°C; IR (KBr) cm^{-1}: 3464, ($NH_{str.}$), 3135 (Ar-$CH_{str.}$), 3047 (Ali-$CH_{str.}$), 1680, 1687 ($C=O_{str.}$), 1609 (C=C); ^{1}H-NMR (400 MHz, $CDCl_3$): δ (ppm): 7.28 (s, 1H, C=CH), 7.32-7.85 (m, 7H, Ar-H), 8.31 (s, I H, NH); ^{13}C-NMR (100 MHz, $CDCl_3$): δ (ppm): 124.2, 126.3, 127.1, 128.5, 129.4, 130.7, 131.9, 133.1, 134.5, 136.0, 138.2, 141.1, 143.4, 143.9, 158.8 and 170.1; ESI-MS m/z: 318.05 $[M+H]^+$.

4-(2-hydroxybenzylidene)isoquinoline-1,3(2*H*,4*H*)-dione (PK-D8): Brown Solid; Yield 56%; Mp: 231-233°C; IR (KBr) cm^{-1}: 3472, ($OH_{str.}$), 3404, ($NH_{str.}$), 3104 (Ar-$CH_{str.}$), 3014 (Ali-$CH_{str.}$), 1688, 1702 ($C=O_{str.}$), 1580 (C=C); ^{1}H-NMR (400 MHz, $CDCl_3$): δ (ppm): 5.47 (s, 1H, OH), 7.27 (s, 1H, C=CH), 7.30-8.12 (m, 8H, Ar-H), 8.32 (s, I H, NH); ^{13}C-NMR (100 MHz, $CDCl_3$): δ (ppm): 121.8, 122.5, 125.9, 127.2, 129.3, 131.8, 133.1, 134.7, 135.5, 138.3, 139.7, 143.8, 145.1, 145.9, 164.2 and 173.2; ESI-MS m/z: 266.12 $[M+H]^+$.

4-(4-methoxybenzylidene)isoquinoline-1,3(2*H*,4*H*)-dione (PK-D9): White Solid; Yield 68%; Mp: 242-244°C; IR (KBr) cm^{-1}: 3395, ($NH_{str.}$), 3116 (Ar-$CH_{str.}$), 2985 (Ali-$CH_{str.}$), 1683, 1691 ($C=O_{str.}$), 1587 (C=C); ^{1}H-NMR (400 MHz, $CDCl_3$): δ (ppm): 3.83 (s, 3H, OCH_3), 7.29 (s, 1H, C=CH), 7.50-8.10 (m, 8H, Ar-H), 8.38 (s, I H, NH); ^{13}C-NMR (100 MHz, $CDCl_3$): δ (ppm): 58.1, 120.9, 123.7, 124.0, 128.5, 131.6, 131.9, 133.7, 135.4, 136.8, 141.3, 142.2, 145.4, 147.9, 158.4, 160.5 and 169.7; ESI-MS m/z: 280.11 $[M+H]^+$.

4-(3,4-dimethoxybenzylidene)isoquinoline-1,3(2*H*,4*H*)-dione (PK-D10): Yellow Solid; Yield 71%; Mp: 223-235°C; IR (KBr) cm^{-1}: 3429, ($NH_{str.}$), 3124 (Ar-$CH_{str.}$), 3039 (Ali-$CH_{str.}$), 1682, 1695 ($C=O_{str.}$), 1592 (C=C); ^{1}H-NMR (400 MHz, $CDCl_3$): δ (ppm): 3.83-3.87 (s, 6H, OCH_3), 7.27 (s, 1H, C=CH), 7.40-7.79 (m, 7H, Ar-H), 8.37 (s, I H, NH); ^{13}C-NMR (100 MHz, $CDCl_3$): δ (ppm): 57.5, 57.9, 121.5, 124.8, 126.1, 128.7, 130.5, 132.4, 134.0, 136.9, 139.1, 144.6, 146.4, 149.3, 157.4, 158.4, 161.3 and 171.3; ESI-MS m/z: 310.34 $[M+H]^+$.

4-(2,5-dimethoxybenzylidene)isoquinoline-1,3(2*H*,4*H*)-dione (PK-D11): Pale Yellow Solid; Yield 73%; Mp: 221-223°C; IR (KBr) cm^{-1}: 3439, ($NH_{str.}$), 3120 (Ar-$CH_{str.}$), 2997 (Ali-$CH_{str.}$), 1678, 1688 ($C=O_{str.}$), 1598 (C=C); ^{1}H-NMR (400 MHz, $CDCl_3$): δ (ppm): 4.05 (s, 6H, OCH_3), 7.13 (s, 1H, C=CH), 7.04-8.20 (m, 7H, Ar-H), 8.33 (s, I H, NH); ^{13}C-NMR (100 MHz, $CDCl_3$): δ (ppm): 58.3, 58.5, 123.1, 124.4, 127.6, 129.3, 130.9, 132.8, 133.8, 137.4, 139.3, 142.6, 146.7, 149.1, 156.8, 158.7, 166.3 and 172.9; ESI-MS m/z: 310.29 $[M+H]^+$.

4-(3,4,5-trimethoxybenzylidene)isoquinoline-1,3(2*H*,4*H*)-dione (PK-D12): Light Brown Solid; Yield 65%; Mp: 236-238°C; IR (KBr) cm^{-1}: 3477, ($NH_{str.}$), 3139 (Ar-$CH_{str.}$), 2987 (Ali-$CH_{str.}$), 1677, 1699 ($C=O_{str.}$), 1614 (C=C); ^{1}H-NMR (400 MHz, $CDCl_3$): δ (ppm): 3.83-3.88 (s, 9H, OCH_3), 7.29 (s, 1H, C=CH), 7.46-7.81 (m, 6H, Ar-H), 8.39 (s, I H, NH); ^{13}C-NMR (100 MHz, $CDCl_3$): δ (ppm): 55.6, 56.2, 57.1, 124.6, 124.9, 126.3, 128.7,

131.4, 132.9, 134.1, 135.8, 139.9, 143.7, 145.1, 155.7, 157.9, 158.4, 169.7 and 171.5; ESI-MS m/z: 340.21 $[M+H]^+$.

4-(4-hydroxy-3-methoxybenzylidene)isoquinoline-1,3(2*H*,4*H*)-dione (PK-D13): Yellow Solid; Yield 59%; Mp: 241-243°C; IR (KBr) cm^{-1}: 3480, ($OH_{str.}$), 3368, ($NH_{str.}$), 3058 (Ar-$CH_{str.}$), 2977 (Ali-$CH_{str.}$), 1696, 1708 ($C=O_{str.}$), 1589 (C=C); ^{1}H-NMR (400 MHz, $CDCl_3$): δ (ppm): 3.86 (s, 3H, OCH_3), 5.54 (s, 1H, OH), 7.30 (s, 1H, C=CH), 7.42-8.14 (m, 7H, Ar-H), 8.38 (s, 1H, NH); ^{13}C-NMR (100 MHz, $CDCl_3$): δ (ppm): 56.6, 120.8, 122.4, 123.9, 127.5, 131.6, 133.4, 134.8, 135.2, 137.4, 141.6, 149.6, 159.3, 159.5, 161.3, 168.6 and 172.3; ESI-MS m/z: 296.18 $[M+H]^+$.

4-(3-ethoxy-4-hydroxybenzylidene)isoquinoline-1,3(2*H*,4*H*)-dione (PK-D14): Brown Solid; Yield 65%; Mp: 240-242°C; IR (KBr) cm^{-1}: 3466, ($OH_{str.}$), 3385, ($NH_{str.}$), 3074 (Ar-$CH_{str.}$), 2968 (Ali-$CH_{str.}$), 1686, 1705 ($C=O_{str.}$), 1612 (C=C); ^{1}H-NMR (400 MHz, $CDCl_3$): δ (ppm): 1.52 (t, 3H, CH_3) 2.89 (q, 2H, OCH_2), 6.25 (s, 1H, OH), 6.78 (s, 1H, C=CH), 7.44-8.16 (m, 7H, Ar-H), 8.32 (s, I H, NH); ^{13}C-NMR (100 MHz, $CDCl_3$): δ (ppm): 16.8, 65.2, 121.7, 123.9, 124.5, 125.8, 127.9, 132.8, 134.2, 136.7, 137.3, 139.7, 140.8, 144.7, 152.8, 158.5, 162.7, 169.1 and 170.8; ESI-MS m/z: 310.21 $[M+H]^+$.

4-(4-(dimethylamino)benzylidene)isoquinoline-1,3(2*H*,4*H*)-dione (PK-D15): Light Yellow Solid; Yield 74%; Mp: 218-220°C; IR (KBr) cm^{-1}: 3472, ($NH_{str.}$), 3136 (Ar-$CH_{str.}$), 2982 (Ali-$CH_{str.}$), 1674, 1692 ($C=O_{str.}$), 1618 (C=C); ^{1}H-NMR (400 MHz, $CDCl_3$): δ (ppm): 2.83-2.85 (s, 6H, CH_3), 7.29 (s, 1H, C=CH), 7.42-7.89 (m, 8H, Ar-H), 8.34 (s, I H, NH); ^{13}C-NMR (100 MHz, $CDCl_3$): δ (ppm): 42.5, 42.6, 117.5, 118.2 122.2, 124.8, 125.3, 126.4, 127.2, 130.7, 135.4, 138.6, 139.8, 142.7, 149.5, 154.4, 159.8, 163.7, 168.3 and 172.4; ESI-MS m/z: 293.31 $[M+H]^+$.

4-((1*H*-indol-3-yl)methylene)isoquinoline-1,3(2*H*,4*H*)-dione (PK-D16): Yellow Solid; Yield 68%; Mp: 252-254°C; IR (KBr) cm^{-1}: 3442, 3385 ($NH_{str.}$), 3128 (Ar-$CH_{str.}$), 2980 (Ali-$CH_{str.}$), 1679, 1695 ($C=O_{str.}$), 1610 (C=C); ^{1}H-NMR (400 MHz, $CDCl_3$): δ (ppm): 7.53-7.56 (s, 2H, C=CH), 7.59-8.81 (m,8H, Ar-H), 8.41 (s, 1H, NH), 8.52 (s, IH, NH); ^{13}C-NMR (100 MHz, $CDCl_3$): δ (ppm): 112.4, 113.8, 118.7, 120.4, 121.8, 123.4, 124.6, 127.5, 129.6, 131.4, 132.2, 133.8, 134.7, 135.4, 141.8, 149.4, 168.2 and 171.8; ESI-MS m/z: 289.06 $[M+H]^+$.

8.2 Results and Discussion

The results of *in vitro* evaluation as well as *in silico* binding energy (Gscore) are given in **table 11**. Compound **PK-D1** having unsubstituted phenyl ring showed, apart from metal coordination with C-3 carbonyl oxygen, hydrogen bonding interactions with Asp 64 (by -NH of isoquinoline ring) and Asn 155

(by carbonyl group at C-1 position of isoquinoline ring) and hydrophobic interactions with Cys 65, His 67 and Lys 159 were also observed. It showed 50.43 % inhibition of IN and G Score was -5.40.

Substitution of electron withdrawing nitro group, either at ortho position (**PK-D2**) or at para position (**PK-D3**), showed hydrogen bonding with Asp 64 (by -NH of isoquinoline ring), Cys 65 (by C-3 carbonyl group), Asn 155 (by carbonyl group at C-1 position of isoquinoline ring) and hydrophobic interactions with Glu 92, Glu 152 and Lys 156. Although the % inhibition profile of both compounds was better than **PK-D1**, substitution at ortho position (compound **PK-D2**) was favored, as compound **PK-D3** lacked of hydrogen bonding interactions with Thr 66 and π-π stacking interaction with His 67, which were present in **PK-D2**.

On substitution of chloro group at ortho, meta and para positions (Compounds **PK-D4** to **PK-D6**), it was found that meta substitution is not favored. These derivatives showed hydrogen bonding with Cys 65 and hydrophobic interactions with Thr 66, His 67, Glu 92, Glu 152, Lys 156 and Lys 159; as also coordinate with magnesium. Compound **PK-D4** (ortho chloro) showed, in addition, hydrogen bonding interactions with Thr 66, His 67 (by carbonyl group at C-1 position of isoquinoline ring), But it lacks interactions with Asp 64 ((by -NH of isoquinoline ring)) which was shown by para chloro substituted compound **PK-D6**, which was also most active of these three (G score -7.76 and % inhibition 84.12). Substitution of chlorine at both ortho and para positions (compound **PK-D7**) showed similar interactions as **PK-D4.** It showed absence of docking interactions with Asp 64 (G score -6.19) leading to reduction in Gscore as well as activity as compared to **PK-D6**.

On Substitution of electron donating hydroxy group at 2 position (**PK-D8**) showed highest docking interactions (G score -7.86) as well significant HIV-1 IN inhibition (% inhibition 87.30) activity. It showed hydrogen bonding interactions with Asp 64 (by -NH of isoquinoline ring), Cys 65 (by carbonyl group of C-3 position of isoquinoline ring) and Asn 155 (by carbonyl group of C-1 position of isoquinoline ring). The ortho hydroxyl group also participated in hydrogen bonding interactions with Cys 65, Thr 66 and His 67. The hydrophobic interactions bond with amino acids Asp 64, Cys 65, His 67 and Lys 159. The 2-hydroxyl substitution also showed metal coordination with Mg 1001 in addition to by carbonyl group of C-3 position of isoquinoline ring.

O-alkylation (4-methoxy substituted **PK-D9**) or di- and tri- substitution (compounds **PK-D10** to **PK-D14**) with electron donating groups was found to decrease the interactions and hence lower docking and % inhibition scores were obtained for these. Specifically, **PK-D9** showed reduction in docking score because 4-methoxy group was found to be solvent exposed. Among dimethoxy substituted compounds, 3,4-dimethoxy (**PK-D10**) was found to have better interactions than 2,5-dimethoxy (**PK-D11**) as it did not

show interaction with Asp 64 but **PK-D10** did. 3,4,5-trimethoxy substitution (**PK-D12**) showed similar interactions as that of **PK-D10** such as hydrogen bonding interactions with Asp 64, Cys 65 (by -NH of isoquinoline ring), Thr 66, Asn 155 (by carbonyl group of C-1 position of isoquinoline ring).

It was found that compound substituted with 4-hydroxy-3-methoxy phenyl (**PK-D13**) also shows similar interactions like **PK-D10** and hence docking score and % inhibition values of **PK-D10, PK-D12** and **PK-D13** were similar. However, replacing methoxy in **PK-D13** with ethoxy (**PK-D14**) was not favored as benzylidene ring comes out of active site and only two hydrogen bonding interactions with Asp 64 (by NH of isoquinoline ring) and Asn 155 (by carbonyl group of C-1 position of isoquinoline ring) were observed. Substitution of *N*,*N*-dimethyl (**PK-D15**) at para position of aryl ring or replacement of substituted phenyl ring with fused ring like indole (**PK-D15**) did not show any difference than **PK-D10**.

Thus, it was observed that the HIV-1 IN inhibitory potency of designed compounds altered with variation in nature as well as position of substituents. Since compounds having 2-nitro (**PK-D2**), 4-chloro (**PK-D6**) and 4-hydroxy substitution (**PK-D8**) exhibited significant IN inhibitory activity (more than 75%), these were further tested for calculation of IC_{50} values (given in **table 8**). It was observed that compounds **PK-D2** and **PK-D6** with electron withdrawing substituent showed IC_{50} value of 5.96 µM and 3.83 µM, respectively. Compound **PK-D8** had IC_{50} value of 1.90 µM.

After analyzing the *in silico* and *in vitro* results, all the compounds were examined for anti-HIV activity against HIV-1 (III_B) and HIV-2 (ROD) in cell based assay. First, cytotoxicity was studied using MTT based cell viability assay against HeLa cell line and then anti-HIV activity against HIV-1 (III_B) and HIV-2 (ROD) at/below their cytotoxic concentration was evaluated. It was however observed that none of the compound showed anti-HIV activity below their cytotoxic concentration (as shown in **table 12**). The compounds showed very good potential *in vitro* however, in cell culture assay the activity was not seen. This indicates that the cytotoxicity rather increases by removing 2-hydroxy substitution and these results support the necessity to have N-hydroxy substitution as proposed by Billiamboz *et al.*

8.3 Oral bioavailability and toxicity prediction

In-silico predicted drug likeness parameters of the designed compounds have been shown in **table 13** and it was observed that predicted drug-likeness parameters like M.Wt, HBD, HBA, logP, and PSA were within their optimum range. All the compounds obeyed Lipinski rule of five. LogP of these derivatives varied from 2.20 to 3.80. The number of hydrogen bond donors ranged between 1 to 2 and hydrogen bond acceptors between 2 to 5. The polar surface area was found to be in range of 110.16 to 140.56.

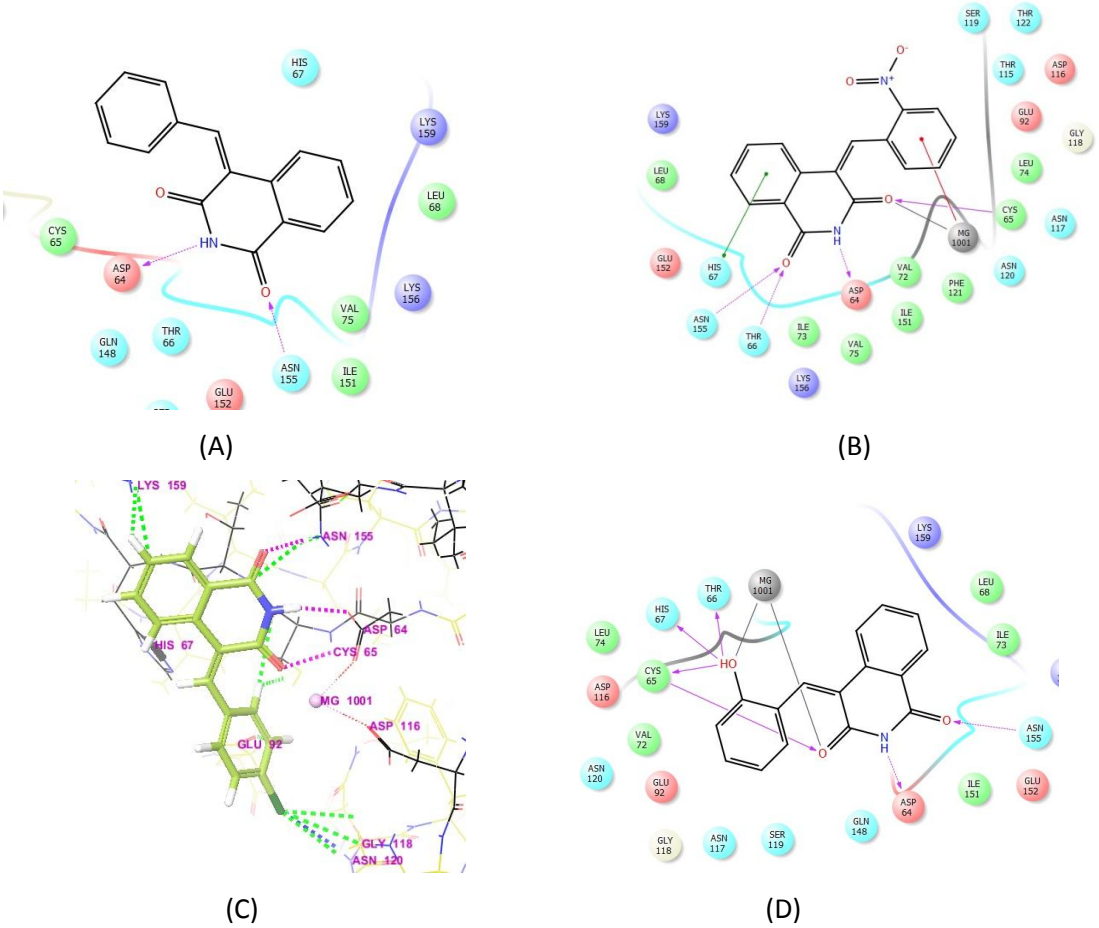

Figure 27: Docking poses of few representative compounds A: 2D interaction plot of PK-D1; B: 2D interaction plot of PK-D2; C: Docking pose of PK-D6; D: 2D interaction plot of PK-D8

Table 11: Results of in-vitro HIV-1 IN inhibition and docking studies of PK-D1 to PK-D16

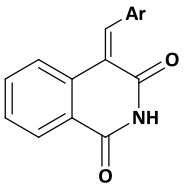

Code	Ar	Docking score	% IN Inhibition*	IC_{50} value**
Dolutegravir		-7.30	95.00	nd
PK-D1	Ph	-5.40	50.43	nd
PK-D2	2-NO_2-Ph	-7.64	77.24	5.96±1.0
PK-D3	4-NO_2-Ph	-6.71	69.04	nd

PK-D4	2-Cl-Ph	-7.13	70.72	nd
PK-D5	3-Cl-Ph	-6.10	63.75	nd
PK-D6	4-Cl-Ph	-7.76	84.12	3.83±0.27
PK-D7	2,4-diCl-Ph	-6.19	67.19	nd
PK-D8	2-OH-Ph	-7.86	87.80	1.90±0.15
PK-D9	4-OMe-Ph	-5.46	54.49	nd
PK-D10	3,4-diOMe-Ph	-6.26	64.55	nd
PK-D11	2,5-diOMe-Ph	-5.72	57.85	nd
PK-D12	3,4,5-triOMe-Ph	-5.87	61.92	nd
PK-D13	4-OH-3-OMe-Ph	-6.08	62.13	nd
PK-D14	4-OH-3-OEt-Ph	-5.28	44.97	nd
PK-D15	4-(N,N-diCH_3)-Ph	-6.03	60.19	nd
PK-D16	1H-indol-3-yl	-6.18	62.48	nd

% inhibition at 10µM concentration, values are mean of duplicate experiment performed independently, nd = not done; ** in µM

Table 12: Anti-HIV activity of synthesized compounds PK-D1 to PK-D16

Compounds	**HIV-1 (III_B)**			**HIV-2 (ROD)**		
	EC_{50}[1] (µM)	**CC_{50}[2] (µM)**	**HIV-1[3] SI**	**EC_{50}[1] (µM)**	**CC_{50}[2] (µM)**	**HIV-2[3] SI**
Dolutegravir	0.0006±0.000001	1.275±0.3	2110.00	0.00232±0.00061	1.495±0.165	597.00
PK-D1	>56.45±2.25	56.45±2.25	<1	>58.19±3.62	58.19±3.62	<1
PK-D2	>45.25±1.75	45.25±1.75	<1	>46.59±1.95	46.59±1.95	<1
PK-D3	>12.35±0.75	12.35±0.75	<1	>13.81±0.69	13.81±0.69	<1
PK-D4	>20.14±0.06	20.14±0.06	<1	>25.18±2.44	25.18±2.44	<1
PK-D5	>15.75±2.35	15.75±2.35	x1	>16.85±2.15	16.85±2.15	<1
PK-D6	>11.50±0.90	11.50±0.90	<1	>11.85±0.85	11.85±0.85	<1
PK-D7	>20.68±0.31	0.68±0.31	<1	>24.25±0.60	24.25±0.60	<1
PK-D8	>51.50±1.45	51.50±1.45	<1	>56.51±2.62	56.51±2.62	<1
PK-D9	>53.10±0.30	53.10±0.30	<1	>55.12±2.23	55.12±2.23	<1
PK-D10	>63.10±2.60	63.10±2.60	<1	>63.87±2.86	63.87±2.86	<1

PK-D11	>12.30±0.50	12.30±0.50	<1	>15.75±2.05	15.75±2.05	<1
PK-D12	>58.50±7.40	58.50±7.40	<1	>62.15±7.30	62.15±7.30	<1
PK-D13	>38.25±7.65	38.25±7.65	<1	>39.77±3.15	39.77±3.15	<1
PK-D14	>56.65±5.85	56.65±5.85	<1	>58.21±5.85	58.21±5.85	<1
PK-D15	>42.85±3.65	42.85±3.65	<1	>44.20±3.65	44.20±3.65	<1
PK-D16	>11.35±3.85	11.35±3.85	<1	>13.62±3.85	13.62±3.85	<1

[1] EC_{50}: concentration of compound required to achieve 50% protection of MT-4 cell cultures against HIV induced cytotoxicity, as determined by MTT method. [2] CC_{50}: concentration required to reduce the viability of mock-infected cells by 50%, as determined by MTT method. [3] SI: selectivity index (CC_{50}/EC_{50}).

Table 13: *In silico* predicted physiochemical parameters of compounds PK-D1 to PK-D16

CODE	Mol. Formula	M.Wt.	log P[a]	RB[b]	HBA[c]	HBD[d]	PSA[e]	log S[f]	PCaco[g]
PK-D1	$C_{16}H_{11}NO_2$	249.26	2.50	1	2	1	110.16	-3.82	1.31
PK-D2	$C_{16}H_{10}N_2O_4$	294.27	2.41	2	4	1	124.78	-3.97	1.02
PK-D3	$C_{16}H_{10}N_2O_4$	294.27	2.41	2	4	1	124.78	-3.97	1.02
PK-D4	$C_{16}H_{10}ClNO_2$	283.71	3.15	1	2	1	120.43	-4.10	1.31
PK-D5	$C_{16}H_{10}ClNO_2$	283.71	3.15	1	2	1	120.43	-4.10	1.31
PK-D6	$C_{16}H_{10}ClNO_2$	283.71	3.15	1	2	1	120.43	-4.10	1.31
PK-D7	$C_{16}H_9Cl_2NO_2$	318.16	3.80	1	2	1	130.73	-4.91	1.35
PK-D8	$C_{16}H_{11}NO_3$	265.27	2.20	1	3	2	114.92	-3.34	1.01
PK-D9	$C_{17}H_{13}NO_3$	279.30	2.51	2	3	1	121.60	-3.96	1.30
PK-D10	$C_{18}H_{15}NO_4$	309.32	2.51	3	4	1	133.08	-3.94	1.02
PK-D11	$C_{18}H_{15}NO_4$	309.32	2.51	3	4	1	133.08	-3.94	1.02
PK-D12	$C_{19}H_{17}NO_5$	339.35	2.52	4	5	1	140.56	-4.28	1.04
PK-D13	$C_{17}H_{13}NO_4$	295.29	2.21	2	4	2	126.40	-3.69	1.03
PK-D14	$C_{18}H_{15}NO_4$	309.32	2.60	3	4	2	132.76	-3.95	1.02
PK-D15	$C_{18}H_{16}N_2O_2$	292.34	2.56	2	3	1	128.62	-3.81	1.27
PK-D16	$C_{18}H_{12}N_2O_2$	288.31	2.98	1	2	2	126.02	-3.98	0.98

[a]Partition coefficient, [b]No. of rotatable bonds, [c] No. of hydrogen bond acceptors, [d] No. of hydrogen bond donors, [e]polar surface area, [f]water solubility, [g]caco-2 permeability.

CHAPTER 9: *N*- SUBSTITUTED PHENYL COUMARIN-3-CARBOXAMIDES

Coumarins contain oxygen as a member of the heterocyclic ring. They are divided into two main categories viz: benzo-α-pyrones and benzo-γ-pyrones (also called as chromones); the second differing from the former only in the position of carbonyl group in heterocyclic ring. Some naturally occurring coumarin derivatives are warfarin, umbelliferone (7-hydroxycoumarin), aesculetin (6,7-dihydroxycoumarin), herniarin (7-methoxycoumarin), psoralen and imperatorin. Both, natural and synthetic coumarins, have widespread biological significance based on their anticoagulation, analgesic, anti-inflammatory, anti-sedative, anti-HIV, anti-proliferative, antidiabetic, antimalarial, antioxidant, antiulcer, dermal photosensitizing, estrogenic, hypothermic, hypnotic, vasodilator activities and also used as agrochemicals, perfumes, food additives (Fylaktakidou, 2004; Wu, 2009).

It is reported that for HIV IN inhibition, the ligand must have two hydrogen bond acceptor groups (such as diketo functionality) and one aromatic ring for the inhibition of HIV IN. Since coumarins offer such structural feature, coumarin derivatives have been explored as HIV-1 integrase (IN) inhibitors. Rosmarinic acid (compound **I**), wherein coumarin ring is open, has showed in vitro inhibition of recombinant integrase with IC_{50} value below 10 µM (Mazumder, 1997).

Later, Mao *et al.* reported modified coumarin dimers (example compounds **II-VI**) with IC_{50} value in the range of 0.5 - 3.9 µM (Mao, 2002). Bailly *et al.* found that caffeoyl-coumarin conjugate compound (compound **VII**) inhibits HIV-1 integrase at IC_{50} of 1.0 µM (Bailly, 2005). It was hypothesized that coumarin nucleus with a phenyl ring separated by appropriate linker will inhibit HIV integrase. For choice of linker, it was observed that in reported integrase inhibitors such as raltegravir, dolutegravir (compound **VIII**) and phenyl ring is separated from nucleus using carboxamide. Therefore, carboxamide linker was selected and it was expected that presence of amide linkage be expected to provide flexibility to optimize the interactions at the receptor. In prototype compounds **PK-E1** to **PK-E18**, modification was done by changing substitution pattern on phenyl ring and its effect on integrase inhibition was evaluated.

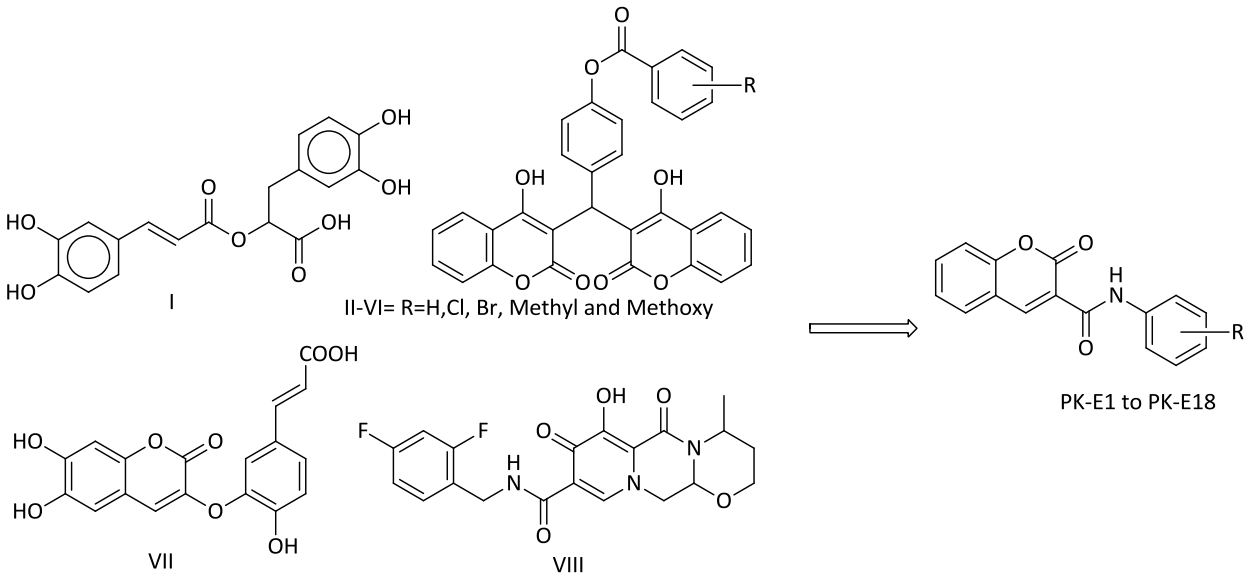

Figure 28: Literature reported potential HIV-1 IN inhibitors and the designed prototype (PK-E1 to PK-E18)

9.2 Chemistry

The synthesis of 3-carbethoxycoumarin involves a transesterification reaction, which further hydrolyzed to coumarin-3-carboxylic acid in strong basic condition. The final 2-Oxo-*N*-substituted phenyl- 2H - chromene- 3- carboxamides **PK-E1** to **PK-E18** were synthesized by treating coumarin-3-carboxylic acid with different substituted anilines.

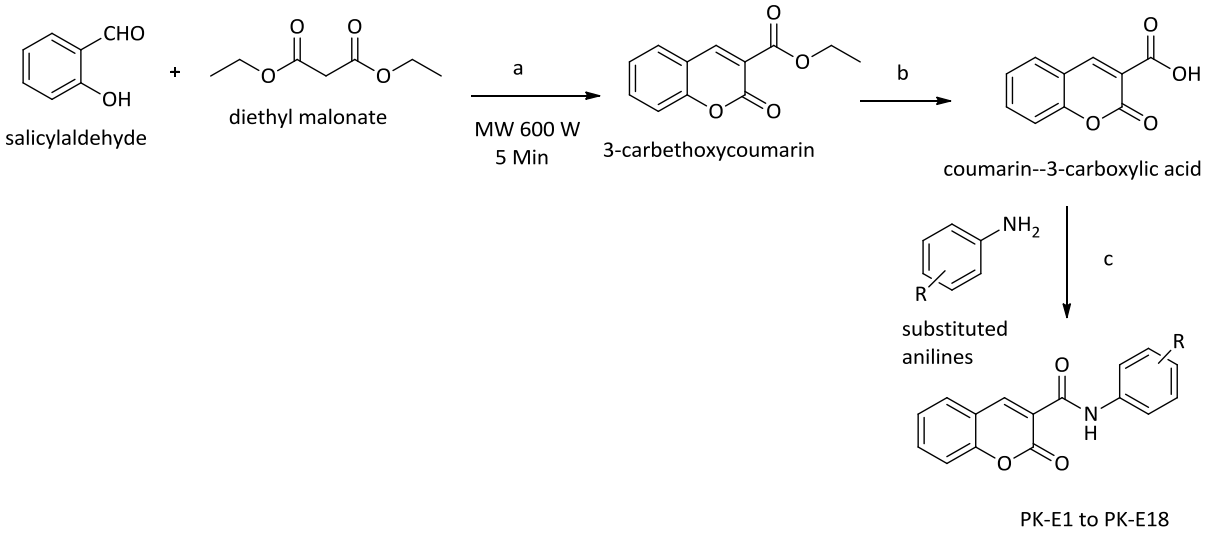

Scheme 5: Reagents and conditions: (a) Piperidine, Gla. acetic acid; MW 600W, 5min; (b) KOH, 6M HCl, 1 h, reflux (c) EDC.HCl, HOBT, triethylamine, dichloromethane, RT, 12 h

Reaction mechanism

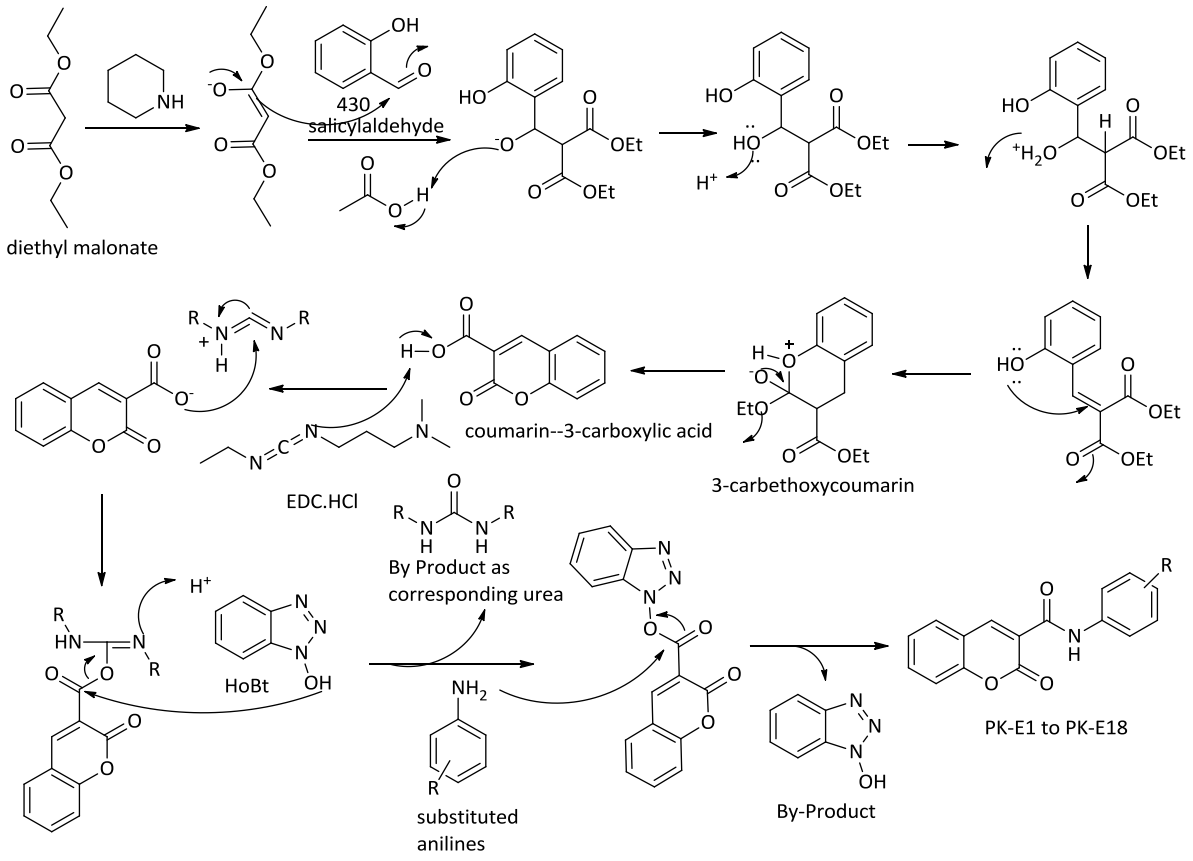

Figure 29: Plausible mechanism for synthesis of chromene- 3- carboxamides (PK-E1 to PK-E18)

Preparation of 3-carbethoxycoumarin involves formation of intermediate nucleophilic enolate ion via deprotonation of diethyl malonate by the non-nucleophilic pyridine base. This stable enolate further attacks on carbonyl group of salicylaldehyde. The consequential alkoxide picks up the acidic proton on the ethanol solvent and the hydroxide formed attacks an intermolecular hydride ion for releasing water followed by formation of stable conjugated enone while the phenol attacks the carboxyl group in an intramolecular fashion eventually causing the ether group to leave. The displaced ether group, which is the conjugate base of ethanol, is highly nucleophilic and attacks the acidic proton on the carboxylic acid and upon tautomerization, 3- carbethoxycoumarin is effectively formed (Klutchko, 1974). The final step of the reaction involves treatment of coumarin--3-carboxylic acid with the series of different substituted anilines using 1-ethyl-3-(3-dimethylamino-propyl)carbodiimide hydrochloride (EDC.HCl) and *N*-hydroxybenzotriazole (HOBt) as a coupling agent yielded a series of 2-Oxo-N-substituted phenyl- 2*H* -chromene- 3- carboxamide (**PK-E1** to **PK-E18**).

Synthesis of 3-carbethoxycoumarin

In 25 ml, RBF Salicylaldehyde (1.0 mL), diethyl malonate (1.5 mL), piperidine (15 drops) and glacial acetic acid (5 drops) were added. The reaction mixture was heated by microwave irradiation for about 5 minute at 600 watt. The progress of the reaction was monitored by using TLC (ethyl acetate/n-hexane: 30:70). After completion of reaction the reaction mixture was cooled to, room temperature until precipitates comes out. The crude product was purified by recrystallization from ethanol (95%) to afford pure product. Yellow Solid; Yield 80%; Mp: 92-94°C; IR (KBr) cm^{-1}: 3106 (Ar-$CH_{str.}$), 2971 (Ali-$CH_{str.}$), 1698, 1715 (C=$O_{str.}$), 1587 (C=C); ^{1}H-NMR (400 MHz, $CDCl_3$): δ (ppm): 1.41 (t, 3H, CH_3), 4.46 (q, 2H, CH_2), 7.28-7.36 (m, 4H, Ar-H), 8.55 (s, 1H, CH-CO); ^{13}C-NMR (100 MHz, $CDCl_3$): δ (ppm): 15.4, 63.8, 114.7, 119.4, 121.4, 122.8, 124.9, 127.6, 129.3, 154.4 and 168.2; ESI-MS m/z: 219.04 $[M+H]^+$.

Synthesis of coumarin-3-carboxylic acid

In 100 ml, RBF 3-carbethoxycoumarin (2.0 g) was dissolved in 30 ml of EtOH: H_2O (1:1). To this solution, potassium hydroxide was added (5.0 eq). The reaction mass was stirred at reflux temperature for 1 hr. The progress of the reaction was monitored by using TLC (ethyl acetate/n-hexane: 50:50). After completion of reaction, the reaction mixture was cooled to room temperature and acidified with 6M HCl solution. The white solid product precipitates out. The crude product was treated with n-hexane to remove non-polar impurities and recrystallized with ethanol. White Solid; Yield 78%; Mp: 188-190°C; IR (KBr) cm^{-1}: 3465 ($OH_{str.}$), 3115 (Ar-$CH_{str.}$), 2948 (Ali-$CH_{str.}$), 1632, 1730 (C=$O_{str.}$), 1587 (C=C); ^{1}H-NMR (400 MHz, $CDCl_3$): δ (ppm): 7.49-7.86 (m, 4H, Ar-H), 8.98 (s, 1H, CH-CO), 12.25 (s, 1H, -COOH); ^{13}C-NMR (100 MHz, $CDCl_3$): δ (ppm): 115.9, 118.6, 122.7, 123.4, 125.2, 126.7, 128.4, 153.9 and 167.4; ESI-MS m/z: 191.03 $[M+H]^+$.

Synthesis of 2-Oxo-N-substituted phenyl-2*H* -chromene- 3- carboxamide (PK-E1 to **PK-E18)**

To the coumarin-3-carboxylic acid (1.0 g) in 20 ml dry DCM was added EDCl-HCl (0.6 g), and HOBt (0.55 g). After stirring at RT for 30 min, the amine (1.1 equiv) was added followed by triethylamine (1 ml). The reaction mixture was stirred at RT for 12 h. The progress of the reaction was monitored by using TLC (ethyl acetate/n-hexane: 30:70). After completion of reaction, the reaction mixture was diluted with DCM and washed with 1M HCl solution. The organic layer was separated and further treated with saturated sodium bicarbonate solution followed by brine solution. The organic layer was dried on sodium sulfate and concentrated by using rota-evaporator. The crude products were recrystallized using Dichloromethane: Pentane (2:8).

2-Oxo-*N*-phenyl-2*H*-chromene-3-carboxamide (PK-E1): Yellow Solid; Yield 72%; Mp: 182-184°C; IR (KBr) cm^{-1}: 3387 ($NH_{str.}$), 3104 (Ar-$CH_{str.}$), 2965, 2864 ($CH_{str.}$), 1642, 1745 ($C=O_{str.}$), 1549 (C=C); ^{1}H-NMR (400 MHz, $CDCl_3$): δ (ppm): 7.38-7.76 (m, 9H, ArH), 9.06 (s, 1H, -C=H), 10.9 (s, 1H, CO-NH); ^{13}C-NMR (100 MHz, $CDCl_3$): δ (ppm): 113.3, 115.2 ,116.2, 118.4, 120.3, 120.9, 123.2, 124.4, 126.1 128.8, 128.8, 130.3, 134.4, 146.6, 153.5 and 160.5; ESI-MS m/z: 266.18 $[M+H]^+$.

***N*-(2-chlorophenyl)-2-Oxo-2H-chromene-3-carboxamide (PK-E2):** Brown Solid; Yield 66%; Mp: 204-206°C; IR (KBr) cm^{-1}: 3452 ($NH_{str.}$), 3097 (Ar-$CH_{str.}$), 3011, 2860 ($CH_{str.}$), 1668, 1740 ($C=O_{str.}$), 1541 (C=C); ^{1}H-NMR (400 MHz, $CDCl_3$): δ (ppm): 7.28-7.79 (m, 8H, ArH), 9.09 (s, 1H, -C=H), 10.81 (s, 1H, CO-NH); ^{13}C-NMR (100 MHz, $CDCl_3$): δ (ppm): 115.7, 116.9, 117.9, 118.2, 120.9, 124.1, 126.2, 127.9, 128.4, 128.5, 132.1, 134.0, 145.5 and 162.1. 113.3, 115.2, 116.2, 118.4, 120.3, 120.9, 123.2, 124.4, 126.1 128.8, 128.8, 130.3, 134.4, 146.6, 153.5 and 160.5; ESI-MS m/z: 300.08 $[M+H]^+$.

***N*-(4-chlorophenyl)-2-Oxo-2H-chromene-3-carboxamide (PK-E3):** Yellow Solid; Yield 64%; Mp: 213–215 °C; IR (KBr) cm^{-1}: 3391 ($NH_{str.}$), 3109 (Ar-$CH_{str.}$), 2951, 2841 ($CH_{str.}$), 1654, 1748 ($C=O_{str.}$), 1540 (C=C); ^{1}H-NMR (400 MHz, $CDCl_3$): δ (ppm): 7.28-7.72 (m, 8H, ArH), 9.04 (s, 1H, -C=H), 10.900 (s, 1H, CO-NH); ^{13}C-NMR (100 MHz, $CDCl_3$): δ (ppm): 114.1, 116.2, 118.1, 119.5, 121.2, 125.1, 127.8, 128.1, 129.5, 133.8, 135.5, 146.50, 152.2 and 163.2; ESI-MS m/z: 300.09 $[M+H]^+$.

***N*-(2-chloro-4-nitrophenyl)-2-Oxo-2H-chromene-3-carboxamide (PK-E4):** Creamish Solid; Yield 64%; Mp: 217–219°C; IR (KBr) cm^{-1}: 3416 ($NH_{str.}$), 3071 (Ar-$CH_{str.}$), 3023, 2874 ($CH_{str.}$), 1662, 1741 ($C=O_{str.}$), 1549 (C=C); ^{1}H-NMR (400 MHz, $CDCl_3$): δ (ppm): 7.26-7.68 (m, 7H, ArH), 9.07 (s, 1H, -C=H), 9.87 (s, 1H, CO-NH); ^{13}C-NMR (100 MHz, $CDCl_3$): δ (ppm): 116.8, 117.6, 118.4, 119.2, 122.2, 124.1, 126.9, 129.6, 130.6, 134.6, 136.6, 145.6, 154.5 and 165.6; ESI-MS m/z: 344.70 $[M+H]^+$.

***N*-(4-fluorophenyl)- 2-Oxo-2H-chromene-3-carboxamide (PK-E5):** Brown Solid; yield 66%; Mp: 208–210 °C; IR (KBr) cm^{-1}: 3424 ($NH_{str.}$), 3068 (Ar-$CH_{str.}$), 3029, 2884 ($CH_{str.}$), 1669, 1747 ($C=O_{str.}$), 1554 (C=C); ^{1}H-NMR (400 MHz, $CDCl_3$): δ (ppm): 7.31-7.82 (m, 8H, ArH), 8.21 (s, 1H, -C=H), 9.41 (s, 1H, CO-NH); ^{13}C-NMR (100 MHz, $CDCl_3$): δ (ppm): 113.9, 115.1, 118.1, 118.8, 120.7, 123.4, 125.6, 128.5, 129.6, 133.5, 134.6, 144.2, 153.6 and 164.0; ESI-MS m/z: 284.24 $[M+H]^+$.

2-Oxo-*N*-(3-(trifluoro methyl)- phenyl-2H-chromene-3-carboxamide (PK-E6): Light Brown Solid; yield 61%; Mp: 224–226°C; IR (KBr) cm^{-1}: 3438 ($NH_{str.}$), 3051 (Ar-$CH_{str.}$), 3045, 2892 ($CH_{str.}$), 1667, 1741 ($C=O_{str.}$), 1562 (C=C); ^{1}H-NMR (400 MHz, $CDCl_3$): δ (ppm): 7.31-7.82 (m, 8H, ArH), 8.21 (s, 1H, -C=H), 9.41 (s, 1H, CO-NH); ^{13}C-NMR (100 MHz, $CDCl_3$): δ (ppm): 114.8, 116.2, 117.9, 118.3, 121.5, 124.1, 126.7, 129.1, 131.3, 131.3, 132.9, 132.9, 138.1, 148.5, 156.5 and 166.5; ESI-MS m/z: 334.16 $[M+H]^+$.

***N*-(5-fluoro-2-methyl phenyl)-2-Oxo-2H-chromene-3-carboxamide (PK-E7):** Yellow Solid; yield 66%; Mp: 216–218°C; IR (KBr) cm^{-1}: 3461 ($NH_{str.}$), 3023 (Ar-$CH_{str.}$), 3014, 2884 ($CH_{str.}$), 1654, 1735 ($C=O_{str.}$), 1557 (C=C); ^{1}H-NMR (400 MHz, $CDCl_3$): δ (ppm): 7.28-7.74 (m, 8H, ArH), 8.15 (s, 1H, -C=H), 9.46 (s, 1H, CO-NH); ^{13}C-NMR (100 MHz, $CDCl_3$): δ (ppm): 20.1, 114.4, 115.8, 118.6, 119.5, 120.1, 122.5, 126.1, 128.6, 129.1, 130.2, 132.4, 133.0, 148.1, 154.1 and 162.6 ppm; ESI-MS m/z: 284.24 $[M+H]^+$.

***N*-(4-bromophenyl)-2-Oxo-2H-chromene-3-carboxamide (PK-E8):** Brown Solid; yield 71%; Mp: 228–230 °C; IR (KBr) cm^{-1}: 3441 ($NH_{str.}$), 3087 (Ar-$CH_{str.}$), 3021, 2896 ($CH_{str.}$), 1669, 1748 ($C=O_{str.}$), 1566 (C=C); ^{1}H-NMR (400 MHz, $CDCl_3$): δ (ppm): 7.52-7.79 (m, 8H, ArH), 9.04 (s, 1H, -C=H), 10.90 (s, 1H, CO-NH); ^{13}C-NMR (100 MHz, $CDCl_3$): δ (ppm): 116.7, 117.4, 118.6, 122.0, 124.7, 125.6, 127.8, 130.0, 132.0, 134.5, 136.7, 149.2, 154.5, 159.3 and 161.8; ESI-MS m/z: 344.02 $[M+H]^+$.

***N*-(2,6-dibromo-4-nitro phenyl)-2-Oxo-2H-chromene-3-carboxamide (PK-E9):** Yellow Solid; yield 66%; Mp: 242–244°C; IR (KBr) cm^{-1}: 3463 ($NH_{str.}$), 3058 (Ar-$CH_{str.}$), 3024, 2964 ($CH_{str.}$), 1657, 1748 ($C=O_{str.}$), 1569 (C=C); ^{1}H-NMR (400 MHz, $CDCl_3$): δ (ppm): 7.41-7.83 (m, 6H, ArH), 8.23 (s, 1H, -C=H), 9.39(s, 1H, CO-NH); ^{13}C-NMR (100 MHz, $CDCl_3$): δ (ppm): 113.9, 116.1, 118.9, 119.9, 124.6, 124.9, 125.1, 127.1, 127.4, 127.8, 149.0, 150.1, 153.4, 159.1 and 163.8; ESI-MS m/z:466.93 $[M+H]^+$.

***N*-(2-hydroxyphenyl)-2-Oxo-2H-chromene-3-carboxamide (PK-E10):** Yellow Solid; yield 66%; Mp: 231–233°C; IR (KBr) cm^{-1}: 3496 ($OH_{str.}$), 3424 ($NH_{str.}$), 3061 (Ar-$CH_{str.}$), 3020, 2897 ($CH_{str.}$), 1659, 1756 ($C=O_{str.}$), 1585 (C=C); ^{1}H-NMR (400 MHz, $CDCl_3$): δ (ppm): 5.58 (s, 1H, OH), 7.37-7.77 (m, 8H, ArH), 8.31 (s, 1H, -C=H), 9.28 (s, 1H, CO-NH); ^{13}C-NMR (100 MHz, $CDCl_3$): δ (ppm): 113.9, 115.8, 116.2, 118.4, 123.5, 126.4, 127.4, 127.5, 128.4, 128.4, 129.2, 130.4, 131.4, 132.4, 144.4, 158.4 and 166.2; ESI-MS m/z: 280.16 $[M+H]^+$.

***N*-(3-hydroxyphenyl)-2-Oxo-2H-chromene-3-carboxamide (PK-E11):** Yellow Solid; yield 52%; Mp: 228–230°C; IR (KBr) cm^{-1}: 3459 ($OH_{str.}$), 3384 ($NH_{str.}$), 3047 (Ar-$CH_{str.}$), 3014, 2884 ($CH_{str.}$), 1652, 1762 ($C=O_{str.}$), 1574 (C=C); ^{1}H-NMR (400 MHz, $CDCl_3$): δ (ppm): 5.64 (s, 1H, OH), 7.43-7.92 (m, 8H, ArH), 8.39 (s, 1H, -C=H), 9.24 (s, 1H, CO-NH); ^{13}C-NMR (100 MHz, $CDCl_3$): δ (ppm): 114.1, 116.1, 117.1, 118.6, 122.5, 124.6, 128.6, 128.7, 130.1, 130.1, 131.4, 132.6, 133.5, 134.5, 145.9, 155.5 and 164.5; ESI-MS m/z: 282.08 $[M+H]^+$.

***N*-(4-hydroxyphenyl)-2-Oxo-2H-chromene-3-carboxamide (PK-E12):** Brown Solid; yield 61%; Mp: 234–236°C; IR (KBr) cm^{-1}: 3471 ($OH_{str.}$), 3442 ($NH_{str.}$), 3038 (Ar-$CH_{str.}$), 3023, 2898 ($CH_{str.}$), 1656, 1767 ($C=O_{str.}$), 1571 (C=C); ^{1}H-NMR (400 MHz, $CDCl_3$): δ (ppm): 4.86 (s, 1H, OH), 6.75-7.72 (m, 8H, ArH), 9.04 (s, 1H, -C=H), 10.75 (s, 1H, CO-NH); ^{13}C-NMR (100 MHz, $CDCl_3$): δ (ppm): 116.2, 117.2, 117.9, 118.0, 120.2,

122.6, 126.6, 126.6, 128.5, 128.5, 131.4 , 133.5, 134.8, 135.9, 146.5, 154.0 and 167.0; ESI-MS m/z: 282.09 $[M+H]^+$.

***N*-(2,4-dimethyl phenyl)-2-Oxo-2H-chromene-3-carboxamide (PK-E13):** Dark Brown Solid; yield 46%; Mp: 226–228°C; IR (KBr) cm^{-1}: 3428 ($NH_{str.}$), 3042 (Ar-$CH_{str.}$), 3013, 2874 ($CH_{str.}$), 1663, 1764 ($C=O_{str.}$), 1570 (C=C); ^{1}H-NMR (400 MHz, $CDCl_3$): δ (ppm): 2.34 (s, 3H, CH_3), 2.41 (s, 3H, CH_3), 7.08 (s, 1H, ArH), 7.49-8.11 (m, 6H, ArH), 9.06 (s, 1H, -C=H), 10.73 (s, 1H, CO-NH); ^{13}C-NMR (100 MHz, $CDCl_3$): δ (ppm): 18.3, 23.3, 112.3, 114.8, 115.9, 118.0, 121.6, 125.4, 128.0, 128.2, 137.1, 140.2, 143.2, 160.2, 161.2 and 163.6; ESI-MS m/z: 294.16 $[M+H]^+$.

***N*-(4-(cyanomethyl) phenyl)-2-Oxo-2H-chromene-3-carboxamide (PK-E14):** Yellow Solid; yield 62%; Mp: 262–264°C; IR (KBr) cm^{-1}: 3462 ($NH_{str.}$), 3071 (Ar-$CH_{str.}$), 3035, 2881 ($CH_{str.}$), 2245 ($CN_{str.}$), 1667, 1769 ($C=O_{str.}$), 1557 (C=C); ^{1}H-NMR (400 MHz, $CDCl_3$): δ (ppm): 4.28 (s, 2H, CH_2CN), 7.24-7.40 (dd, 4H, ArH), 7.44-7.72 (m, 4H, ArH), 8.48 (s, 1H, -C=H), 9.17 (s, 1H, CO-NH); ^{13}C-NMR (100 MHz, $CDCl_3$): δ (ppm): 21.5, 112.3, 113.6, 116.6, 116.9, 117.3, 120.4, 123.8, 126.5, 126.6, 131.0, 132.4, 140.2, 148.0, 157.1 and 161.8; ESI-MS m/z: 305.14 $[M+H]^+$.

2-Oxo -*N*-(4-(phenyldiazenyl) phenyl)-2H-chromene-3-carboxamide (PK-E15): Yellow Solid; yield 66%; Mp: 252–254°C; IR (KBr) cm^{-1}: 3469 ($NH_{str.}$), 3036 (Ar-$CH_{str.}$), 3027, 2868 ($CH_{str.}$), 1652, 1744 ($C=O_{str.}$), 1552 (C=C); ^{1}H-NMR (400 MHz, $CDCl_3$): δ (ppm): 7.20-8.15 (m, 8H, ArH), 7.82-8.12 (dd, 4H, ArH), 8.36 (s, 1H, -C=H), 9.12 (s, 1H, CO-NH); ^{13}C-NMR (100 MHz, $CDCl_3$): δ (ppm): 110.1, 113.6, 118.2, 118.2, 119.2, 122.5, 122.6, 124.2, 128.6, 128.7, 130.1, 130.1, 134.2, 136.5, 143.5, 149.3, 154.6 and 163.8; ESI-MS m/z: 370.08 $[M+H]^+$.

2-Oxo -*N*-(pyridine-2-yl)- 2H-chromene-3-carboxamide (PK-E16): White Solid; yield 66%; Mp: 209–211 °C; IR (KBr) cm^{-1}: 3484 ($NH_{str.}$), 3048 (Ar-$CH_{str.}$), 3019, 2915 ($CH_{str.}$), 1652, 1754 ($C=O_{str.}$), 1569 (C=C); ^{1}H-NMR (400 MHz, $CDCl_3$): δ (ppm): 7.24 (d, 1H, ArH), 7.37-7.40 (d, 2H, ArH), 7.68-7.72 (d, 2H, ArH), 8.15-8.18 (d, 2H, ArH), 8.79(s, 1H, -C=H), 8.94-8.95 (dd, 2H, ArH), 10.85 (s, 1H, CO-NH); ^{13}C-NMR (100 MHz, $CDCl_3$): δ (ppm): 109.3, 116.6, 117.9, 120.2, 124.3, 125.2, 126.2, 128.9, 134.4, 140.2, 153.1, 154.5, 154.8 and 158.8; ESI-MS m/z: 267.31 $[M+H]^+$.

***N*-(3-hydroxy-pyridin-2-yl)-2-Oxo-2H-chromene-3-carboxamide (PK-E17):** Yellow Solid; yield 69%; Mp: 214–216°C; IR (KBr) cm^{-1}: 3552 ($OH_{str.}$), 3442 ($NH_{str.}$), 3072 (Ar-$CH_{str.}$), 3029, 2915 ($CH_{str.}$), 1658, 1759 ($C=O_{str.}$), 1573 (C=C); ^{1}H-NMR (400 MHz, $CDCl_3$): δ (ppm): 3.52 (s, 1H, CO-NH), 7.20 (d, 1H, ArH), 7.25-7.28 (dd, 2H, ArH), 7.47-7.50 (dd, 2H, ArH), 7.78-8.03 (m, 3H, ArH), 9.08 (s, 1H, -C=H); ^{13}C-NMR (100 MHz, $CDCl_3$): δ (ppm): 117.0, 118.4, 118.6, 121.9, 123.2, 125.7, 128.0, 130.2, 135.3, 139.3, 146.0, 150.2, 154.8 and 161.02; ESI-MS m/z: 267.31 $[M+H]^+$.

2-Oxo -*N*-(6-methylpyridine-2-yl)-2H-chromene-3-carboxamide (PK-E18): Light Yellow Solid; yield 46%; Mp: 198–200°C; IR (KBr) cm^{-1}: 3462 ($NH_{str.}$), 3064 (Ar-$CH_{str.}$), 3031, 2884 ($CH_{str.}$), 1668, 1762 ($C=O_{str.}$), 1592 (C=C); ^{1}H-NMR (400 MHz, $CDCl_3$): δ (ppm): 2.54 (s, 3H, CH_3), 6.96 (d, 1H, ArH), 7.47-7.75 (m, 5H, ArH), 8.16 (t, 1H, ArH), 9.03 (s, 1H, -C=H), 11.15 (s, 1H, CO-NH); ^{13}C-NMR (100 MHz, $CDCl_3$): δ (ppm): 22.6, 113.1, 116.1, 117.3, 118.9, 120.5, 122.4, 127.1, 127.2, 134.5, 138.6, 142.6, 147.3, 153.2 and 162.6; ESI-MS m/z: 281.51 $[M+H]^+$.

9.2 Results and Discussion

The percentage inhibition of all compounds and IC_{50} value of few highly active compounds is reported in **table 14**. The results of cytoxicity and anti-HIV assay are shown in **table 15**. It was observed that unsubstituted phenyl derivative (**PK-E1**) lacks interactions with catalytic trial and shows only hydrophobic interactions with amino acids Cys 65, Thr 66, His 67, Glu 92 and Asn 155. It was also least active against IN in vitro and also showed lowest Gscore. Substitution of electron withdrawing chloro group at ortho position (**PK-E2**) and para position (**PK-E3**) displayed slight improvement in Gscore and IN inhibitory activity. Both compounds showed hydrophobic interactions with Glu 152, Lys 156 and Lys 159. Compound **PK-E2** showed hydrogen bonding interaction with Cys 65 (by amidic NH) while in case of **PK-E3** similar interaction was observed with Gln 148 (by carbonyl group of ring). The slightly higher Gscore of **PK-E2** may be due to presence of π-π stacking interaction with His 67 which was absent in **PK-E3**.

Substitution of p-nitro group in compound **PK-E2** gave compound **PK-E4**, which showed hydrogen bonding interactions with Lys 156 (by p-NO_2 group) and Gln 148 (by carbonyl group of ring) while showing similar hydrophobic interactions as that of **PK-E2**, but there was no significant increase in activity and Gscore.

Compound **PK-E5** having fluoro substitution at para position also showed less activity, may due to absence of hydrogen bonding interactions with DDE motif. However, substitution of trifluoromethyl group on meta position (**PK-E6**) showed slight enhancement in activity as it had hydrogen bonding interactions with Cys 65 and Asn 155. Additionally, hydrophobic interactions with Asp 64, Thr 66, His 67, Gln 148, Glu 152 and Lys 159 were also seen. By substituting methyl as well as fluoro on phenyl ring (m-fluoro, o-methyl; **PK-E7**) marginal increase in docking interactions as well as in vitro IN inhibitory activity. It might be due to presence of hydrogen bonding interactions with Cys 65 (by carbonyl groups), His 67 and Glu 92 (by -NH of amidic bond). Additionally, **PK-E7** showed π-π stacking interaction with His 67 which was absent in **PK-E6**.

Significant increase in activity as well as Gscore was observed with substitution of 4-bromo (compound **PK-E8**, Gscore -6.86 and 89.94% inhibition at 10 µM concentration). It showed hydrogen bonding interactions with Cys 65 (by amidic carbonyl group), Gln 148 (by carbonyl group of ring) and hydrophobic interactions with Asp 64, Asp 116, Glu 152, Asn 155 and Lys 159. The diketo functionality also formed co-ordinate bonds with Mg1001.

2,6-dibromo-4-nitro substituted derivative (**PK-E9**) also showed hydrogen bonding interactions with His 67 (by NH of amidic bond), Ser 119, Asn 120 (by p-NO2 group) and Asn 155 (by oxygen of coumarin ring). Carbonyl groups of coumarin ring and amidic bond displayed metal coordination with magnesium ion (Mg 001). Halogen bonds and salt bridge were also seen with Cys 65, Asn 120 (by o-Br group) and Glu 92 (by p-NO2 group), respectively. Other hydrophobic interactions with His 67, Ser 119 and Lys 159 were also detected. The Gscore of **PK-E9** was -6.62 and showed 88.47 % inhibition *in vitro* at 10 µM concentration. When the phenyl ring was substituted with electron donating hydroxyl group, it was observed that 4-hydroxy (**PK-E12**) substitution favored the inhibitory potential as compared to 2- or 3-hydroxyl substitution (**PK-E10** and **PK-E11**, respectively).

Compound **PK-E10** having 2-hydroxy substitution showed hydrogen-bonding interactions with Thr 66 (by 2-hydroxy group) and Asn 155 (by amidic carbonyl group). Other hydrophobic interactions with Asp 64, Asp 116, His 67, Gln 148, Glu 152 and Lys 159 were also detected. Compound **PK-E11** also showed similar hydrogen-bonding interactions and hydrophobic interactions. Additional hydrophobic interactions with Thr 66, His 67, Gln 148, Glu 152, Asn 155 and Lys 159 were also seen.

The most active compound (**PK-E12**) showed highest docking score (-7.20) and 90.14 % inhibition at 10 µM concentration. Hydroxy group substitution at para position forms hydrogen bond with amino acid Asn 120. Amidic -NH group interacts with Asp 64, Cys 65 and Thr 66 via hydrogen bonding. Carbonyl group of chromene ring and amidic –NH shows hydrogen bond interactions with amino acid Cys 65 and Mg^{+2} ion via coordination bond. Hydrophobic interactions were also observed with amino acid residues such as His 67, Asp 116, Gln 148, Glu 152 and Lys 159.

Reduction in activity and Gscore was observed with either dimethyl substitution (**PK-E13**) or extending the length of substituent at 4th position (cyanomethyl phenyl (**PK-E14**) and phenyl diazenyl (**PK-E15**)), respectively. In all three cases, it was observed that there was no hydrogen bonding interactions with DDE motif but presence of hydrophobic interactions along with hydrogen bonding (Asn 155 by amidic carbonyl group). Additionally, compound **PK-E14** showed hydrogen-bonding interactions with His 67, Lys 159 (by 4-cyanomethyl group) and Gln 148 (by oxygen of chromene ring).

Compound **PK-E15** showed only one hydrogen bond with Gln 148 via carbonyl group of coumarin ring. Amidic linkage and diazo group did not participate in any type of interaction. Replacing phenyl ring with heterocycles such as pyridine was also considered to study the effect of activity. When phenyl ring was replaced with pyridin-2-yl (**PK-E16**), it exhibited better docking score, interactions and biological activity as compared to **PK-E1**. It showed hydrogen-bonding interactions with Asp 64, Asp 116 (amidic NH group), Cys 65 (by NH of pyridine ring and amidic carbonyl), Thr 66 (by coumarin ring), His 67 (amidic NH group) and Asn 155 (by oxygen of coumarin ring). Both, NH of pyridine ring and amidic carbonyl group, also formed metal coordination bond with magnesium (Mg 1001). Apart from these, hydrophobic interactions with Asp 64, Cys 65, Thr 66, His 67, Glu 152, Asn 155 and Lys 159 were also seen. Substitution on pyridine ring was found to reduce activity as was the case with 3-hydroxypyridin-2-yl (**PK-E17**) and 6-methylpyridin-2-yl (**PK-E18**) having 80.91 and 76.38 % inhibition, respectively at 10 µM concentration. Compounds **PK-E17** and **PK-E18** showed absence of hydrogen bonding interactions with Asp 64 and Asp 116 that were observed in **PK-E16**. Additionally **PK-E18** also showed absence of interaction with His 67 that might be responsible for less docking score as compare to **PK-E16** and **PK-E17**, respectively. Overall, it was observed that the HIV-1 IN inhibitory potency of designed compounds altered significantly with variation in nature as well as position of substituent.

In general, compounds having electron withdrawing group like 4-bromo (**PK-E8**) and 2,6-dibromo-4-nitro substitution (**PK-E5**); electron donating group like 4-hydroxy substitution (**PK-E12**); derivatives containing pyridin-2-yl (**PK-E16**) and 3-hydroxypyridin-2-yl (**PK-E17**) ring in place of phenyl ring exhibited significant IN inhibitory activity. Since these compounds showed % inhibition more than 80%, these were further tested for calculation of IC_{50} values (given in table 10). It was observed that compounds **PK-E8** and **PK-E5** with electron withdrawing substituent showed IC_{50} value of 1.52 µM and 1.59 µM, respectively. Compound **PK-E12** had IC_{50} value of 1.42 µM and compounds containing pyridin-2-yl (**PK-E16**) and 3-hydroxypyridin-2-yl (**PK-E17**) displayed IC_{50} value of 1.62 µM and 1.65 µM, respectively. Encouraged by the in silico and in vitro results, all the compounds were tested for anti-HIV activity against HIV-1 (III_B) and HIV-2 (ROD) in cell based assay. It was however observed that no compound showed anti-HIV activity below their cytotoxic concentration (as shown **in table 15**). The compounds showed very good potential in vitro however, in cell culture assay the activity was absent.

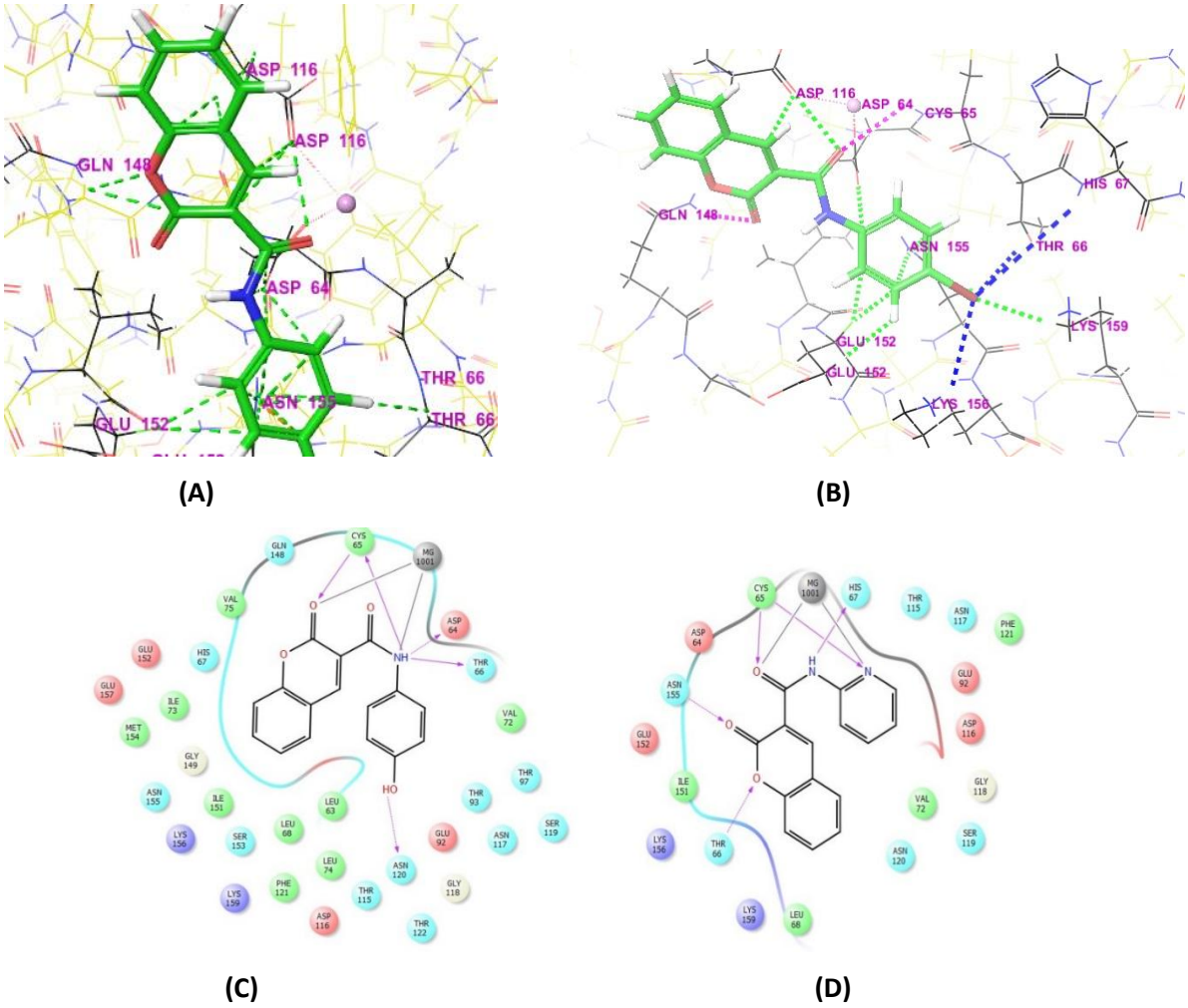

Figure 30: Docking poses of few representative compounds A: Docking pose of PK-E1; B: Docking pose of PK-E8; C: 2D interaction plot of PK-E12; D: 2D interaction plot of PK-E16

Table 14: Results of in-vitro HIV-1 IN inhibition and docking studies of PK-E1 to PK-E18

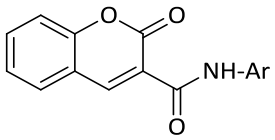

COMPOUND CODE	Ar	DOCKING SCORE	% IN Inhibition*	IC_{50} value**
Dolutegravir	-----	-7.30	95.00	nd
PK-E1	-Ph	-5.10	34.67	nd
PK-E2	2-Cl-Ph	-5.41	40.71	nd
PK-E3	4-Cl-Ph	-5.37	38.16	nd
PK-E4	2-Cl,4- NO_2-Ph	-5.42	42.25	nd
PK-E5	4-F-Ph	-5.38	39.17	nd
PK-E6	3-CF_3-Ph	-5.54	58.29	nd
PK-E7	2-Me, 5-F-Ph	-5.81	63.31	nd
PK-E8	4-Br-Ph	-6.86	89.94	1.52±0.08
PK-E9	2,6-diBr-4-NO_2-Ph	-6.62	88.47	1.59±0.09
PK-E10	2-OH-Ph	-6.14	46.68	nd
PK-E11	3-OH-Ph	-6.59	54.77	nd
PK-E12	4-OH-Ph	-7.20	90.14	1.42±0.12
PK-E13	2,4-diCH_3 -Ph	-5.53	58.82	nd
PK-E14	4-(cyanomethyl)phenyl	-5.48	53.26	nd
PK-E15	4-(phenyldiazenyl)phenyl	-5.43	44.72	nd
PK-E16	pyridin-2-yl	-6.69	89.94	1.62±0.12
PK-E17	3-hydroxypyridin-2-yl	-6.48	80.91	1.65±0.13
PK-E18	6-methylpyridin-2-yl	-6.01	76.38	nd

*% inhibition at 10µM concentration, values are mean of duplicate experiment performed independently, nd = not done; ** in µM

Table 15: Anti-HIV activity of synthesized compounds of PK-E1 to PK-E18

Compounds	HIV-1 (III_B)			HIV-2 (ROD)		
	EC_{50}[1] (µM)	CC_{50}[2] (µM)	HIV-1[3] SI	EC_{50}[1] (µM)	CC_{50}[2] (µM)	HIV-2[3] SI
Dolutegravir	0.0006±0.000001	1.275±0.3	2110.00	0.00232±0.00061	1.495±0.165	597.00
PK-E1	>44.25±3.15	44.25±3.15	<1	>47.00±4.40	47.00±4.40	<1
PK-E2	>11.03±1.77	11.03±1.77	<1	>12.10±2.10	12.10±2.10	<1
PK-E3	>17.10±1.00	17.10±1.00	<1	>18.70±5.10	18.70±5.10	<1
PK-E4	>39.80±20.13	39.80±20.13	<1	>43.09±2.30	43.09±2.30	<1
PK-E5	>22.15±4.05	22.15±4.05	<1	>24.40±5.60	24.40±5.60	<1
PK-E6	>34.10±4.00	34.10±4.00	<1	>34.40±5.60	34.40±5.60	<1
PK-E7	>31.05±5.25	31.05±5.25	<1	>35.10±3.50	35.10±3.50	<1
PK-E8	>24.50±3.10	24.50±3.10	<1	>29.00±8.30	29.00±8.30	<1
PK-E9	>4.68±2.40	4.68±2.40	<1	>5.05±7.40	5.05±7.40	<1
PK-E10	>21.06±11.55	21.06±11.55	<1	>22.50±8.30	22.50±8.30	<1
PK-E11	>24.95±9.15	24.95±9.15	<1	>32.40±7.20	32.40±7.20	<1
PK-E12	>33.75±7.25	33.75±7.25	<1	>36.50±8.50	36.50±8.50	<1
PK-E13	>40.80±3.00	40.80±3.00	<1	>44.50±8.20	44.50±8.20	<1
PK-E14	>35.85±11.15	35.85±11.15	<1	>38.50±4.53	38.50±4.53	<1
PK-E15	>12.04±7.86	12.04±7.86	<1	>13.05±6.40	13.05±6.40	<1
PK-E16	>42.55±13.05	42.55±13.05	<1	>44.05±3.50	44.05±3.50	<1
PK-E17	>53.30±7.50	53.30±7.50	<1	>56.30±4.50	56.30±4.50	<1
PK-E18	>50.45±23.55	50.45±23.55	<1	>52.04±6.80	52.04±6.80	<1

[1] EC_{50}: concentration of compound required to achieve 50% protection of MT-4 cell cultures against HIV induced cytotoxicity, as determined by MTT method. [2] CC_{50}: concentration required to reduce the viability of mock-infected cells by 50%, as determined by MTT method. [3] SI: selectivity index (CC_{50}/EC_{50}).

9.3 Oral bioavailability and toxicity prediction

All compounds were obeying the Lipinski rule of five. Water solubility reflects the bioavailability of the compound and it was in the range (-6.5 to 0.5 log mol/L).

Table 16: *In silico* predicted physiochemical parameters of the designed compounds PK-E1 to PK-E18

CODE	Mol.Formula	M.Wt.	log P[a]	RB[b]	HBA[c]	HBD[d]	PSA[e]	log S[f]	PCaco[g]
PK-E1	$C_{16}H_{11}NO_3$	265.26	3.04	3	3	1	114.21	-3.62	1.26
PK-E2	$C_{16}H_{10}ClNO_3$	299.71	3.69	3	3	1	124.51	-3.93	1.30
PK-E3	$C_{16}H_{10}ClNO_3$	299.71	3.69	3	3	1	124.51	-3.92	1.28
PK-E4	$C_{16}H_9ClN_2O_5$	334.15	4.35	3	3	1	134.81	-4.27	1.32
PK-E5	$C_{16}H_{10}FNO_3$	283.25	3.18	3	3	1	118.37	-3.49	1.25
PK-E6	$C_{17}H_{10}F_3NO_3$	333.26	4.06	4	3	1	133.07	-4.14	1.34
PK-E7	$C_{17}H_{12}FNO_3$	297.08	3.49	3	3	1	124.74	-3.53	1.27
PK-E8	$C_{16}H_{10}BrNO_3$	344.16	3.80	3	3	1	128.80	-3.98	1.29
PK-E9	$C_{16}H_8Br_2N_2O_5$	423.06	4.57	3	3	1	141.94	-4.38	1.34
PK-E10	$C_{16}H_{11}NO_4$	281.26	2.75	3	4	2	119.07	-3.56	1.06
PK-E11	$C_{16}H_{11}NO_4$	281.26	2.75	3	4	2	119.07	-3.44	1.12
PK-E12	$C_{16}H_{11}NO_4$	281.26	2.75	3	4	2	119.07	-3.30	1.09
PK-E13	$C_{18}H_{15}NO_3$	293.32	3.66	3	3	1	126.94	-3.93	1.28
PK-E14	$C_{18}H_{12}N_2O_3$	304.30	3.11	4	4	1	131.33	-3.71	1.03
PK-E15	$C_{22}H_{15}N_3O_3$	369.38	5.46	5	5	1	159.36	-5.39	0.52
PK-E16	$C_{15}H_{10}N_2O_3$	266.25	2.44	3	4	1	113.43	-3.09	1.32
PK-E17	$C_{15}H_{10}N_2O_4$	282.25	2.14	3	5	2	118.22	-3.14	0.92
PK-E18	$C_{16}H_{12}N_2O_3$	280.28	2.74	3	4	1	119.79	-3.30	1.32

[a]Partition coefficient, [b]No. of rotatable bonds, [c] No. of hydrogen bond acceptors, [d] No. of hydrogen bond donors, [e]polar surface area, [f]water solubility, [g]caco-2 permeability.

CHAPTER 10: 3-(1,3-DIOXOISOINDOLIN-2-YL)-*N*-SUBSTITUTED PHENYL BENZAMIDE DERIVATIVES

Compounds having 1,3-dioxoisoindolin-2-yl scaffold (phthalimide analogues) exhibit various pharmacological activities such as anti-angiogenic activity, anti-inflammatory, anticonvulsant, immunomodulatory activities, hypolipidimic, antibacterial, antioxidant and hemolytic activities. They also found to have significant inhibitory activity against HIV-1 RT (Sharma, 2010; Nayab, 2017).

In addition, two hydrogen bond acceptor groups (such as diketo acid functionality) and one aromatic ring are also essential (Santo, 2006). An extensive scrutiny of literature revealed that little work has been done on 1,3-dioxoisoindolin-2-yl derivatives as HIV-1 integrase inhibitors. In view of these facts and our interest on the development of novel HIV-1 IN inhibitors, we have chosen novel 3-(1,3-dioxoisoindolin-2-yl)-*N*-substituted phenyl benzamide scaffold as one of the pharmacophore.

Verschueren *et al.* reported tricyclic phthalimide analogs (example, compound **I**) as HIV-1 IN inhibitors (Verschueren, 2005). Later, much of the work on these analogs has been done by Zhao et al. (Zhao, 2007; Zhao, 2009; Zhao, 2011; Zhao, 2012). They initially reduced the tricyclic structure to bicyclic 6,7-dihydroxy isoindol-1-one derivatives (compound **II**) (Zhao, 2007) which retained potent anti-HIV IN inhibitory activity; later modified it to 4,5-dihydroxy-isoindole-1,3-dione (compound **III**) (Zhao, 2009). However, these compounds were considered not much useful due to cytotoxicity resulting from the embedded catechol functionality. Therefore, they hypothesized that removal of catechol nature by introduction of a nitrogen substituent would lead to reduction in cytotoxicity and synthesized tricyclic hydroxyl-pyrrolopyridine-triones (exemplified by compound **IV**) (Zhao, 2011). Although, they observed reduced cytotoxicity for these compounds, there was also loss of IN inhibitory potential. Since it was not clear to them whether the reduced HIV IN inhibitory activity was due to tricyclic scaffold, they synthesized bicyclic hydroxy-1H-pyrrolopyridine-triones (compound**V**) (Zhao, 2012). These compounds had reduced cytotoxicity as well as activity. After that, there is no report on isoindoline diones in literature.

Considering these reports and the fact that there are many scaffolds lacking diketo functionality but having HIV IN inhibition, compound **III** was modified by removing the catechol hydroxyls and substituting phenyl benzamide on indole nitrogen (compounds **PK-F1** to **PK-F18**). Phthalimide ring and amide moiety can participate in hydrogen bonding, hydrophobic interactions and π-π interactions with HIV-1 integrase enzyme (Noguchi, 2005; Bach, 2017). It was hypothesized that removal of catechol might reduce cytotoxicity and phenyl benzamide functionality can increase binding affinity as it is reported that the aryl group can bind in one or more hydrophobic pockets of IN-DNA complex. Proposed

prototype compound PK-F1 to PK-F18 constitutes three parts: isoindoline-1,3-dione ring at one terminal, central benzamide and aromatic ring at the other terminal. Presence of amide linkage was expected to provide flexibility to optimize the interactions at the receptor site. The effect of substitution of electron donating and withdrawing substituents on the aromatic ring was studied to generate structure-activity relationship.

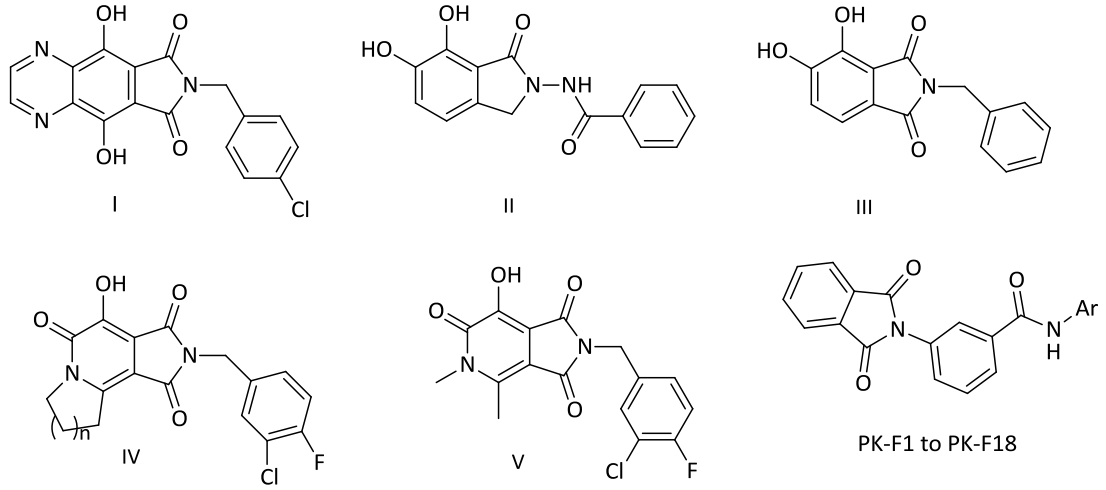

Figure 31: Reported isoindol-1-one and isoindole-1,3-diones having anti-HIV IN activity (I-V) and proposed structure (PK-F1 to PK-F18)

10.1 Chemistry

Designed compounds (**PK-F1** to **PK-F18**) were synthesized in two steps, details of the optimum reaction conditions used for the synthesis of target compounds are shown below (**Scheme 6**). The commercially available 2-benzofuran-1,3-dione was condensed with 3-aminobenzoic acid in microwave to give the key intermediate 3-(1,3-dioxoisoindolin-2-yl)benzoic acid. Then treatment of compound 3-(1,3-dioxoisoindolin-2-yl)benzoic acidwith different substituted anilines was carried out by using *N*-(3-Dimethylaminopropyl)-*N*'-ethylcarbodiimide·HCl (EDC.HCl) and 1-hydroxybenzotriazole (HOBt) in methylene chloride leading to the formation of final products **PK-F1** to **PK-F18**, in 60-75% yields. The synthesized compounds have been characterized using ^{1}H NMR, ^{13}C NMR and MS (ESI).

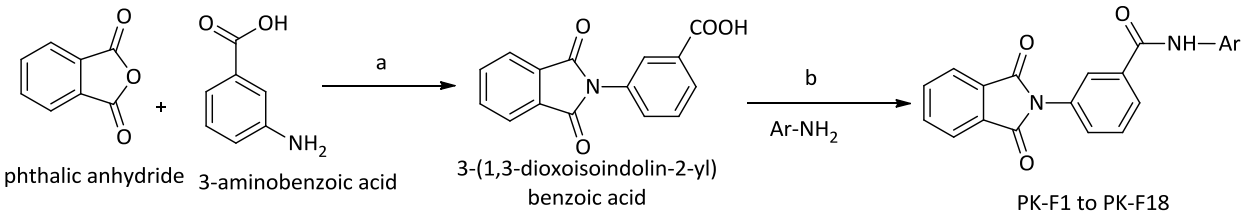

Scheme 6: Reagents and conditions: (a) MW 595W, 5min; (b) EDC.HCl, HOBT, triethylamine, dichloromethane, RT, 12 h

Reaction mechanism

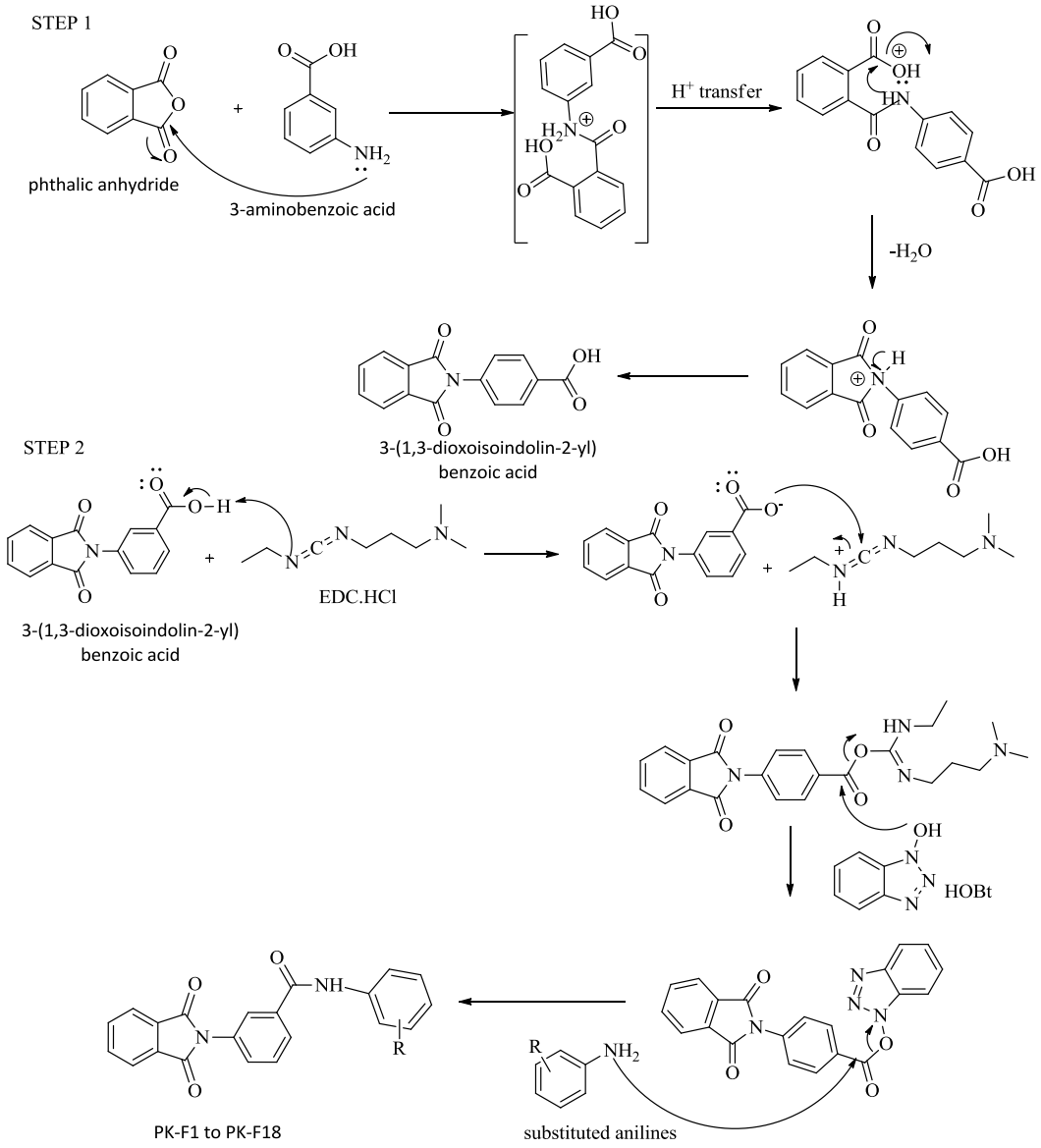

Figure 32: Reaction mechanism of Synthesis of 3-(1,3-dioxoisoindolin-2-yl)-*N*-substituted phenyl benzamide analogues (PK-F1 to PK-F18)

Synthesis of 3-(1,3-dioxoisoindolin-2-yl)benzoic acid

In mortar pestle 0.020 moles of 2-benzofuran-1,3-dione (phthalic anhydride) was mixed with 0.0205 moles of 3-aminobenzoic acid properly with continuous triturating. The reaction mixture is then heated in microwave at 200^0C for 5 minutes (Power 7 watt 595) by using CATAR microwave. The progress of reaction was monitored by TLC (ethyl acetate: hexane; 5:5). After completion of reaction, crude 3-(1,3-dioxoisoindolin-2-yl)benzoic acid as light white solid was used as such for next step. Yield 86%; Mp: 190–

192 °C; IR (KBr) cm^{-1}: 3584 ($OH_{str.}$), 3004 (Ar-$CH_{str.}$), 1617, 1684, 1722 (C=$O_{str.}$), 1512 (C=C); ^{1}H-NMR (400 MHz, $CDCl_3$): δ (ppm): 7.46-8.38 (m, 8H, ArH), 10.53 (s, 1H, -COOH); ^{13}C-NMR (100 MHz, $CDCl_3$): δ (ppm): 118.4, 122.5, 122.7, 127.6, 128.2, 132.5, 133.6, 134.9, 168.6, 170.6 and 170.8; ESI-MS m/z: 268.06 $[M+H]^+$.

Synthesis of 3-(1,3-dioxoisoindolin-2-yl)-N-substituted phenylbenzamide (**PK-F1** to **PK-F18**)

Three necked RBF was charged with 0.0018 moles of 3-(1,3-dioxoisoindolin-2-yl)benzoic acid (0.5 g) dissolved in 25 ml of dichloro methane (DCM) under N_2 atmosphere. The mixture was cooled to 0^0 C and treated with EDC.HCl (0.394 g, 0.0020 mol), HOBt (0.3 g, 0.0022 mol), and the substituted anilines (0.0020 moles). The reaction mixture was stirred at RT overnight. After completion, the mixture was diluted with H_2O (50 mL) and extracted with DCM (50 mL). The organic layer was washed with 1N hydrochloric solution (30 ml) and saturated sodium bicarbonate solution (30 ml), respectively, dried over sodium sulphate and concentrated in vacuum. The resulting crude material was purified by silica gel column chromatography to provide the product as a solid **PK-F1** to **PK-F18** in excellent yields. All the products were characterized from their spectral data.

3-(1,3-dioxoisoindolin-2-yl)-*N*-phenylbenzamide (PK-F1): Light Yellow Solid; yield 76%; Mp: 230–232°C; IR (KBr) cm^{-1}: 3410 ($NH_{str.}$), 3069 (Ar-$CH_{str.}$), 1714, 1655, 1603 (C=$O_{str.}$), 1507 (C=C, aromatic); ^{1}H-NMR (400 MHz, $CDCl_3$): δ (ppm): 7.10-8.14 (m, 13H, Ar-H), 10.25 (s, 1H, NH-Amide); ^{13}C-NMR (100 MHz, $CDCl_3$): δ (ppm): 118.3, 119.2, 121.2, 122.4, 123.3, 123.9, 127.2, 127.3, 128.4, 128.9, 129.8, 129.9, 130.3, 132.4, 133.6, 135.1, 135.3, 140.1, 160.5, 163.7 and 164.5; ESI-MS m/z: 343.17 $[M+H]^+$.

3-(1,3-dioxoisoindolin-2-yl)-*N*-(4-hydroxyphenyl)benzamide (PK-F2): Dark Brown Solid; yield 63%; Mp: 264–266°C; IR (KBr) cm^{-1}: 3486 ($OH_{str.}$), 3368 ($NH_{str.}$), 3057 (Ar-$CH_{str.}$), 1714, 1652, 1611 (C=$O_{str.}$), 1508 (C=C, aromatic); ^{1}H-NMR (400 MHz, $CDCl_3$): δ (ppm): 6.39 (s, 1H, OH-Alcohol), 6.80-7.87 (m, 12H, Ar-H), 9.05 (s, 1H, NH-Amide); ^{13}C-NMR (100 MHz, $CDCl_3$): δ (ppm): 118.4, 121.2, 122.4, 123.1, 125.8, 126.8, 127.9, 128.6, 129.8, 131.4, 132.5, 133.6, 134.8, 136.2, 139.6, 140.2, 144.5, 160.4, 162.8 and 163.6; ESI-MS m/z: 359.18 $[M+H]^+$.

3-(1,3-dioxoisoindolin-2-yl)-*N*-(3-hydroxyphenyl)benzamide (PK-F3): Brown Solid; yield 67%; Mp: 262–264°C; IR (KBr)cm^{-1}: 3482 ($OH_{str.}$), 3380 ($NH_{str.}$), 3054 (Ar-$CH_{str.}$), 1719, 1658, 1605 (C=$O_{str.}$), 1501 (C=C, aromatic); ^{1}H-NMR (400 MHz, $CDCl_3$): δ (ppm): 6.32 (s, 1H, OH-Alcohol), 6.80-7.87 (m, 12H, Ar-H), 9.05 (s, 1H, NH-Amide); ^{13}C-NMR (100 MHz, $CDCl_3$): δ (ppm): 117.2, 120.6, 123.6, 124.8, 126.1, 127.4, 128.2, 128.9, 130.6, 131.2, 132.3, 133.5, 135.2, 138.6, 139.2, 140.5, 142.5, 161.6, 162.6 and 163.9; ESI-MS m/z: 359.16 $[M+H]^+$.

3-(1,3-dioxoisoindolin-2-yl)-*N*-(3-methoxyphenyl)benzamide (PK-F4): Yellow Solid; yield 69%; Mp: 228–230°C; IR (KBr) cm^{-1}: 3361 ($NH_{str.}$), 3041 ($CH_{3str.}$), 2974 (Ar-$CH_{str.}$), 1713, 1647, 1619 (C=$O_{str.}$), 1520 (C=C, aromatic); ^{1}H-NMR (400 MHz, $CDCl_3$): δ (ppm): 3.86 (s, 3H, OCH_3), 7.04-7.99 (m, 12H, Ar-H), 10.04 (s, 1H, NH-Amide); ^{13}C-NMR (100 MHz, $CDCl_3$): δ (ppm): 56.7, 109.1, 115.1, 117.5, 119.1, 121.8, 123.9, 124.3, 126.9, 128.1, 129.1, 132.4, 132.5, 135.1, 136.1, 139.1, 144.8, 152.7, 158.6, 161.8, 163.5, and 166.8; ESI-MS m/z: 373.20 $[M-H]^+$.

***N*-(2,4-dimethylphenyl)-3-(1,3-dioxoisoindolin-2-yl)benzamide (PK-F5):** Pale Yellow Solid; yield 63%; Mp: 198–200°C; IR (KBr) cm^{-1}: 3374 ($NH_{str.}$), 3081 ($CH_{3str.}$) 2991 (Ar-$CH_{str.}$), 1715, 1643, 1614 (C=$O_{str.}$), 1521 (C=C, aromatic); ^{1}H-NMR (400 MHz, $CDCl_3$): δ (ppm): 2.18 (s, 3H, CH_3), 2.40 (s, 3H, CH_3), 7.01-8.01 (m, 11H, Ar-H), 9.78 (s, 1H, NH-Amide); ^{13}C-NMR (100 MHz, $CDCl_3$): δ (ppm): 19.5, 19.6, 116.4, 118.1, 120.7, 123.3, 123.4, 123.7, 124.8, 126.5, 129.5, 131.1, 131.5, 131.8, 133.4, 135.5, 136.9, 143.8, 150.9, 162.5, 165.1 and 167.2; ESI-MS m/z: 411.06 $[M+H]^+$.

3-(1,3-dioxoisoindolin-2-yl)-*N*-(2-hydroxy-5-nitrophenyl)benzamide (PK-F6): Yellow Solid; yield 67%; Mp: 210–212°C; IR (KBr) cm^{-1}: 3451 ($OH_{str.}$), 3364 ($NH_{str.}$), 3051 (Ar-$CH_{str.}$), 1718, 1647, 1615 (C=$O_{str.}$), 1520 (C=C, aromatic); ^{1}H-NMR (400 MHz, $CDCl_3$): δ (ppm): 6.36 (s, 1H, OH-Alcohol), 7.14-8.25 (m, 13H, Ar-H), 9.67 (s, 1H, NH-Amide); ^{13}C-NMR (100 MHz, $CDCl_3$): δ (ppm): 112.5, 114.3, 118.2, 122.3, 123.8, 123.7, 123.7, 126.9, 130.2, 130.9, 131.8, 132.4, 132.3, 133.4, 134.6, 144.1, 152.1, 161.9, 164.5 and 166.2; ESI-MS m/z: 404.17 $[M+H]^+$.

N-(2-chlorophenyl)-3-(1,3-dioxoisoindolin-2-yl)benzamide (PK-F7): White Solid; yield 62%; Mp: 268–270 °C; IR (KBr) cm^{-1}: 3364 ($NH_{str.}$), 2962 (Ar-$CH_{str.}$), 1717, 1652, 1619 (C=$O_{str.}$), 1506 (C=C, aromatic); ^{1}H-NMR (400 MHz, $CDCl_3$): δ (ppm): 7.13-8.13 (m, 12H, Ar-H), 9.68 (s, 1H, NH-Amide); ^{13}C-NMR (100 MHz, $CDCl_3$): δ (ppm): 118.2, 119.1, 120.3, 123.5, 123.7, 124.6, 125.9, 126.4, 128.6, 131.4, 131.8, 132.6, 133.6, 134.6, 136.5, 145.6, 151.2, 161.2, 163.5 and 166.5; ESI-MS m/z: 375.09 $[M-H]^+$.

***N*-(4-bromophenyl)-3-(1,3-dioxoisoindolin-2-yl)benzamide (PK-F8):** Yellow Solid; yield 68%; Mp: 280–282 °C; IR (KBr) cm^{-1}: 3374 ($NH_{str.}$), 3042 (Ar-$CH_{str.}$), 1708, 1657, 1614 (C=$O_{str.}$), 1508 (C=C, aromatic); ^{1}H-NMR (400 MHz, $CDCl_3$): δ (ppm): 7.37-7.99 (m, 12H, Ar-H), 10.04 (s, 1H, NH-Amide); ^{13}C-NMR (100 MHz, $CDCl_3$): δ (ppm): 115.1, 121.4, 123.5, 124.6, 124.7, 125.5, 125.8, 126.3, 131.5, 132.8, 133.1, 134.6, 136.8, 139.6, 142.6, 151.4, 160.2, 163.5 and 166.5; ESI-MS m/z: 419.11 $[M-H]^+$.

3-(1,3-dioxoisoindolin-2-yl)-*N*-(4-fluorophenyl)benzamide (PK-F9): Brown Solid; yield 71%; Mp: 224–226°C; IR (KBr) cm^{-1}: 3374 ($NH_{str.}$), 3042 (Ar-$CH_{str.}$), 1708, 1657, 1614 (C=$O_{str.}$), 1508 (C=C, aromatic); ^{1}H-NMR (400 MHz, $CDCl_3$): δ (ppm): 7.37-7.99 (m, 12H, Ar-H), 10.04 (s, 1H, NH-Amide); ^{13}C-NMR (100 MHz,

$CDCl_3$): δ (ppm): 117.4, 120.5, 122.4, 123.4, 124.1, 125.6, 125.8, 127.1, 130.2, 131.5, 132.6, 133.8, 137.5, 140.2, 144.4, 152.4, 161.1, 163.9 and 167.2; ESI-MS m/z: 361.17 $[M+H]^+$.

3-(1,3-dioxoisoindolin-2-yl)-*N*-(3-(trifluoromethyl)phenyl)benzamide (PK-F10): Yellow Solid; yield 60%; Mp: 231–233°C; IR (KBr) cm^{-1}: 3356 ($NH_{str.}$), 3048 ($Ar\text{-}CH_{str.}$), 1710, 1652, 1619 ($C{=}O_{str.}$), 1514 (C=C, aromatic); ^{1}H-NMR (400 MHz, $CDCl_3$): δ (ppm): 7.24-7.96 (m, 12H, Ar-H), 9.57 (s, 1H, NH-Amide); ^{13}C-NMR (100 MHz, $CDCl_3$): δ (ppm): 116.1, 120.2, 121.4, 123.9, 124.8, 125.7, 125.9, 126.5, 126.7, 129.4, 130.48, 131.6, 132.8, 136.8, 139.8, 142.5, 151.6, 164.2, 166.8 and 167.7; ESI-MS m/z: 409.12 $[M-H]^+$.

***N*-(3,4-dichlorophenyl)-3-(1,3-dioxoisoindolin-2-yl)benzamide (PK-F11):** White Solid; yield 63%; Mp: 248–250°C; IR (KBr) cm^{-1}: 3379 ($NH_{str.}$), 2981 ($Ar\text{-}CH_{str.}$), 1714, 1656, 1613 ($C{=}O_{str.}$), 1508 (C=C, aromatic); ^{1}H-NMR (400 MHz, $CDCl_3$): δ (ppm): 7.11-8.08 (m, 11H, Ar-H), 10.04 (s, I H, NH-Amide); ^{13}C-NMR (100 MHz, $CDCl_3$): δ (ppm): 116.4, 118.1, 120.7, 123.4, 123.6, 123.7, 124.8, 126.5, 129.8, 131.1, 131.5, 132.2, 133.0, 135.5, 136.9, 143.2, 150.9, 162.0, 165.1, and 167.2; ESI-MS m/z: 409.06 $[M-H]^+$.

***N*-(2,6-dichloro-4-nitrophenyl)-3-(1,3-dioxoisoindolin-2-yl)benzamide (PK-F12):** Yellow Solid; yield 58%; Mp: 229–231°C; IR (KBr) cm^{-1}: 3367 ($NH_{str.}$), 2986 ($Ar\text{-}CH_{str.}$), 1712, 1661, 1619 ($C{=}O_{str.}$), 1504 (C=C, aromatic); ^{1}H-NMR (400 MHz, $CDCl_3$): δ (ppm): 7.09-8.12 (m, 10H, Ar-H), 9.78 (s, 1H, NH-Amide); ^{13}C-NMR (100 MHz, $CDCl_3$): δ (ppm): 119.1, 121.0, 123.1, 123.3, 124.3, 124.5, 124.7, 126.9, 130.4, 131.2, 131.5 132.4, 133.8, 134.0, 135.5, 143.2, 153.2, 162.2, 165.5 and 167.6; ESI-MS m/z: 456.07 $[M+H]^+$.

***N*-(2,6-dibromo-4-nitrophenyl)-3-(1,3-dioxoisoindolin-2-yl)benzamide (PK-F13):** Pale Yellow Solid; yield 56%; Mp: 247–249°C; IR (KBr) cm^{-1}: 3381 ($NH_{str.}$), 2989 ($Ar\text{-}CH_{str.}$), 1710, 1665, 1621 ($C{=}O_{str.}$), 1507 (C=C, aromatic); ^{1}H-NMR (400 MHz, $CDCl_3$): δ (ppm): 6.83-8.29 (m, 10H, Ar-H), 10.05 (s, 1H, NH-Amide); ^{13}C-NMR (100 MHz, $CDCl_3$): δ (ppm): 118.4, 122.5, 123.4, 123.6, 124.8, 125.3, 126.1, 127.2, 129.6, 131.8, 132.6, 133.9, 134.8, 136.7, 142.9, 152.1, 161.7, 164.4 and 166.8; ESI-MS m/z: 543.84 $[M+H]^+$.

***N*-(3-acetylphenyl)-3-(1,3-dioxoisoindolin-2-yl)benzamide (PK-F14):** Yellow Solid; yield 58%; Mp: 258–260°C; IR (KBr) cm^{-1}: 3408 ($NH_{str.}$), 3121 ($CH_{3str.}$) 2987 ($Ar\text{-}CH_{str.}$), 1712, 1698, 1647, 1619 ($C{=}O_{str.}$), 1514 (C=C, aromatic); ^{1}H-NMR (400 MHz, $CDCl_3$): δ (ppm): 2.67 (s, 3H, $COCH_3$), 7.66-8.14 (m, 12H, Ar-H), 10.04 (s, I H, NH-Amide); ^{13}C-NMR (100 MHz, $CDCl_3$): δ (ppm): 26.7, 110.4, 120.2, 120.6, 123.9, 124.2, 124.9, 126.5, 127.7, 129.4, 130.9, 131.5, 131.7, 132.1, 133.2, 134.6, 138.0, 162.5, 167.4, 167.8 and 197.2; ESI-MS m/z: 385.22 $[M+H]^+$,383.14 $[M-H]^+$.

***N*-(4-(cyanomethyl)phenyl)-3-(1,3-dioxoisoindolin-2-yl)benzamide (PK-F15):** Creamish Solid; yield 58%; Mp: 208–210°C; IR(KBr) cm^{-1}: 3384 ($NH_{str.}$), 2987 ($Ar\text{-}CH_{str.}$), 1712, 1644, 1621 ($C{=}O_{str.}$), 1517 (C=C, aromatic); ^{1}H-NMR (400 MHz, $CDCl_3$): δ (ppm): 4.25 (s, 2H, CH_2CN), 7.29-8.06 (m, 12H, Ar-H), 10.02 (s, 1H, NH-Amide); ^{13}C-NMR (100 MHz, $CDCl_3$): δ (ppm): 23.2, 117.2, 120.6, 121.2, 123.4, 124.0, 124.3,

126.4, 126.6, 128.2, 130.5, 131.9, 132.2, 132.6, 135.7, 138.9, 144.1, 152.2, 163.5, 165.5, and 168.0; ESI-MS m/z: 382.14 $[M-H]^+$.

3-(1,3-dioxoisoindolin-2-yl)-*N*-(pyridin-2-yl)benzamide (PK-F16): Yellow Solid; yield 66%; Mp: 226–228 °C; IR (KBr) cm^{-1}: 3398 ($NH_{str.}$), 3144 ($CH_{3str.}$) 2962 (Ar-$CH_{str.}$), 1717, 1691, 1640 ($C=O_{str.}$), 1518 (C=C, aromatic); ^{1}H-NMR (400 MHz, $CDCl_3$): δ (ppm): 6.98-8.10 (m, 12H, Ar-H), 9.84 (s, I H, NH-Amide); ^{13}C-NMR (100 MHz, $CDCl_3$): δ (ppm): 115.2, 118.4, 120.0, 122.4, 123.6, 125.7, 126.4, 129.5, 130.4, 130.9, 131.8, 132.5, 132.6, 133.5, 134.3, 136.9, 141.5, 161.2, 164.2 and 166.2; ESI-MS m/z: 344.14 $[M+H]^+$.

3-(1,3-dioxoisoindolin-2-yl)-*N*-(pyridin-4-yl)benzamide (PK-F17): Yellow Solid; yield 69%; Mp: 231–233°C; IR (KBr) cm^{-1}: 3377 ($NH_{str.}$), 2952 (Ar-$CH_{str.}$), 1712, 1695, 1643, ($C=O_{str.}$), 1515 (C=C, aromatic); ^{1}H-NMR (400 MHz, $CDCl_3$): δ (ppm): 7.12-8.37 (m, 12H, Ar-H), 9.94 (s, I H, NH); ^{13}C-NMR (100 MHz, $CDCl_3$): δ (ppm): 117.2, 118.7, 120.5, 123.5, 124.4, 125.1, 126.4, 127.0, 128.1, 128.6, 133.0, 134.0, 134.5, 135.1, 135.6, 136.4, 142.7, 163.4, 166.8 and 167.1; ESI-MS m/z: 344.12 $[M+H]^+$.

3-(1,3-dioxoisoindolin-2-yl)-*N*-(3-hydroxypyridin-2-yl)benzamide (PK-F18): Yellow Solid; yield 62%; Mp: 242–244°C; IR (KBr) cm^{-1}: 3458 ($OH_{str.}$), 3361 ($NH_{str.}$), 3054 (Ar-$CH_{str.}$), 1716, 1657, 1614 ($C=O_{str.}$), 1504 (C=C, aromatic); ^{1}H-NMR (400 MHz, $CDCl_3$): δ (ppm): 3.88 (s, 1H, OH), 7.23-8.11 (m, 11H, Ar-H), 9.91 (s, IH, Ar-H) 10.60 (s, IH, NH-Amide); ^{13}C-NMR (100 MHz, $CDCl_3$): δ (ppm): 116.2, 119.2, 121.8, 122.4, 123.0, 124.2, 125.7, 128.4, 129.6, 130.5, 132.0, 133.6, 133.9, 134.8, 135.5, 137.1, 143.0, 164.1, 164.8 and 167.0; ESI-MS m/z: 360.11 $[M+H]^+$.

10.2 Results and Discussion

It was observed that all compounds showed metal coordination with Mg 1001 by C1-carbonyl of phthalimide ring. This meant that in all compounds, the phthalimide ring occupied same cavity whereas the differences in docking scores resulted from change of substituents on terminal phenyl and its interactions with active site.

The results of *in-vitro* assay revealed that, compounds **PK-F3, PK-F8, PK-F9, PK-F13, PK-F14** and **PK-F18** exhibited significant percentage inhibition (up to 87.05%) of HIV-1 IN with IC_{50} ≤3.90 µM. Further, compounds **PK-F6, PK-F7, PK-F11** and **PK-F12** displayed moderate potency (percentage inhibition in range of 58.25% to 80.25%), while rest of compounds exhibited weak to least HIV-1 IN inhibitory activity. It was observed that weakly deactivating groups like halides display significant inhibition as compared to electron donating groups like amino, methoxy, etc.

Compound **PK-F1** (percentage inhibition 47.61, G Score -5.91) having un-substituted phenyl ring showed weak activity because of absence of hydrogen docking interactions with amino acid residues Asp 64, Asp

116 and Glu 152 present in DDE motif of integrase active site. Substitution of hydroxy at para position (**PK-F2**) and ortho position (**PK-F3,** (**IC_{50} 4.39 µM**), showed improvement in docking score and HIV-1 IN inhibitory activity. This may be due to interaction of hydroxy group with Cys 65, Lys 159 *via* hydrogen bonding. Amidic carbonyl, keto group of phthalimide ring and terminal aromatic ring showed hydrophobic interactions with Asp 116 and His 67, respectively.

Further modifying the **PK-F3** by placing *m*- methoxy substitution **(PK-F4)** shows less docking score and IN inhibitory activity due to absence of hydrogen bonding interactions with DDE motif. Diketo groups of isoindoline moiety did not interact with any amino acids. Only amidic carbonyl and ethereal oxygen formed hydrogen bonding with Asn 155 and Lys 159, respectively. Compound **PK-F5** having dimethyl substitution at ortho and positions, showed only two hydrogen bonding interactions with Asn 117 and Gln 148 (by both carbonyl groups of phthalimide ring). *P*-methyl group showed hydrophobic interactions with Glu 152 and Asn 155, but no interactions was observed with *o*-methyl group. Other hydrophobic interactions with Asp 116, Phe 139, Gly 140 and Gln 148 were also observed.

Further modifying the **PK-F1** by placing hydroxy and nitro groups at 2,5 positions (**PK-F6**), expressive improvement in G score and HIV-1 IN inhibitory was observed. Hydrogen bonding interactions with amino acid residues Thr 66 (by amidic carbonyl group and hydroxy group), His 67 (by carbonyl group of amidic linkage) and Asn 155 (by carbonyl group of phthalimide ring). Other hydrophobic interactions were observed with amino acid residues Asp 64, Cys 65, His 67, Gln 148, Lys 156 and Lys 159.

Among all, compounds **PK-F8 (IC_{50} 4.01 µM)** and **PK-F9** having electron withdrawing substitution (p-bromo and p-fluoro, respectively) on aromatic ring, displayed very high potency (82.24% and 87.05%), comparable to standard drug Dolutegravir. Compound **PK-F8** showed hydrogen bonding interactions with amino acid residues Asp 64 (by amidic NH group), Gln 148 (by carbonyl group of phthalimide ring), Lys 159 and hydrophobic interaction with amino acids Asp 116 via chelating with magnesium metal ions (Mg 1001), while second aromatic wing (phenyl ring) exhibited hydrophobic interactions with Asp 64 Gln 148, Ile 151 and Glu 152. The –NH and keto group of the amide linkage showed hydrogen bonding and hydrophobic interaction with Asp 64, Asn 155 and Glu 152, respectively. The terminal hydrophobic phenyl ring substituted with electron withdrawing bromo group at para position displayed hydrogen bonding and hydrophobic interactions with amino acid residues Lys 159, Thr 66 and His 67, respectively.

Compound **PK-F9** showed most significant HIV-1 IN inhibitory activity with an IC_{50} value of 3.90 µM. It may be due to better docking interactions by keto groups present in structures. Hydrogen bonding interactions were observed with Asp 64 (by amidic NH group) and Gln 148 (by carbonyl group of phthalimide ring), respectively. Fluoro group substituted at para positions displayed hydrophobic

interactions with Thr 66 and Lys 159. Carbonyl group of phthalimide ring and amide linkage showed hydrophobic interactions with Asp 116 *via* forming salt bridge with Mg metal ion and Glu 152 amino acid residues of DDE motif. Other hydrophobic interactions with Thr 66, His 67, Gln 148, Ile 151 and Lys 159 were also observed. These results were concomitant with the docking scores.

Among electron withdrawing substitutions, para position (**PK-F8** and **PK-F9**) is preferred as compare to ortho position (**PK-F7**). These results are also supported by docking interaction studies wherein the docking scores are higher for para substituted compound than ortho or meta substituted compounds. As compared to other deactivating groups like fluoro and bromo at para position, chlorine is found to be least active. This can be explained from docking study whereby it is observed that chlorine being highly electronegative gets solvent exposed while bromine and fluorine does not. On substitution of trifluoro methyl group at meta positions (**PK-F10**) showed similar docking score as compare to un substituted ring, but improvement in activity is due to hydrogen bonding interaction with amino acid residue Gln 148(by carbonyl group of phthalimide ring) and hydrophobic interactions with Asp 64, Asp 116 *via* chelating with magnesium metal ion present in active site of DDE motif. Other hydrophobic interactions with Thr 66, Ile 151, Glu 152, Asn 155 and Lys 159 were also observed.

On substitution of chloro group at 3,4 positions (compound **PK-F11**), slightly reduction in docking score as well as activity was observed, compared to **PK-F7**. It may be due to absence of any interactions of chlorine group with in ST cavity. Further, it was observed that more hydrophobic interactions were present in **PK-F13** containing 2,6-dibromo-4-nitro substitution as compared to **PK-F12** having 2,6-dichloro-4-nitro substation. **PK-F13** showed inhibition at IC_{50} value of 4.53 µM and also exhibited three hydrogen bonding interactions with Thr 66, His 67 (by nitro group) and Asn 117 (by carbonyl group of phthalimide ring), respectively. Other hydrophobic interactions were observed with Asp 116, Phe 139, Gly 140, Gln 148, Glu 152, Asn 155 and Lys 156.

Placing acetyl group at para position (**PK-F14, IC_{50} 4.25 µM**) shows significant inhibition of HIV-1 integrase, it may be because of presence of hydrogen bonding interactions with amino acid residues Thr 66, Asn 155 (by amidic carbonyl group), Gln 148 (by carbonyl group of phthalimide ring) and Lys 159 (by carbonyl group of *p*-acetyl group). The π-π stacking was also observed with Lys 156. However, when para position is replaced with cyano methyl (compound **PK-F15**), least docking interactions and decreased potency were observed. It showed hydrogen bonding interactions with Asn 155 (by amidic carbonyl) and Lys 159 (by CH_2CN). Replacement of phenyl ring with more basic pyridin-2-yl ring (**PK-F16**) showed improvement in docking interactions and biological activity. This may be due to more hydrogen bonding interactions with amino acid residues Cys 65, Asn 155 (by both carbonyl groups of phthalimide

ring), Thr 66, Lys 159 (by amidic carbonyl group) and Lys 156 (by NH of pyridin-2-yl ring). It also had hydrophobic interaction with Asp 116, which then forms salt bridge with magnesium ion (Mg 1001). However, replacement of **PK-F16** with pyridin-4-yl ring (**PK-F17**) showed reduction in potency.

Further, substitution of hydroxy group at ortho position (**PK-F18, IC_{50} 4.30 µM**) showed rise in docking score, docking interactions and IN inhibitory activity. Keto group of phthalimide ring and amidic linkage interacts with Asn 155, Thr 66 and His 67, respectively by hydrogen bonding. Terminal pyridin-2-yl ring also formed hydrogen bonds with amino acid residues Lys 156 (by -OH group) and Lys 159 (by -NH group), respectively. Nitrogen of phthalimide rings also showed interactions with As 64 and asp 116 *via* salt bridge with magnesium metal ion (Mg 1001).

Overall, it was observed that the HIV-1 IN inhibitory potency of designed compounds altered significantly with variation in nature as well as position of substituent. In general, compounds having *m*-hydroxy (**PK-F3**), *p*-bromo (**PK-F8**), *p*-fluoro substitution (**PK-F9**), 2,6-dibromo-4-nitro (**PK-F13**), *p*- acetyl group substitution (**PK-F14**) and 3-hydroxypyridin-2-yl ring in place of phenyl ring (**PK-F18**) exhibited significant IN inhibitory activity. Since these compounds showed % inhibition more than 80%, these were further tested for calculation of IC_{50} values (given in **table 17**). It was observed that compounds **PK-F3**, **PK-F8**, **PK-F9**, and **PK-F13** with electron withdrawing substituent showed IC_{50} value of 4.39 µM, 4.01 µM, 3.90 µM and 4.53 µM respectively. Compound **PK-F14** had IC_{50} value of 4.25 µM and 3-hydroxypyridin-2-yl ring substituted compound **PK-F18** displayed IC_{50} value of 4.30 µM. Encouraged by the above results, all compounds were tested for anti-HIV activity against HIV-1 (III_B) and HIV-2 (ROD) in cell based assay.

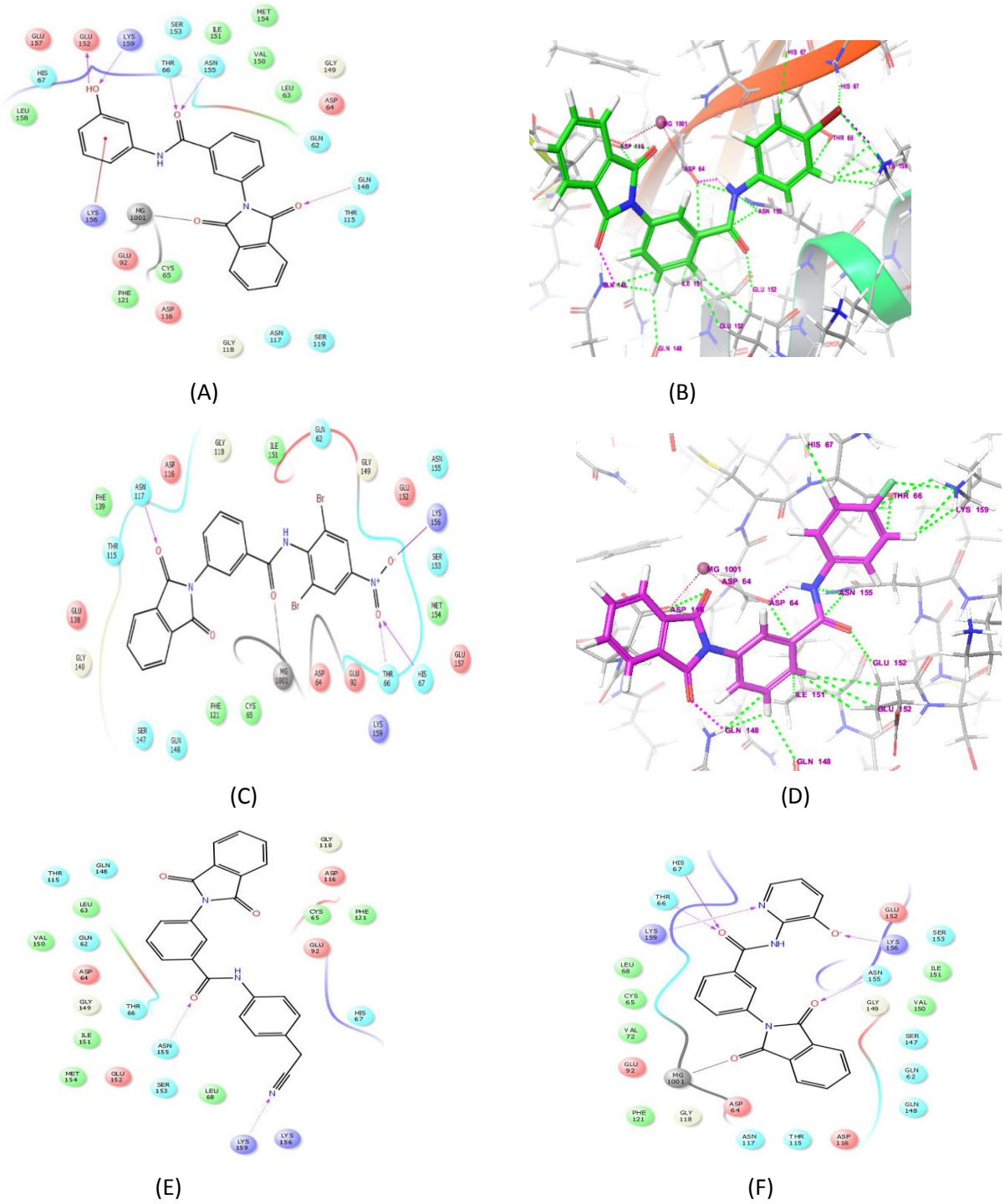

Figure 33: Docking poses of few representative compounds A: 2D interaction plot of PK-F3; B: Docking pose of PK-F8; C: 2D interaction plot of PK-F13; D: Docking pose of PK-F14; E: 2D interaction plot of PK-F15; F: 2D interaction plot of PK-F18

Table 17: Results of *In-vitro* HIV-1 IN inhibition studies and G Score of PK-F1 to PK-F18

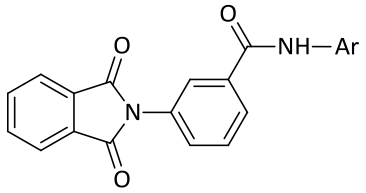

COMPOUND CODE	Ar	G SCORE	% IN INHIBITION*	IC_{50} value**
Dolutegravir	----	-7.30	95.00	nd
PK-F1	Ph	-5.91	47.61	nd
PK-F2	4-OH-Ph	-5.73	63.68	nd
PK-F3	3-OH-Ph	-6.34	82.37	4.39±0.033
PK-F4	3-OMe-Ph	-4.39	34.39	nd
PK-F5	2,4-diMe-Ph	-5.37	43.38	nd
PK-F6	2-OH-5-NO_2-Ph	-7.31	71.95	nd
PK-F7	2-Cl-Ph	-6.62	78.25	nd
PK-F8	4-Br-Ph	-7.38	83.24	4.01±0.012
PK-F9	4-F-Ph	-7.15	87.05	3.90±0.017
PK-F10	3- CF_3-Ph	-5.90	70.71	nd
PK-F11	3,4-diCl-Ph	-5.96	69.31	nd
PK-F12	2,6-diCl-4-NO_2-Ph	-5.57	58.25	nd
PK-F13	2,6-diBr-4-NO_2-Ph	-6.16	81.42	4.53±0.025
PK-F14	4-COMe-Ph	-7.01	82.30	4.25±0.020
PK-F15	4-CH_2CN-Ph	-4.63	24.86	nd
PK-F16	pyridin-2-yl	-7.16	80.25	nd
PK-F17	pyridin-4-yl	-5.80	48.15	nd
PK-F18	3-hydroxypyridin-2-yl	-7.36	82.08	4.30±0.071

*% inhibition at 10µM concentration, values are mean of duplicate experiment performed independently; nd: not done; nd: not done; ** in µM

Table 18: Anti-HIV activity of synthesized compounds PK-F1 to PK-F18

Compounds	HIV-1 (III_B)			HIV-2 (ROD)		
	EC_{50}[1] (µM)	CC_{50}[2] (µM)	HIV-1[3] SI	EC_{50}[1] (µM)	CC_{50}[2] (µM)	HIV-2[3] SI
Dolutegravir	0.0006±0.000001	1.275±0.3	2110.00	0.00232±0.00061	1.495±0.165	597.00
PK-F1	>110.50±5.50	110.50±5.50	<1	>117.50±8.40	117.50±8.40	<1
PK-F2	>125.00±15.50	>125.00±15.50	<1	>125.10±12.10	125.10±12.10	<1
PK-F3	107.40±16.60	>125.00±12.50	<1	>118.78±15.10	118.78±15.10	<1
PK-F4	>125.00±8.50	>125.00±8.50	<1	>123.49±12.30	123.49±12.30	<1
PK-F5	>68.90±11.50	68.90±11.50	<1	>69.40±15.60	69.40±15.60	<1
PK-F6	>69.85±5.35	69.85±5.35	<1	>74.45±5.60	74.45±5.60	<1
PK-F7	>102.30±22.70	102.30±22.70	<1	>105.10±23.50	105.10±23.50	<1
PK-F8	>77.75±10.45	77.75±10.45	<1	>77.50±8.30	77.50±8.30	<1
PK-F9	>71.80±14.40	71.80±14.40	<1	>71.85±8.40	71.85±8.40	<1
PK-F10	>99.20±25.80	99.20±25.80	<1	>98.50±14.30	98.50±14.30	<1
PK-F11	>79.85±6.95	79.85±6.95	<1	>82.40±7.20	82.40±7.20	<1
PK-F12	>125.00±9.30	>125.00±9.30	<1	>124.50±8.50	124.50±8.50	<1
PK-F13	>8.105±0.68	8.105±0.68	<1	>9.50±8.20	9.50±8.20	<1
PK-F14	>114.50±10.50	114.50±10.50	<1	>116.50±14.53	116.50±14.53	<1
PK-F15	>125.00±9.30	>125.00±9.30	<1	>125.05±6.40	>125.05±6.40	<1
PK-F16	>124.00±1.00	124.00±1.00	<1	>124.05±3.50	124.05±3.50	<1
PK-F17	>125.00±5.50	>125.00±5.50	<1	>125.30±4.50	>125.30±4.50	<1
PK-F18	>125.00±11.5	>125.00±11.5	<1	>125.04±6.80	>125.04±6.80	<1

[1] EC_{50}: concentration of compound required to achieve 50% protection of MT-4 cell cultures against HIV induced cytotoxicity, as determined by MTT method. [2] CC_{50}: concentration required to reduce the viability of mock-infected cells by 50%, as determined by MTT method. [3] SI: selectivity index (CC_{50}/EC_{50}).

10.3 Oral bioavailability and toxicity prediction

Drug likeness parameters such as mol. wt., logP, hydrogen bond acceptor, hydrogen bond donors, no of rotatable bonds and ADME found within the optimum range. All compounds exhibited correlation between bioavailability of the compound and water solubility (logS -5.67 to -3.81).

Table 19: *In-silico* predicted drug likeliness parameters of compounds PK-F1 to PK-F18

CODE	Mol. Formula	M.Wt.	log P[a]	RB[b]	HBA[c]	HBD[d]	PSA[e]	log S[f]	PCaco[g]
PK-F1	$C_{21}H_{14}N_2O_3$	342.35	3.74	4	3	1	139.43	-4.77	0.92
PK-F2	$C_{21}H_{14}N_2O_4$	358.35	3.45	4	4	2	141.22	-4.60	0.95
PK-F3	$C_{21}H_{14}N_2O_4$	358.35	3.45	4	4	2	144.22	-4.00	1.05
PK-F4	$C_{22}H_{16}N_2O_4$	372.38	3.75	5	4	1	150.91	-4.27	1.05
PK-F5	$C_{23}H_{18}N_2O_3$	370.40	4.36	4	3	1	142.16	-5.01	0.98
PK-F6	$C_{21}H_{13}N_3O_6$	403.36	3.35	5	6	2	148.88	-4.41	-0.05
PK-F7	$C_{21}H_{13}ClN_2O_3$	376.79	4.39	4	3	1	139.73	-4.60	0.99
PK-F8	$C_{21}H_{13}BrN_2O_3$	421.25	4.50	4	3	1	153.30	-5.10	0.95
PK-F9	$C_{21}H_{13}FN_2O_3$	360.34	3.88	4	3	1	143.59	-4.91	0.97
PK-F10	$C_{22}H_{13}F_3N_2O_3$	410.35	4.76	5	3	1	138.29	-4.92	1.07
PK-F11	$C_{21}H_{12}Cl_2N_2O_3$	411.24	5.05	4	3	1	149.04	-5.52	0.98
PK-F12	$C_{21}H_{11}Cl_2N_3O_5$	456.24	4.95	5	5	1	144.69	-5.59	0.91
PK-F13	$C_{21}H_{11}Br_2N_3O_5$	545.14	5.17	5	5	1	161.82	-5.67	0.93
PK-F14	$C_{23}H_{16}N_2O_4$	384.39	3.94	5	4	1	146.32	-4.41	1.05
PK-F15	$C_{23}H_{15}N_3O_3$	381.39	3.81	5	4	1	136.55	-4.50	0.91
PK-F16	$C_{20}H_{13}N_3O_3$	343.34	3.13	4	4	1	138.65	-3.96	0.92
PK-F17	$C_{20}H_{13}N_3O_3$	343.34	3.13	4	4	1	142.65	-3.91	1.00
PK-F18	$C_{20}H_{13}N_3O_4$	359.34	2.84	4	5	2	143.44	-3.81	0.90

[a]Partition coefficient, [b]No. of rotatable bonds, [c] No. of hydrogen bond acceptors, [d] No. of hydrogen bond donors, [e]polar surface area, [f]water solubility, [g]caco-2 permeability.

CHAPTER 11: SUBSTITUTED 1*H*-INDOLE-3-CARBALDEHYDE DERIVATIVES

Indole nucleus containing analogues have privileged position in the medicinal chemistry, such compounds are reported for diverse biological activities like anti-inflammatory, analgesic, anticancer, antidiabetic, antiviral, antifungal, antioxidant, antitubercular, antimicrobial, antidepressant, tranquillizing, anticonvulsant and Glycoprotein IIb\IIIa inhibitor (Ali, 2013; Kaushik, 2013). Indole derivatives have been reported to have antiviral activity. The first molecule, 5-CITEP (1-(5-chloroindol-3-yl)-3-hydroxy-3-(2*H*-tetrazol-5-yl)-propenone) (compound **I**) was found to block integration in extracellular assays and exhibit good antiviral effects against HIV-infected cells (Goldgur, 1999). Further, using 5-CITEP as prototype, Pais et al. reported indolyl derivatives (compound **II**) having β-diketo acid substitution (Pais, 2002). Based on these, several *N*-substituted indole derivatives were prepared with β-hydroxy or β-amino ketone at 3 positions having IN inhibitory potency (Fujishita, 2004). Sechi et al. also evaluated a series of *N*-substituted dihydroxyindole-2-carboxylic acid (DHICA, **III**) and Indole β-diketo acids, concluding that indole nucleus allows a consistent and selective inhibition of HIV-1 IN and carbonyl groups at either 2 or 3 of the indole significantly affects the activity (Sechi, 2004; Sechi, 2004). However, Xu et al. observed that *N*-arylindoles having no other substitution on indole (compound **IV**) also show potent anti HIV-1 IN activity (Xu, 2008). Ferro et al. mostly worked on compounds having diketo acid substitution or enclosing the diketo function in furan ring and checked the effect of various substitutions on indole (Ferro, 2007; Hombrouck, 2008; Ferro, 2009, De Luca, 2011; Ferro, 2011), though it was concluded that the modifications did not improve the biological profile of their lead compound (compound **V**) (De Luca, 2011; Ferro, 2011). Later, *N*-arylsulfonylindoles (compound **VI**) and its acetyl derivative (compound **VII**) was reported to have significant inhibition of HIV-1 IN and replication (Fan, 2009; Ran, 2010; Che, 2015). Thus, on basis of reported structures and taking into account the structural requirements necessary to form a ligand-Mg^{2+}-IN complex, a new series of 12 (**PK-G1** to **PK-G12**) indole-3-carbaldehyde derivatives having linkers such as sulfonyl or phenacyl expecting to inhibit the ST step of HIV-1 IN were synthesized.

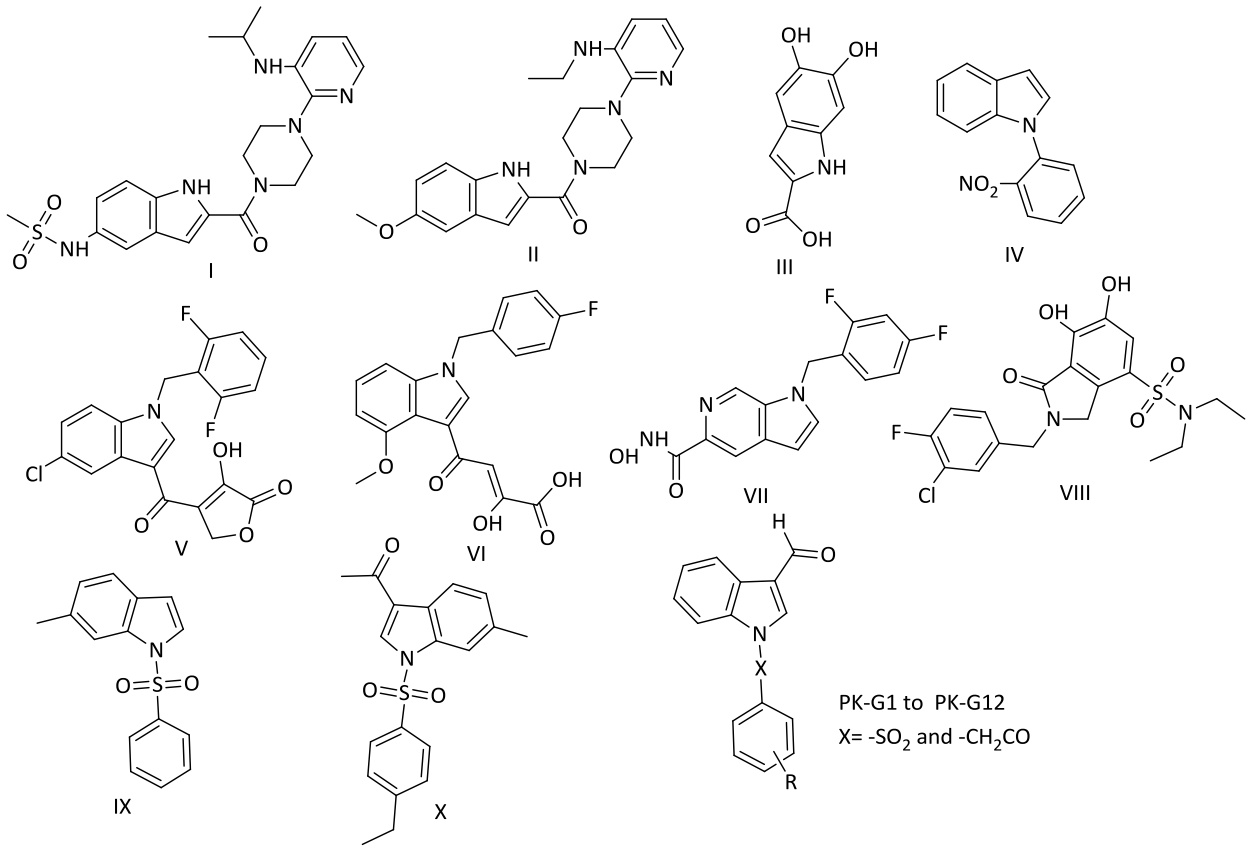

Figure 34: Literature reported HIV-1 IN inhibitors and general structure of designed molecule (PK-G1 to PK-G12)

11.1 Chemistry

The compounds were synthesized in two steps as shown in Scheme 7. First indole-3-carbaldehyde was synthesized from indole by use of mixture of phosphorous oxychloride and dimethyl formamide (DMF) (Vilsmeier-Haack reaction). The first step of this reaction involves generation of substituted chloroiminium ion, also called the Vilsmeier reagent, from dimethyl formamide (DMF) and phosphorus oxychloride. The reaction of substituted chloroiminium ion with electron-rich indole nitially produces an iminium ion, which is hydrolyzed to the corresponding aldehyde during workup. The product was further treated with different substituted sulfonyl chlorides to give **PK-G1** to **PK-G8** and substituted phenyl acetyl chlorides to obtain **PK-G9** to **PK-G12** in presence of base trimethylamine to give moderate yields (60-78%).

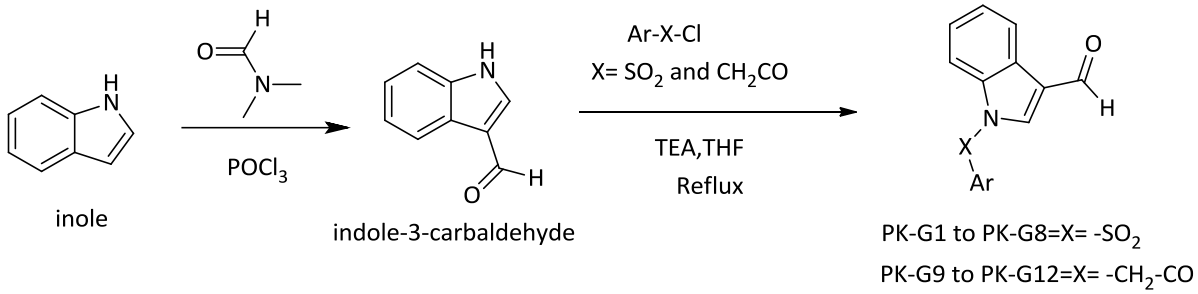

Scheme 7: General synthetic pathway of the target compounds

Reaction Mechanism

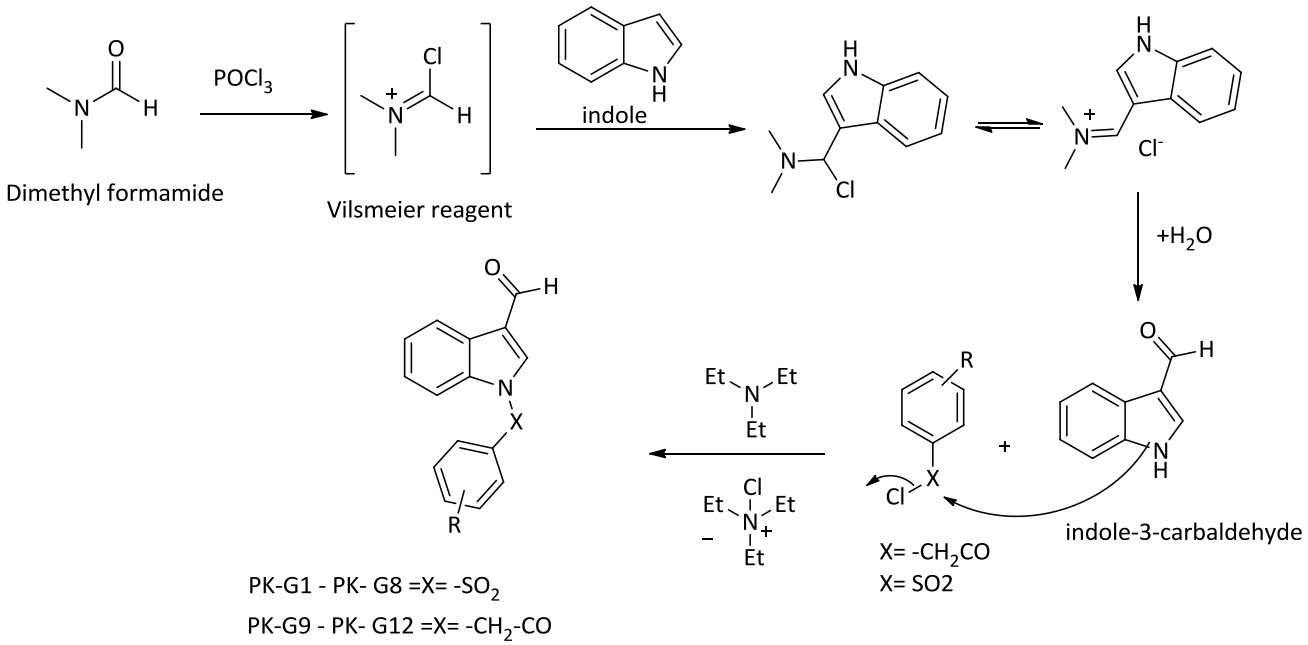

Figure 35: Plausible mechanism for synthesis of substituted indole-3-carbaldehyde derivatives (PK-G1 to PK-G12)

Synthesis of indole-3-carbaldehyde

Three necked 100 ml RBF was charged with Dimethylformamide (0.0684 mol) at 0^{o}C. Then Phosphoryl chloride (0.171 mol) was subsequently added with continuous stirring to the dimethylformamide over a period of 0.5 hour. The reaction mixture turned into pinkish color then indole (0.0171 mol) dissolved in 3 ml of DMF was added with stirring at temperature below 10^{o}C. The change in solution color from pink to yellow was observed. The ice bath was removed and reaction mixture was stirred efficiently at RT for 2 hrs. To the resulting solution, aqueous solution of base sodium hydroxide (0.15 mol) was added slowly and heated to boiling for another 90 minutes. The reaction mixture was cooled to room temperature

and obtain precipitate was filtered. The solid product was recrystallized with ethanol and dried in hot air oven. Off-white Solid; yield 78%; Mp: 196- 198°C IR (KBr) cm^{-1}: 3348 ($NH_{str.}$), 2976 ($CH_{str.}$), 1713 ($C=O_{str.}$), 1563 (C=C, aromatic); ^{1}H-NMR (400 MHz, $CDCl_3$): δ (ppm): 7.27 (s, 1H, ArH), 7.30 – 7.79 (m, 4H, ArH), 8.72 (s, 1H, NH), 9.79 (s, 1H, CHO); ^{13}C-NMR (100 MHz, $CDCl_3$): δ (ppm): 110.2, 119.6, 120.8, 121.4, 122.1, 127.2, 135.7, 138.6 and 190.6; ESI-MS m/z: 146.13 $[M+H]^+$.

Synthesis of Novel substituted indole-3-carbaldehyde derivatives (**PK-G1** to **PK-G12**)

Three-necked round-bottomed flask fitted with a thermometer and N_2 inlet, was charged with indole-3-carbaldehyde (0.0068 mol) and dry THF (20 ml) at room temperature. Triethylamine (0.0238 mol) was added slowly *via* syringe. The reaction mixture was allowed to stir for 20 minutes. Substituted sulfonyl chlorides (0.0068 mol) and phenyl acetyl chlorides (0.0068 mol) dissolved in dry THF (5 ml). The reaction mixture was stirred at RT for 5-8 h. Progress of reaction was monitored by TLC (ethyl acetate: hexane; 3:7). After completion of reaction, the residue was diluted with ethyl acetate (50 ml) and washed successively with aqueous water (60 ml). Concentration of solvent under vacuum gave crude solids (**PK-G1** to **PK-G12**). The compounds were further purified by column chromatography.

1-(phenylsulfonyl)-1*H*-indole-3-carbaldehyde (PK-G1): Light Yellow Solid; yield 76%; Mp: 164–166°C; IR (KBr) cm^{-1}: 2947 ($CH_{str.}$), 1719 ($C=O_{str.}$), 1563 (C=C, aromatic), 1350 ($O=S=O_{str.}$); ^{1}H-NMR (400 MHz, $CDCl_3$): δ (ppm): 7.24 (s, 1H, ArH), 7.31-8.63 (m, 9H, ArH), 9.68 (s, 1H, CHO); ^{13}C-NMR (100 MHz, $CDCl_3$): δ (ppm): 112.5, 116.8, 118.6, 120.5, 123.7, 124.2, 125.9, 126.7, 126.8, 132.5, 133.8, 136.4 and 183.2; ESI-MS m/z: 286.08 $[M+H]^+$.

1-((2-nitrophenyl)sulfonyl)-1*H*-indole-3-carbaldehyde (PK-G2): Yellow Solid; yield 72%; Mp: 219–221°C; IR (KBr) cm^{-1}: 2955 ($CH_{str.}$), 1685 ($C=O_{str.}$), 1569 (C=C, aromatic), 1378 ($O=S=O_{str.}$); ^{1}H-NMR (400 MHz, $CDCl_3$): δ (ppm): 6.94 (s, 1H, ArH), 7.24-8.41 (m, 8H, ArH), 9.64 (s, 1H, CHO); ^{13}C-NMR (100 MHz, $CDCl_3$): δ (ppm): 114.2, 115.6, 116.9, 121.5, 124.6, 124.8, 128.3, 129.1, 130.2, 131.4, 135.4, 144.8 and 183.8; ESI-MS m/z: 331.04 $[M+H]^+$.

1-((3-nitrophenyl)sulfonyl)-1*H*-indole-3-carbaldehyde (PK-G3): Yellow Solid; yield 68%; Mp: 207–209°C; IR (KBr) cm^{-1}: 2967 ($CH_{str.}$), 1668 ($C=O_{str.}$), 1541 (C=C, aromatic), 1380 ($O=S=O_{str.}$); ^{1}H-NMR (400 MHz, $CDCl_3$): δ (ppm): 7.11 (s, 1H, ArH), 7.29-8.31 (m, 8H, ArH), 9.60 (s, 1H, CHO); ^{13}C-NMR (100 MHz, $CDCl_3$): δ (ppm): 113.6, 114.9, 115.7, 120.3, 123.8, 124.5, 127.9, 128.4, 131.6, 133.5, 136.1, 145.2 and 183.3; ESI-MS m/z: 331.09 $[M+H]^+$.

1-((4-nitrophenyl)sulfonyl)-1*H*-indole-3-carbaldehyde (PK-G4): Yellow Solid; yield 75%; Mp: 211–213°C; IR (KBr) cm^{-1}: 2981 ($CH_{str.}$), 1662 ($C=O_{str.}$), 1548 (C=C, aromatic), 1372 ($O=S=O_{str.}$); ^{1}H-NMR (400 MHz, $CDCl_3$): δ (ppm): 7.18 (s, 1H, ArH), 7.41-8.48 (m, 8H, ArH), 9.71 (s, 1H, CHO); ^{13}C-NMR (100 MHz, $CDCl_3$):

δ (ppm): 115.7, 116.4, 117.2, 122.6, 123.9, 125.7, 127.4, 128.8, 129.6, 132.6, 134.8, 146.2 and 184.2; ESI-MS m/z: 331.05 $[M+H]^+$.

1-((2-chlorophenyl)sulfonyl)-1*H*-indole-3-carbaldehyde (PK-G5): White Solid; yield 60%; Mp: 214–216 °C; IR (KBr) cm^{-1}: 2946 ($CH_{str.}$), 1671 ($C=O_{str.}$), 1552 (C=C, aromatic), 1385 ($O=S=O_{str.}$); ^{1}H-NMR (400 MHz, $CDCl_3$): δ (ppm): 7.23 (s, 1H, ArH), 7.34-8.54 (m, 8H, ArH), 9.76 (s, 1H, CHO); ^{13}C-NMR (100 MHz, $CDCl_3$): δ (ppm): 112.8, 114.7, 117.2, 119.5, 120.5, 123.9, 125.6, 128.2, 128.9, 132.6, 134.7, 140.4 and 186.4; ESI-MS m/z: 320.21 $[M+H]^+$.

1-tosyl-1*H*-indole-3-carbaldehyde (PK-G6): Brown Solid; yield 62%; Mp: 204–206°C; IR (KBr) cm^{-1}: 2985, 2938 ($CH_{str.}$), 1666 ($C=O_{str.}$), 1562 (C=C, aromatic), 1410 ($O=S=O_{str.}$); ^{1}H-NMR (400 MHz, $CDCl_3$): δ (ppm): 2.38 (s, 1H, CH_3), 7.19 (s, 1H, ArH), 7.32-8.32 (m, 8H, ArH), 9.76 (s, 1H, CHO); ^{13}C-NMR (100 MHz, $CDCl_3$): δ (ppm): 25.5, 113.5, 116.2, 117.7, 118.4, 118.9, 122.6, 124.2, 126.1, 127.3, 128.1, 130.8, 136.4 and 186.8; ESI-MS m/z: 300.15 $[M+H]^+$.

1-((4-methoxyphenyl)sulfonyl)-1*H*-indole-3-carbaldehyde (PK-G7): Creamish Solid; yield 71%; Mp: 230–232°C; IR (KBr) cm^{-1}: 2973, 2951 ($CH_{str.}$), 1668 ($C=O_{str.}$), 1535 (C=C, aromatic), 1395 ($O=S=O_{str.}$); ^{1}H-NMR (400 MHz, $CDCl_3$): δ (ppm): 3.84 (s, 1H, OCH_3), 7.24 (s, 1H, ArH), 7.38-8.47 (m, 8H, ArH), 9.73 (s, 1H, CHO); ^{13}C-NMR (100 MHz, $CDCl_3$): δ (ppm): 62.4, 114.5, 115.3, 118.6, 119.2, 120.4, 121.8, 123.5, 127.4, 130.4, 131.7, 132.9, 160.4 and 183.7; ESI-MS m/z: 316.04 $[M+H]^+$.

***N*-(4-((3-formyl-1*H*-indol-1-yl)sulfonyl)phenyl)acetamide (PK-G8):** Light Yellow Solid; yield 61%; Mp: 216–218°C; IR (KBr) cm^{-1}: 2986, 2930 ($CH_{str.}$), 1714, 1674 ($C=O_{str.}$), 1530 (C=C, aromatic), 1372 ($O=S=O_{str.}$); ^{1}H-NMR (400 MHz, $CDCl_3$): δ (ppm): 2.72 (s, 1H, $COCH_3$), 7.29 (s, 1H, ArH), 7.40-8.52 (m, 8H, ArH), 8.67 (s, 1H, NH), 9.76 (s, 1H, CHO); ^{13}C-NMR (100 MHz, $CDCl_3$): δ (ppm): 28.4, 115.1, 116.4, 117.7, 118.2, 119.6, 120.8, 122.3, 124.2, 126.2, 128.9, 133.5, 146.7, 168.2 and 185.3; ESI-MS m/z: 342.20 $[M+H]^+$.

1-(2-oxo-2-phenylethyl)-1*H*-indole-3-carbaldehyde (PK-G9): White Solid; yield 73%; Mp: 227–229°C; IR (KBr) cm^{-1}: 2970, 2884 ($CH_{str.}$), 1721, 1664 ($C=O_{str.}$), 1518 (C=C, aromatic); ^{1}H-NMR (400 MHz, $CDCl_3$): δ (ppm): 5.72 (s, 2H, CH_2CO), 7.41 (s, 1H, ArH), 7.45-8.32 (m, 9H, ArH), 9.71 (s, 1H, CHO); ^{13}C-NMR (100 MHz, $CDCl_3$): δ (ppm): 64.4, 110.5, 112.4, 113.9, 114.6, 115.8, 118.6, 119.9, 121.5, 123.4, 126.2, 129.6, 131.5, 135.8, 137.5, 186.4 and 189.2; ESI-MS m/z: 264.38 $[M+H]^+$.

1-(2-oxo-2-(p-tolyl)ethyl)-1*H*-indole-3-carbaldehyde (PK-G10): Light Yellow Solid; yield 71%; Mp: 197–199°C; IR (KBr) cm^{-1}: 2973, 2934, 2860 ($CH_{str.}$), 1723, 1669 ($C=O_{str.}$), 1542 (C=C, aromatic); ^{1}H-NMR (400 MHz, $CDCl_3$): δ (ppm): 2.39 (s, 3H, CH_3), 5.64 (s, 2H, CH_2CO), 7.23 (s, 1H, ArH), 7.28-8.41 (m, 8H, ArH), 9.78 (s, 1H, CHO); ^{13}C-NMR (100 MHz, $CDCl_3$): δ (ppm): 25.4, 66.2, 111.9, 112.8, 114.9, 117.4, 118.2,

119.3, 120.1, 122.4, 124.9, 125.8, 127.3, 130.2, 133.3, 135.1, 185.9 and 190.4; ESI-MS m/z: 277.09 $[M+H]^+$.

1-(2-(4-methoxyphenyl)-2-oxoethyl)-1*H*-indole-3-carbaldehyde (PK-G11): Yellow Solid; yield 62%; Mp: 201–203°C; IR (KBr) cm^{-1}: 2951, 2962, 2865 ($CH_{str.}$), 1720, 1663 ($C=O_{str.}$), 1548 (C=C, aromatic); ^{1}H-NMR (400 MHz, $CDCl_3$): δ (ppm): 3.89 (s, 3H, OCH_3), 5.89 (s, 2H, CH_2CO), 7.19 (s, 1H, ArH), 7.23-8.39 (m, 8H, ArH), 9.70 (s, 1H, CHO); ^{13}C-NMR (100 MHz, $CDCl_3$): δ (ppm): 63.9, 66.7, 110.4, 113.1, 114.4, 115.2, 116.7, 118.1, 120.6, 121.8, 123.2, 126.4, 128.9, 131.6, 134.6, 137.6, 185.1 and 191.6; ESI-MS m/z: 294.18 $[M+H]^+$.

1-(2-(4-chlorophenyl)-2-oxoethyl)-1*H*-indole-3-carbaldehyde (PK-G12): White Solid; yield 64%; Mp: 215–217°C; IR (KBr) cm^{-1}: 2962, 2862 ($CH_{str.}$), 1717, 1667 ($C=O_{str.}$), 1521 (C=C, aromatic); ^{1}H-NMR (400 MHz, $CDCl_3$): δ (ppm): 5.91 (s, 2H, CH_2CO), 7.27 (s, 1H, ArH), 7.33-8.36 (m, 8H, ArH), 9.76 (s, 1H, CHO); ^{13}C-NMR (100 MHz, $CDCl_3$): δ (ppm): 68.2, 114.1, 116.5, 118.9, 121.3, 122.5, 126.7, 129.1, 132.4, 133.6, 135.2, 136.8, 137.5, 137.8, 147.4, 184.6 and 189.9; ESI-MS m/z: 264.38 $[M+H]^+$.

11.2 Results and Discussion

The results of *in vitro* evaluation as well as Gscore of designed compounds are given in **table 20**. The results of cytoxicity and anti-HIV assays are shown in **table 21**.

Overall, it was observed that compounds with phenacyl linker were weakly active as compared to compounds with sulfonyl linker. In silico, it was observed that the carbaldehyde group in sulfonyl linker compounds co-ordinates with Mg1001. Replacing sulfonyl with phenacyl changes the conformation in such way that acyl carbonyl co-ordinates with Mg1001 and aromatic group does not occupy the hydrophobic cavity.

Compounds **PK-G1** having unsubstituted phenyl ring showed hydrogen bonding with Cys 65 (by carbaldehyde), His 67 and Asn 155 (by sulfonyl group) and hydrophobic interactions with Asp 64, Ile 151, Glu 152 and Lys 159 were also observed apart from Mg coordination. It was moderately active HIV-1 IN inhibitor and showed 55.36% inhibition at 10µM concentration.

Substitution of electron withdrawing nitro group, either at ortho (**PK-G2**) or para (**PK-G4**) position, showed higher Gscore as well as HIV-1 IN inhibitory potential (85.90 and 76.87 %, respectively), as compared to meta substituted derivative (**PK-G3**, 63.21%). Analysis of docked poses revealed that both **PK-G2** showed hydrogen bonding with Cys 65 (by carbaldehyde), Thr 66, His 67, Lys 156, Lys 159 (by ortho nitro and sulfonyl group, respectively) and hydrophobic interactions with Asp 64, His 67, Glu 152 and Lys 156 apart from metal coordination. Although **PK-G4** showed almost similar interactions, **PK-G2**

also displayed π-π stacking between indole ring and His 67 that might be responsible for better activity. **PK-G3** lacked hydrogen bonding interactions with Cys 65 and π-π stacking, might be reason for less activity as compare to **PK-G2** and **PK-G4**. Chloro substitution (**PK-G5**) also showed reduction in HIV-1 IN inhibitory activity and docking score**.** This may be due to lack of hydrogen bonding interactions with Thr 66 and π-π stacking.

Substitution of electron donating methyl group at para position (**PK-G6**) displayed hydrogen bonding with Cys 65 and Mg coordination (by carbaldehyde group) and hydrophobic interactions with Glu 152, Asn 155 and Lys 159. However, replacement of methyl with methoxy group (**PK-G7**) showed significant increase in IN inhibitory activity (80.92 %). It showed hydrogen bonding interactions with Cys 65 (as well as Mg coordination by carbaldehyde group), Thr 66, Asn 155 (by sulfonyl group) and Gln 148 (by *p*-methoxy group) and hydrophobic interactions with Asp 64 and Glu 152, respectively. The π-π stacking between indole ring and Lys 159 was also seen. The higher activity of nitro and methoxy substitution could be due to bulk and the ability to stabilize adjacent anion, resulting in more binding interactions and thus, docking score. However, when the bulk was increased further by *N*-acetyl substitution (**PK-G8**) reduced interactions with the active site.

Since compounds having *o*-nitro (**PK-G2**) and *p*-nitro (**PK-G4**) and *p*-methoxy substitution (**PK-G7**) and sulfonyl linker exhibited significant IN inhibitory activity (inhibition more than 75%), these were further tested for calculation of IC_{50} values. It was observed that compounds **PK-G2** and **PK-G4** showed IC_{50} value of 4.78 µM and 5.35 µM respectively and **PK-G7** showed IC_{50} value of 5.15 µM. These values are in accordance with the Gscore and % inhibition values.

Table 20: Docking Score and inhibition data of compounds PK-G1 to PK-G12

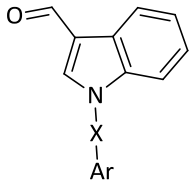

Code	X	Ar	Docking Score	% IN Inhibition*	IC_{50} value**
Dolutegravir	-------	-------	-7.30	95.00	nd
PK-G1	$-SO_2$	-Ph	-5.49	55.36	nd
PK-G2	$-SO_2$	2-NO_2-Ph	-6.78	85.90	4.78
PK-G3	$-SO_2$	3-NO_2-Ph	-5.60	63.21	nd

PK-G4	$-SO_2$	4-NO_2-Ph	-5.75	76.87	5.32
PK-G5	$-SO_2$	2-Cl-Ph	-5.63	69.31	nd
PK-G6	$-SO_2$	4-Me-Ph	-5.42	53.77	nd
PK-G7	$-SO_2$	4-OMe-Ph	-6.26	80.92	5.15
PK-G8	$-SO_2$	4-$NHCOCH_3$-Ph	-5.38	50.72	nd
PK-G9	$-CH_2CO$	-Ph	-5.41	51.76	nd
PK-G10	$-CH_2CO$	4-Me-Ph	-4.17	39.69	nd
PK-G11	$-CH_2CO$	4-OMe-Ph	-5.18	48.24	nd
PK-G12	$-CH_2CO$	2-Cl-Ph	-6.25	60.80	nd

*% inhibition at 10μM concentration, values are mean of duplicate experiment performed independently, nd = not done; ** in μM

Table 21: Anti-HIV activity of synthesized compounds PK-G1 to PK-G12

Compounds	**HIV-1 (III_B)**			**HIV-2 (ROD)**		
	EC_{50}[1] (μM)	**CC_{50}[2] (μM)**	**HIV-1[3] SI**	**EC_{50}[1] (μM)**	**CC_{50}[2] (μM)**	**HIV-2[3] SI**
Dolutegravir	0.0006±0.000001	1.275±0.3	2110.00	0.00232±0.00061	1.495±0.165	597.00
PK-G1	>11.02±1.50	11.02±1.50	<1	>11.50±1.40	11.50±1.40	<1
PK-G2	3.16±0.25	7.32±2.25	<1	>5.10±0.40	5.10±0.40	<1
PK-G3	>11.24±1.70	11.24±1.70	<1	>12.78±1.10	12.78±1.10	<1
PK-G4	>6.04±1.10	6.04±1.10	<1	>7.49±1.30	7.49±1.30	<1
PK-G5	>51.80±4.25	51.80±4.25	<1	>53.40±1.60	53.40±1.60	<1
PK-G6	>5.39±0.80	5.39±0.80	<1	>7.45±1.12	7.45±1.12	<1
PK-G7	>2.37±0.35	2.37±0.35	<1	>3.10±0.50	3.10±0.50	<1
PK-G8	>8.12±1.35	8.12±1.35	<1	>8.50±0.30	8.50±0.30	<1
PK-G9	>53.80±2.65	53.80±2.65	<1	>54.85±1.70	54.85±1.70	<1
PK-G10	>33.48±1.90	33.48±1.90	<1	>34.50±1.30	34.50±1.30	<1
PK-G11	nd	nd	nd	nd	nd	nd
PK-G12	>24.90±2.65	24.90±2.65	<1	>24.50±2.50	24.50±2.50	<1

[1]EC_{50}: concentration of compound required to achieve 50% protection of MT-4 cell cultures against HIV induced cytotoxicity, as determined by MTT method. [2]CC_{50}: concentration required to reduce the viability of mock-infected cells by 50%, as determined by MTT method. [3] SI: selectivity index (CC_{50}/EC_{50}); nd: not done.

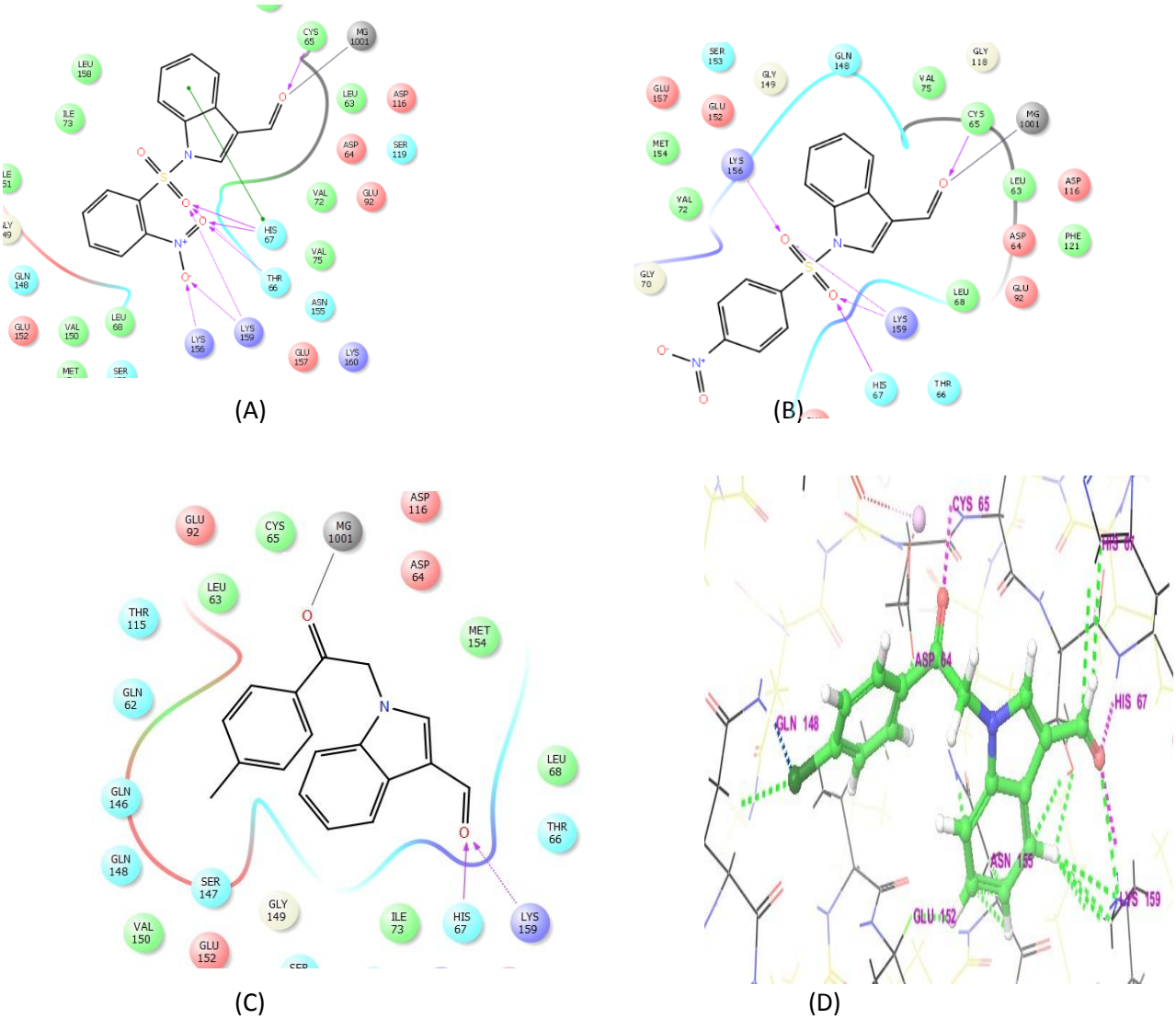

Figure 36: Docking poses of few representative compounds A: 2D interaction plot of PK-G2; B: 2D interaction plot of PK-G3; C: 2D interaction plot of PK-G10; D: Docking pose of PK-G12

11.3 Oral bioavailability and toxicity prediction

Drug likeness parameters such as mol. wt., logP, hydrogen bond acceptor, hydrogen bond donors, no of rotatable bonds found within the optimum range. All compounds exhibited correlation between bioavailability of the compound and water solubility (logS -4.51 to -3.70).

Table 22: *In silic*o predicted ADME parameters of compounds PK-G1 to PK-G12

CODE	Mol. Formula	M.Wt.	log P[a]	RB[b]	HBA[c]	HBD[d]	PSA[e]	log S[f]	PCaco[g]
PK-G1	$C_{15}H_{11}NO_3S$	285.32	2.69	3	4	0	115.77	-3.70	1.28
PK-G2	$C_{15}H_{10}N_2O_5S$	330.32	2.60	4	6	0	130.53	-4.39	0.99
PK-G3	$C_{15}H_{10}N_2O_5S$	330.32	2.60	4	6	0	130.53	-4.28	0.98
PK-G4	$C_{15}H_{10}N_2O_5S$	330.32	2.60	4	6	0	130.53	-4.28	0.94
PK-G5	$C_{15}H_{10}ClNO_3S$	319.77	3.34	3	4	0	126.18	-4.33	1.34
PK-G6	$C_{16}H_{13}NO_3S$	299.35	3.00	3	4	0	122.24	-3.95	1.29
PK-G7	$C_{16}H_{13}NO_4S$	315.35	2.70	4	5	0	127.36	-4.11	1.06
PK-G8	$C_{17}H_{14}N_2O_4S$	342.38	2.65	5	5	1	138.32	-4.00	1.04
PK-G9	$C_{17}H_{13}NO_2$	263.30	3.34	4	3	0	116.01	-3.89	1.73
PK-G10	$C_{18}H_{15}NO_2$	277.32	3.65	4	3	0	122.37	-4.15	1.57
PK-G11	$C_{18}H_{15}NO_3$	293.32	3.35	5	4	0	127.49	-4.18	1.33
PK-G12	$C_{17}H_{12}ClNO_2$	297.74	3.99	4	3	0	126.31	-4.51	1.58

[a]Partition coefficient, [b]No. of rotatable bonds, [c] No. of hydrogen bond acceptors, [d] No. of hydrogen bond donors, [e]polar surface area, [f]water solubility, [g]caco-2 permeability.

CHAPTER 12: SUMMARY AND CONCLUSION

Acquired immune deficiency syndrome (AIDS) is caused by infection with human immunodeficiency virus (HIV). HIV IN has been shown to be a potential target for the management of AIDS, with the entry of raltegravir, elvitegravir and dolutegravir in the clinic. Moreover, due to absence of HIV-1 IN homologue in human cells, it is an attractive target for development of new anti HIV therapy. The search for small molecule HIV-1 IN inhibitors has proven to be challenging due to toxicity and bioavailability issues. The aim was therefore; to design, synthesize and evaluate small molecular HIV-1 IN inhibitors of various structural scaffolds.

To start with, the compounds reported to inhibit strand transfer step of HIV-1 IN were studied to find a suitable prototype. Then various structural modifications of prototype compounds were done to derive series of analogues. After synthesis, HIV IN inhibition was studied at 10µM in enzyme inhibition assay and most active compounds were screened further for IC_{50} determination. To verify hypotheses, docking analysis with Schrodinger suite was performed for which pdb ID 1QS4 was chosen and docking protocol was validated. Further, cell based anti-HIV activity was done to evaluate the effect on HIV infection and cell viability.

In first series, *N*-(4-fluorophenyl)-6-methyl-2-oxo-4-substituted phenyl-1,2,3,4-tetrahydro pyrimidine-5-carboxamide derivatives were synthesized. Docking and *in vitro* studies revealed that these compounds showed interactions with catalytical site of HIV-1 IN and four compounds **PK-A5, PK-A6, PK-A16** and **PK-A18** exhibited significant percentage inhibition of HIV-1 IN with IC_{50} values less than 4.91 µM. There was reasonably good correlation between docking simulation and isolated enzyme assay results. However, none of the derivative was active against HIV-1 and HIV-2 below their cytotoxic concentration. This indicates that these types of compounds can be excluded from further exploration for anti-HIV activity.

Next, 4-oxo-6-substituted phenyl-2-thioxo-1,2,3,4-tetrahydropyrimidine-5-carbonitrile derivatives were synthesized and evaluated. These compounds showed very good docking score in the range of -6.39 to -5.39. We observed that nitrile group play a key role as hydrogen bond acceptors by withdrawing electrons from the aromatic ring and acquiring a negative charge. It was also reported that in many cases the nitrile functions as a ketone bioisostere with the nitrile engaging in non-specific, polar interactions. It was observed that unsubstituted derivative (**PK-B1**) showed inhibition of HIV-1 IN at IC_{50} 7.45 µM. Compound **PK-B5** having electron withdrawing substitution (*p*-chloro), displayed very high potency (84.18%) with IC_{50} 2.31 µM. Compound **PK-B8** having electron donating substitution (*p*-hydroxy) showed potent activity with an IC_{50} value of 6.24 µM. Overall series shows less docking interactions with

DDE motif. However, none of the derivative was active against HIV-1 and HIV-2 below their cytotoxic concentration.

Fourteen 7,7-dimethyl-4-substituted phenyl-3,4,7,8-tetrahydroquinazoline-2,5(1*H*,6*H*)-dione analogues were synthesized and evaluated. Three compounds **PK-C2, PK-C4** and **PK-C13** exhibited significant percentage inhibition of HIV-1 IN with IC_{50} value less than 5.36 µM. However, none of the derivative was active against HIV-1 and HIV-2 below their cytotoxic concentration.

Further, 4-substituted-benzylideneisoquinoline-1,3(2*H*,4*H*)-dione derivatives were synthesized. It was observed that three compounds **PK-D2, PK-D6** and **PK-D8** exhibited significant percentage inhibition of HIV-1 IN with IC_{50} values less than 5.96 µM. Eighteen *N*- substituted phenyl coumarin-3-carboxamide derivatives were also considered of which five compounds **PK-E8, PK-E9, PK-E12, PK-16** and **PK-E17** exhibited significant percentage inhibition (up to 90.14%) of HIV-1 IN with IC_{50} ≤1.69 µM. Again, none of the derivative was active against HIV-1 and HIV-2 below their cytotoxic concentration.

Next, 3-(1,3-dioxoisoindolin-2-yl)-*N*-substituted phenyl benzamide derivatives synthesized based on literature reports. Their docking results reveled that these derivatives formed hydrogen-bonding interactions with DDE motif. It was also observed that keto group of phthalimide ring and amidic linkage interacts with Asn 155, Thr 66 and His 67, respectively by hydrogen bonding. Six compounds **PK-F3, PK-F8, PK-F9, PK-F13, PK-F14** and **PKF18** exhibited significant percentage inhibition (up to 87.05%) of HIV-1 IN with IC_{50} ≤3.90 µM. Two compounds **PK-F8** (IC_{50} 4.01 µM) and **PK-F9** (IC_{50} 3.90 µM) exhibited significant activity comparable to those of the standard drug dolutegravir. But all the compounds, except 3-hydroxy substituted **PK-F3** did not show any anti-HIV activity below their cytotoxic concentration.

Last, a series of indole-3-carbaldehydes having substituted *N*-sulfonyl phenyl or N-phenacyl was synthesized and evaluated for anti-HIV activity. Three compounds (**PK-G2, PK-G3** and **PK-G7**) exhibited significant inhibition of HIV-1 IN (IC_{50} ≤5.32 µM). Compound **PK-G2** also exhibited significant anti-HIV activity against HIV-1 strain IIIB (IC_{50} 3.16 µM). HIV integrase inhibitors are also reported to inhibit reverse transcriptase.

Since compounds **PK-F3** and **PK-G2** showed the antiHIV activity below their cytotoxic concentration, these were examined against various single and double mutant reverse transcriptase (RT) strains. As shown in table 23, only **PK-G2** showed promising activity against E138K with IC50 value of 2.43 µM with safety index of 3.

Table 23: Anti-HIV activity of the PK-F3 , PK-G2 and Reference drugs against RT mutated HIV strains

Compounds	**L100I[a]**	**K103N[a]**	**Y181C[a]**	**Y188L[a]**	**E138K[a]**	**RES175[a]**	**F227L+V106A[a]**	**RES056[a]**	**SI[b]**
PK-F3	>125	>125	>125	>125	>125	>125	>125	>125	>1
PK-G2	>8.09	>8.09	>8.09	>8.09	2.43	>8.09	>8.09	>8.09	3
Dolutegravir	0.00062	0.00065	0.00067	0.00068	0.00079	0.0026	0.00043	0.00092	1558
Efavirenz	0.0010	0.0019	0.0015	0.0059	0.0016	0.00092	0.050	0.040	>50
Azidothymidine	0.0013	0.0019	0.0017	0.0016	0.0022	0.00084	0.0010	0.0015	>1311
Nevirapine	0.40	1.85	>4.00	>4.00	0.058	nd	>4.00	>4.00	X1
Etravirine	0.0027	0.0015	0.0079	0.0079	0.0073	nd	0.0070	0.0010	>194

[a]average IC_{50} (µM) and [b] SI: selective index, the ratio of CC_{50}/EC_{50}. X1 stand for ≥ 1 or < 1.

To conclude, the specific contribution of the present work can be given as:

1. A Total of 110 compounds belonging to seven structurally diverse scaffolds were synthesized.
2. Among these, 28 compounds showed promising results and the IC_{50} range was 0.65- 7.45 µM.
3. Most active compound of all was PK-A6 belonging to tetrahydropyrimidine-5-carboxamides class.
4. Compound **PK-G2** showed dual inhibition of HIV IN and RT (RNaseH). Therefore, compound **PK-G2** can be a starting point for development of dual inhibitors of HIV integrase as well as reverse transcriptase.
5. These compounds can be good starting point for future modifications to reduce cytoxicity and enhance HIV IN inhibitory potency.

CHAPTER 13: FUTURE PERSPECTIVES

The present work mainly focused on generation of structurally diverse library of small molecules to obtain leads of different structural scaffolds using computer aided drug design. Based on this work, following future studies may be planned:

1. Using this information, several libraries can be designed of the molecules having improved binding interactions with HIV-1 IN active site and thus improved potency.
2. Reasons for failure of these compounds in cell based assays can be studied further; in particular, cytotoxicity aspect can be explored.
3. One compound showed IN as well as RT inhibition. Such dual inhibitors may be explored based on these structures.
4. More scaffolds may be tapped to get potent IN inhibitors.

CHAPTER 14: REFERENCES

Ali S, Ali N, et al., *Mini Rev Med Chem.* 13 (2013) 1792-1800.

Artico M, Di Santo R, et al., *J Med Chem.* 41 (1998) 3948-3960.

Arts EJ, Hazuda DJ, *Cold Spring Harb Perspect Med.* 2 (2012) 1-23.

Babu AV, Navudu R, et al., *Med Chem Res.* 23 (2014) 877-881.

Bach DH, Liu JY, et al., *Bioorg Med Chem.* 25 (2017) 3396-3405.

Bailly F, Queffélec C, et al., *Eur J Med Chem.* 43 (2008) 1222-1229

Bailly F, Queffelec C, et al., *Bioorg Med Chem Lett.* 15 (2005) 5053-5056.

Bénard C, Zouhiri F, et al., *Bioorg Med Chem Lett.* 14 (2004) 2473-2476.

Billamboz M, Bailly F, et al., *Eur J Med Chem.* 46 (2011) 535-546.

Billamboz M, Bailly F, et al., *J Med Chem.* 51 (2008) 7717-7730.

Billamboz M, Bailly F, et al., *J Med Chem.* 54 (2011) 1812-1824.

Billamboz M, Suchaud V, et al., *ACS Med Chem Lett.* 4 (2013) 606-611.

Billamboz M, Suchaud V, et al., *Eur J Med Chem.* 117 (2016) 256-268.

Boros EE, Johns BA, et al., *Bioorg Med Chem Lett.* 16 (2006) 5668-5672.

Brzozowski Z, Saczewski F, et al., *Bioorg Med Chem.* 12 (2004) 3663-3672.

Brzozowski Z, Saczewski F, et al., *Eur J Med Chem.* 44 (2009) 190-196.

Brzozowski Z, Sławiński J, et al., *Eur J Med Chem.* 43 (2008) 1188-1198.

Che Z, Liu S, et al., *Pharmaceuticals.* 8 (2015) 221-229.

Chen JCH, Krucinski J, et al., *Proc Natl Acad Sci USA.* 97 (2000) 8233-8238.

Chi G, Nair V, et al., *Bioorg Med Chem Lett.* 17 (2007) 1266-1269.

Chiang CC, Mouscadet JF, et al., *Chem Pharm Bull.* 55 (2007) 1740-1743.

Costi R, Di Santo R, et al., *Bioorg Med Chem Lett.* 14 (2004) 1745-1749.

Costi R, Di Santo R, et al., *Bioorg Med Chem Lett.* 14 (2004) 1745-1749.

Costi R, Di Santo R, et al., *Bioorg Med Chem.* 12 (2004) 199-215.

Costi R, Métifiot M, et al., *J Med Chem.* 56 (2013) 8588-8598.

Costi R, Métifiot M, et al., *J Med Chem.* 57 (2014) 3223-3234.

Crandall KA, Kelsey CR, Imamichi H, et al., *Mol Biol Evol.* 16 (1999) 372-382.

Dayam R, Neamati N, *Bioorg Med Chem.* 12 (2004) 6371-6381.

Debyser Z, Cherepanov P, et al., *Methods Mol Biol.* 160 (2001) 139-155.

De Clercq E, *Int J Antimicrob Agents.* 33 (2009) 307-320.

De Luca L, Barreca ML, et al., *Bioorg Med Chem Lett.* 18 (2008) 2891-2895.

De Luca L, Ferro S, et al., *Bioorg Med Chem.* 18 (2010) 7515-7521.

De Luca L, Gitto R, et al., *Antiviral Res.* 92 (2011) 102-107.

De Luca L, Grazia SD, et al., *Eur J Med Chem.* 46 (2011) 756-764.

Di Francescoet ME, Pace P, et al., *Bioorg Med Chem Lett.* 18 (2008) 2709-2713.

Di Santo R, Costi R, et al., *J Med Chem.* 51 (2008) 4744-4750.

Di Santo R, Costi R, et al., *J Med Chem.* 49 (2006) 1939-1945.

Di Santo R, Costi R, et al., *J Med Chem.* 51 (2008) 4744-4750.

Donghi M, Kinzel OD, et al., *Bioorg Med Chem Lett.* 19 (2009) 1930-1934.

Dupont R, Jeanson L, et al., *Bioorg Med Chem Lett.* 11 (2001) 3175-3178.

Egbertson MS, Moritz HM, et al., *Bioorg Med Chem Lett.* 17 (2007) 1392-1398.

Elumalai K, Ali MA, et al., *Biotechnol Rep.* 5 (2015) 1-6.

Embrey MW, Wai JS, et al., *Bioorg Med Chem Lett.* 15 (2005) 4550-4554.

Fan LL, Liu WQ, et al., *Chem Pharm Bull.* 57 (2009) 797-800.

Fan X, Zhang FH, et al., *Bioorg Med Chem.* 19 (2011) 4935-4952.

Fardis M, Jin H, et al., *Bioorg Med Chem Lett.* 16 (2006) 4031-4035.

Fátima Â de, Braga TC, et al., *J Adv Res.* 6 (2015) 363-373.

Faure A, Calmels C, Desjobert C, et al., *Nucleic Acids Res.* 33 (2005) 977-986.

Fernandes J, Gattass CR, *J Med Chem.* 52 (2009) 1214-1218.

Ferrara M, Fiore F, et al., *Bioorg Med Chem Lett.* 20 (2010) 5031-5034.

Ferro S, Barreca ML, et al., *Arch Pharm.* 340 (2007) 292-298.

Ferro S, De Luca L, et al., *Bioorg Med Chem.* 18 (2010) 5510-5518.

Ferro S, De Luca L, et al., *Bioorg Med Chem.* 22 (2014) 2269-2279.

Ferro S, De Luca L, et al., *J Med Chem.* 52 (2008) 569-573.

Ferro S, Grazia SD, et al., *Molecules*. 16 (2011) 6858-6870.

Fisher TE, Kim B, et al., *Bioorg Med Chem Lett.* 17 (2007) 6511-6515.

Foye WO, Foye's principles of medicinal chemistry, Lippincott Williams & Wilkins, (2008).

Friesner RA, Banks JL, et al., *J Med Chem.* 47 (2004) 1739-1749.

Fujishita T, Yoshinaga T, in Google Patents, 2004.

Fumakia M, Yang S, Gu J, Ho EA. *Rev Med Virol.* 26 (2016) 4-20.

Fylaktakidou KC, Hadjipavlou-Litina DJ, et al., *Curr Pharm Des.* 10 (2004) 3813-3833.

Gardelli C, Nizi E, et al., *J Med Chem.*, 50 (2007) 4953-4975.

Garvey EP, Johns BA, et al., *Antimicrob Agents Chemother.* 52 (2008) 901-908.

Goldgur Y, Craigie R, et al., *Proc Natl Acad Sci USA.* 96 (1999) 13040-13043.

Goodman & Gillman's The Pharmacological basis of therapeutics, by Laurence Brunton, Bruce A. Chabner, Bjorn Knollman, 12th edition, 2011.

Guare JP, Wai JS, et al., *Bioorg Med Chem Lett.* 16 (2006) 2900-2904.

Hajimahdi Z, Zarghi A, et al., *Med Chem Res.* 22 (2013) 2467-2475.

Hajimahdi Z, Zarghi A. *Iran J Pharm Res.* 15 (2016) 595.

Hazuda DJ, Felock P, et al., *Science.* 287 (2000) 646-650.

He QQ, Zhang X, et al., *Bioorg Med Chem.* 19 (2011) 5553-5558.

Hombrouck A, Van Remoortel B, et al., *Antimicrob Agents Chemother.* 52 (2008) 2861-2869.

Hu L, Li Z, et al., *Med Chem.* 11 (2015) 180-187.

Hu L, Zhang S, et al., *Bioorg Med Chem.* 20 (2012) 177-182.

Ingale KB, Bhatia MS. *Antivir Chem Chemother.* 22 (2011) 95-105.

Jain KS, Arya N, et al., *Curr Top Med Chem.* 16 (2016) 3133-3174.

Jiao ZG, He HQ, et al., *Molecules*. 15 (2010) 1903-1917.

Jin H, Cai RZ, et al., *Bioorg Med Chem Lett.* 16 (2006) 3989-3992.

Jin H, Metobo S, et al., *Bioorg Med Chem Lett.* 19 (2009) 2263-2265.

Jin H, Wright M, et al., *Bioorg Med Chem Lett.* 18 (2008) 1388-1391.

Johns BA, Kawasuji T, et al., *Bioorg Med Chem Lett.* 24 (2014) 3104-3107.

Johns BA, Kawasuji T, Velthuisen EJ. Successful Strategies for the Discovery of Antiviral Drugs. Chapter 6: HIV Integrase inhibitors, (2013) 149-188.

Johns BA, Weatherhead JG, et al., *Bioorg Med Chem Lett.* 19 (2009) 1802-1806.

Johnson TW, Tanis SP, et al., *J Med Chem.* 54 (2011) 3393-3417.

Jones ED, Vandegraaff N, et al., *Bioorg Med Chem Lett.* 20 (2010) 5913-5917.

Kaushik NK, Kaushik N, et al., *Molecules.* 18 (2013) 6620-6662.

Kawasuji T, Fuji M, et al., *Bioorg Med Chem.* 15 (2007) 5487-5492.

Kawasuji T, Johns BA, et al., *J Med Chem.* 55 (2012) 8735-8744.

Kawasuji T, Yoshinaga T, et al., *Bioorg Med Chem.* 14 (2006) 8430-8445.

Kehlenbeck S, Betz U, et al., *J Virol.* 80 (2006) 6883-6894.

Klutchko S, Shavel JJ, et al., *J Org Chem.* 39 (1974) 2436-2437.

Ladani NK, Patel MP, et al., *Arkivoc.* 7 (2009) 292-302.

Langford HM, Williams PD, et al., *Bioorg Med Chem Lett.* 18 (2008) 721-725.

Lee JY, Park JH, et al., *Arch Pharm.* 335 (2002) 277-282.

Lee JY, Yoon KJ, et al., *Bioorg Med Chem Lett.* 13 (2003) 4331-4334.

Li BW, Zhang, et al., *Bioorg Med Chem.* 22 (2014) 3146-3158.

Li X, Krishnan L, et al., *Virology.* 411 (2011) 194-205.

Li X, Vince R, *Bioorg Med Chem.* 14 (2006) 2942-2955.

Long YQ, Jiang XH, et al., *J Med Chem.* 47 (2004) 2561-2573.

Luo Z, Zhao Y, et al., *Arch Pharm.* 348 (2015) 206-213.

Lv Z, Chu Y, Wang Y. *HIV/AIDS (Auckl).* 7 (2015) 95.

Ma K, Wang P, et al., *Bioorg Med Chem Lett.* 21 (2011) 6724-6727.

Maertens GN, Hare S, Cherepanov P. *Nature.* 468 (2010) 326-329.

Mao PCM, Mouscadet JF, et al., *Chem Pharm Bull.* 50 (2002) 1634-1637.

Marchand C, Beutler JA, et al., *Antimicrob Agents Chemother.* 52 (2008) 361-364.

Maurin C, Bailly F, et al., *Bioorg Med Chem.* 14 (2006) 2978-2984.

Maurin C, Lion C, et al., *Bioorg Med Chem.* 18 (2010) 5194-5201.

Mazumder A, Neamati N, et al., *J Med Chem.* 40 (1997) 3057-3063.

Mazumder A, Raghavan K, et al., *Biochem Pharmacol.* 49 (1995) 1165-1170.

Meadows DC, Mathews TB, et al., *J Med Chem.* 48 (2005) 4526-4534.

Meadows DC, Sanchez T, et al., *Bioorg Med Chem.* 15 (2007) 1127-1137.

Metobo S, Jin H, et al., *Bioorg Med Chem Lett.* 16 (2006) 3985-3988.

Metobo S, Mishet M, et al., *Bioorg Med Chem Lett.* 19 (2009) 1187-1190.

Middleton T, Lim HB, et al., *Antiviral Res.* 64 (2004) 35-45.

Mugnaini C, Rajamaki S, et al., *Bioorg Med Chem Lett.* 17 (2007) 5370-5373.

Muraglia E, Kinzel O, et al., *J Med Chem.* 51 (2008) 861-874.

Nagasawa JY, Songet J, et al., *Bioorg Med Chem Lett.* 21 (2011) 760-763.

Naidu BN, Sorenson ME, et al., *Bioorg Med Chem Lett.* 25 (2015) 717-720.

Nair V, Chi G, et al., *J Med Chem.* 49 (2006) 445-447.

Nayab PS, Irfan M, et al., *Luminescence.* 32 (2017) 298-308.

Neamati N, Hong H, et al., *J Med Chem.* 41 (1998) 3202-3209.

Neamati N, Lin Z, et al., H.E. Winslow, *J Med Chem.* 45 (2002) 5661-5670.

Nizi E, Orsale MV, et al., *Bioorg Med Chem Lett.* 19 (2009) 4617-4621.

Noguchi T, Fujimoto H, et al., *Bioorg Med Chem Lett.* 15 (2005) 5509-5513.

Nowotny M, *EMBO Rep.* 10 (2009) 144-151.

Pace P, Di Francescoet ME, et al., *J Med Chem.* 50 (2007) 2225-2239.

Pais GC, Zhang X, et al., *J Med Chem.*, 45 (2002) 3184-3194.

Pasquini S, Mugnaini C, et al., *J Med Chem.* 51 (2008) 5125-5129.

Patil S, Kamath S, et al., *Bioorg Med Chem.* 15 (2007) 1212-1228.

Pawar R, Das T, et al., *Bioorg Med Chem Lett.* 24 (2014) 302-307.

Pendri A, Troyer TL, et al., *J Comb Chem.* 12 (2009) 84-90.

Peterson CW, Younan P, Jerome KR, Kiem HP. *Gene Ther.* 20 (2013) 695-702.

Petrocchi A, Jones P, et al., *Bioorg Med Chem Lett.* 19 (2009) 4245-4249.

Petrocchi A, Koch U, et al., *Bioorg Med Chem Lett.* 17 (2007) 350-353.

Pires DE, Blundell TL, et al., *J Med Chem.* 58 (2015) 4066-4072.

Plewe MB, Butler SL, et al., *J Med Chem.* 52 (2009) 7211-7219.

Queffélec C, Bailly F, et al., *Bioorg Med Chem Lett.* 18 (2008) 4736-4740.

Rajamaki S, Innitzer A, et al., *Bioorg Med Chem Lett.* 19 (2009) 3615-3618.

Ramajayam R, Mahera NB, et al., *Arch Pharm.* 342 (2009) 710-715.

Ran JQ, Huang N, et al., *Bioorg Med Chem Lett.* 20 (2010) 3534-3536.

Ribeiro ANJ, Ramos MJ, Fernandes PA, *J Am Chem Soc.* 134 (2012) 13436-13447.

Ryabinin VA, Sinyakov AN, et al., *Eur J Med Chem.* 35 (2000) 989-1000.

Sanchez TW, Debnath B, et al., *Bioorg Med Chem.* 21 (2013) 957-963.

Sato M, Kawakami H, et al., *J Med Chem.* 52 (2009) 4869-4882.

Sato M, Motomura T, et al., *J Med Chem.* 49 (2006) 1506-1508.

Sechi M, Derudas M, et al., *J Med Chem.* 47 (2004) 5298-5310.

Sechi M, Rizzi G, et al., *Bioorg Med Chem.* 17 (2009) 2925-2935.

Sechi M, Sannia L, et al., *Antivir Chem Chemother.* 16 (2005) 41-61.

Seo YH, Carroll KS, *Angew Chem Int Ed Engl.* 50 (2011) 1342-1345.

Sepehri S, Gharagani S, et al., *Med Chem Res.* 24 (2015) 1707-1724.

Serafin K, Mazur P, et al., *Bioorg Med Chem.* 19 (2011) 5000-5005.

Sharma H, Patil S, et al., *Bioorg Med Chem.* 19 (2011) 2030-2045.

Sharma H, Sanchez TW, et al., *Bioorg Med Chem Lett.* 23 (2013) 6146-6151.

Sharma U, Kumar P, et al., *Mini Rev Med Chem.,* 10 (2010) 678-704.

Su CX, Mouscadet JF, et al., *Chem Pharm Bull.* 54 (2006) 682-686.

Suchaud V, Bailly F, et al., *J Med Chem.* 57 (2014) 4640-4660.

Summa V, Petrocchi A, et al., *J Med Chem.* 49 (2006) 6646-6649.

Tandon V, Yadav P, et al., *ACS Med Chem Lett.* 6 (2015) 1065-1070.

Tang J, Maddali K, et al., Z. Wang, *J Med Chem.* 54 (2011) 2282-2292.

Tang J, Maddali K, et al., *ACS Med Chem Lett.* 2 (2010) 63-67.

Tang J, Maddali K, et al., *Bioorg Med Chem Lett.* 20 (2010) 3275-3279.

Tang J, Maddali K, et al., *Bioorg Med Chem Lett.* 21 (2011) 2400-2402.

Tanis SP, Plewe MB, et al., *Bioorg Med Chem Lett.* 20 (2010) 7429-7434.

Tsou HR, Otteng M, et al., *J Med Chem.* 51 (2008) 3507-3525.

Tupchiangmai W, Choksakulporn S, et al., *Chem Pharm Bull.* 62 (2014) 754-763.

UNAIDS Reports 2017.

Vandurm P, Cauvin C, et al., *Bioorg Med Chem Lett.* 19 (2009) 4806-4809.

Vandurm P, Guiguen A, et al., *Eur J Med Chem.* 46 (2011) 1749-1756.

Vercruysse T, Basta B, et al., *Retrovirology.* 9 (2012) 95-95.

Verschueren WG, Dierynck I, et al., *J Med Chem.* 48 (2005) 1930-1940.

Wadhwa P, Jain P, et al., *Curr Drug Discov Technol.* 15(2018) 2-19.

Wai JS, Egbertson MS, et al., *J Med Chem.* 43 (2000) 4923-4926.

Wai JS, Kim B, et al., *Bioorg Med Chem Lett.* 17 (2007) 5595-5599.

Walker MA, Johnson T, et al., *Bioorg Med Chem Lett.* 16 (2006) 2920-2924.

Walker MA, Johnson T, et al., *Bioorg Med Chem Lett.* 16 (2006) 5818-5821.

Walker MA, Johnson T, et al., *Bioorg Med Chem Lett.* 17 (2007) 4886-4890.

Wang B. HIV-1 integrase: mechanism and inhibitor design, John Wiley & Sons, (2011).

Wang P, Liu C, et al., *Bioorg Med Chem Lett.* 19 (2009) 4574-4578.

Wang Z, Tang J, et al., *Bioorg Med Chem.* 18 (2010) 4202-4211.

Wang Z, Vince R. *Bioorg Med Chem.* 16 (2008) 3587-3595.

Wang Z, Wang M, et al., *Eur J Med Chem.* 53 (2012) 275-282.

Wiscount CM, Williams PD, et al., *Bioorg Med Chem Lett.* 18 (2008) 4581-4583.

Wu L, Wang X, et al., *Curr Med Chem.* 16 (2009) 4236-4260.

Xu H, Liu WQ, et al., *Chem Pharm Bull.* 56 (2008) 720-722.

Xu YW, Zhao GS, et al., *Bioorg Med Chem.* 11 (2003) 3589-3593.

Yoshinaga T, Sato A, et al., in: 9th conference on retroviruses and opportunistic infections, Seattle, WA, 2002, pp. 55.

Yu S, Sanchez TW, et al., *Bioorg Med Chem Lett.* 23 (2013) 6134-6137.

Zabihollahi R, Vahabpour R, et al., *Acta Virol.* 56 (2012) 11-18.

Zeng LF, Jiang XH, et al., *Bioorg Med Chem.* 16 (2008) 7777-7787.

Zeng LF, Zhang HS, et al., *Bioorg Med Chem Lett.* 18 (2008) 4521-4524.

Zhang D, Debnath B, et al., *Bioorg Med Chem.* 22 (2014) 5446-5453.

Zhang X, Pais GC, et al., *Bioorg Med Chem Lett.* 13 (2003) 1215-1219.

Zhao XZ, Maddali K, et al., *Bioorg Med Chem Lett.* 21 (2011) 2986-2990.

Zhao XZ, Maddali K, et al., *Chem Biol Drug Des.* 79 (2012) 157-165.

Zhao XZ, Maddali K, et al., *Bioorg Med Chem Lett.* 22 (2012) 7309-7313.

Zhao XZ, Maddali K, et al., *Bioorg Med Chem Lett.* 19 (2009) 2714-2717.

Zhao XZ, Semenova EA, et al., *J Med Chem.* 51 (2007) 251-259.

Zhao XZ, Smith SJ, et al., *J Med Chem.* 57 (2014) 1573-1582.

Zhuang L, Wai JS, et al., *J Med Chem.* 46 (2003) 453-456.

Appendix I

List of publications

Journal Publications from thesis

Published

- Quinoline, Coumarin and Other Heterocyclic analogues as Potent Inhibitors of HIV-1 Integrase. Current Drug Discovery and Technology, 2018, 15(1), 2-19.
- Synthesis and Biological Evaluation of N-(4-Fluorophenyl)-6-Methyl-2-Oxo-1, 2, 3, 4-Tetrahydropyrimidine-5-Carboxamides as HIV Integrase Strand Transfer Inhibitors. Der Pharmacia Lettre, 2018, 10 (4), 100-114.

Communicated (Under Review)

- 2-Oxo-N-substituted phenyl-2H-chromene-3-carboxamide derivatives as HIV integrase strand transfer inhibitors: Design, synthesis and in vitro evaluation. Communicated in Medicinal Chemistry.
- 4-Substituted Benzylideneisoquinoline-1,3(2*H*,4*H*)-dione Derivatives: Synthesis and Biological Evaluation as Potential HIV-1 Integrase Inhibitors. Communicated in Der Pharmacy Lettre.
- 4-oxo-6-substituted phenyl-2-thioxo1,2,3,4-tetrahydropyrimidine-5-carbonitrile derivatives as HIV integrase strand transfer inhibitors: Design, synthesis and in vitro evaluation. Under revision in Letters in Drug Design & Discovery.
- Synthesis and anti-HIV Evaluation of substituted indole-3-carbaldehyde derivatives. Communicated in Letters in Drug Design & Discovery.
- Design, synthesis and anti-HIV-1 evaluation of a series of tetrahydroquinazoline-2,5(1H,6H)-dione derivatives as possible integrase inhibitors. Communicated in Medicinal Chemistry Research.
- Synthesis and evaluation of 3-(1,3-dioxoisoindolin-2-yl)-*N*-substituted phenyl benzamide analogues as HIV integrase strand transfer inhibitors. Communicated in Anti-Infective Agents.

Journal Publications other than thesis

- Rational design, synthesis and in vitro evaluation of allylidene hydrazinecarboximidamide derivatives as BACE-1 inhibitors. Bioorganic & Medicinal Chemistry Letters, 2016, 26(1), 33-7.
- Design, synthesis and in vitro evaluation studies of Sulfonyl-amino-acetamides as small molecule BACE-1 inhibitors. Bioorganic & Medicinal Chemistry, 2016, 24(11), 2567-2575.

- Design, synthesis and evaluation of Acridin-9-yl hydrazide derivatives as BACE-1 inhibitors. Medicinal Chemistry Research, 2016, 25(7), 1507-1513.
- QSAR and docking studies of N-hydroxy urea derivatives as Flap endonuclease-1 inhibitors. Current Computer-Aided Drug Design, 2015, 11, 279-290.
- Reactive Astrogliosis: Role in Alzheimer's disease. CNS & neurological disorders drug targets 2015, 14 (7), 872-9.
- Design and docking of 6-Methyl-3-Phenoxy-N-Phenylquinoline-4-Carboxamide derivatives as flap Endonuclease-1 Inhibitors. International Journal of Pharmaceutical Sciences and Research, 2015, 386-388 for Conference Proceedings of APTICON 2015 - (20th annual national convention of Association of Pharmaceutical Teachers of India, October 9th-11th 2015, Indore, MP, India).

Poster Presentations

- "Design, synthesis and evaluation of 2-Oxo-N-Substituted Phenyl- 2H - Chromene- 3- Carboxamide Derivatives As Potent Inhibitors Of HIV-1 Integrase Strand Transfer'", Poster presented at ICDD 2017, April 8-9, 2017, JNU, New Delhi.
- "Design, synthesis and evaluation of novel substituted Indole-3-Carboxaldehyde derivative as potent HIV-1 Integrase Inhibitors", Poster presented at International Conference on Challenges in Drug Discovery and Delivery (ICCD3-2017), March 2-4, 2017, BITS Pilani.
- "Design, synthesis and evaluation of novel *N* -(4-fluorophenyl)-6-methyl-2-oxo-4-substituted-phenyl-1,2,3,4-tetrahydropyrimidine-5-carboxamide as HIV integrase inhibitors", orally presented at 'Chem-Cys-2016 ', March 16-19, 2016, Belgium.
- "Flap endonuclease-1 inhibitors: In-silico studies using 2-hydroxy-6-methyl-4-oxo-N-substituted-phenyl-4H-pyran-3-carboxamides", Poster presented at 'Current Trends in Drug Discovery & Research - CTDDR-2016 ', February 24-28, 2016, CDRI Lucknow.
- "Anthranilate urea hydroxamate derivatives: In silico Design, Synthesis and Evaluation as TACE inhibitors", Poster presented at 'Current Trends in Drug Discovery & Research - CTDDR-2016 ', February 24-28, 2016, CDRI Lucknow.
- "Design and Docking of N-(2,6 -dioxo-1,2,3,6-tetrahydropyrimidin-4-yl)- *N*-(4-hydroxyphenyl) benzamide Derivatives as Flap Endonuclease-1 Inhibitors ", Poster presented at "NDCS-2015: International Conference on Nascent Developments in Chemical Sciences", 16-18 October, 2015, BITS Pilani, Pilani campus

- “Design and Docking of 6-Methyl-3-Phenoxy-N-Phenylquinoline-4-Carboxamide Derivatives as Flap Endonuclease-1 Inhibitors”, Poster presented at ‘APTICON-2015: 20th Annual Convention of Association of Pharmaceutical Teachers of India’, October 9-11, 2015, Indore.
- "Docking study of indole derivatives as Flap endonuclease inhibitors", Poster presented at 'International Conference on recent advances in Computational Drug Design', September 16-17, 2013, IISc Bangalore.

Workshops Attended

- Attended One Day National Workshop on “recent advances in computational lead optimization techniques.” April 7th (2017) organized by Schrodinger at JNU, New Delhi, India.
- Attended Ten Day National Workshop on “RESEARCH METHODOLGY” March15th-24th (2015) organized by School of Commerce and Business Studies, Jiwaji University, Gwalior (M.P) , India.

Brief Biography of Ms. Pankaj Wadhwa

Mr. Pankaj Wadhwa has completed his Bachelor's degree in Pharmacy from Swami Keshvanand Institute of Pharmacy, Bikaner (SKIP, Bikaner) in the year 2009. He acquired his Master's degree in Pharmacy in Pharmaceutical Chemistry from Lord Shiva College Of Pharmacy, Sirsa in year 2009. After that, he worked in Jubilant Chemsys, Noida, UP as Research Associate from November 2009 to January 2012. He joined BITS Pilani, Pilani campus as PhD Research Scholar in February 2012. He has published 8+ research articles in peer reviewed journals and presented his work in various national and international conferences.

Brief Biography of Dr. Hemant R. Jadhav

Dr. Hemant R Jadhav is presently working as Associate Professor, Department of Pharmacy, BITS Pilani, Pilani Campus. He also holds administrative position as Associate Dean, Academic Research (Ph. D. Programme) Division and Associate Dean, Sponsored Research and Consultancy Division, Birla Institute of Technology and Science Pilani, Pilani campus. He received his PhD degree in the year 2004 from National Institute of Pharmaceutical Education and Research (NIPER), Mohali, India. He has been involved in the research for last 17 years and in teaching for last 13 years. He has authored more than 35 research papers and 2 book chapters. He has presented his work in more than 50 national and international conferences. He is an expert reviewer of many national and international journals. He is a lifetime member of Association of Pharmacy Teachers of India. He has served as the postgraduate and doctoral examiner for various universities. He has successfully completed two research projects, one under DST Fast Track Young Scientist Scheme and another sponsored by UGC, New Delhi. He also has completed one industrial project. Presently he has an Indo-Polish joint collaborative DST project. He has guided six Ph. D students apart from this thesis.